UNIL | Université de Lausanne

Faculté de biologie
et de médecine

Transfusion Interrégionale CRS SA

New routes in additive solution formulations to improve the quality of stored red blood cells

Thèse de doctorat ès sciences de la vie (PhD)

présentée à la

Faculté de biologie et de médecine
de l'Université de Lausanne

par

Manon BARDYN

Master en sciences de la vie de l'École Polytechnique Fédérale de Lausanne

Jury

Prof. Massimo Bongiovanni, Président
Prof. Jean-Daniel Tissot, Directeur de thèse
Privat-Docent Dr Michel Prudent, Co-directeur de thèse
Prof. Pierre Goloubinoff, Expert
Prof. Anastasios G. Kriebardis, Expert
Privat-Docent Dr Raffaele Renella, Expert

Lausanne
2019

TABLE OF CONTENTS

ABSTRACT

Blood transfusion is a procedure that enables us to save lives every day. In Switzerland, 221'100 red cell concentrates, 38'947 platelet concentrates, and 30'552 units of fresh frozen plasma have been used in 2018 (Swiss Transfusion SRC). Red Blood Cells (RBCs), once separated from other blood components, can be stored for several weeks (generally between 6 and 7) at 4°C in gas-permeable plastic bags. To this end, an additive solution containing all necessary elements for cell survival is routinely added. Such storage conditions, however, differ from the physiological environment in which cells naturally live, leading to metabolic, oxidative and functional changes called RBC "storage lesions" which can be irreversible and progressively accumulate after transfusion.

As of today, scientific consensus has not been reached concerning the clinical impact of these RBC storage lesions. In fact, some studies demonstrated that patients transfused with "old" blood, *i.e.* close to expiration date, have an increased risk of developing transfusion-related adverse effects, whereas others showed no such correlations. The only certainty is that such RBCs no longer have their original properties, potentially reducing their effectiveness. In this context, this thesis aims at proposing novel cheaper ways of improving RBC storage, thereby improving the quality of transfusions for patients.

The first part of this thesis provides a deeper understanding of the causes and mechanisms linked to storage lesions. Using a variety of measurement tools, key parameters of RBC metabolism, antioxidant defenses, and morphology, are reported. The analysis of this data demonstrates that RBCs are prematurely impacted by changes in their environment, including depletion of the uric acid naturally present in high concentration in blood plasma. Based on these results, improvements to storage solutions are proposed. In particular, the effect of adding uric acid with or without vitamin C is tested. Results show significant improvements at level of the cell metabolism, suggesting that proposed treatments are effective. However, limited changes are found for other parameters such as hemolysis, raising the question of dosage and efficacy. To address this issue, the second part of this thesis is devoted to the development of an assay compatible with high-throughput screening to quickly and easily evaluate antioxidant properties of a wide range of molecules. This test provides a way to better define the amount of chemical or natural compounds to add in blood bags to have a positive impact on the aging of RBCs in storage units to prolong the quality of transfusions for patients.

RÉSUMÉ

La transfusion sanguine est une procédure qui permet de sauver des vies quotidiennement. En Suisse, 221'100 concentrés érythrocytaires, 38'947 concentrés thrombocytaires et 30'552 unités de plasma frais congelés ont ainsi été consommés en 2018 (Transfusion CRS Suisse). Les globules rouges (GR) une fois séparés des autres composants sanguins peuvent être conservés plusieurs semaines (généralement entre 6 et 7) à 4°C dans une poche plastique perméable aux gaz. Pour ce faire, une solution additive contenant les éléments nécessaires à leur survie est ajoutée. Ces conditions de stockage diffèrent de l'environnement physiologique dans lequel ces cellules évoluent normalement. Au cours du temps des lésions métaboliques, oxydatives et fonctionnelles, qui peuvent être réversibles ou irréversibles après transfusion, communément nommées « lésions de stockage des GR » s'accumulent.

La communauté scientifique n'est aujourd'hui pas unanime sur la question de l'impact clinique de ces lésions sur le patient traité. En effet, certaines études ont démontré que les receveurs du sang « vieux », c'est-à-dire proche de la péremption, couraient un risque accru de développer des effets indésirables en lien avec la transfusion, alors que d'autres travaux n'ont montré aucune corrélation. La certitude qui demeure néanmoins est que ces GR n'ont plus les mêmes propriétés, réduisant ainsi potentiellement leur efficacité. C'est dans ce contexte que s'inscrit cette thèse de doctorat dont le but fût de proposer de nouvelles solutions simples et peu coûteuses permettant d'améliorer le stockage des GR, et ainsi la qualité du produit pour le patient.

La première partie de ce travail a consisté à acquérir une meilleure compréhension des causes et mécanismes liés à ces lésions. Les différents outils utilisés ont permis de suivre l'évolution de paramètres reflétant le métabolisme, les défenses antioxydantes et la morphologie cellulaire. Cette étude a notamment démontré que les GR étaient impactés précocement par le changement de leur milieu et notamment la déplétion de l'acide urique contenu dans le plasma. C'est sur la base de ces observations que diverses modifications de la composition de la solution de stockage furent ensuite proposées. L'effet de l'ajout d'acide urique avec ou sans vitamine C a ainsi été testé. Les résultats ont montré des modifications significatives au niveau du métabolisme cellulaire, suggérant un effet du traitement, mais des effets limités sur d'autres paramètres telle que l'hémolyse. Ces résultats ont soulevé la question de la dose et de l'efficacité. C'est pourquoi, la dernière partie de cette thèse fut consacrée au développement d'un test (compatible avec le criblage à haut débit) permettant d'évaluer rapidement et simplement les propriétés antioxydantes d'un large panel de composés. Ce test devrait également permettre de mieux définir la quantité de molécule à ajouter afin d'avoir un impact réel sur le vieillissement des GR dans les poches de stockage, et ainsi d'assurer un produit de qualité constante pour le patient transfusé.

ACKNOWLEDGEMENTS

ABBREVIATIONS

2,3-DPG	2,3-Diphosphoglycerate
AA	Ascorbic Acid
AAPH	2,2'-Azobis(2-amidinopropane) dihydrochloride
ABTS	2,2'-Azino-bis-(3-ethylbenzothiazoline-6-sulfonic acid)
ACD	Acid-Citrate-Dextrose
AI	Artificial Intelligence
ALD	Aldolase
AMP	Adenosine Monophosphate
AMPK	AMP-activated Kinases
AMVN	2,2'-Azobis(2,4-dimethylvaleronitrile)
AOP	Antioxidant Power
AS	Additive Solution
ATP	Adenosine Triphosphate
AUC	Area Under the Curve
BSF	Biomolecular Screening Facility
Ca^{2+}	Calcium
CAA	Cellular Antioxidant Assay
CCD	Charge-Coupled Device
CCT	Chaperonin-Containing Tailless complex polypeptide 1
CE	Counter Electrode
CHUV	Lausanne University Hospital
CMF	Cell Membrane Fluctuation
CMV	Cytomegalovirus
CO_2	Carbon Dioxide
CPA	CellProfiler Analyst
CP2D	Citrate-Phosphate-double Dextrose
CPD	Citrate-Phosphate-Dextrose
CPDA	Citrate-Phosphate-Dextrose-Adenine
Cu	Copper
CumOOH	Cumene hydroperoxide
DC	Direct Current
DCFH-DA	2',7'-Dichlorofluorescin Diacetate
dH_2O	Deionized water
DHA	Dehydroascorbic Acid
DHM	Digital Holographic Microscope or Microscopy
DIC	Disseminated Intravascular Coagulation
DTNB	5,5'-Dithio-bis-[2-nitrobenzoic acid]
EPFL	Ecole Polytechnique Fédérale de Lausanne
EPO	Erythropoietin
ESC	Embryonic Stem Cell
ET	Electron Transfer

FDP or PLYO	Freeze-Dried or Lyophilized Plasma
FDR	False Discovery Rate
Fe	Iron
Fe^{3+}	Ferric Iron
Fe^{2+}	Ferrous Iron
FFP	Fresh Frozen Plasma
FITC	Fluorescein
FLyP	French Lyophilized Plasma
FRAP	Ferric Reducing Ability of Plasma
FSC	Forward Scatter
G6PD	Glucose-6-Phosphate Dehydrogenase
GAPDH	Glyceraldehyde 3-Phosphate Dehydrogenase
GMP	Guanosine Monophosphate
GPx	Glutathione Peroxidase
GR	Glutathione Reductase
GSH	Reduced Glutathione
GSSG	Oxidized Glutathione
GVHD	Graft-Versus-Host Disease
H_2O_2	Hydrogen peroxide
HAT	Hydrogen Transfer
Hb	Hemoglobin
HBOC	Hemoglobin-Based Oxygen Carrier
HBV	Hepatitis B Virus
HCT	Hematocrit
HCV	Hepatitis C Virus
HEV	Hepatitis E Virus
HIV	Human Immunodeficiency Virus
HLA	Human Leukocyte Antigen
HPLC	High-Pressure Liquid Chromatography
HSC	Hematopoietic Stem Cell
HSP	Heat Shock Protein
HTS	High-Throughput Screening
HU	Hydroxyurea
iPSC	Induced Pluripotent Stem Cell
KI	Kinase Inhibitor
LDH	Lactate Dehydrogenase
LSV	Linear Sweep Voltammogram
MCHC	Mean Corpuscular Hemoglobin Concentration
MCV	Mean Corpuscular Volume
MDA	Malondialdehyde
MetHb	Methemoglobin
MRM	Multiple Reaction Monitoring
MS	Mass Spectrometry

MSM	Men having Sex with Men
MV	Microvesicle
N_2	Nitrogen
NAC	N-Acetylcysteine
NAD	Nicotinamide Adenine Dinucleotide
NADH	Reduced Nicotinamide Adenine Dinucleotide
NADPH	Reduced Nicotinamide Adenine Dinucleotide Phosphate
NAT	Nucleic Acid Test
NEM	*N*-Ethylmaleimide
NO	Nitric Oxide
NP	Natural Product
NTBI	Non-Transferrin Bound Iron
O_2	Oxygen
$O_2{}^{\bullet-}$	Superoxide anion
$OH^{\bullet}$	Hydroxyl radical
OPD	Optical Path Difference
OPD avg	Average of the Optical Path Difference distribution
OPL	Optical Path Length
ORAC	Oxygen Radical Absorbance Capacity
OV	Sodium Orthovanadate
OxyHb or HbO_2	Oxygenated Hemoglobin
PAGGSM	Phosphate-Adenine-Glucose-Guanosine-Saline-Mannitol
PBM	Patient Blood Management
PBS	Phosphate Buffered Saline
PC	Platelet Concentrate
PE	Phosphatidylethanolamine
PEG	Polyethylene Glycol
PFK	Phosphofructokinase
pi-FFP	Pathogen-inactivated Fresh Frozen Plasma
PKA and PKC	Protein Kinase A and C
PPP	Pentose Phosphate Pathway
Prx	Peroxiredoxin
PS	Phosphatidylserine
PTP	Protein Tyrosine Phosphatase
PTR	Post-Transfusion Recovery
PUFA	Polyunsaturated Fatty Acid
PVDF	Polyvinylidene Fluoride
pY	Tyrosine-phosphorylation
q-FFP	Quarantine Fresh Frozen Plasma
QPM	Quantitative Phase Microscopy
RBC	Red Blood Cell
RCC	Red Cell Concentrate
RE	Reference Electrode

RES	Reticuloendothelial System
ROS	Reactive Oxygen Species
RT	Room Temperature
S	Serine
SAGM	Saline-Adenine-Glucose-Mannitol
SAM	S-Adenosylmethionine
SCD	Sickle Cell Disease
SD	Standard Deviation
SD-OPD	Standard Deviation of Optical Path Difference
SD-RDW	Standard Deviation of Red Blood Cell Distribution Width
SOD	Superoxide Dismutase
SPE	Screen-Printed Electrodes
SSC	Side Scatter
T	Threonine
TCA	Tricarboxylic Acid
TIR	Transfusion Interrégionale CRS SA
TNB	5-Thio-2-nitrobenzoic Acid
TRALI	Transfusion-Related Acute Lung Injury
Trx	Thioredoxin
TrxR	Thioredoxin Reductase
TSOX	Test of Sensitivity to OXidation
TTP	Thrombotic Thrombocytopenic Purpura
UA	Uric Acid
UPLC	Ultra-Performance Liquid Chromatography
WB	Western Blot
WE	Working Electrode
wFWB	Warm Fresh Whole Blood
WHO	World Health Organization
WNV	West Nile Virus
XO	Xanthine Oxidase
Y	Tyrosine

INTRODUCTION

THE PRESENT AND FUTURE OF TRANSFUSION

Blood transfusion consists in administrating a labile blood product by venous route. It is a life-saving procedure which required, in 2018 and in Switzerland alone, 221'100 Red Cell Concentrates (RCCs), 38'947 Platelet Concentrates (PCs) and 30'552 Fresh Frozen Plasma (FFP) units[1]. Worldwide, around 117.4 million blood donations are collected every year, according to the World Health Organization WHO)[2].

Types of blood products and indications

Two different procedures exist for blood collection, *i.e.* whole blood donation or apheresis (plasmapheresis, thrombocytapheresis, erythrocytapheresis, or combined apheresis). Various labile blood products, *i.e.* RCCs or suspensions, PCs and plasma (*e.g.* FFP units), can be prepared from human whole blood, with differences between countries. It should be emphasized that, in Switzerland since 1999, every standard blood preparation is leuko-depleted and subjected to at least the following tests: anti-HIV (Human Immunodeficiency Virus) and HIV-NAT (Nucleic Acid Test), anti-HCV (Hepatitis C Virus) and HCV-NAT, HBV (Hepatitis B Virus) antigen and HBV-NAT, anti-treponema pallidum, and blood group (ABO/Rhesus D) determination[3]. Each labile blood product has specific storage conditions and given indications[4].

Transfusion of Red Blood Cells (RBCs) is indicated for patients suffering from insufficient oxygen (O_2) delivery to organs and tissues. Anemia can be caused by acute or chronic blood loss (*e.g.* trauma or surgery), deficiency in RBC production (*e.g.* defects in erythropoiesis due to a lack of folate, iron or Erythropoietin [EPO] hormone), cancer (the co-morbidities, the cancer itself or the treatment)[5], or RBC destruction (*e.g.* in Sickle Cell Disease [SCD]). In some cases, massive or exchange blood transfusion is also a means to reduce the incidence of damaged cells in circulation by diluting the endogenous RBCs or repressing the patient erythropoiesis[6–8]. RCCs are stored between 2 and 6°C (which limits bacterial growth), for up to 6 or 7 weeks, depending on the additive solution used (*e.g.* 42 days in Saline-Adenine-Glucose-Mannitol [SAGM], or 49 days in Phosphate-Adenine-Glucose-Guanosine-Saline-Mannitol [PAGGSM]). Cryopreservation of RBCs is also used in specific circumstances, for example to maintain an inventory of rare RBC units[9].

Platelets are used to prevent (prophylactic) or treat (therapeutic) bleeding due to thrombocytopenia or a platelet function defect, *e.g.* in patients having a hemato-oncological disease, or undergoing major cardiovascular surgery. The PCs are either produced from a pool of buffy coat (multiple donors), or from an apheresis procedure (single-donor). They can be kept during 5 to 7 days at room temperature (20 to 24°C) under gentle agitation[10]. To reduce the risks associated with bacterial or unknown/unscreened pathogen contamination, blood banks have different pathogen inactivation technologies at their disposal, such as the INTERCEPT™ system (Cerus Corporation), which takes advantage of amotosalen and UVA radiation to induce cross-linking of nucleic acids; the

Mirasol® system (Terumo BCT), which uses riboflavin, a photosensitizer, to generate Reactive Oxygen Species (ROS) upon UV illumination, or the THERAFLEX® UV-Platelets system (Macopharma), which uses only UVC light[11]. Different products are currently under development, such as the cryopreserved, thermocycled, or dried platelets. Storing the platelets at 4°C could also become a valuable alternative. Indeed, in addition to being less prone to contamination and to potentially having a longer shelf life, such platelets were shown to retain a more acute capacity for hemostasis, and are therefore particularly indicated in emergency situations[12]. Cold-stored platelets, however, have a shorter time of recirculation, which makes them less interesting for prophylaxis, *e.g.* in hemato-oncology. Therefore, why not take a step towards personalized medicine by giving products most suited to each situation rather than simply continuing to apply the current "one-size-fits-all" approach?[13].

The third labile blood product available for transfusion is the plasma, kept for example as a quarantine plasma (q-FFP), during a minimum of 4 months after blood donation, or pathogen inactivated (pi-FFP), as such or as a pool of 1 to 6 buffy coats. The FFP can be conserved at -30°C for 2 years maximum. A commercial product (OctaplasLG®, Octapharma) produced by pooling 380 to 1500 L of plasma inactivated by solvent/detergent treatment, is also available on the Swiss market. Plasma is transfused in case of coagulation defects subsequent to, *e.g.* 1) liver disease, 2) anticoagulant (warfarin) overdoses, 3) depletion of coagulation factors associated for example with large volume transfusions, 4) Disseminated Intravascular Coagulation (DIC), 5) Thrombotic Thrombocytopenic Purpura (TTP), or 6) plasma exchange during pregnancy. Freeze-Dried or Lyophilized Plasma (FDP or PLYO), such as the licensed and FDA approved French Lyophilized Plasma (FLyP)[14], represents an alternative to the FFP for the rapid management of trauma as it reduces the administration time (does not need to be unfrozen), and resolves key logistic issues, such as preservation temperature and time)[15]. FDP is mainly used by the army, though it can also be valuable in crisis situations such as terrorist attacks or natural disasters, and in case of geographic remoteness. The various plasma preparations have an influence on coagulation factors with more or less clinical impact[16]. Similarly, transfusion of warm Fresh Whole Blood (wFWB), which can be stored for 6 hours between 20 and 24°C, is frequently performed during military operations.

Whole blood transfusions are also a standard in low-income countries where only 50 % of the blood is separated into components as compared to 97 % in high-income countries. This product, which is indicated in case of massive transfusion or hemorrhagic shock, could replace the stored component therapy where whole blood is reconstituted from individual components, *i.e.* 1 RCC: 1 FFP: 1 PC, reducing the quantity of anticoagulant and additive solutions transfused to patients[17]. Whole blood can be stored for 21 days in Citrate-Phosphate-Dextrose (CPD) or Citrate-Phosphate-

double Dextrose (CP2D), or for 35 days in Citrate-Phosphate-Dextrose-Adenine 1 (CPDA-1), between 1 to 6°C[18].

The near future of transfusion is not the same throughout the world

Ideally, transfusions should be able to meet all demand, with blood donated by voluntary unpaid donors, providing only what is necessary, and offering an excellent quality, perfectly compatible and completely safe. Numerous obstacles are still barring the way to reach this goal, and the amount of work that remains to be done is not the same in different countries around the world[19]. Indeed, the WHO reported that, in 2015, only 45 % of low-income countries had a national blood policy as compared to 79 % for high-income nations, with a blood donation rate of 4.4 donations for 1'000 people against 32.6, rendering the access to blood difficult, and a screening rate of only 76.2 % in comparison to 99.9 %, considerably increasing the prevalence of transfusion-transmitted infections, *i.e.* HIV, HBV, HCV and syphilis. Today, even applications of blood products are different: in low-income countries, 52 % of transfusions are performed on children under 5 after complications related to pregnancy, and to treat childhood anemia, which is often related to malaria and SCD. In contrast, blood products in high-income countries are mostly used for supportive care, and primarily (in 75 % of cases) for patients over 65 years old. The near future of transfusion in low-income regions will therefore be to build the necessary infrastructure, to find the most appropriate procedures (e.g. pathogen inactivation of whole blood), and spread the knowledge required for a more effective access to safer blood products.

Instead, the current trend is to reduce blood utilization in wealthier regions of the world. Patient Blood Management (PBM) initiatives are implemented by many hospitals to rationalize the use of labile blood products to limit costs, but also to decrease residual or unknown risks associated with transfusions of human blood products. This goal can be reached by: 1) an efficient diagnostic of iron deficiency and anemia, with corrective measures such as supplementation of iron, EPO, ferric carboxymaltose, folic acid and/or vitamin B12 before elective surgeries; 2) limiting blood losses during hospitalization (reduction in the volume of blood samples taken for biological analyses), or during surgeries including less invasive techniques, *i.e.* optimization of the patient position, temperature and pressure, administration of tranexamic acid (fibrine analog that blocks the fibrinolysis and reduces bleeding), or *via* the use of cell salvage devices; 3) optimizing the management of post-operative anemia, and implementing more restrictive blood transfusion policies, based on the evaluation of clinical criteria instead of the Hemoglobin (Hb) level only[20]. Realizing this ambitious plan will require substantial and continuous improvements in the expertise, techniques and equipment used in the field of transfusion.

Changing needs and evolving threats in the future of transfusion

Transfusion will have to adapt to a world in constant evolution. Indeed, demographic changes such as global population growth and aging are expected to increase the demand for blood products. In 2016, Volken *et al.* predicted a shortage of up to 77'000 RCCs by 2035 in Switzerland alone[21]. Advances made in the medical field also play a role in this issue[22]: some of the diseases that were acute and uncurable in the past have now become chronic, and will therefore require frequent transfusions. Today, only 2.8 % of the Swiss population is donating blood, whereas 80 % will need some blood product at least once in their life[23]. The maintenance and renewal of the pools of donors are thus a daily challenge which requires to rethink, modernize and adapt recruitment models to target people of different ages and cultures. The use of less restrictive blood donation deferral policies (*e.g.* for Men having Sex with Men [MSM], people who came back from a trip, or received a transfusion once in their life) could also be an option, provided that security is guaranteed for both the donor and the transfused patient. In such cases, improvements in the sensitivity and specificity of screening tests and the implementation of global pathogen inactivation procedures could play a major role in balancing risks and benefits.

In addition, current and upcoming migration crises (political, economic and/or environmental) lead to further complications. In particular, intra-ethnic transfusions are complicated as the HLA (Human Leukocyte Antigen) diversity correlates with geography. It is especially problematic for patients needing chronic transfusion (*e.g.* SCD patients), for whom a systemic match for Rh (C,E,c,e) and K is required to avoid the risks of alloimmunization as much as possible.

The field of transfusion is also under pressure due to the emergence of new pathogens, as well as the outbreak and spread of epidemics. Such events are becoming more likely due to climate change, mass agriculture, deforestation and evolving travel habits. Emerging diseases require to adapt screening tests on a regular basis to stay one step ahead and avoid crises. Today, the selective screening of Malaria, Chagas, and of the West Nile Virus (WNV) has already been implemented at Transfusion Interrégionale CRS SA (TIR), and is ready to be deployed on a larger scale if needed. Improvements in pathogen inactivation technologies and their applications to RBCs and whole blood could also help reduce the threat. Phase III clinical trials were recently completed for the INTERCEPT™ S-303 system as well as for the Mirasol® system for pathogen inactivation in RCCs and whole blood[24].

Nevertheless, questions remain regarding the safety and efficiency of pathogen inactivated blood products, and the associated costs. As far as safety is concerned, will it require to still perform all screening tests to reduce costs once pathogen inactivation is implemented? As for efficiency, is an inactivated product equivalent a standard one?

Research and innovation at the service of transfusion

Research and innovation are key to better understand current issues, to develop new tools in the field of transfusion, and, hence, to look at the future with more confidence and optimism despite potential threats. New discoveries also contribute to the improvement of current practices. A good example is the development of personalized medicine: for example, one could imagine to select donors with the "best" characteristics (knowing that great biological variability exists), and apply the "best" preparation processes and storage conditions, to obtain the "best" product at the "best" time, in order to match the "best" specific needs of each patient[25].

To get rid of biological variability and of blood products shortages, artificial blood substitutes are currently explored, such as the Hb-Based Oxygen Carriers (HBOCs). However, the different clinical trials conducted up to 2008 failed as these substances were shown to interact with endogenous Nitric Oxide (NO), triggering unwanted side effects. Today, efforts are made to improve the design of HBOCs (*e.g.* by adding Polyethylene Glycol [PEG] chains to Hb)[26]. However, such products will not be available on the market soon[27].

Another innovation serving similar purposes is the *in vitro* culture at large scale of RBCs. Several research teams are currently working on it, such as the group of Professor Luc Douay and EryPharm,[28] and a team at the Sanquin Research and Landsteiner Laboratory[29,30]. Cultured RBCs can be produced from different sources of stem cells, *i.e.* Hematopoietic Stem Cells (HSCs), Embryonic Stem Cells (ESCs), or induced Pluripotent Stem Cells (iPSCs). Presumably, the preferred one will be immortalized iPSCs selected to present the most universal blood group possible, thus providing blood products adapted to most needs. Moreover, cultured RBCs could allow us to get rid of the risks of transfusion-related pathogen transmission, to become independent of the donor blood source. Currently, a proof of concept for this approach has been demonstrated. The next goal will be to upscale the production in larger bioreactors.

State of the art of red blood cell storage lesions. Why do we need to optimize storage conditions?

As above-mentioned innovations are unlikely to become available in the near future, "traditional" blood donation remains relevant. Moreover, once fully developed and authorized for marketing, the prices of more innovating products could remain prohibitively high. For example, Prof. Luc Douay and his team expect the cost of a single cultured RBC unit to reach about USD 3'000 (in case of routine implementation), which is not much for rare blood groups, but completely unpractical for routine applications[31].

This is why optimizing the storage of blood products is a key part of the transfusion problematics. Good storage is simply essential as the quality of blood products unavoidably decreases over time in blood banks. Degradation can reduce the efficiency of treatments, and possibly be detrimental to transfused patients.

The next sections detail the changes that generically appear in RBCs during storage under standard blood bank conditions, *i.e.* storage at 4°C in additive solutions for 6 to 7 weeks[32].

Effects of storage on red blood cell metabolism

Non-physiological storage conditions lead to a profound remodeling of the RBC metabolism (Figure 1). First, because hypothermia modifies metabolic fluxes by reducing reaction rates[33]. Second, because bags in which RBCs are placed with an additive solution is equivalent to a quasi-closed environment (only gas exchanges), in which nutrients are progressively consumed and possibly depleted, while waste products accumulate inside the cells and in the supernatant.

The low pH of additive solutions together with the acidification of RCC supernatant subsequent to lactate accumulation (glycolysis end-product) induce a negative feedback for enzymatic activity[34]: key metabolites are progressively lost, such as: 1) the O_2-Hb affinity regulator 2,3-Diphosphoglycerate (2,3-DPG), which is depleted after 2 weeks of storage[35]; 2) the reduced Nicotinamide Adenine Dinucleotide (NADH), an essential redox cofactor which is either produced by Glyceraldehyde 3-Phosphate Dehydrogenase (GAPDH) in glycolysis, or from malate by malate dehydrogenase; and finally 3) the Adenosine Triphosphate (ATP), which mediates all metabolic pathways outside glycolysis and protein activity. Moreover, metabolic remodeling can also be triggered by different salvage mechanisms activated by the accumulation of storage lesions. Instead of a monotonic decay, the RBC metabolism exhibits three distinct phases during storage, at 0-10 days, 10-18 days, and after 18 days. This metabolic signature was first identified by Bordbar *et al.* from the analysis with system biology methods of quantitative metabolomics data measured in RCCs stored in SAGM[36,37]. The same trend was observed in other additive solutions such as Additive Solution Formula 3 (AS-3)[38].
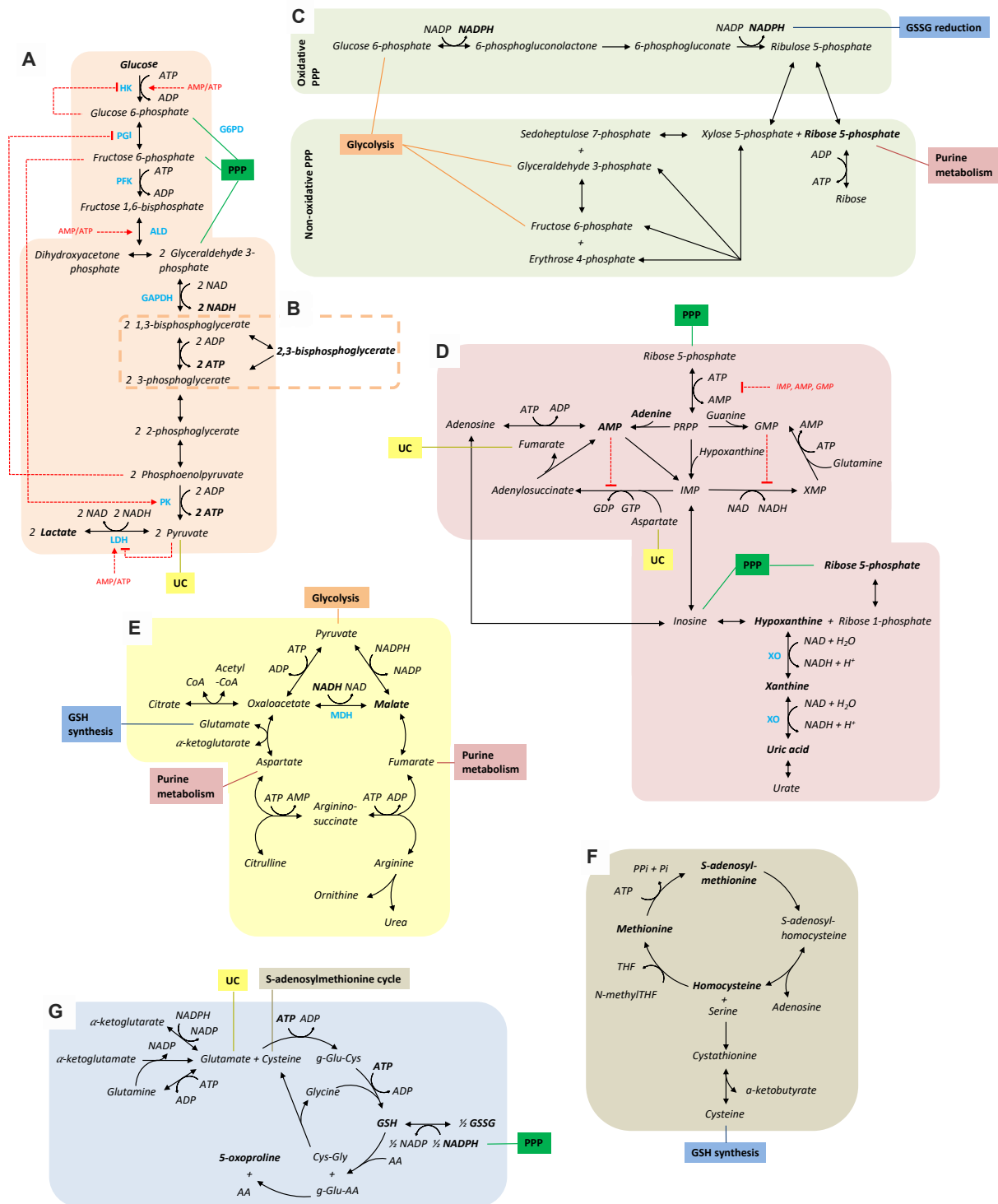
Figure 1 – **Simplified view of the metabolic pathways in red blood cells (RBCs) related to energy and redox metabolisms**. [A] Glycolysis, [B] Rapoport-Luebering cycle, [C] Pentose Phosphate Pathway (PPP), [D] purine and GMP (Guanosine Monophosphate) metabolism , [E] urea cycle and remnants of Krebs cycle, [F] SAM cycle (S-Adenosylmethionine), [G] GSH (reduced Glutathione) synthesis and GSSG (oxidized Glutathione) recycling.

The first phase is characterized by an increase of ATP production, likely due to the excess of glucose supplemented in SAGM which boosts glycolysis. Anaerobic glycolysis is the main source of ATP (90 %) in RBCs, as these cells do not contain mitochondria. Phase 1 is also characterized by an extensive use of adenine by the purine metabolism, and by the consumption of methionine in the S-Adenosylmethionine Cycle (SAM) that forms the homocysteine. This metabolite enters in the synthesis of reduced Glutathione (GSH), still active at this stage (glutathione pool increases). In addition, methionine was shown to be consumed for the methylation of oxidized isoaspartate moieties in asparagine/aspartate residues, and thus contributes to the repair of oxidatively damaged proteins[39]. Next, due to rising oxidative burden, the Pentose Phosphate Pathway (PPP) that takes over glycolysis, during the second metabolic phase, tries to restore the cellular redox balance. The metabolism of the RBCs was also shown to be modulated by the levels of Oxygenated-Hb (OxyHb or HbO_2), which increase during storage due to 2,3-DPG depletion[40].
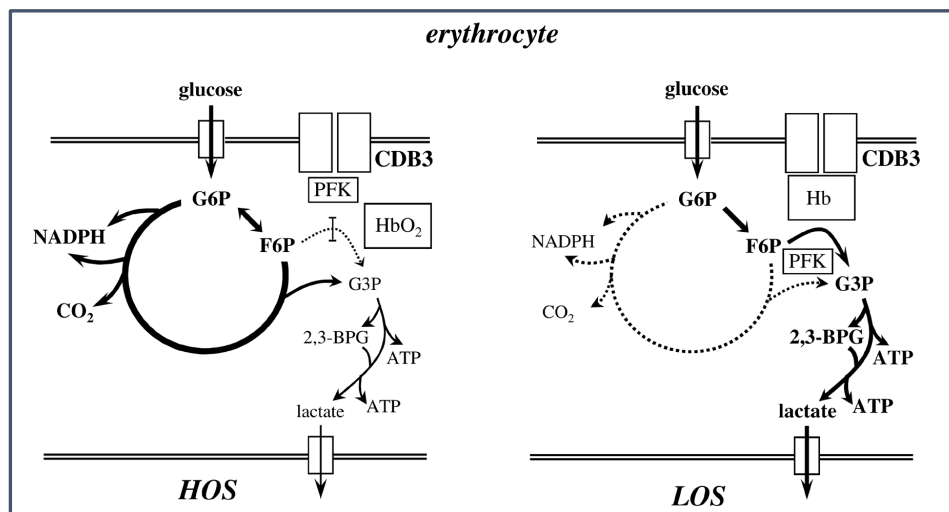
Figure 2 – **Oxygen (O_2)-linked modulation of the red blood cell (erythrocyte) metabolism.** Taken from Castagnola et al.[41]. HOS: high-oxygenation state, LOS: low-oxygenation state, CDB3: band 3, PFK: phosphofructokinase, Hb: hemoglobin.

Indeed, as shown in Figure 2, in high oxygenation state, HbO_2 is released from the N-terminal cytoplasmic domain Band 3, which becomes free to bind and thus inhibits different glycolytic enzymes, *i.e.* the Aldolase (ALD), GAPDH, Phosphofructokinase (PFK) and Lactate Dehydrogenase (LDH)[41,42]. Sugars are thus shifted towards the PPP (about two times more active in high oxygenation state[41]), promoting the production of reduced Nicotinamide Adenine Dinucleotide Phosphate (NADPH, light green boxes in Figure 1), which is necessary for recycling oxidized Glutathione (GSSG) into its reduced form (GSH). Finally, the last metabolic phase is characterized by the release of hypoxanthine, when purine bases are not recycled anymore. The Adenosine Monophosphate (AMP) metabolism in which glycolysis intermediates are shuttled in phase 2 is inhibited, and AMP is catabolized into adenosine and ribose phosphate sugar as a last effort to support glycolysis.

In conclusion, the metabolic alterations trigger and accelerate a cascade of lesions incurred to RBCs during storage. For example, the reduction of ATP levels (a predictor of *in vivo* recovery of RBCs[43]) impairs many key processes, such as the *de* novo synthesis of GSH (blue box in Figure 1) and the recycling of antioxidants, the maintenance of the ion homeostasis (the Na^+/K^+ and the Ca^{2+} pumps that are ATP-dependent), and membrane phospholipids asymmetry, leading to modifications of the cell morphology and deformability. This suggests that metabolic signatures could provide an estimation of the state of RBCs which is more sensitive and precise than with classical hematologic analyses. In this vein, Paglia *et al.*[44] proposed 8 biomarkers, *i.e.* the extracellular levels of lactic acid, nicotinamide, 5-oxoproline, xanthine, hypoxanthine, glucose, malic acid, and adenine, which enable to differentiate the 3 metabolic phases in SAGM as well as in AS-3, and therefore to estimate the metabolic age of stored RBCs. In the future, *in silico* modeling of dynamic metabolic fluxes using omics and system biology will help better understand the *ex vivo* aging of RBCs, providing tools to predict the effects of modified storage conditions more accurately[45,46].

Accumulation of oxidative lesions during storage

To be fully functional, the antioxidant protective system requires energy, and is therefore negatively impacted by the depletion of key cofactors (ATP, NADPH, NADH) associated with storage-related metabolic dysregulation. In addition, O_2 saturation increases with storage duration, reaching 95 to 100 % after three weeks of storage. This leads to ROS accumulation reaching a plateau in the same timeframe[47]. Consequently, oxidative forces begin to overwhelm the antioxidant system, leading to a state defined as oxidative stress. The following model (Figure 3) was proposed by Dr Julien Delobel to describe the pathway and consequences of oxidative stress in stored RBCs[48].
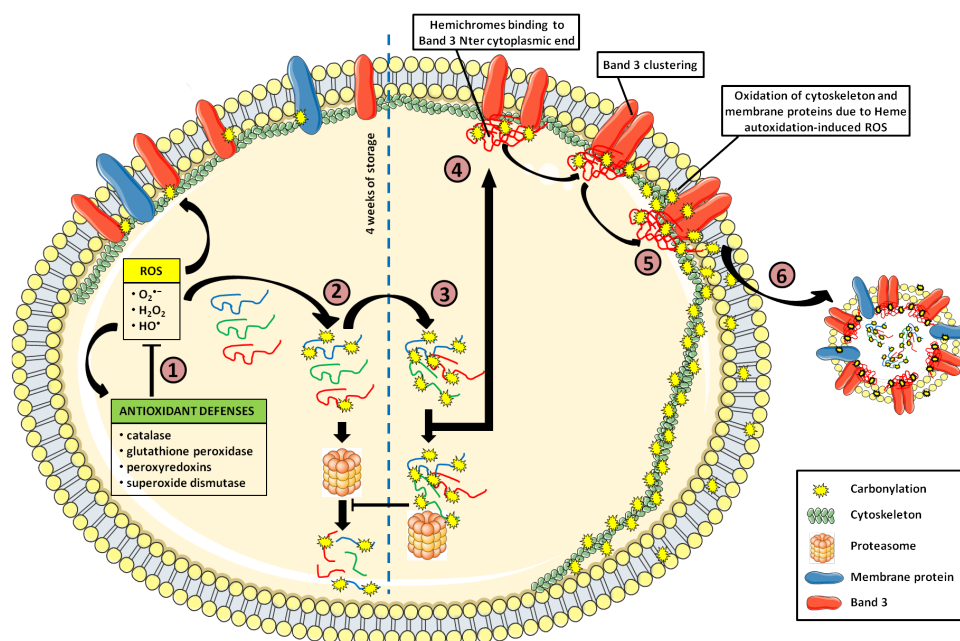
*Figure 3 – **Protein carbonylation pathway in the RBCs during storage**. Reproduced from the PhD thesis of Dr Julien Delobel.*

Under physiologic conditions, exogenous and endogenous ROS are reduced by RBC antioxidant defenses (phase 1 in Figure 3). However, during storage, the declining metabolism fails to replenish essential cofactors, and is thus directly associated with the exhaustion of the antioxidant protective system. Specifically, the rapid decline of ATP concentration impairs the *de novo* synthesis of GSH, representing 90 % of the RBC non-enzymatic reducing system. Indeed, ATP is necessary for: 1) the uptake of GSH precursors glutamine, glutamate, cysteine and glycine through Na^+-dependent carriers, and 2) GSH synthesis, which is catalyzed by ATP-dependent glutamate cysteine ligase and GSH synthetase. Whillier *et al.* and Dumaswala *et al.* reported that 27 ± 6.5 % and 26 % of GSH was lost after 6 weeks of storage in leukoreduced SAGM and AS-1 units, respectively[49,50]. After 10 days of storage, the metabolism shifts from anaerobic glycolysis towards PPP. Such metabolic reprogramming depends directly on oxidative stress, as shown by Rinalducci *et al.* and Reisz *et al.*[51,52]. The latter demonstrated that oxidative modification of redox-sensitive amino acid in the glycolytic enzyme GAPDH promoted its association with Band 3, leading to its inactivation. This bottleneck in glycolysis in turns promotes PPP to replenish the NADPH pool, which is necessary for recycling GSSG into GSH. This compensatory mechanism, however, does not suffice to fully protect the cell against the rising oxidative burden, and to compensate the reduction of glutathione anabolism. Moreover, glycolysis slowdown negatively impacts on the NADH pool, a co-factor required for methemoglobin (metHb) reduction back to OxyHb by the NADH-dependent cytochrome b_5 metHb reductase. This ferric form of Hb is unable to bind O_2 and is rapidly degraded in reversible and irreversible hemichromes, and finally in globin and haemin. These compounds can participate in the Fenton reaction, further accelerating the accumulation of oxidative stress. Consequently, ROS progressively accumulate in stored RBCs, reaching a maximal plateau values after 21 weeks of storage, as shown by D'Alessandro *et al.*[47].

As storage goes on, the balance between the antioxidant defenses and the ROS is progressively lost (phase 2). Consequently, the extent of irreversible damages to the cellular components increases: lipids peroxidation markers, such as the 8-isoprostane or Malondialdehyde (MDA), increase during storage[47,53,54]. Fu *et al.* also highlighted the accumulation of Polyunsaturated Fatty Acids (PUFA) and their oxidation products oxylipins in RCC supernatants[55]. Similarly, the level of protein carbonylation, an hallmark of protein oxidation, was shown to increase in membrane and cytoskeletal proteins[48,56–59]. Generation of advanced glycation end-products mediated by ROS was also reported[60].

Normally, irreversibly oxidized membrane and cytosolic proteins are degraded by the 20S proteasome[59]. Other chaperone proteins, such as the Heat Shock Proteins (HSP) 70, HSP 90, and Chaperonin-Containing Tailless complex polypeptide 1 (CCT), combine with misfolded or aggregated proteins[61]. This defense system, however, can be altered after 4 weeks of storage[48] (phase 3). A

possible explanation could be the following: 1) an extensive cross-linking of over-oxidized proteins could inhibit the proteasome; 2) damaged proteins, such as Hb[56] or Peroxiredoxin 2 (Prx 2)[62], are recruited at the cell membrane, and thus become less accessible; and 3) the activity of numerous enzymes of the repair/elimination systems requires ATP.

When the oxidative stress becomes excessive, RBCs begin to lose their functionality and integrity. In fact, the progressive accumulation of hemichromes at the membrane was shown to induce band 3 clustering[63] (phase 4), which constitutes a known eryptosis signal[64]. Autoxidation of the heme close to the membrane further accelerates the oxidation of membrane proteins (phase 5), leading to cytoskeletal alterations that impact RBC rheology and causes modifications, *i.e.* oxidation of the CD47 marker, rendering RBCs prone to clearance *in vivo*. Ultimately, Microvesicles (MVs) containing damaged material (such as the carbonylated proteins, which have irreversible post-translational modifications) are released as a self-protective mechanism (phase 6)[65–67]. Delobel *et al.* demonstrated that the carbonylation content decreases in the integral membrane fraction between the days 29 and 43 of storage, whereas it increases with the same order of magnitude in the RBC-derived MVs[48].

Alterations of red blood cell rheological properties

Following the accumulation of lesions, RBC rheological properties, defined by their morphology and capacity for deformation, are modified. A main cause is the irreversible membrane loss subsequent to the release of vesicles, which was previously shown to constitute a protective mechanism to shed oxidized cellular elements. The analysis of the content of vesicles isolated in RCC units showed aggregates of Hb, degraded or dimerized band 3, lipid rafts proteins, Fas, FADD, pro-caspases 3 and 8, and their cleavage products, CD47, IgG and stomatin[66–68]. RBC-derived vesicles are also produced when the interactions between the cytoskeleton and the membrane are disturbed and/or when the lipid membrane asymmetry is lost, which occurs when the cation homeostasis is lost due to ATP depletion. Indeed, the phospholipid bilayer organization, *i.e.* maintenance of negatively charged Phosphatidylserine (PS) and Phosphatidylethanolamine (PE) in the inner side of the cell membrane, is controlled by the activity of the flippase enzyme (a translocase), which is inhibited when the Ca^{2+} concentration increases[69]. The excess of Ca^{2+} also impacts a broad range of other processes[70]: 1) it triggers the Gardos effect, which corresponds to an efflux of K^+ induced by the opening of the Ca^{2+}-dependent K^+ Gardos channels, and results in extracellular K^+ accumulation and cell dehydration; 2) Ca^{2+} activates proteins kinases, such as the Protein Kinase C and A (PKC, PKA) and AMP-activated Kinases (AMPK), leading to changes in phosphorylation levels; and 3) Ca^{2+} promotes proteolytic enzymes such as the μ-calpain proteases, which were shown to degrade the ankyrin, band 3, protein 4.1, adducin and dematin; all part of the cytoskeleton-membrane junction protein complexes[71].

Interestingly, calpain-1 knockout mouse RBCs did not exhibited Ca^{2+}-induced sphero-echinocytic transition[72].

Long-term stored RBCs exhibit changes in cell morphology and increased cell rigidity[73–76]. Blasi *et al.* showed that 50.2 % of the RBCs exhibit reversible (echinocytes and stomatocytes) and irreversible (sphero-echinocytes, sphero-stomatocytes and spherocytes) morphological changes after 21 days of storage, and that the proportion of non-discocytes RBCs reached 77.1 % at day 42[77]. More recently, Roussel *et al.* demonstrated that in addition to morphological changes, stored RBCs exhibit a decrease in projected surface area after 28 days of storage, which makes them prone to splenic retention[78]. The RBC shape and deformability can be influenced by 1) the release of vesicles that reduces the membrane surface-to-volume ratio, 2) the osmolarity and ion homeostasis, and 3) the interactions between the membrane and cytoskeleton[79,80]. Deformability is an essential characteristic for the RBCs, as they need to pass through small capillaries to efficiently deliver O_2 to peripheral organs/tissues[79,81–83]. Hence, RBCs that are poorly deformable (*i.e.* lost more than 18 % of surface area[84] and/or express senescent markers, such as modified band 3 conformation, increased externalized PS or reduced CD47 levels) are retained by macrophages in the recipient Reticuloendothelial System (RES)[85]. Ultimately, extensively damaged RBCs can lyse in the blood bag, releasing their cytosolic content.

New routes and additive solution formulations to improve the storage quality of red blood cells

Different cost-effective approaches are currently studied to deal with storage-associated damages:

First, rejuvenation consists in incubating the RBCs during 1 hour at 37°C in a solution composed of sodium pyruvate, inosine, adenine, mono- and dibasic sodium phosphate (*i.e.* rejuvesol™ from CitraLabs, the only FDA approved rejuvenation solution). It reactivates the RBC metabolism and restores the 2,3-DPG and ATP levels post-storage. However, this does not repair irreversible lesions, which increase with storage duration[86–89].

Second, the reduction in the O_2 in blood bags: it has been shown that reducing the O_2 saturation level below 20 % generally helps maintain ATP and 2,3-DPG levels, reducing the percentage of hemolysis[90] and the deterioration of mechanical properties[91]. Moreover, oxygenation reduction enhances the uniformity between RCC units[90]. Total depletion of O_2 is not desirable, as it impairs the O_2-dependent metabolic shift towards PPP which generates the electron carrier NADPH necessary for the replenishment/recycling of GSH.

The third solution is the modification of storage solutions[92]. Indeed, SAGM (mostly used in Europe) and AS-1 (Adsol from Baxter, mostly used in the USA) were introduced in the 1970s and are still used today. Since then, slightly different formulations have been proposed and licensed, such as

the PAGGSM (from MacoPharma), AS-3 (Nutricel from Pall Medical) and AS-5 (Optisol from Terumo). Subsequently, solutions based on the concept of "chloride shift" were also developed. The idea was to replace extracellular chloride anion by citrate or gluconate anions, which cannot enter the cell, to have an alkaline solution instead of acidic one. As a result, the internal chloride that leaks because of the Donnan membrane equilibrium is replaced by hydroxyl ions, resulting in an increased intracellular pH and therefore in a better maintenance of ATP and 2,3-DPG levels. Based on this concept, the AS-7 (commercialized under the name SOLX® by Haemonetics Corporation) was developed by Hess and Greenwalt[93], the E-sol 5 by Högmann *et al.*[94], the PAGGGM by Korte *et al*[95]. Finally, one could imagine shortening the RCC shelf life. A threshold set at 28 days, for example, would reduce the risks associated with storage time. This approach would require to rethink the stocks management, which may be feasible judging by the case of the PCs[96].

OBJECTIVES OF THIS PHD THESIS

The main objective of this research conducted at the "Laboratoire de Recherche sur les Produits Sanguins (LRPS)" from TIR was to find new ways to improve the storage of RBCs by simple and cost-effective means, to offer a product of higher quality to transfused patients. Specifically, the focus was on the addition of molecules that a) could limit the metabolic shift associated with the RCC preparation procedure, and b) could have antioxidant properties, to better protect RBCs against oxidative-related storage lesions. To achieve these goals, a better characterization of storage lesions in RCCs was required.

The first chapter of this thesis is devoted to the characterization and quantification of storage lesions (metabolic, oxidative and morphological). With this aim, routine and newly developed methods were used to pinpoint the hallmarks of RBC storage lesions in blood bags. RBC microvesiculation and the percentage of hemolysis and hematological parameters were evaluated. Oxidative stress was determined by measuring the total Antioxidant Power (AOP) and the ratio of intracellular reduced/oxidized glutathione. Extracellular glucose and lactate concentrations, which reflect RBC metabolic activity, were quantified. Morphological changes, as well as membrane fluctuations, were recorded using a label-free Digital Holographic Microscope (DHM)[97,98]. The impact of storage on membrane protein Tyrosine-phosphorylation (pY) during aging was also investigated[99].

In the second chapter, the focus moves to the evolution of AOP in RCCs from donation to transfusion[100]. Indeed, the lesions from which the RBCs suffers during cold storage depend in part on their ability to counterbalance oxidative stress by activating their antioxidant defenses. An improved understanding of AOP evolution and the identification of underlying causes was therefore necessary to implement corrective strategies.

The third chapter addresses the modification of the additive solution formulation *per se* based on Chapter 2 and the literature. A first strategy simply consisted to add Uric Acid (UA, whose level was shown to be closely correlated to the AOP), or UA plus Ascorbic Acid (AA) at physiological levels to prevent a potential metabolic shift, as well as a drop of AOP subsequent to the RCC preparation. Indeed, the replacement of plasma by an additive solution drastically reduces the concentration of endogenous antioxidant molecules. A second approach was to add exogenous molecules in order to increase the basal load of antioxidant protection, either by replenishing the endogenous antioxidant pool (*e.g.* the N-Acetylcysteine [NAC] that promotes *de novo* synthesis of GSH[101]), or taking advantage of their direct antioxidant effect. Molecules with known effects against oxidative stress in SCD were tested[102].

Finally, the fourth chapter presents preliminary data obtained during the development of the TSOX, namely, "Test of Sensitivity to OXidation". This assay aims at evaluating the susceptibility of

RBCs to oxidative stress, and will thus be useful to monitor their antioxidant defense system (*e.g.* during storage or in other conditions). In particular, it could provide a tool for high-throughput screening and evaluation (EC_{50}, cytotoxicity, mechanism of action, etc.) of potential protective molecules against oxidative stress.

Based on the characterization of RBCs at the cellular and molecular level, and on investigations of chemical additives, this thesis brings new knowledge about RBC aging within RCCs, offering potential opportunities to rethink RBC storage.

REFERENCES

1.   Chiffres 2018: don de sang - rapport annuel 2018. Transfusion CRS Suisse Available at: https://rapportannuel2018.transfusion.ch/chiffres/.

2.   Blood safety and availability. World Health Organization. Available at https://www.who.int/news-room/fact-sheets/detail/blood-safety-and-availability.

3.   Préparations Sanguines. Transfusion CRS Suisse. Available at: https://www.blutspende.ch/fr/medecine/medecine_transfusionnelle/preparations_sanguines.

4.   The Clinical Use of Blood. Handbook. World Health Organization. Available at: https://www.who.int/bloodsafety/clinical_use/en/Handbook_EN.pdf.

5.   Dicato M, Plawny L, Diederich M. Anemia in cancer. *Ann. Oncol.* 2010;21(suppl_7):vii167–vii172.

6.   Francis RO, Spitalnik SL. Red blood cell components: Meeting the quantitative and qualitative transfusion needs. *Presse Médicale*. 2016;45(7–8):e281–e288.

7.   Klein AA, Arnold P, Bingham RM, et al. AAGBI guidelines: the use of blood components and their alternatives 2016. *Anaesthesia*. 2016;71(7):829–842.

8.   1 RBC Concentrates. *Transfus. Med. Hemotherapy*. 2009;36(6):362–370.

9.   Lagerberg JW. Cryopreservation of Red Blood Cells. *Cryopreserv. Free.-Dry. Protoc.* 2015;1257:353–367.

10.   Holbro A, Infanti L, Sigle J, Buser A. Platelet transfusion: basic aspects. *Swiss Med. Wkly.* 2013;143(4950).

11.   Schlenke P. Pathogen Inactivation Technologies for Cellular Blood Components: an Update. *Transfus. Med. Hemotherapy*. 2014;41(4):309–325.

12.   Stubbs JR, Tran SA, Emery RL, et al. Cold platelets for trauma-associated bleeding: regulatory approval, accreditation approval, and practice implementation—just the "tip of the iceberg." *Transfusion*. 2017;57(12):2836–2844.

13.   Cap AP. Platelet storage: a license to chill!: EDITORIAL. *Transfusion*. 2016;56(1):13–16.

14.   Garrigue D, Godier A, Glacet A, et al. French lyophilized plasma versus fresh frozen plasma for the initial management of trauma-induced coagulopathy: a randomized open-label trial. *J. Thromb. Haemost. JTH*. 2018;16(3):481–489.

15.   Buckley L, Gonzales R. Challenges to producing novel therapies – dried plasma for use in trauma and critical care. *Transfusion*. 2019;59(S1):837–845.

16.   Garraud O, Folléa G, Lassale B, Pirenne F. The way forward in transfusion medicine, from a French perspective…. *Transfus. Clin. Biol. J. Soc. Francaise Transfus. Sang.* 2018;25(1):1.

17.   Spinella PC, Perkins JG, Grathwohl KW, Beekley AC, Holcomb JB. Warm fresh whole blood is independently associated with improved survival for patients with combat-related traumatic injuries. *J. Trauma*. 2009;66(4 Suppl):S69-76.

18.   Cap AP, Beckett A, Benov A, et al. Whole Blood Transfusion. *Mil. Med.* 2018;183(suppl_2):44–51.

19.   Haddad A, Bou Assi T, Garraud O. How Can Eastern/Southern Mediterranean Countries Resolve Quality and Safety Issues in Transfusion Medicine? *Front. Med.* 2018;5:45.

20.   Zacharowski K, Spahn DR. Patient blood management equals patient safety. *Best Pract. Res. Clin. Anaesthesiol.* 2016;30(2):159–169.

21.   Volken T, Buser A, Castelli D, et al. Red blood cell use in Switzerland: trends and

demographic challenges. *Blood Transfus*. 2016;1–10.

22. Greinacher A, Weitmann K, Schönborn L, et al. A population-based longitudinal study on the implication of demographic changes on blood donation and transfusion demand. *Blood Adv.* 2017;1(14):867–874.

23. Don du sang …car le sang ne peut pas être synthétisé. Transfusion Interrégionale CRS; Available at : https://www.jedonnemonsang.ch/fr/don-du-sang.html.

24. Drew VJ, Barro L, Seghatchian J, Burnouf T. Towards pathogen inactivation of red blood cells and whole blood targeting viral DNA/RNA: design, technologies, and future prospects for developing countries. *Blood Transfus.* 2017;15(6):512–521.

25. Tissot J-D, Bardyn M, Sonego G, Abonnenc M, Prudent M. The storage lesions: From past to future. *Transfus. Clin. Biol.* 2017;24(3):277-284.

26. Kluger R. Red cell substitutes from hemoglobin--do we start all over again? *Curr. Opin. Chem. Biol.* 2010;14(4):538–543.

27. Moradi S, Jahanian-Najafabadi A, Roudkenar MH. Artificial Blood Substitutes: First Steps on the Long Route to Clinical Utility. *Clin. Med. Insights Blood Disord.* 2016;9:33–41.

28. Douay L. Why industrial production of red blood cells from stem cells is essential for tomorrow's blood transfusion. *Regen. Med.* 2018;13(6):627–632.

29. Burger P, Varga E, Heshusius S, et al. Large scale culture and differentiation of erythroblasts from PBMC and iPSC. *Cytotherapy*. 2017;19(5):S49–S50.

30. Claessen M, Varga E, Heshusius S, et al. Large Scale Culture and Differentiation of Erythroblasts from PBMC and iPSC. *Blood*. 2018;132(Suppl 1):2319–2319.

31. Rousseau GF, Giarratana M-C, Douay L. Large-scale production of red blood cells from stem cells: What are the technical challenges ahead? *Biotechnol. J.* 2014;9(1):28–38.

32. Yoshida T, Prudent M, D'Alessandro A. Red blood cell storage lesion: causes and potential clinical consequences. *Blood Transfus.* 2019;17(1):27–52.

33. Yurkovich JT, Zielinski DC, Yang L, et al. Quantitative time-course metabolomics in human red blood cells reveal the temperature dependence of human metabolic networks. *J. Biol. Chem.* 2017;jbc.M117.804914.

34. Gevi F, D'Alessandro A, Rinalducci S, Zolla L. Alterations of red blood cell metabolome during cold liquid storage of erythrocyte concentrates in CPD–SAGM. *J. Proteomics*. 2012;76:168–180.

35. Bennett-Guerrero E, Veldman TH, Doctor A, et al. Evolution of adverse changes in stored RBCs. *Proc. Natl. Acad. Sci.* 2007;104(43):17063–17068.

36. Bordbar A, Johansson PI, Paglia G, et al. Identified metabolic signature for assessing red blood cell unit quality is associated with endothelial damage markers and clinical outcomes. *Transfusion*. Cytoskeletal Control of Red Blood Cell Shape: Theory and Practice of Vesicle Formation;56(4):852–862.

37. Prudent, M., et al. Targeted Metabolomics of SAGM red blood cell storage. *Clin. Lab.* 2014;60(8):S3–S3.

38. D'Alessandro A, Nemkov T, Kelher M, et al. Routine storage of red blood cell (RBC) units in additive solution-3: a comprehensive investigation of the RBC metabolome: Metabolomics of AS-3 RBCs. *Transfusion*. 2015;55(6):1155–1168.

39. Reisz JA, Nemkov T, Dzieciatkowska M, et al. Methylation of protein aspartates and deamidated asparagines as a function of blood bank storage and oxidative stress in human red blood cells. *Transfusion*. 2018;58(12):2978–2991.

40.   Yoshida T, AuBuchon JP, Dumont LJ, et al. The effects of additive solution pH and metabolic rejuvenation on anaerobic storage of red cells. *Transfusion*. 2008;48(10):2096–2105.

41.   Castagnola M, Messana I, Sanna MT, Giardina B. Oxygen-linked modulation of erythrocyte metabolism: state of the art. *Blood Transfus.* 2010;8(Suppl 3):s53–s58.

42.   Low PS, Rathinavelu P, Harrison ML. Regulation of glycolysis via reversible enzyme binding to the membrane protein, band 3. *J. Biol. Chem.* 1993;268(20):14627–14631.

43.   Zimring JC. Established and theoretical factors to consider in assessing the red cell storage lesion. *Blood*. 2015;125(14):2185–2190.

44.   Paglia G, D'Alessandro A, Rolfsson Ó, et al. Biomarkers defining the metabolic age of red blood cells during cold storage. *Blood*. 2016;128(13):e43–e50.

45.   Nishino T, Yachie-Kinoshita A, Hirayama A, et al. Dynamic Simulation and Metabolome Analysis of Long-Term Erythrocyte Storage in Adenine–Guanosine Solution. *PLoS ONE*. 2013;8(8):e71060.

46.   Bordbar A, Jamshidi N, Palsson BO. iAB-RBC-283: A proteomically derived knowledge-base of erythrocyte metabolism that can be used to simulate its physiological and patho-physiological states. *BMC Syst. Biol.* 2011;5:110.

47.   D'Alessandro A, D'Amici GM, Vaglio S, Zolla L. Time-course investigation of SAGM-stored leukocyte-filtered red bood cell concentrates: from metabolism to proteomics. *Haematologica*. 2012;97(1):107–115.

48.   Delobel J, Prudent M, Rubin O, et al. Subcellular fractionation of stored red blood cells reveals a compartment-based protein carbonylation evolution. *J. Proteomics*. 2012;76:181–193.

49.   Dumaswala UJ, Wilson MJ, Wu YL, et al. Glutathione loading prevents free radical injury in red blood cells after storage. *Free Radic. Res.* 2000;33(5):517–529.

50.   Whillier S, Raftos JE, Sparrow RL, Kuchel PW. The effects of long-term storage of human red blood cells on the glutathione synthesis rate and steady-state concentration. *Transfusion*. 2011;51(7):1450–1459.

51.   Rinalducci S, Marrocco C, Zolla L. Thiol-based regulation of glyceraldehyde-3-phosphate dehydrogenase in blood bank-stored red blood cells: a strategy to counteract oxidative stress. *Transfusion*. 2015;55(3):499–506.

52.   Reisz JA, Wither MJ, Dzieciatkowska M, et al. Oxidative modifications of glyceraldehyde 3-phosphate dehydrogenase regulate metabolic reprogramming of stored red blood cells. *Blood*. 2016;128(12):e32–e42.

53.   Chaudhary R, Katharia R. Oxidative injury as contributory factor for red cells storage lesion during twenty eight days of storage. *Blood Transfus.* 2012;10(1):59–62.

54.   Dumaswala UJ, Zhuo L, Jacobsen DW, Jain SK, Sukalski KA. Protein and lipid oxidation of banked human erythrocytes: Role of glutathione. *Free Radic. Biol. Med.* 1999;27(9):1041–1049.

55.   Fu X, Felcyn JR, Odem-Davis K, Zimring JC. Bioactive lipids accumulate in stored red blood cells despite leukoreduction: a targeted metabolomics study. *Transfusion*. 2016;56(10):2560–2570.

56.   Kriebardis AG, Antonelou MH, Stamoulis KE, et al. Progressive oxidation of cytoskeletal proteins and accumulation of denatured hemoglobin in stored red cells. *J. Cell. Mol. Med.* 2007;11(1):148–155.

57.   Kriebardis AG, Antonelou MH, Stamoulis KE, et al. Membrane protein carbonylation in non-

leukodepleted CPDA-preserved red blood cells. *Blood Cells. Mol. Dis.* 2006;36(2):279–282.

58. Delobel J, Prudent M, Crettaz D, et al. Cysteine redox proteomics of the hemoglobin-depleted cytosolic fraction of stored red blood cells. *Proteomics Clin. Appl.* 2016;10(8):883–893.

59. Delobel J, Prudent M, Tissot J-D, Lion N. Proteomics of the red blood cell carbonylome during blood banking of erythrocyte concentrates. *Proteomics Clin. Appl.* 2016;10(3):257–266.

60. D'Alessandro A, Mirasole C, Zolla L. Haemoglobin glycation (Hb1Ac) increases during red blood cell storage: a MALDI-TOF mass-spectrometry-based investigation. *Vox Sang.* 2013;105(2):177–180.

61. Finka A, Mattoo RUH, Goloubinoff P. Experimental Milestones in the Discovery of Molecular Chaperones as Polypeptide Unfolding Enzymes. *Annu. Rev. Biochem.* 2016;85(1):715–742.

62. Bayer SB, Hampton MB, Winterbourn CC. Accumulation of oxidized peroxiredoxin 2 in red blood cells and its prevention. *Transfusion*. 2015;55(8):1909–1918.

63. Kriebardis AG, Antonelou MH, Stamoulis KE, et al. Storage-dependent remodeling of the red blood cell membrane is associated with increased immunoglobulin G binding, lipid raft rearrangement, and caspase activation. *Transfusion*. 2007;47(7):1212–1220.

64. Pantaleo A, Giribaldi G, Mannu F, Arese P, Turrini F. Naturally occurring anti-band 3 antibodies and red blood cell removal under physiological and pathological conditions. *Autoimmun. Rev.* 2008;7(6):457–462.

65. Freikman I, Amer J, Cohen JS, Ringel I, Fibach E. Oxidative stress causes membrane phospholipid rearrangement and shedding from RBC membranes—An NMR study. *Biochim. Biophys. Acta BBA - Biomembr.* 2008;1778(10):2388–2394.

66. Kriebardis AG, Antonelou MH, Stamoulis KE, et al. RBC-derived vesicles during storage: ultrastructure, protein composition, oxidation, and signaling components. *Transfusion*. 2008;48(9):1943–1953.

67. Rubin O, Crettaz D, Canellini G, Tissot J-D, Lion N. Microparticles in stored red blood cells: an approach using flow cytometry and proteomic tools. *Vox Sang.* 2008;95(4):288–297.

68. Rubin O, Delobel J, Prudent M, et al. Red blood cell-derived microparticles isolated from blood units initiate and propagate thrombin generation: RMPs Generate Thrombin. *Transfusion*. 2013;53(8):1744–1754.

69. Rubin O, Canellini G, Delobel J, Lion N, Tissot J-D. Red Blood Cell Microparticles: Clinical Relevance. *Transfus. Med. Hemotherapy*. 2012;39(5):342–347.

70. Bogdanova A, Makhro A, Wang J, Lipp P, Kaestner L. Calcium in Red Blood Cells—A Perilous Balance. *Int. J. Mol. Sci.* 2013;14(5):9848–9872.

71. O'Neill GM, Prasanna Murthy SN, Lorand L, et al. Activation of transglutaminase in mu-calpain null erythrocytes. *Biochem. Biophys. Res. Commun.* 2003;307(2):327–331.

72. Wieschhaus A, Khan A, Zaidi A, et al. Calpain-1 knockout reveals broad effects on erythrocyte deformability and physiology. *Biochem. J.* 2012;448(1):141–152.

73. Hess JR, Lippert LE, Derse-Anthony CP, et al. The effects of phosphate, pH, and AS volume on RBCs stored in saline-adenine-glucose-mannitol solutions. *Transfusion*. 2000;40(8):1000–1006.

74. Sparrow RL, Sran A, Healey G, Veale MF, Norris PJ. In vitro measures of membrane changes reveal differences between red blood cells stored in saline-adenine-glucose-mannitol and AS-1 additive solutions: a paired study. *Transfusion*. 2014;54(3):560–568.

75.   Moon I, Yi F, Lee YH, et al. Automated quantitative analysis of 3D morphology and mean corpuscular hemoglobin in human red blood cells stored in different periods. *Opt. Express*. 2013;21(25):30947–30957.

76.   Kozlova E, Chernysh A, Moroz V, et al. Morphology, membrane nanostructure and stiffness for quality assessment of packed red blood cells. *Sci. Rep.* 2017;7(1):7846.

77.   Blasi B, D'Alessandro A, Ramundo N, Zolla L. Red blood cell storage and cell morphology. *Transfus. Med.* 2012;22(2):90–96.

78.   Roussel C, Dussiot M, Marin M, et al. Spherocytic shift of red blood cells during storage provides a quantitative whole cell-based marker of the storage lesion. *Transfusion*. 2017;57(4):1007–1018.

79.   Mohandas N, Gallagher PG. Red cell membrane: past, present, and future. *Blood*. 2008;112(10):3939–3948.

80.   Lang F, Busch GL, Ritter M, et al. Functional significance of cell volume regulatory mechanisms. *Physiol. Rev.* 1998;78(1):247–306.

81.   Diez-Silva M, Dao M, Han J, Lim C-T, Suresh S. Shape and Biomechanical Characteristics of Human Red Blood Cells in Health and Disease. *MRS Bull.* 2010;35(05):382–388.

82.   Mohandas N, Evans E. Mechanical properties of the red cell membrane in relation to molecular structure and genetic defects. *Annu. Rev. Biophys. Biomol. Struct.* 1994;23(1):787–818.

83.   Park Y, Best CA, Auth T, et al. Metabolic remodeling of the human red blood cell membrane. *Proc. Natl. Acad. Sci.* 2010;107(4):1289–1294.

84.   Safeukui I, Buffet PA, Deplaine G, et al. Quantitative assessment of sensing and sequestration of spherocytic erythrocytes by the human spleen. *Blood*. 2012;120(2):424–430.

85.   Lutz HU, Bogdanova A. Mechanisms tagging senescent red blood cells for clearance in healthy humans. *Front. Physiol.* 2013;4:387.

86.   Barshtein G, Arbell D, Livshits L, Gural A. Is It Possible to Reverse the Storage-Induced Lesion of Red Blood Cells? *Front. Physiol.* 2018;9:914.

87.   Gehrke S, Srinivasan AJ, Culp-Hill R, et al. Metabolomics evaluation of early-storage red blood cell rejuvenation at 4°C and 37°C. *Transfusion*. 2018;58(8):1980–1991.

88.   Meyer EK, Dumont DF, Baker S, Dumont LJ. Rejuvenation capacity of red blood cells in additive solutions over long-term storage: RBC REJUVENATION CAPACITY. *Transfusion*. 2011;51(7):1574–1579.

89.   Tchir JDR, Acker JP, Holovati JL. Rejuvenation of ATP during storage does not reverse effects of the hypothermic storage lesion: Rejuvenation and RBC Storage Lesion. *Transfusion*. 2013;53(12):3184–3191.

90.   Yoshida T, Blair A, D'alessandro A, et al. Enhancing uniformity and overall quality of red cell concentrate with anaerobic storage. *Blood Transfus.* 2017;15(2):172–181.

91.   Burns JM, Yoshida T, Dumont LJ, et al. Deterioration of red blood cell mechanical properties is reduced in anaerobic storage. *Blood Transfus.* 2016;14(1):80.

92.   de Korte D. New additive solutions for red cells. *ISBT Sci. Ser.* 2016;11(S1):165–170.

93.   Cancelas JA, Dumont LJ, Maes LA, et al. Additive solution-7 reduces the red blood cell cold storage lesion. *Transfusion*. 2014;55(3):491-8.

94.   Högman CF, Löf H, Meryman HT. Storage of red blood cells with improved maintenance of 2,3-bisphosphoglycerate. *Transfusion*. 2006;46(9):1543–1552.

95. de Korte D, Kleine M, Korsten HGH, Verhoeven AJ. Prolonged maintenance of 2,3-diphosphoglycerate acid and adenosine triphosphate in red blood cells during storage. *Transfusion*. 2008;48(6):1081–1089.

96. Koch CG, Figueroa PI, Li L, et al. Red Blood Cell Storage: How Long Is Too Long? *Ann. Thorac. Surg.* 2013;96(5):1894–1899.

97. Bardyn M, Rappaz B, Jaferzadeh K, et al. Red blood cells ageing markers: a multi-parametric analysis. *Blood Transfus. Trasfus. Sangue*. 2017;15(3):239–248.

98. Jaferzadeh K, Moon I, Bardyn M, et al. Quantification of stored red blood cell fluctuations by time-lapse holographic cell imaging. *Biomed. Opt. Express*. 2018;9(10):4714.

99. Prudent M, Rappaz B, Hamelin R, et al. Loss of Protein Tyr-phosphorylation During in vitro Storage of Human Erythrocytes: Impact on RBC Morphology. *Transfusion*. 2014;54:49A-50A.

100. Bardyn M, Maye S, Lesch A, et al. The antioxidant capacity of erythrocyte concentrates is increased during the first week of storage and correlated with the uric acid level. *Vox Sang.* 2017;112(7):638–647.

101. Pallotta V, Gevi F, D'Alessandro A, Zolla L. Storing red blood cells with vitamin C and N-acetylcysteine prevents oxidative stress-related lesions: a metabolomics overview. *Blood Transfus.* 2014;12(3):376–387.

102. Silva DGH, Belini Junior E, de Almeida EA, Bonini-Domingos CR. Oxidative stress in sickle cell disease: An overview of erythrocyte redox metabolism and current antioxidant therapeutic strategies. *Free Radic. Biol. Med.* 2013;65:1101–1109.

INTRODUCTION

CHAPTER 1

CHANGES IN THE RED BLOOD CELLS DURING STORAGE

GENERAL INTRODUCTION

The *ex vivo* journey of a Red Blood Cell (RBC) for transfusion (Figure 1) starts after donation of whole blood or after an apheresis procedure (automated cell separation).
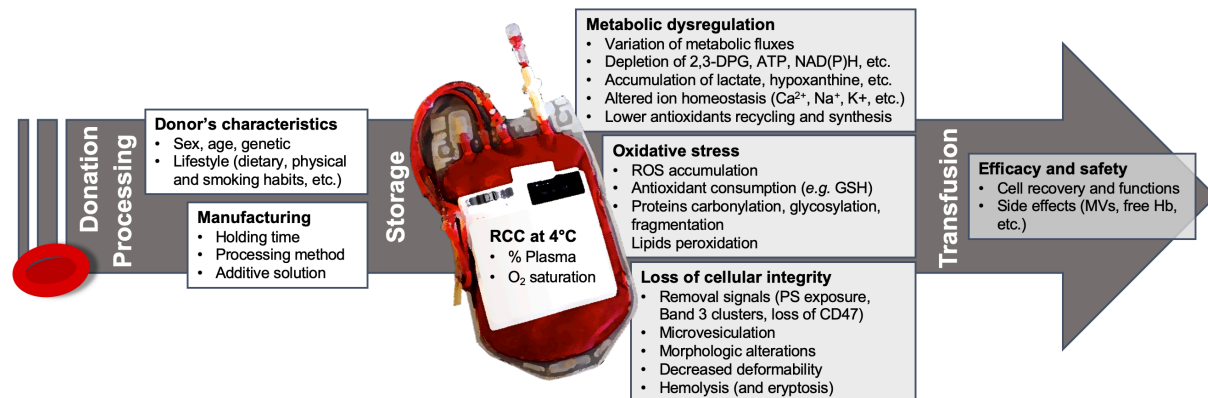
*Figure 1 – **The** ex vivo **journey of a Red Blood Cell (RBC) for transfusion.** The Red Cell Concentrate (RCC) characteristics are dependent on the donor's characteristics and the manufacturing processes. During storage, the RBCs progressively accumulate storage lesions that can impair cell recovery when a transfusion is carried out, with possible deleterious side effects for the patient. 2,3-DPG: 2,3-Diphosphoglycerate, ATP: Adenosine Triphosphate, GSH: reduced Glutathione, Hb: Hemoglobin, MVs: Microvesicles, NAD(P)H: reduced Nicotinamide Aadenine Dinucleotide (phosphate), PS: Phosphatidylserine, ROS: Reactive Oxygen Species.*

Whole blood is collected in an anticoagulant solution, *i.e.* Citrate-Phosphate-Dextrose (CPD) or Acid-Citrate-Dextrose (ACD). Then, to obtain a Red Cell Concentrate (RCC), the blood components are separated by centrifugation and distributed into different storage bags. The RBCs are generally filtrated to minimize the number of residual leukocytes and platelets. This procedure reduces: 1) the risk of non-hemolytic transfusion reactions (allergic, anaphylactic and febrile, as well as Transfusion-Related Acute Lung Injury [TRALI]), 2) the probability of Graft-Versus-Host Disease ([GVHD], to note that irradiation is required for immunocompromised patients) and 3) the transmission of blood-borne pathogens (such as Cytomegalovirus [CMV] and probably also the Hepatitis E Virus [HEV]) following transfusion. Moreover, it was shown that filtration reduces early senescence of RBCs during storage[1,2]. The RBCs are then re-suspended at a Hematocrit (HCT) comprised between 50 and 70 % in an additive solution, and stored in a gas-permeable plastic bag, at 4°C, without agitation until transfusion. Different types of additive solution are licensed and used worldwide (Table 1).

Table 1 – **Licensed additive solutions for red blood cell storage.** *Composition, pH, associated anti-coagulant, and countries used. Table modified from Sparrow L. R.[3].*

Constituents / mM	SAGM	AS-1 (Adsol)	AS-3 (Nutricel)	AS-5 (Optisol)	MAP	PAGGSM
NaCl	150	154	70	150	85	72
$NaHCO_3$	-	-	-	-	-	-
Na_2HPO_4	-	-	-	-	-	16
NaH_2PO_4	-	-	23	-	6	8
Citric acid	-	-	2	-	1	-
Sodium citrate	-	-	23	-	5	-
Adenine	1.25	2	2	2.2	1.5	1.4
Guanosine	-	-	-	-	-	1.4
Dextrose	45	111	55	45	40	47
Mannitol	30	41	-	45.5	80	55
pH	5.7	5.5	5.8	5.5	5.7	5.7
Anti-coagulant	CPD	CPD	CP2D	CPD	ACD	CPD
Countries used	Europe UK Australia Canada New Zealand	USA	USA Canada	USA	Japan	Germany Switzerland

SAGM: saline-adenine-glucose-mannitol, AS: Additive Solution, PAGGSM: Phosphate-Adenine-Glucose-Guanosine-Saline-Mannitol, CPD: Citrate-Phosphate-Dextrose, CP2D: Citrate-Phosphate-double Dextrose, ACD: Acid-Citrate-Dextrose, UK: United Kingdom, USA: United States of America.

In Switzerland, the RCCs are generally stored at 4°C for 42 days in Saline-Adenine-Glucose-Mannitol (SAGM) and 49 days in Phosphate-Adenine-Glucose-Guanosine-Saline-Mannitol (PAGGSM) additive solutions. During storage, important changes appear at the level of the RBC metabolism, followed by the occurrence of oxidative stress (imbalance in the redox homeostasis), which ultimately results in the alteration of the cell rheological properties[4,5]. The progressive deterioration in the RCC quality during storage is multi-factorial: *i.e.* the normal aging of the cells (RBCs have a lifespan of 120 days in the circulation), the stress induced by the preparation procedure (mechanical stress, exposition to plastic materials, to light, etc.) and finally the storage conditions themselves, that are not physiological.

This chapter will be focused on the identification of aging markers and on the improvement of the understanding of the storage lesions, using standard as well as innovative analysis tools. It is a necessary step before implementing correcting strategies to improve the quality of the blood products for transfusion. Therefore, we first characterized and quantified storage lesions by looking at multiple aging markers simultaneously. This study is presented in the first part of this chapter and is the subject of a paper published in the journal *Blood Transfusion*[6]. Then, the impact of the protein phosphorylation, which is hypothesized to regulate the RBC membrane shape and deformability, was studied.

PART 1: OVERWIEW OF THE RED BLOOD CELL STORAGE LESIONS

Introduction

During storage, the RBCs accumulate a broad range of lesions, that are either reversible or irreversible following transfusion[4,5,7]. The aim of this study is to better characterize and quantify storage lesions by analyzing various aging hallmarks that altogether provide an overview of the evolution of the cell metabolism, antioxidant defenses, morphology and membrane dynamics during storage.

Study design

In this study, different aging markers were quantified simultaneously on five RCCs prepared in SAGM and stored under conventional conditions in Switzerland (Figure 2).
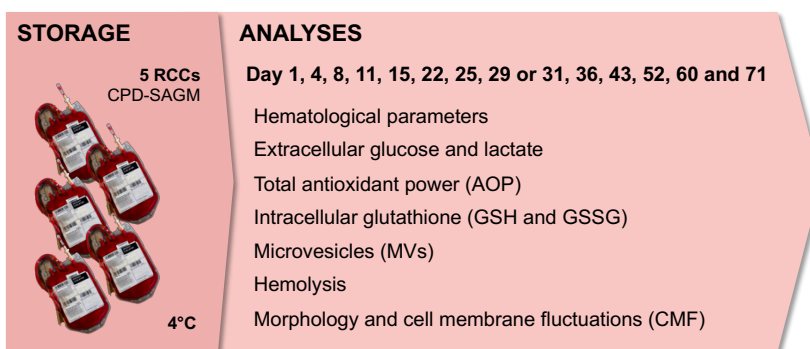
Figure 2 – *Experimental workflow: follow-up of the Red Cell Concentrates (RCCs).* The RCCs were followed during 71 days of storage at 4°C. The hematological parameters, extracellular glucose and lactate concentrations, pH, global antioxidant power, intracellular reduced and oxidized glutathione levels, microvesiculation, hemolysis, morphology and cell membrane fluctuations were analyzed at given timepoints.

Metabolic parameters such as glucose consumption and extracellular lactate accumulation were quantified. The Antioxidant Power (AOP) was determined *via* the electrochemical pseudo-titration of water-soluble antioxidants, as well as the measurement of the intracellular reduced and oxidized Glutathione (GSH and GSSG) levels. The percentage of hemolysis and degree of microvesiculation were also assessed. Since morphological damages are related to biochemical lesions, Digital Holographic Microscopy (DHM) was used to follow the changes of RBC morphology and the levels of dynamic cell membrane fluctuations, a parameter reflecting the cell health state. To capture deep storage lesions, the follow-up period was prolonged to 71 days (29 days after the expiration date).

Material and methods

Five milliliters of each sample were collected using a sampling site weekly for 71 days (twice during week 1, 2 and 4). The five RCCs used in this study came from two women and three men (donors' characteristics are listed in Table 2).

Table 2 – **Donor's characteristics**. *Sex, age and blood group (ABO and Rhesus D) of the donor.*

Sample	Sex	Age / year	Blood group
RCC 1	Female	58	O+
RCC 2	Female	43	O-
RCC 3	Male	50	A+
RCC 4	Male	49	O+
RCC 5	Male	33	O+

RCC: Red Cell Concentrate.

Hematological, AOP and Microvesicles (MVs) analyses were done directly on RCC samples without processing. Hemolysis, glucose and lactate were quantified in the RCC supernatant collected after centrifugation of the RCC samples at 2000 *g* during 10 min at 4°C. The observations of morphology and membrane fluctuations were done on washed RBCs.

Preparation of the red cell concentrates

The RCCs were prepared using a top/bottom processing method. Whole blood (450 ± 50 mL) donated under signed consent was collected in 63 mL of CPD anticoagulant (CompoFlow CQ32250, Fresenius Kabi). After a holding time (minimum 1h and maximum 24h) at Room Temperature (RT, 22 ± 2°C), the bags were centrifuged (5'047 *g* for 13 min at 22°C on a Roto Silenta 630 RS, Hettich) to separate the blood components, and a semi-automated pressure was applied (CompoMat, Fresenius Kabi) to distribute the fractions into sterile inter-connected bags. Finally, the RBCs were filtered to remove residual leukocytes and were stored at 4°C in 100 mL of SAGM additive solution. To fulfill the quality control criteria, the RCCs must have a final volume of 275 ± 75 mL and an HCT of 0.6 ± 0.1 v/v.

Hematological analysis

The hematological data such as the RBC count, HCT, total and intracellular Hemoglobin (Hb) content, Mean Corpuscular Volume (MCV), Standard Deviation of the RBC Distribution Width (SD-RDW), etc., were recorded with an automated hematology analyzer (KX-21N, Sysmex). This instrument uses a Direct Current (DC) method, based on the impedance (electrical resistance) of the cell against a current, for cell count (number of pulses) and volume determination (pulse height); and the photometric non-cyanide Hb method for Hb quantification.

Electrochemical antioxidant power measurement

The EdelMeter potentiostat was used to measure electrochemically the AOP in RCCs (or supernatants) samples. For further details, please refer to the Chapter 2[8,9]. Few microliters (approx. 3 µL) of sample were loaded in the electrochemical cell of the disposable screen-printed electrode strip. For each measurement, a fresh electrode strip is used. The AOP is recorded three seconds after loading the sample. Each measurement was performed at least in duplicate and was generally repeated when the difference between two measurements exceeded 7 EDEL.

Microvesicles quantification

The MVs were quantified by flow cytometry (FACScalibur flow cytometer with CellQuest pro software, BD Biosciences)[10]. Five microliters of RCC (or supernatant) were mixed with 5 µL of Fluorescein (FITC) anti-human CD47 antibody and incubated 20 min at RT under agitation. Before analysis, Trucount™ tubes (BD Biosciences), that contain a known number of fluorescent beads enabling quantitation, were filled with 400 µL of 0.9 % NaCl and 5 µL of labelled sample. The different populations in the sample were discriminated according to their size (Forward Scatter, FSC), granularity (Side Scatter, SSC) and fluorescence. Small (< 1 µm) and CD47-positive events were considered as MVs.

Hemolysis quantitation

The concentration of Hb in the supernatant was determined according to the Harboe method with the 3-point "Allen correction" (Equation 1)[11]. The absorbance at 380, 415 and 450 nm was measured with a spectrophotometer (NanoDrop 2000c, Thermo Scientific). This instrument measures the absorbance on microvolumes sample sizes (0.5 to 2 µL) over a 1 mm light path.

$$Hb\ supernatant\ (g/l) = \frac{167.2 \times A_{415} - 83.6 \times (A_{380} + A_{450})}{100} \times dilution\ factor \qquad \text{Equation 1}$$

When hemolysis was too high (*i.e.* A_{415} above 1.5 A.U.), the samples were diluted in deionized water (dH$_2$O). dH$_2$O also used for the blank. The Hb supernatant value was then used to calculate the percentage of hemolysis using Equation 2.

$$Hemolysis\ (\%) = \frac{Hb\ supernatant\ (g/l) \times (1 - HCT)}{Hb\ total\ (g/l)} \times 100 \qquad \text{Equation 2}$$

To be noted that the HCT and total Hb where determined during the hematological analysis.

Measurement of extracellular glucose and lactate concentrations

Extracellular concentrations of glucose and lactate were measured in supernatant samples (stored at -80°C) using commercial colorimetric assays. The glucose was quantified using a Biochain assay (kit Z5030025, BioChain) and the lactate with a BioVision assay (kit II, K627-100, BioVision).

Determination of intracellular reduced and oxidized glutathione levels

Quantification of the intracellular levels of GSH and GSSG, was performed according to the protocol proposed by Giustarini *et al.*[12] with small modifications. Two RCC samples were collected for the analysis. The first one was used *per se* for total glutathione quantification and the second one was treated with the derivatizing agent *N*-Ethylmaleimide (NEM) for GSSG measurement. NEM is added to prevent oxidation of GSH into GSSG during the acid deproteinization step, avoiding GSSG overestimation. This assay is based on GSH reaction with Ellman's reagent (5,5'-Dithio-bis-[2-

nitrobenzoic acid], DTNB) that produces the chromophore 5-Thio-2-nitrobenzoic acid (TNB) quantifiable by spectrophotometry at 412 nm. GSSG is recycled into GSH in the presence of the enzyme Glutathione Reductase (GR) and the redox cofactor Nicotinamide Adenine Dinucleotide Phosphate (NADPH).

Two mL of each RCC were collected for the analysis, from which 750 µL were transferred into an empty tube for total glutathione quantification and 750 µL into a second tube containing 225 µL of NEM (NEM 300 mM, Sigma-Aldrich) for GSSG measurement. Samples were centrifuged at 10'000 *g* during 38 s at 4°C and supernatant was discarded. RBCs were then washed twice in two volumes of 1x phosphate buffered saline (PBS, Laboratorium Dr. G. Bichsel). RBC pellet was resuspended in one volume of 1x PBS, and a hematological measurement was done to determine intracellular Hb concentration of each sample for normalization. Two aliquots of 400 µL were transferred into new tubes, centrifuged as before and supernatant was discarded. The samples were stored as dry pellets of RBCs at -80°C until analysis. The rest of the analysis followed the procedure described in the protocol.

Morphology and membrane fluctuation analyses using digital holographic microscopy

DHM is a Quantitative Phase Microscopy (QPM) interferometric technique which has many advantages over the classical microscopy methods. Firstly, because it is label-free and uses a low intensity laser as light source for specimen illumination. Here, the 684 nm laser source that was used delivered roughly 200 µW/cm^2 at the specimen plane - that is some six orders of magnitude less than intensities typically associated with confocal fluorescence microscopy. With that amount of light, the exposure time is only 0.4 ms. DHM is therefore less invasive, time consuming and costly. Secondly, because it not only provides a visual information (image) but also delivers a quantitative measurement of the Optical Path Length (OPL), a parameter related to the volume and cell refractive index. Thirdly, because it enables the refocusing of the images post-acquisition and is therefore compatible with 3-D samples.

The principle of the QPM is based on the fact that even if an object is transparent, and therefore (almost) invisible when looked with intensity contrast, it will induce a retardation of the phase of the transmitted wave (Figure 3).
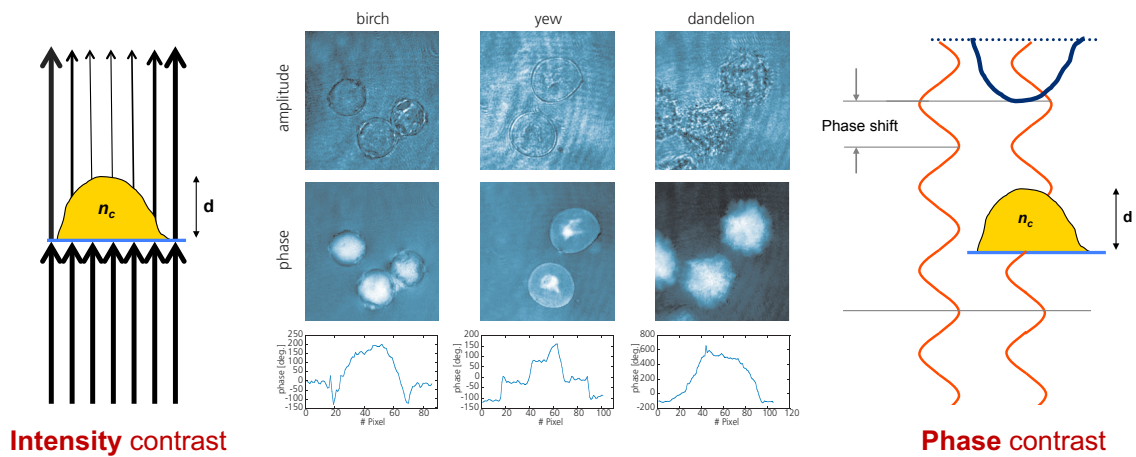
*Figure 3 – **Intensity** versus **phase contrast for imaging of transparent objects.** Different pollen particles imaged with transmission DHM™ T1000 and profiles extracted from phase images. d: distance or cell thickness, n_c: refractive index of the cell. Images modified from the website of Lyncée Tec SA and from the slides of a presentation made by Dr. Benjamin Rappaz.*

The DHM records the phase images in a two-step process where a hologram consisting of a 2-D interference pattern is first recorded on a digital camera (Figure 4). Then, the quantitative OPL images are reconstructed numerically off-line using a specific algorithm. The numerical reconstruction consists in the simulation of re-illumination with the reference wave plus a correction for aberration, as classical interferometric phase shift measurements are sensitive to experimental noise.
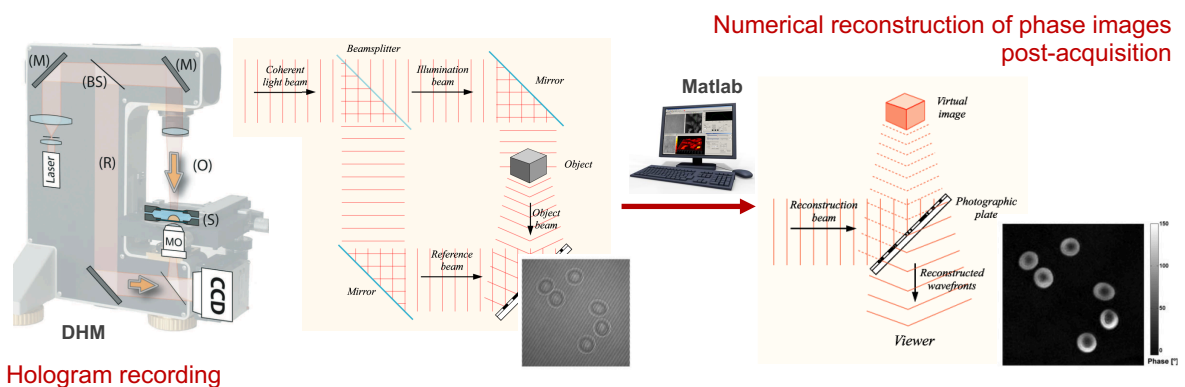
*Figure 4 – **Workflow for phase image acquisition using Digital Holographic Microscopy (DHM).** The DHM is composed of a laser, as set of lenses, mirrors (M), a beam splitter (BS), microscope objectives (MO), a condenser and a Charge-Coupled Device (CCD) camera. The beam is split into a reference wave (R) and an object wave (O) that passes through the sample (S). As the phase cannot be directly recorded, it is encoded by interferometry. The interference pattern,* i.e. *the hologram is then numerically reconstructed post-acquisition into a phase image. Images modified from Depeursinge et al.[13], Rappaz et al.[14], and Bob Mellish from Creative Commons.*

The phase information in DHM is quantitatively related to the Optical Path Difference (OPD), expressed in terms of cell biophysical parameters as described in Equation 3.

$$OPD_{(x,y)} = d_{(x,y)} \times (n_{cell_{(x,y)}} - n_m)$$

where $d_{(x,y)}$ is the cell thickness, $n_{cell_{(x,y)}}$ is the mean z-integrated intracellular refractive index at the (x, y) position and n_m is the refractive index of the surrounding culture medium[15]. As far as RBCs are concerned, the value of the intracellular refractive index results primarily from Hb concentration, and the cell thickness to the RBC morphology[13,14,16–18].
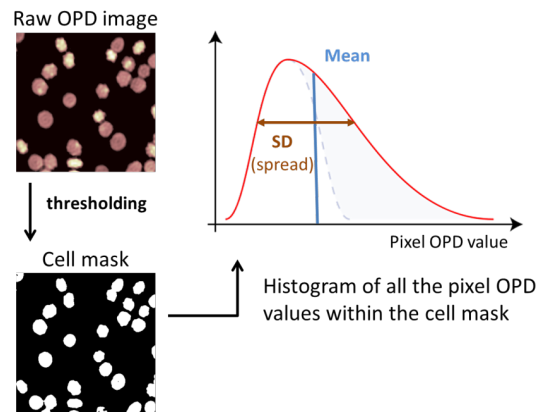
*Figure 5 – **Population analysis with the Optical Path Difference (OPD) parameter.** A cell mask is applied to the raw OPD image and all the pixel OPD values within the mask are plotted as a histogram. SD: Standard Deviation.*

For quantitative analysis, the raw OPD images are thresholded with a fixed value (slightly above background level to discard noisy pixels) to create the "cell mask". All the pixel OPD values that are within the cell mask are plotted in a histogram (Figure 5). The reconstruction software automatically provides multiple analysis parameters such as the average OPD (avg OPD), Standard Deviation of OPD (SD-OPD), kurtosis, skewness, sum of OPD and confluency values for each image (rapid "on-the-fly" analysis).

The general workflow for RBC analysis using DHM is presented in Figure 6. Before analysis, the RBCs were washed twice with 0.9 % NaCl and spun-down at 2000 *g* during 10 min at 4°C. Two volumes of HEPA buffer (composition described in ANNEX-1) were added on the RBC pellets and a Sysmex analysis was done to determine the RBC count. Just before the analysis, the RBCs were further diluted in HEPA and seeded in the wells at a density of 75'000 cells for 100 µL per well (3 wells/ RCC) in a 96-well imaging plate (BD Falcon) coated with 0.1 mg/mL poly-L-ornithine (details of the coating procedure can be found in ANNEX-2). The plate was centrifuged at 140 *g*, 2 min at RT to speed up the sedimentation process. During image acquisition, the plate was placed in a plate incubator set at 37°C with high humidity and 5 % CO_2.
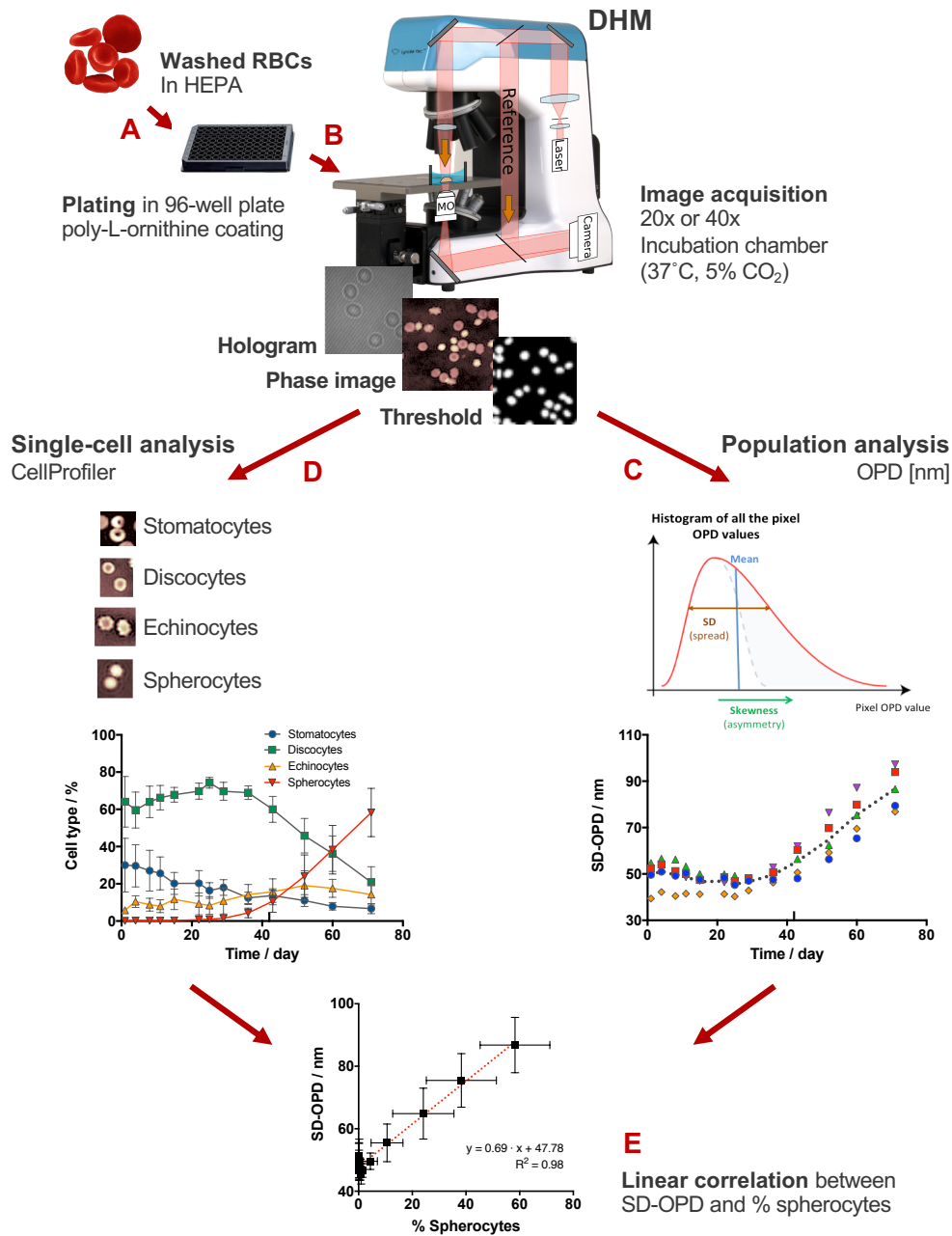
*Figure 6 – **Workflow of Red Blood Cell (RBC) image acquisition using digital holographic microscopy (DHM) and image analysis**. [A] Washed RBCs are plated into a multiwell imaging plate coated with poly-L-ornithine. [B] Holograms of the seeded RBCs are acquired at 20x or 40x magnification. For timelapse analyses, the plate can be placed into an incubation chamber set at 37°C and 5 % CO_2. The phase images are then reconstructed, and a threshold is applied to keep only the pixel Optical Path Difference (OPD) values from cells. [C] Population "on-the-fly" analysis of OPD parameters, or [D] single-cell analysis using CellProfiler and CellProfiler Analyst (CPA). [E] The Standard Deviation of OPD (SD-OPD) and the percentage of spherocytes in the sample are linearly correlated.*

The microscope used was a DHM® T1000 (Lyncée Tec SA) equipped with a motorized microscope stage (Märzhäuser Wetzlar GmbH & CO. KG), an incubator system (LCI Live Cell Instrument), and 20x/0.40 NA and 40x/0.75 NA objectives (Leica Microsystems GmbH). Quantitative phase images (four images per well) of the RBCs were acquired at 20x magnification to analyze RBC morphology.

The quantitative phase images were analyzed in two ways. First, a population analysis (yielding a single output per image) was performed by automatic calculation of the OPD value during the reconstruction of the images. It has the advantage of being directly available without further analysis, enabling High-Throughput Screening (HTS). Single-cell analysis was also performed using CellProfiler[19,20] (Broad Institute, www.CellProfiler.org, 2.2.0, rev 9969f42) and CellProfiler Analyst[21,22] ([CPA], 2.2.1). CellProfiler is a free open-source cell image analysis software that can be used to identify, segment and measure different parameters of the individual RBCs, such as their size, shape, intensity, and texture. CPA then uses these features during the supervised machine learning to classify RBCs according to their phenotype. Generally, four classes were defined, *i.e.* "stomatocytes", "discocytes", "echinocytes" and "spherocytes". An additional "errors" class was added to eliminate objects resulting from segmentation errors. Of interest was a strong correlation shown between the number of spherocytes present in the sample (based on CPA) and the SD-OPD (the results of the correlation analysis are presented in ANNEX-3).

In addition, DHM was used for the quantification of the RBC membrane fluctuations. To that end, short movies (at 40x magnification, during 10 s, with a frame rate of 20 images per second) were acquired. This analysis was done in collaboration with Professor Inkyu Moon and Keyvan Jaferzadeh from the Chosung University in South Korea, who carried out the analyses. DHM phase images from each time-frame of the recorded movies were first registered using the StackReg ImageJ plugin (to cancel the spatial displacement of RBCs) and then, using ImageJ software, manually segmented into individual RBCs to measure membrane fluctuations at the single-RBC level. The amplitude of Cell Membrane Fluctuation (CMF) was measured on individual cells according to the method described by Rappaz *et al.*[23]. More details about this analysis are presented in ANNEX-4.

Results and discussion

The mean values for the observed parameters at day 1, 29, 43 and 71 are summarized in Table 3.

*Table 3 – **Main Red Blood Cell (RBC) aging parameters.** Followed during storage at day 1, 29, 43 and 71.*

	Day 1	Day 29	Day 43	Day 71
RBCs (1·1012/L)	6.47 ± 0.46	6.34 ± 0.51	6.34 ± 0.51	6.51 ± 0.48
MCV (fL)	91.6 ± 6.0	97.8 ± 11.9	99.7 ± 12.2	100.8 ± 8.3 **
SD-RDW (fL)	48.2 ± 1.8	54.0 ± 7.7	55.6 ± 8.5	58.8 ± 13.3
Glucose (mg/dL)	481.4 ± 33.0	254.0 ± 31.5 **	211.1 ± 34.4 **	174.1 ± 37.1 **
Lactate (mM)	6.57 ± 0.96	32.66 ± 3.42 **	37.24 ± 3.64 **	35.95 ± 3.87 **
MVs (1/µL)	3628 ± 1047	7980 ± 832 ++ *	15'860 ± 4219 **	258'654 ± 106'413 *
Hemolysis (%)	0.079 ± 0.017	0.233 ± 0.062 *	0.441 ± 0.135 **	3.817 ± 1.391 **
AOP (nW)	71.4 ± 5.3	62.3 ± 9.2 ++	61.4 ± 5.6 *	62.2 ± 6.5
GSH (µmol/g Hb)	5.27 ± 0.42 +	5.46 ± 0.62	4.08 ± 0.33 *	2.21 ± 0.38 **
GSSG (nmol/g Hb)	28.2 ± 5.2	35.0 ± 4.9 *	27.3 ± 4.4	178.0 ± 118.7
SD-OPD (nm)	49.6 ± 6	46.6 ± 2.2 *	55.5 ± 6	86.8 ± 8.9 **
Stomatocytes (%)	30.0 ± 14.4	18.0 ± 4.2	13.7 ± 3.7	6.7 ± 2.7
Discocytes (%)	64.0 ± 13.6	69.7 ± 4.8	60.0 ± 7.0	20.8 ± 8.4 *
Echinocytes (%)	5.8 ± 1.8	10.8 ± 7.0	15.7 ± 7.0	14.2 ± 5.7
Spherocytes (%)	0.1 ± 0.1	1.5 ± 0.8 *	10.6 ± 5.9 *	58.3 ± 13.0 **
CMF discocytes (nm)	30.4 ± 3.5 +	29.5 ± 2.9	29.9 ± 3.1	29.0 ± 2.9
CMF spherocytes (nm)	32.1 ± 4.1 +	27.5 ± 3.2	28.1 ± 3.4	27.9 ± 3.4

Mean values for the five red cell concentrates ± Standard Deviation (SD). Measurements done at day 4+ instead of day 1, or day 31++ instead of day 29. * p-value < 0.05, ** p-value < 0.01 compared to day 1.
MCV: Mean Corpuscular Volume, SD-RDW: Standard deviation of Distribution Width, MVs: Microvesicles, AOP: Antioxidant Power, GSH and GSSG: reduced and oxidized Glutathione, SD-OPD: Standard Deviation of the Optical Path Difference, CMF: Cell Membrane Fluctuation.

The hematological data (Figure 7) evolved similarly for all RCCs at the exception of RCC5. The MCV, initially of 89.5 ± 4.3 fL, gained on average 5.1 fL at day 43 and 7.9 fL at day 71 (without considering RCC 5). The increasing MCV is the result of the progressive loss of cation gradient[24]. Sizes of RBCs in the population became more heterogeneous during storage, as indicated by an increasing SD-RDW, a parameter providing information about the anisocytosis.
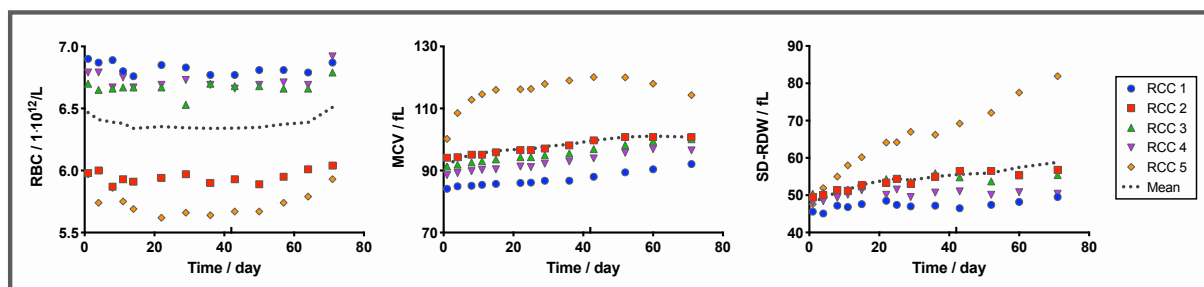
*Figure 7 – **Red Blood Cell (RBC) aging parameters. Part 1: hematological data.** RBC count [left], Mean Corpuscular Volume (MCV) [middle] and Standard Deviation of Distribution Width (SD-RDW) [right], measured with Sysmex analyzer. RCC: Red Cell Concentrate.*

The extracellular glucose was progressively consumed by the cells at a decreasing rate during storage (Figure 8, left). At day 52, a plateau value was reached and did not further decrease, which indicates that the activity of RBC energetic metabolism was almost completely stopped. During the 71 days of storage, RBCs consumed on average 64 % of the available glucose. On the other hand, lactate (glycolysis end-product) accumulated until day 36 (5.6-fold increase) and then stagnated (Figure 8, right).
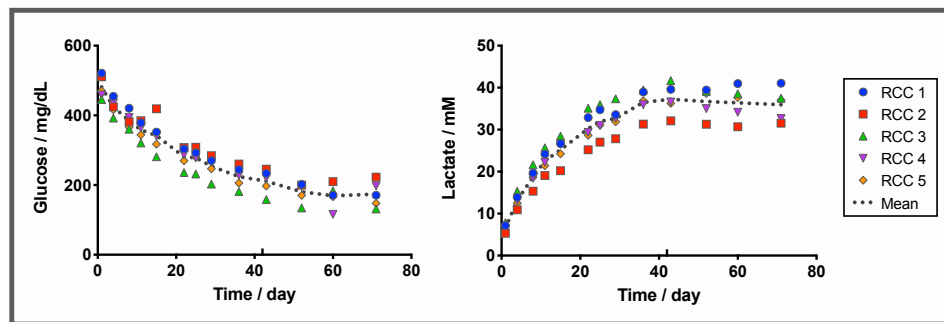
*Figure 8 – **Red Blood Cell (RBC) aging parameters. Part 2: metabolism.** Glucose [left] and lactate concentrations [right], determined using commercial assays. RCC: Red Cell Concentrate.*

The global AOP in the 5 RCCs increased during the first week following blood collection, reaching a maximum at day 4. Then, it decreased gradually back to its initial value (at day 22) and remained stable until the end of the follow-up (Figure 9A). This behavior suggests that RBCs are impacted by blood processing. This response can be passive, RBCs equilibrating with their new environment, or active. This subject will be further discussed in Chapter 2.

Similarly to the AOP, the intracellular concentration of GSH increased during the first two weeks of storage from day 4 up to day 15 (Figure 9B, left), before dropping off linearly until the end of the storage. In the 5 RCCs, the GSSG level (Figure 9B, right) remained low until day 43 and then increased drastically. These results correlate with the increased metabolic activity observed by ours and other groups between 7 and 14 days of storage, followed by its decrease due to a lactate associated drop of pH[25,26]. Indeed, as glycolysis is progressively inhibited by low temperature and pH, glucose is consumed *via* the Pentose Phosphate Pathway (PPP), producing NADPH. This metabolite is the cofactor of the GR responsible for the recycling of GSSG into GSH. GSH is a major thiol-based antioxidant in RBCs. However, the PPP does not produce enough NADPH to sustain recycling of glutathione all along the storage. Additionally, the *de novo* synthesis of GSH is dependent on Adenosine Triphosphate (ATP) and is therefore impaired when the stocks of intracellular ATP are depleted.
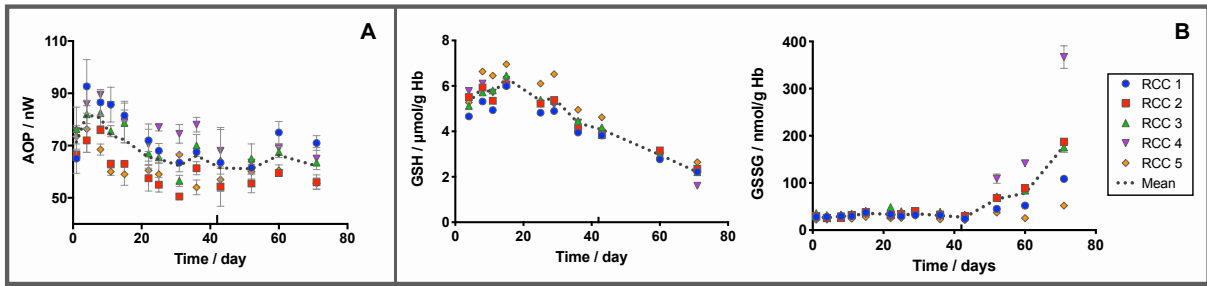
*Figure 9 – **Red Blood Cell (RBC) aging parameters. Part 3: antioxidants.** [A] Global Antioxidant Power (AOP) quantified by pseudotitration voltammetry with EdelMeter, and [B] intracellular concentration of reduced and oxidized Glutathione (GSH and GSSG, respectively). Mean value ± standard deviation. RCC: Red Cell Concentrate.*

The loss of metabolites and antioxidant defenses correlates with the appearance of irreversible lesions such as the microvesiculation and hemolysis. The number of MVs in the RCCs raised first linearly from day 1 to 36 (2.4-fold increase) and then exponentially between day 43 (4.4-fold increase) and 71 (71.3-fold increase) (Figure 10, left). Similarly, the increase of mean hemolysis (0.079 ± 0.017 % at day 1) (Figure 10, right) was linear until day 36, and then followed an exponentially trend. The mean hemolysis percentage was 0.44 ± 0.14 % at day 43, and of 3.82 ± 1.39 % after 71 days of storage. Exponential release of MVs, as well as hemolysis, are reflecting of waste products accumulation inside the cell and appearance of irreversible lesions at the level of the cytoskeleton and membrane, leading together to the destabilization of the RBC membrane (to be mentioned that cell debris coming from hemolyzed RBCs could be wrongly detected as MVs by the flow cytometer). Again, it is interesting to notice that the measured values were quite different among the five RCCs.
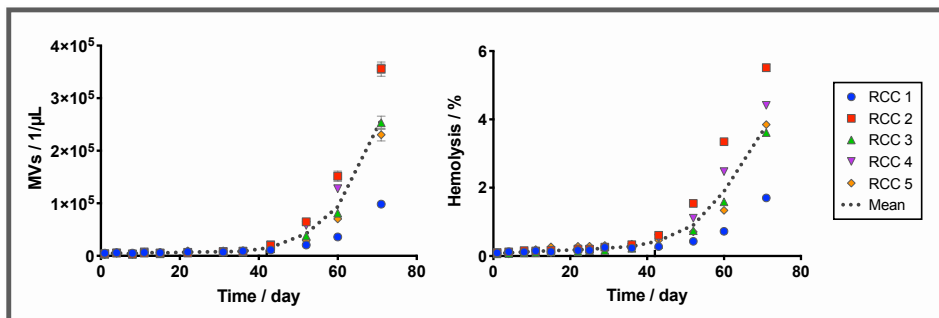
*Figure 10 – **Red Blood Cell (RBC) aging parameters. Part 4: cellular integrity.** Microvesicles (MVs) in the RCC supernatant counted by flow cytometry [left], and percentage of hemolysis in the blood bag determined with the Harboe spectrophotometric method [right]. Mean value ± standard deviation. RCC: Red Cell Concentrate.*

The appearance of irreversible lesions at the level of the cytoskeleton and plasma lead to the destabilization of the RBC membrane and to changes of RBC morphology. All RCCs, at the exception of RCC 5, had a similar SD-OPD at the beginning of the storage. SD-OPD value remained stable until day 29 (Figure 11A, left). The interestingly increasing SD-OPD value was strongly correlated with the transformation of discocytes into transient echinocytes and finally spherocytes (Figure 11B). At day 1,

RBCs were mostly discocytes (64.0 ± 13.6 %) or stomatocytes (30.0 ± 14.4 %) (Figure 11A, right). Until day 29, the stomatocytes transformed into discocytes. Together these two cell types represented approximately 95 % of the population. The percentage of discocytes started to drop linearly from day 36. After 29 days, spherocytes that represented less than 1 % of the population at the beginning of storage started to appear in RCCs. From this point, the percentage of spherocytes also increased linearly in the sample to reach 10.6 ± 5.9 % at day 43 and 58.3 ± 13.0 % at day 71. Echinocytes are a transitional intermediate between discocytes and spherocytes, which is why their number did not increase. Morphological changes followed biochemical alterations, thus suggesting causative events.
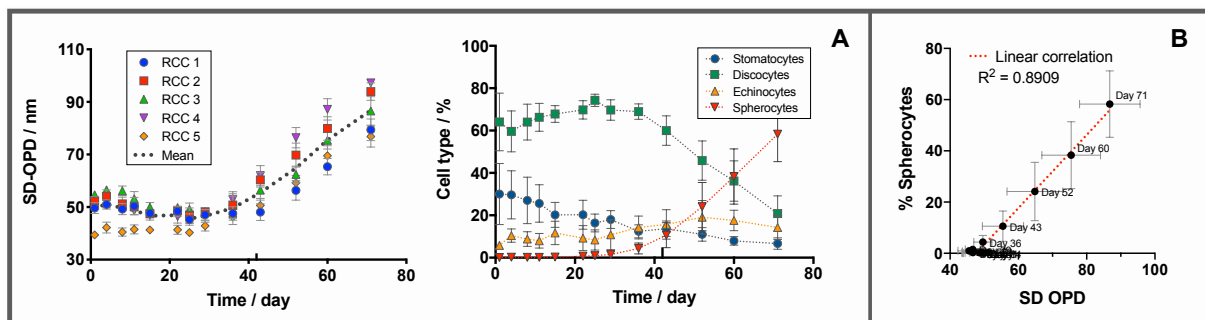
*Figure 11 – **Red Blood Cell (RBC) aging parameters. Part 5: morphology.** Morphology analysis with Digital Holographic Microscope (DHM): [A] population analysis using the Standard Deviation of OPD (SD-OPD) parameter [left], and single-cell analysis with CellProfiler and CellProfiler Analyst (CPA) [right]. Mean value for each cell type ± Standard Deviation (SD). [B] Correlation between the spherocytes percentage and SD-OPD, each point represents a mean value at different storage time ± SD. RCC: Red Cell Concentrate.*

Morphological classes of RBCs can be distinguished on the basis of their CFM map (Figure 12A). The CMF values can be ranked in the following order (by decreasing order of CMF amplitude): stomatocyte, discocyte, echinocyte and spherocyte. Stomatocytes that have a loose central part show an important fluctuation in this region. Discocytes present a symmetric fluctuation in their center and their ring and exhibit the highest CMF, while echinocytes have a decreased center fluctuation. The spherocytes exhibit no more fluctuations in their central area and have the lower CMF values which corroborates their loss of flexibility[27].
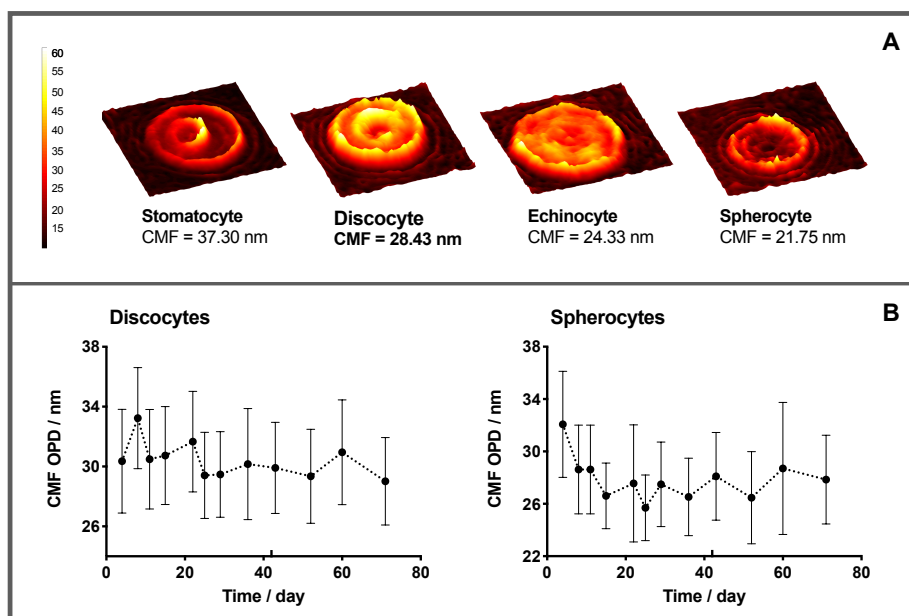
*Figure 12 – **Red Blood Cell (RBC) aging parameters. Part 5: membrane fluctuations.** [A] Cell Membrane Fluctuation (CMF) maps for different classes of RBCs and [B] CMF changes for discocytes and spherocytes. Mean value ± standard deviation.*

A general analysis showed a decrease of the CMF during the storage. The discocytes lost 10 % of their CMF at the expiration date (Figure 12B, left), even though the shape was kept. It suggests that aging not only induces morphological changes from discocytes to spherocytes, but also alter the state of the RBCs that keep a normal shape. During the first three weeks of storage and following the main metabolism lesions, RBCs lost a part of their fluctuation capacity. Several mechanisms could participate into it, such as phosphorylation events that are dependent on energy metabolism[28]. Regarding spherocytes, after a decrease phase, a plateau was reached at day 18 (Figure 12B, right). However, no statistical differences were reported.

Conclusions

RBCs accumulate a broad range of lesions during storage under standard blood transfusion practice. Of particular interest is the sequence of events that lead the storage lesions with two cornerstones and three zones[29], in close relation with the evolution of the cell metabolism[29,25].

Metabolic changes can directly impact the RBC rheological properties. Indeed, even when the RBCs keep an intact shape, their fluctuation amplitude changes, suggesting that aging not only induces morphological changes from discocytes to spherocytes, but also alter the state of apparently normal RBCs. Several mechanisms could participate to it, such as phosphorylation events that are dependent of energy metabolism[30,28]. Indeed, several groups demonstrated that the maintenance of the biconcave shape and membrane deformability was regulated by dynamic ATP-dependent remodeling of the membranes/cytoskeleton interactions[30–34]. The impact of phosphorylation on RBCs morphology will be discussed in the next part of this chapter.

PART 2: PHOSPHORYLATION OF RED BLOOD CELL MEMBRANE PROTEINS

Introduction

During aging, RBCs suffer from lesions[4,5] that are characterized amongst other parameters by changes in cell morphology and increased cell rigidity[35–38] (as reported in Part 1 of this chapter). Cell shape is the result of different features (of which membrane deformability) influenced by cell vesiculation, osmolarity and ion transport, and membrane proteins/lipids organization in active or passive events[39,40]. Protein phosphorylation processes are involved in several mechanisms[41]. It was hypothesized that they regulate RBC membrane deformability which is a key parameter in tissue oxygenation.

The interactions membrane/cytoskeleton (whose rupture is observed in several diseases[39]) regulate the RBC shape change in an ATP-dependent manner[31,42]. Park *et al.* showed the participation of ATP in membrane fluctuations in addition to thermal effects[30]. They concluded that the non-equilibrium dynamism was due to the dissociation of the cytoskeleton at the spectrin junctions powered by ATP. However, once dissociated from the cytoskeleton, membrane fluctuations are thermally governed[43]. Several groups evoked the hypothesis of protein phosphorylation in the regulation of membrane deformability[30–34].

In RBCs, protein phosphorylation, *e.g.* of band 3, is known to regulate enzymatic activity[44–46]. More recently, phosphorylation of cytoskeleton and membrane proteins have been reported to modulate protein-protein interactions and to potentially affect membrane mechanical properties[47–51]. These phosphorylations involve adducin, β-spectrin, protein 4.1 as well as band 3. A few proteomic studies focusing on sickle cell disease identified several phosphoproteins and phophosites[52,53]. They pointed out their roles in signaling and in RBC deformability (through the phosphorylation of junctional complex proteins[54]).

Phosphorylation of band 3 has been studied since the 80s[55,56]. In 1991, Low and colleagues detected the presence of two kinases: p72[syk] (Syk) and p56/53[lyn] (Lyn) in RBCs, and demonstrated that Syk was responsible for band 3 phosphorylation under pervanadate treatment[57]. Later, Brunati *et al.* reported the sequential phosphorylation of band 3 by Syk on Tyr8 and Tyr21 and by Lyn on Tyr359 and Tyr904 (independent of Syk in the case of chorea-acanthocytosis[58])[59]. The same group also discovered the role of SHP-2 tyrosine phosphatase in the dephosphorylation of band 3 and Syk-mediated phosphorylation[60,61]. Protein Tyrosine Phosphatase (PTP) 1B participates also to the dephosphorylation of band 3[62]. Minetti *et al.* have shown that these two PTPs were differentially located. Under vesiculation, PTP1B remains on RBC membrane whereas SHP-2 tyrosine phosphatase

was present in MVs . Moreover, they pointed out that Syk was involved in cell volume-dependent response[64].

Protein phosphorylation could favor morphological changes in response to stress . Ferru *et al.* proposed a phosphorylation-induced oxidation mechanism where Syk binds to oxidized band 3, phosphorylates it and causes the weakening of the cytoskeleton and the formation of band 3 clusters that are released in MVs in thalassemia and Glucose-6-Phosphate Dehydrogenase (G6PD) deficiency[65,66]. On the opposite, Minetti *et al.* suggested that band 3 phosphorylation was not required in Ca^{2+}/ionophore-induced MVs[67]. Under blood banking conditions, where oxidative processes play an important role[68–70], MVs accumulate during storage[10], and the link to phosphorylation is unknown. Several questions remain open regarding all these regulation mechanisms and phosphorylation of proteins during storage of RBCs.

Study design

The aim of this study was to investigate the role of Tyrosine-phosphorylation (pY) of RBC membrane proteins in the context of transfusion. To do so, RBCs taken in 6 RCCs stored in SAGM for 2, 22 and 42 days were treated during 1 or 4 h at 37°C with 2 mM of Sodium Orthovanadate (OV). OV is an inhibitor of protein tyrosine phosphatases, which preparation described in ANNEX-5. Qualitative and quantitative analyses of the pY sites were conducted on the membrane proteins by Western Blot (WB) and phosphoproteomics. The impact of the treatment on the cell integrity was determined by measuring the microvesiculation and hemolysis (Figure 13).
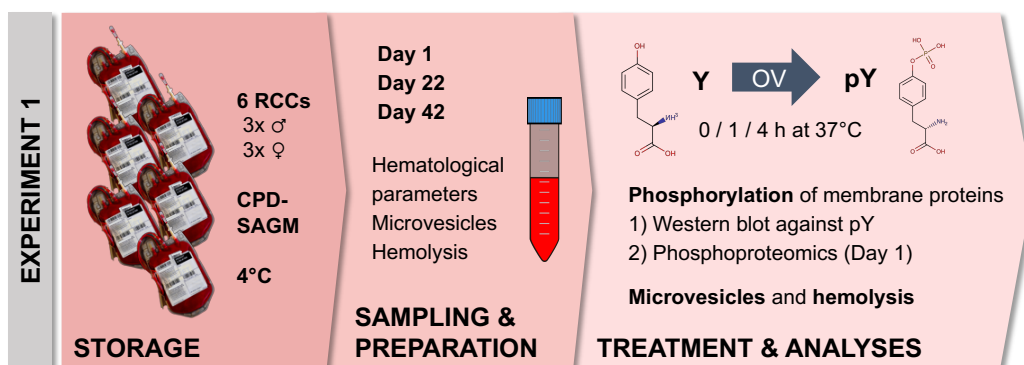
*Figure 13 – **Experimental workflow: sample preparation, treatment and analyses (experiment 1).** Six Red Cell Concentrates (RCCs) were sampled at day 1, 22 and 42, and hematological parameters, microvesicles and hemolysis were quantified. Then, the Red Blood Cells (RBCs) were treated with 2 mM Sodium Orthovanadate (OV) for 0, 1 or 4 h at 37°C and tyrosine phosphorylation (pY) of the membrane proteins was assessed by western blot and phosphoproteomics. The release of microvesicles and hemolysis triggered by the treatment were also quantified.*

A second experiment was then conducted to analyze the impact of the pY events on RBC morphology (Figure 14).
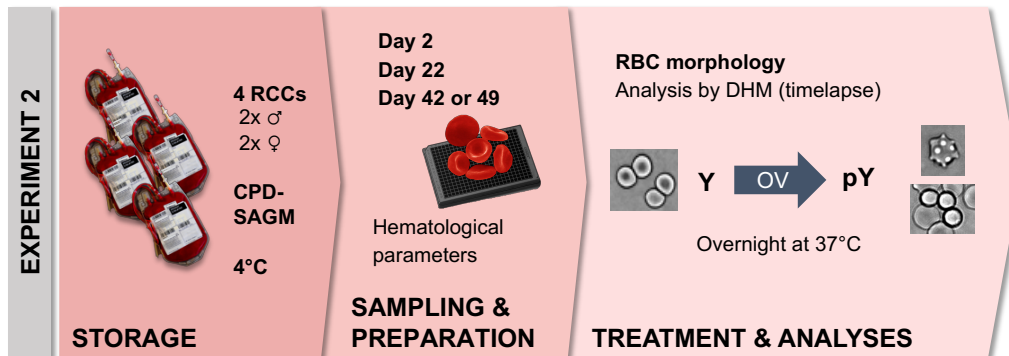
*Figure 14 – **Experimental workflow: sample preparation, treatment and analyses (experiment 2).** Four Red Cell Concentrates (RCCs) were sampled at day 2, 22 and 42 or 49, and hematological parameters, were analyzed. Then, the Red Blood Cells (RBCs) were treated with 2 mM Sodium Orthovanadate (OV) at 37°C and the impact of the treatment on the cell morphology was analyzed by Digital Holographic Microscopy (DHM).*

In the second experiment, RBCs withdrawn from four RCCs stored in SAGM for 2, 22 and 42 or 49 days were plated in a multiwell imaging plate and treated with 2 mM OV (37°C). The evolution of the cell morphology was followed during several hours with DHM.

Material and methods

Experiment 1

Treatment of the red blood cell with sodium orthovanadate and preparation of the membranes
Fourteen milliliters of RBCs were collected from six RCCs (see Table 4) after 1 day, 22 days and 42 days of storage.

*Table 4 – **Donor's characteristics**. Sex, age and blood group (ABO and Rhesus D) of the donor.*

Sample	Sex	Age / year	Blood group
RCC 1	Female	25	A+
RCC 2	Male	71	O+
RCC 3	Female	57	O+
RCC 4	Male	31	A+
RCC 5	Female	62	A+
RCC 6	Male	53	B+

RCC: Red Cell Concentrate.

A small amount (≈ 200 µL) of sample was put aside for Sysmex and MVs quantification (RCC sample), the rest was distributed into two tubes to optimize the wash and centrifuged at 2000 *g* during 10 min at 4°C. The supernatant was collected to measure the percentage of hemolysis in the blood bags. The RBCs were then washed (once at day 1 and twice at days 22 and 42) in 0.9 % NaCl (centrifugation as

before). The cell pellets were resuspended in two volumes of HEPA$_{noCalcium}$ (composition described in ANNEX-1) and incubated 1h at RT under agitation. To have samples as homogeneous as possible, the two aliquots were pooled and split again (2x 12 mL), and 240 µL of either dH$_2$O for control (Ctrl) or 100 mM OV (final concentration of 2 mM OV) were added. Immediately, Sysmex and MVs analyses were performed. Treated RBCs were incubated at 37°C on a roller for 1 and 4 h. Again, a small aliquot was put aside for Sysmex and MVs quantification and 5 mL of sample were centrifuged at 2000 g during 10 min at 4°C. The supernatant was again collected to measure the percentage of hemolysis and the RBCs were washed twice in HEPA$_{noCalcium}$. Finally, the cells were lysed by incubation in hypotonic buffer (PBS 0.1x) during 1h at 4°C on a roller, in presence (OV) or absence (Ctrl) of 2 mM OV. To separate the membranes from the intracellular content, the cell lysates were centrifuged at 100'000 g, 30 min, 4°C. The membranes were then transferred into 1.5-mL tubes for more washing steps (centrifugation at 21'500 g, 4°C, 30 min) until obtaining white membranes. Membrane aliquots were saved at -80°C until protein extraction for WB analysis or phosphoproteomics.

Western blot analysis against phosphorylated tyrosine

Membrane proteins were extracted from pelleted membranes with 4 volumes of DC buffer: 1 % deoxycholate in 50 mM Tris–HCl, 150 mM NaCl, pH 8.1. A final centrifugation was performed at 21'500 g, 30 min, 4°C and the supernatant, containing membrane proteins and cytoskeleton, was saved at 4°C[69]. Protein amounts were determined using the NanoDrop spectrophotometric method based on A280 absorbance. Ten µg of proteins from each sample and 10 µL of BenchMark Prestained Protein Ladder (Invitrogen™, ThermoFisher Scientific) were loaded on SDS-PAGE (Mini-PROTEAN TGX gels, 4-15 %, BIO-RAD). WB were performed on a Polyvinylidene Fluoride (PVDF) membrane (transfer 1h at 100 V in Tris-Glycine buffer inside a Mini Trans-Blot Electrophoretic Transfer cell) against pY-containing proteins. Membranes were blocked 1h at RT under agitation with Top Block buffer (Sigma-Aldrich, 4 % in TBS-T [1x TBS + 0.05 % Tween-20]). Then, the membranes were rinsed and washed 2x 5 min in TBS-T. The blot was incubated overnight at 4°C under agitation with the primary anti-pY antibody (pY PY99 1/6000 from Santa Cruz Biotechnology, in Top Block buffer). After a quick rinse and three washes of 5 min at RT in TBS-T, the membranes were re-incubated in Top block buffer at least 30 min at RT under agitation and were incubated 1h at RT under agitation with the secondary antibody (polyclonal goat anti-mouse immunoglobulins HRP, Dako) diluted at 1/10'000 in Top Block buffer. The membranes were finally washed 1 x 15 min and 2 x 5 min with TBS-T. The ECL reaction was achieved using the ECL western blotting detection reagents (GE Healthcare) 1 min in the dark, the images were acquired by means of ImageQuant LAS 500 (GE Healthcare) and quantitation of protein phosphorylation content was achieved with the ImageQuant TL 7.0 software (GE Healthcare). WB membranes were finally stained with Ponceau red and scanned with a Personal Densitometer SI (GE healthcare).

Phosphoproteomics

Protein extracts from short-term stored RCCs (RCC 1-6), OV-treated or not, were prepared in 4 volumes of extraction buffer (8 M Urea, 2 M Thiourea, 0.5 % SDS and 10 mM DTE). Each sample (300 µg) was buffered in with Tris-HCl, pH 8.5 at final concentration of 30 mM and 0.3 % RapiGest. Reduction was performed at 37°C for 1 h. Samples were buffered to pH 8.5 using Tris pH 10-11 and protein alkylation was performed with 40 mM iodoacetamide at 37°C in the dark for 45 min. Reaction was quenched using DTE to a final concentration of 10 mM. A two-step digestion was performed using first Lys-C (1:50 enzyme/protein) for 2 h at 37°C. Samples were then diluted 5-fold with 50 mM ammonium bicarbonate and the second digestion was performed overnight using Trypsin gold (1:50 enzyme/protein) and 10 mM CaCl$_2$. Reaction was stopped and RapiGest cleaved by addition of pure Trifluoroacetic Acid (TFA) during a final 1 h incubation at 37°C. Samples were concentrated by vacuum centrifugation to a final volume of 0.6 mL and desalted using Sep-Pak SPE cartridges 1cc/100 mg following manufacturer's instructions. Samples were dried by vacuum centrifugation and stored at -20°C before further phosphopeptide enrichment. Phosphopeptide capture was performed on homemade titania tips as described previously[71]. For LC-MS/MS analysis, enriched phosphopeptides were resuspended in 2 % ACN, 0.1 % FA and separated by reversed phase chromatography on a Dionex Ultimate 3000 RSLC nanoUPLC system connected on-line with an Orbitrap Q-Exactive HF.

Raw data were analyzed using MaxQuant 1.6.0.1[72] with Andromeda as internal database search engine[73]. Fragmentation spectra were searched against the human UniProt database (July 2017 - 71'567 sequences). A threshold of 1 % False Discovery Rate (FDR) was fixed at peptide and protein levels. Mass spectra were searched with a mass tolerance of 6 ppm in MS mode and 0.5 Da in MS/MS mode. Up to two missed cleavages were allowed and carbamidomethylation was set as a fixed modification. Oxidation (M), acetylation (Protein N-term) and phosphorylation (Serine [S], Threonine [T], Tyrosine [Y]) were considered as variable modifications. A minimum peptide length of seven amino acids and at least one peptide for protein identification was required. A minimum of seven amino acids was required as peptide length and at least one peptide was required for protein identification. Class1 phosphosites (*i.e.* localization probability > 0.75)[74] quantified in at least twelve of the seventeen (Ctrl group) or eighteen (OV treated group) LC-MS/MS runs per biological condition were analyzed in Perseus, a tool from the MaxQuant suite. Missing values were imputed with random numbers from a normal distribution (width = 0.7, down-shift = 1.8)[75]. Normalized intensities were compared between OV-treated and not treated protein extracts, using a statistical Welsch t-test with a permutation-based FDR of 0.05 for multiple testing. A threshold based on both t-test values and the ratios (SO = 1) was used to discriminate differentially quantified phosphosites[75,76]. Graphical views were generated with homemade programs written in the R environment[77].

Experiment 2

Preparation of the red blood cells for analysis with digital holographic microscopy

Samples (3.2 mL) were collected from four RCCs (see Table 5) at different lengths of storage, *i.e.* 2 days, 22 days and 42 days for RCC 1 and 2, or 49 days for RCC 3 and 4.

Table 5 – **Donor's characteristics**. *Sex, age and blood group (ABO and Rhesus D) of the donor.*

Sample	Sex	Age / year	Blood group
RCC 1	Male	37	A+
RCC 2	Male	52	O+
RCC 3	Male	57	O-
RCC 4	Male	61	A+

RCC: Red Cell Concentrate.

Approximatively 200 μL of sample were kept for hematological analysis (Sysmex). The RBCs were washed twice in 0.9 % NaCl and spun down (centrifugation at 2000 g for 10 min at 4°C). The cell pellets were then resuspended in two volumes of HEPA$_{noCalcium}$ and a Sysmex analysis was done to determine the cell count, before diluting the sample (still in HEPA$_{noCalcium}$) to obtain a concentration of 1×10^9 cells/L. Eighty μL of RBCs were seeded (which is equivalent to 80'000 cells per well) in 96-well imaging plate coated with 0.1 mg/ml poly-L-ornithine. To speed up the sedimentation process, the plate was centrifuged 2 min at 140 g and RT.

Treatment with sodium orthovanadate and image acquisition with digital holographic microscope

For image acquisition, the plate was placed in the DHM incubator system set at 37°C with high humidity and 5 % CO$_2$. The cells were observed at a 20x magnification and four images per well were taken. First, 3 baseline images were acquired at 5 min interval. The RBCs were then treated with 0.2 % DMSO and incubated in the same conditions during 60 min (10 image acquisitions, each 5 min). Finally, the RBCs were treated with 2 mM OV (10 μL of 20 mM OV) or control dH$_2$O (Ctrl). Time-lapse images were taken once every hour during approximately 18 h.

Results and discussion

The six RCCs used for this experiment evolved normally during storage with an increase in volume (Figure 15A), MV count and percentage of hemolysis (Figure 15B).
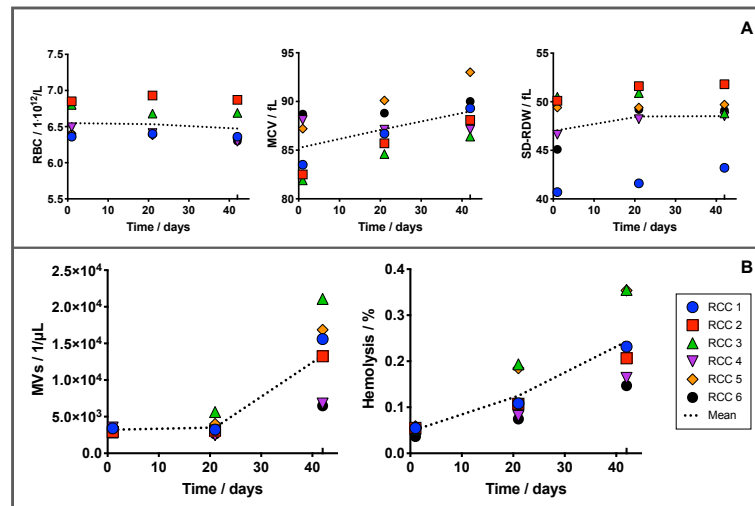
*Figure 15 – **Evolution of some Red Blood Cell (RBC) aging parameters in Red Cell Concentrates (RCCs).** [A] Hematological data: RBC count [left], Mean Corpuscular Volume (MCV) [middle] and Standard Deviation of Distribution Width (SD-RDW) [right]. [B] Microvesicle (MV) count [left] and percentage of hemolysis [right]. Data for the 6 RCCs. Individual (symbols) and mean values (dotted line).*

OV treatment inhibits the PTP and thus lead to the accumulation of the pY. Figure 16A shows the pY signal after the OV treatment for 1 and 4 h (and the corresponding negative control). The pY phosphorylation was observed on specific proteins. They correspond (from top to bottom) to α-spectrin, β-spectrin, ankyrin-1; α-adducin, β-adducin, band 3, protein 4.1 and two bands around 70 kDa that could correspond to Syk and Lyn kinases. In the course of RBC storage, the effect of OV and therefore the capacity to phosphorylate was progressively decreased (Figure 16B).
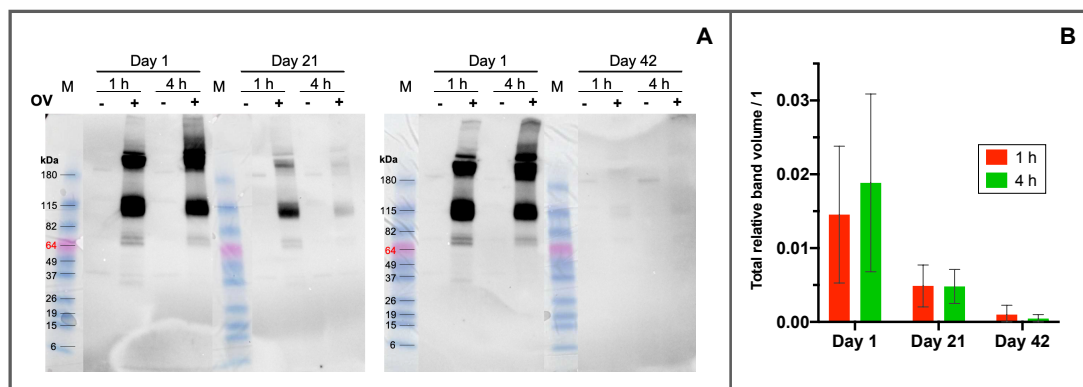
*Figure 16 – **Western blot (WB) analysis of tyrosine-phosphorylation (pY) in red blood cell (RBC) membranes proteins under sodium orthovanadate (OV) treatment in function of storage time.** [A] Representative image of a WB experiment (sample 2) against pY-containing membrane proteins. OV: OV-treated RBCs, M: molecular weight marker. To be noted that the marker bands is coming from the white light image and was superimposed on the chemiluminescence picture. [B] Mean of the total relative pY signal (i.e. sum of pY-positive bands normalized by total protein loading [Ponceau red]) for the 6 red cell concentrates $\pm$ standard deviation.*

The loss of kinase activity could be explained by the decreasing level of available ATP throughout storage because of the metabolic shift from glycolysis to PPP and the general slow-down of the metabolism (1.5- to 2-fold decrease over the storage period)[35,78,79].

To identify and quantify phosphoproteins, a label-free quantitative phosphoproteomic analysis of RBC membrane proteins treated or not with OV was carried out. T-tests were performed on 17 different conditions for the control and 18 for the OV treatment. From the quality control analysis, it appeared that one triplicate of the RCC 5 control sample was clearly an outlier (based on the ClassI phosphosites). This sample was thus removed from the analysis. Proteins with at least 12 valid values in at least one group (OV or Ctrl) were kept for the analysis.
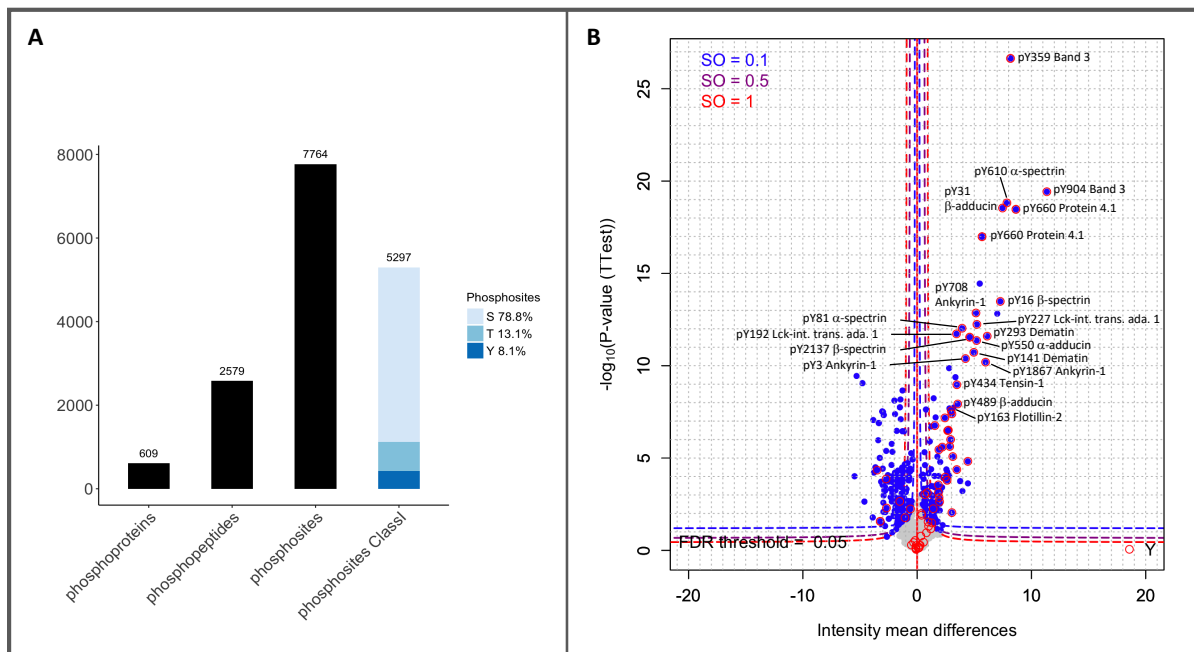
*Figure 17 – **Phosphoproteomics of Red Blood Cell (RBC) membranes proteins under Sodium Orthovanadate (OV) treatment.** [A] Phosphoproteome depth: number of identified phosphoproteins, phospho-peptides, phospho-sites and ClassI phospho-sites. In different colors of blue are represented the number of phosphorylated Serine ([S], 78.8 %), Threonine ([T], 13.1 %) and Tyrosine ([Y], 8.1 %). [B] Comparison of phospho-sites after 1 h of OV treatment versus without any treatment. Volcano plot showing t-test p-values versus phospho-site fold changes (log₁₀). Dark blue points correspond to phospho-sites differentially quantified and unchanged phospho-sites are in grey. Phosphorylated Tyrosines (pY) are surrounded by a red circle.*

The analysis revealed the presence of 2'579 phosphopeptides (5'297 ClassI phosphosites, *i.e.* localization probability > 0.75) corresponding to 609 phosphoproteins (Figure 17A). The distribution of pS, pT, and pY sites is 78.8 %, 13.1 %, and 8.1 % respectively. Upon OV treatment, 40 pY-sites belonging to 21 different proteins were significantly upregulated (Figure 17B) and 5 were downregulated (the complete list of proteins is provided in ANNEX-6). The first 20 upregulated pY-sites belong to proteins mainly involved in the cell structure, *i.e.* Band 3, α- and β-spectrin, α- and β-adducin, protein 4.1, ankyrin-1, dematin, tensin-1 and flotillin-2, which is coherent with the WB analysis.

The OV treatment induced the release of MVs (Figure 18, left) and hemolysis (Figure 18, right). This effect was mainly visible after 4 h of incubation but not after 1 h. Consistently with the phosphorylation levels, RBCs stored for 1 day released a higher number of MVs and hemolyzed more compared to RBCs stored for 22 or 42 days.
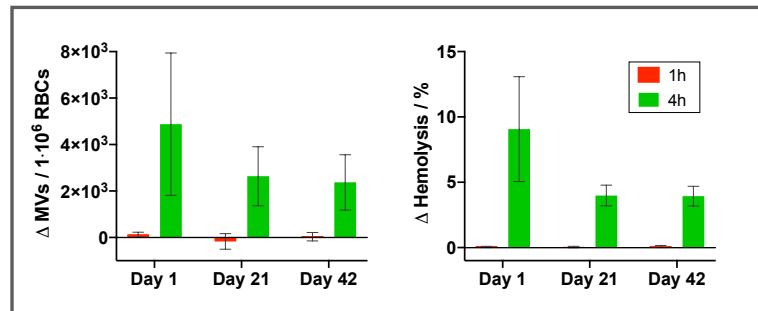
*Figure 18 – **Microvesiculation and hemolysis induced by 1 or 4 h Sodium Orthovanadate (OV) treatment**. Number of Microvesicles (MVs) released per million Red Blood Cells (RBCs) because of the treatment, i.e. number of MVs in OV sample minus Ctrl sample, corrected by the number of RBCs in the sample [left]. Hemolysis induced by the treatment, i.e. percentage of hemolysis in OV sample minus control sample [right]. Mean value for the 6 red cell concentrates ± standard deviation.*

Finally, the DHM analysis indicated that the RBC morphology was impacted by the OV treatment, *i.e.* increase of SD-OPD (Figure 19A). As shown before (refer to ANNEX-3), this parameter is positively correlated with the number of spherocytes in the sample. The increase of SD-OPD signal corresponded to the transformation of RBCs from discocytes to echinocytes and finally spherocytes (Figure 19C).
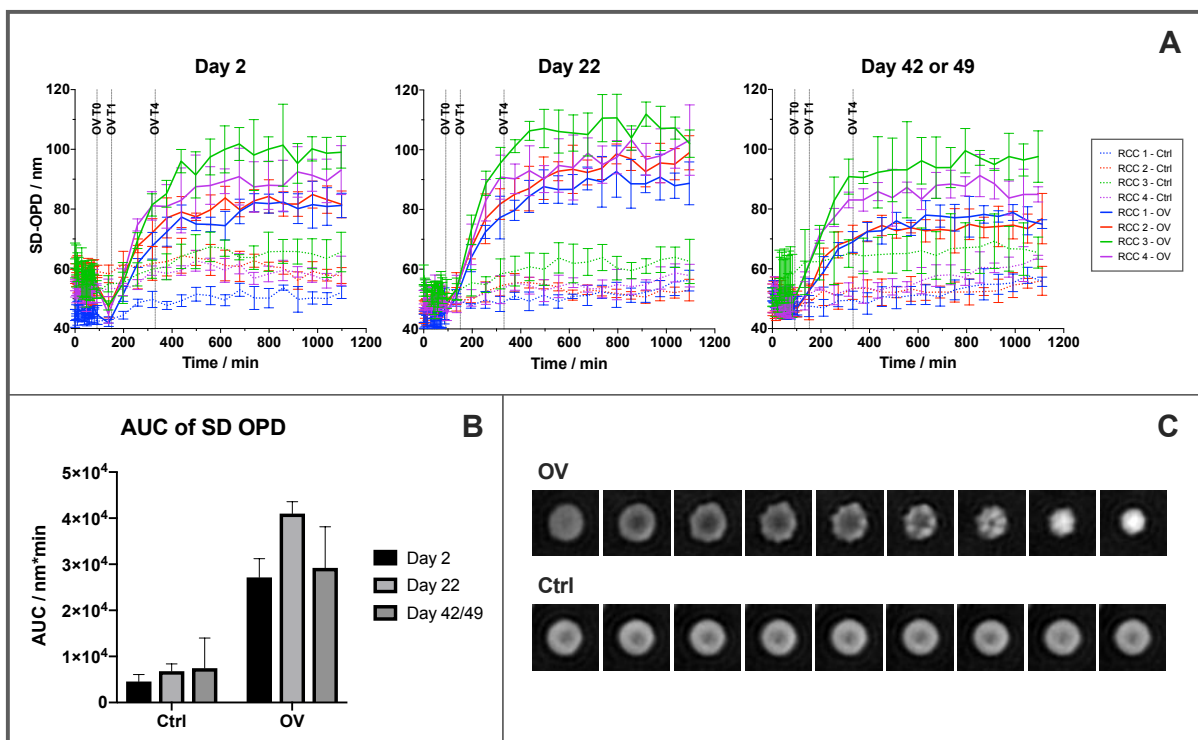
*Figure 19 – **Red Blood Cell (RBC) morphology and effect of Sodium Orthovanadate (OV) treatment evaluated using Digital Holographic Microscopy (DHM).** [A] OV-induced morphology changes in RBCs stored for 2, 22 and 42 (for Red Cell Concentrate [RCC] 1 and 2) or 49 days (for RCC 3 and 4), measured with DHM. The RBCs were plated in a 96-well imaging plate and were*

then treated with 0.2 % DMSO (dotted lines) or 2 mM OV (solid lines). The plate was incubated at 37°C, 5 % CO$_2$ and high humidity during the timelapse analysis (approx. 18 h). Mean SD-OPD for twelve wells ± Standard Deviation (SD). [B] Area Under the Curve (AUC) of Standard Deviation of Optical Path Difference (SD-OPD) curves presented in [A]. Mean values for the four RCCs ±SD. [C] Illustration of the morphological changes induced by 2 mM OV treatment (top) or Ctrl (bottom). Phase images were acquired with DHM at 20x magnification.

The results of the morphological analysis seem to indicate that the effect of OV is not only related to the phosphorylation. Indeed, the morphology of RBC stored for 22 days was even more impacted by the OV treatment (Figure 19B), although less pY were detected by WB analysis. Similarly, OV induced changes of morphology in long-term stored RBCs, whereas the no pY could be detected. Hence, the effect of OV could: 1) be related to side-effects, because the vanadate can also inhibits the enzymes alkaline phosphatase, ATPase, adenosine kinase and phosphofructokinase[80,81], or 2) to the sensitivity of the RBCs to the treatment. Hence, one could imagine that aged RBCs will be more impacted by a small level of phosphorylation than young ones.

Conclusions

The data presented in this Part 2 focused on phosphorylation events of membrane proteins, where band 3, β-spectrin and Lyn kinase play a key role. The phosphorylation was here forced inducing the release of MVs, morphological changes and hemolysis (OV treatment exacerbated the phosphorylation). The capacity of phosphorylation is clearly lost during the storage of RBCs because of the progressive ATP depletion. Indeed, rejuvenation experiments (which consists in incubating the RBCs during 60 min at 37°C with sodium pyruvate, inosine, adenine, mono- and dibasic sodium phosphate) conducted during preliminary tests enabled to fully recover the pY signal in WB analysis. It indicates that the kinases are still functional and that the decrease in phosphorylation is a metabolic issue. The proteins targeted were then deeply investigated by phosphoproteomics. This analysis highlights also the potential differences between *in vivo* and *ex vivo* aging[82]. Indeed, the absence of phosphorylation in long-term stored RCCs indicates that the microvesiculation should be triggered by other mechanism such as the accumulation of oxidized proteins at the membrane and/or membrane perturbation and reorganization. In future experiments, it is planned to use Kinase Inhibitors (KI) in order to elucidate the regulation mechanisms and individual contribution of the different pY events to the morphological changes.

GENERAL CONCLUSIONS

A blood bag is a confined, static and artificial environment where the RBCs are surrounded by additive solution, plastic, other RBCs and, as storage goes on, waste products, rather than plasma and cells from the circulation (*i.e.* leucocytes, platelets and endothelial cells), which implies that the exchanges and equilibrium with the environment are totally upset. Moreover, placing the RBCs in hypothermia, *i.e.* 4°C, is not without consequences, notably for the rate of the metabolic fluxes. The two studies presented in this Chapter confirmed that the storage impacts profoundly the RBCs.

Nowadays, RCCs fulfill quality controls if they exhibit, at the end of the storage period, a level of hemolysis below 0.8 % and if 75 % percent of the transfused RBCs are still viable 24-h post-transfusion. These two parameters are however impossible to test for each RCC and for defined time-points, but are also difficult to measure, for example, assessment of the cell viability requires to transfuse RBCs labelled with [51]chromium. Other criteria are thus necessary to assess the quality of the transfused RCCs.

To this day, much efforts were made by the transfusion community to find a marker reflecting with accuracy the health status of the RBCs within the RCCs in order to predict their efficiency post-transfusion. For example, a positive relationship between the intracellular ATP concentration and the percentage of 24-h recovery post transfusion was demonstrated[83]. Recently, Paglia *et al*. proposed 8 extracellular metabolites to describe the different metabolic phases during storage[84]. More particularly, hypoxanthine levels were shown to be negatively correlated with the recirculation rate post-transfusion[85]. The appearance of cytosolic Peroxiredoxin 2 (Prx 2) at the inner cell membrane was proposed by Rinalducci *et al.* as it reflects the oxidative stress[86]. Proteins biomarkers in the supernatant were also highlighted by D'Alessandro *et al.*[87]. Finally, Roussel *et al.* demonstrated by imaging flow cytometry a marked accumulation of small RBCs after 28 days of storage, which are more prone to be eliminated after transfusion[88].

Here, different analysis parameters were used as they offer unique tools to assess RBC health state. AOP can be an easy-to-monitor single parameter allowing to obtain a quick glance at the cell state. Moreover, combining multiple easy-to-obtain parameters providing different information like AOP yielding information on oxidative stress, percentage of spherocytes yielding information about morphological perturbation and CMF yielding information on membrane state could greatly help quantifying RBC aging and helping discard prematurely old RBC pouches before transfusion.

Interestingly, important differences appeared when looking at RCCs aging markers individually, which opens the question of the uniformity of the blood products quality. Indeed, many studies showed that the extent of RBCs storage lesions and their capacity for post-transfusion recovery can be subject to important variability[89]. One factor explaining such discrepancy is the "donor-variation

effect"[90,91]. Indeed, blood is a biological product derived from female and male donors, from different ages and blood groups, who are genetically distinct, and with specific body constitution and lifestyle (dietary, physical, sleeping and smoking habits, etc.)[92–94]. Then, not just one kind of additive solution is used worldwide, but different types with diverse formulations, pH and osmolarity that may impact RBCs differently. In addition, the manufacturing parameters, such as the holding time between the whole blood donation and the blood component separation, the processing method (whole-blood or buffy-coat), the preparation parameters (centrifugation time and speed) and the type of commercial kit used, certainly have an effect on the final RCC characteristics[95–97]. For example, it was demonstrated that RBCs from donors exhibiting high levels of plasma uric acid antioxidant are better storers than those from low-levels of uric acid[98]. Inter-donor variability is linked to gender, age, ethnic groups, blood group, weight, genetic background and lifestyle[99].

The second study has shown that phosphorylation events of membrane proteins are related to various morphological lesions in RBCs. Therefore, problems in phosphorylation may render RBCs less efficient in crossing capillaries. Even though this ATP-dependent mechanism was restored *in vitro* or *in vivo* a few hours after transfusion[100], it is important to keep constantly a high level of phosphorylation capacity to ensure transfusion efficiency. This capacity could be conserved by boosting metabolism (particularly the lower part of glycolysis and the PPP, RBCs being devoid of mitochondria). As a benefit, the formation of lesions that decrease the shape change capacity should be postponed[29].

REFERENCES

1. Antonelou MH, Tzounakas VL, Velentzas AD, et al. Effects of pre-storage leukoreduction on stored red blood cells signaling: A time-course evaluation from shape to proteome. *J. Proteomics*. 2012;76:220–238.

2. Kim Y, Xia BT, Chang AL, Pritts TA. Role of Leukoreduction of Packed Red Blood Cell Units in Trauma Patients: A Review. *Int. J. Hematol. Res.* 2016;2(2):124–129.

3. Sparrow RL. Time to revisit red blood cell additive solutions and storage conditions: a role for "omics" analyses. *Blood Transfus.* 2012;10(Suppl 2):s7-11.

4. D'Alessandro A, Kriebardis AG, Rinalducci S, et al. An update on red blood cell storage lesions, as gleaned through biochemistry and omics technologies. *Transfusion*. 2015;55(1):205–219.

5. Yoshida T, Prudent M, D'Alessandro A. Red blood cell storage lesion: causes and potential clinical consequences. *Blood Transfus.* 2019;17(1):27–52.

6. Bardyn M, Rappaz B, Jaferzadeh K, et al. Red blood cells ageing markers: a multi-parametric analysis. *Blood Transfus*. 2017;15(3):239–248.

7. Hess JR. Red cell changes during storage. *Transfus. Apher. Sci.* 2010;43(1):51–59.

8. Tacchini P, Lesch A, Neequaye A, et al. Electrochemical Pseudo-Titration of Water-Soluble Antioxidants. *Electroanalysis*. 2013;25(4):922–930.

9. Lesch A, Cortés-Salazar F, Prudent M, et al. Large scale inkjet-printing of carbon nanotubes electrodes for antioxidant assays in blood bags. *J. Electroanal. Chem.* 2014;717–718:61–68.

10. Rubin O, Crettaz D, Canellini G, Tissot J-D, Lion N. Microparticles in stored red blood cells: an approach using flow cytometry and proteomic tools. *Vox Sang.* 2008;95(4):288–297.

11. Han V, Serrano K, Devine DV. A comparative study of common techniques used to measure haemolysis in stored red cell concentrates. *Vox Sang.* 2010;98(2):116–123.

12. Giustarini D, Dalle-Donne I, Milzani A, Fanti P, Rossi R. Analysis of GSH and GSSG after derivatization with N-ethylmaleimide. *Nat. Protoc.* 2013;8(9):1660–1669.

13. Depeursinge C, Colomb T, Emery Y, et al. Digital holographic microscopy applied to life sciences. *Conf. Proc. IEEE Eng. Med. Biol. Soc*. 2007;6243–6246.

14. Rappaz B, Barbul A, Emery Y, et al. Comparative study of human erythrocytes by digital holographic microscopy, confocal microscopy, and impedance volume analyzer. *Cytometry A*. 2008;73A(10):895–903.

15. Rappaz B, Marquet P, Cuche E, et al. Measurement of the integral refractive index and dynamic cell morphometry of living cells with digital holographic microscopy. *Opt. Express*. 2005;13(23):9361–9373.

16. Kühn J, Shaffer E, Mena J, et al. Label-Free Cytotoxicity Screening Assay by Digital Holographic Microscopy. *Assay Drug Dev. Technol.* 2013;11(2):101–107.

17. Marquet P, Rappaz B, Magistretti PJ, et al. Digital holographic microscopy: a noninvasive contrast imaging technique allowing quantitative visualization of living cells with subwavelength axial accuracy. *Opt. Lett.* 2005;30(5):468.

18. Rappaz B, Breton B, Shaffer E, Turcatti G. Digital Holographic Microscopy: a quantitative label-free microscopy technique for phenotypic screening. *Comb. Chem. High Throughput Screen.* 2014;14(1):80.

19. Carpenter AE, Jones TR, Lamprecht MR, et al. CellProfiler: image analysis software for identifying and quantifying cell phenotypes. *Genome Biol.* 2006;7(10):R100.

20. Kamentsky L, Jones TR, Fraser A, et al. Improved structure, function and compatibility for

CellProfiler: modular high-throughput image analysis software. *Bioinformatics*. 2011;27(8):1179–1180.

21. Jones TR, Kang I, Wheeler DB, et al. CellProfiler Analyst: data exploration and analysis software for complex image-based screens. *BMC Bioinformatics*. 2008;9(1):482.

22. Jones TR, Carpenter AE, Lamprecht MR, et al. Scoring diverse cellular morphologies in image-based screens with iterative feedback and machine learning. *Proc. Natl. Acad. Sci.* 2009;106(6):1826–1831.

23. Rappaz B, Barbul A, Hoffmann A, et al. Spatial analysis of erythrocyte membrane fluctuations by digital holographic microscopy. *Blood Cells. Mol. Dis.* 2009;42(3):228–232.

24. Flatt JF, Bawazir WM, Bruce LJ. The involvement of cation leaks in the storage lesion of red blood cells. *Front. Physiol.* 2014;5:214.

25. Bordbar A, Johansson PI, Paglia G, et al. Identified metabolic signature for assessing red blood cell unit quality is associated with endothelial damage markers and clinical outcomes. *Transfusion*. 2016;56(4):852-862.

26. D'Alessandro A, D'Amici GM, Vaglio S, Zolla L. Time-course investigation of SAGM-stored leukocyte-filtered red bood cell concentrates: from metabolism to proteomics. *Haematologica*. 2012;97(1):107–115.

27. Evans J, Gratzer W, Mohandas N, Parker K, Sleep J. Fluctuations of the red blood cell membrane: relation to mechanical properties and lack of ATP dependence. *Biophys. J.* 2008;94(10):4134–4144.

28. Prudent M, Rappaz B, Hamelin R, et al. Loss of Protein Tyr-phosphorylation During in vitro Storage of Human Erythrocytes: Impact on RBC Morphology. *Transfusion*. 2014;54:49A-50A.

29. Prudent M, Tissot J-D, Lion N. In vitro assays and clinical trials in red blood cell aging: Lost in translation. *Transfus. Apher. Sci.* 2015;52(3):270–276.

30. Park Y, Best CA, Auth T, et al. Metabolic remodeling of the human red blood cell membrane. *Proc. Natl. Acad. Sci.* 2010;107(4):1289–1294.

31. Gov NS, Safran SA. Red blood cell membrane fluctuations and shape controlled by ATP-induced cytoskeletal defects. *Biophys. J.* 2005;88(3):1859–1874.

32. Cluitmans JC, Hardeman MR, Dinkla S, Brock R, Bosman GJ. Red blood cell deformability during storage: towards functional proteomics and metabolomics in the Blood Bank. *Blood Transfus.* 2012;10 Suppl 2:s12-18.

33. Boivin P. Role of the phosphorylation of red blood cell membrane proteins. *Biochem. J.* 1988;256(3):689–695.

34. Levin S, Korenstein R. Membrane fluctuations in erythrocytes are linked to MgATP-dependent dynamic assembly of the membrane skeleton. *Biophys. J.* 1991;60(3):733–737.

35. Hess JR, Lippert LE, Derse-Anthony CP, et al. The effects of phosphate, pH, and AS volume on RBCs stored in saline-adenine-glucose-mannitol solutions. *Transfusion*. 2000;40(8):1000–1006.

36. Sparrow RL, Sran A, Healey G, Veale MF, Norris PJ. In vitro measures of membrane changes reveal differences between red blood cells stored in saline-adenine-glucose-mannitol and AS-1 additive solutions: a paired study. *Transfusion*. 2014;54(3):560–568.

37. Moon I, Yi F, Lee YH, et al. Automated quantitative analysis of 3D morphology and mean corpuscular hemoglobin in human red blood cells stored in different periods. *Opt. Express*. 2013;21(25):30947–30957.

38. Kozlova E, Chernysh A, Moroz V, et al. Morphology, membrane nanostructure and stiffness

for quality assessment of packed red blood cells. *Sci. Rep.* 2017;7(1):7846.

39. Mohandas N, Gallagher PG. Red cell membrane: past, present, and future. *Blood*. 2008;112(10):3939–3948.

40. Lang F, Busch GL, Ritter M, et al. Functional significance of cell volume regulatory mechanisms. *Physiol. Rev.* 1998;78(1):247–306.

41. Pantaleo A, De Franceschi L, Ferru E, Vono R, Turrini F. Current knowledge about the functional roles of phosphorylative changes of membrane proteins in normal and diseased red cells. *J. Proteomics*. 2010;73(3):445–455.

42. Gov N, Cluitmans J, Bosman GJ. Chapter 4 Cytoskeletal Control of Red Blood Cell Shape: Theory and Practice of Vesicle Formation. In: A. Leitmannova L, Aleš I. Advances in Planar Lipid Bilayers and Liposomes. Vol. 10 ed. Academic Press; 2009:95-119.

43. Boss D, Hoffmann A, Rappaz B, et al. Spatially-resolved eigenmode decomposition of red blood cells membrane fluctuations questions the role of ATP in flickering. *PloS One*. 2012;7(8):e40667.

44. Harrison ML, Rathinavelu P, Arese P, Geahlen RL, Low PS. Role of band 3 tyrosine phosphorylation in the regulation of erythrocyte glycolysis. *J. Biol. Chem.* 1991;266(7):4106–4111.

45. Low PS, Rathinavelu P, Harrison ML. Regulation of glycolysis via reversible enzyme binding to the membrane protein, band 3. *J. Biol. Chem.* 1993;268(20):14627–14631.

46. Lewis IA, Campanella ME, Markley JL, Low PS. Role of band 3 in regulating metabolic flux of red blood cells. *Proc. Natl. Acad. Sci. U. S. A.* 2009;106(44):18515–18520.

47. Ferru E, Giger K, Pantaleo A, et al. Regulation of membrane-cytoskeletal interactions by tyrosine phosphorylation of erythrocyte band 3. *Blood*. 2011;117(22):5998–6006.

48. Gauthier E, Guo X, Mohandas N, An X. Phosphorylation-dependent perturbations of the 4.1R-associated multiprotein complex of the erythrocyte membrane. *Biochemistry*. 2011;50(21):4561–4567.

49. Manno S, Takakuwa Y, Mohandas N. Modulation of erythrocyte membrane mechanical function by protein 4.1 phosphorylation. *J. Biol. Chem.* 2005;280(9):7581–7587.

50. Kalfa TA, Pushkaran S, Mohandas N, et al. Rac GTPases regulate the morphology and deformability of the erythrocyte cytoskeleton. *Blood*. 2006;108(12):3637–3645.

51. George A, Pushkaran S, Li L, et al. Altered phosphorylation of cytoskeleton proteins in sickle red blood cells: the role of protein kinase C, Rac GTPases, and reactive oxygen species. *Blood Cells. Mol. Dis.* 2010;45(1):41–45.

52. Soderblom EJ, Thompson JW, Schwartz EA, et al. Proteomic analysis of ERK1/2-mediated human sickle red blood cell membrane protein phosphorylation. *Clin. Proteomics*. 2013;10(1):1.

53. Siciliano A, Turrini F, Bertoldi M, et al. Deoxygenation affects tyrosine phosphoproteome of red cell membrane from patients with sickle cell disease. *Blood Cells. Mol. Dis.* 2010;44(4):233–242.

54. Burton NM, Bruce LJ. Modelling the structure of the red cell membrane. *Biochem. Cell Biol.* 2011;89(2):200–215.

55. Dekowski SA, Rybicki A, Drickamer K. A tyrosine kinase associated with the red cell membrane phosphorylates band 3. *J. Biol. Chem.* 1983;258(5):2750–2753.

56. Low PS, Allen DP, Zioncheck TF, et al. Tyrosine phosphorylation of band 3 inhibits peripheral protein binding. *J. Biol. Chem.* 1987;262(10):4592–4596.

57. Harrison ML, Isaacson CC, Burg DL, Geahlen RL, Low PS. Phosphorylation of human erythrocyte band 3 by endogenous p72syk. *J. Biol. Chem.* 1994;269(2):955–959.

58. De Franceschi L, Tomelleri C, Matte A, et al. Erythrocyte membrane changes of chorea-acanthocytosis are the result of altered Lyn kinase activity. *Blood*. 2011;118(20):5652–5663.

59. Brunati AM, Bordin L, Clari G, et al. Sequential phosphorylation of protein band 3 by Syk and Lyn tyrosine kinases in intact human erythrocytes: identification of primary and secondary phosphorylation sites. *Blood*. 2000;96(4):1550–1557.

60. Bordin L, Ion-Popa F, Brunati AM, Clari G, Low PS. Effector-induced Syk-mediated phosphorylation in human erythrocytes. *Biochim. Biophys. Acta*. 2005;1745(1):20–28.

61. Bordin L, Brunati AM, Donella-Deana A, et al. Band 3 is an anchor protein and a target for SHP-2 tyrosine phosphatase in human erythrocytes. *Blood*. 2002;100(1):276–282.

62. Zipser Y, Kosower NS. Phosphotyrosine phosphatase associated with band 3 protein in the human erythrocyte membrane. *Biochem. J.* 1996;314 (Pt 3):881–887.

63. Minetti G, Ciana A, Balduini C. Differential sorting of tyrosine kinases and phosphotyrosine phosphatases acting on band 3 during vesiculation of human erythrocytes. *Biochem. J.* 2004;377(Pt 2):489–497.

64. Minetti G, Seppi C, Ciana A, et al. Characterization of the hypertonically induced tyrosine phosphorylation of erythrocyte band 3. *Biochem. J.* 1998;335 (Pt 2):305–311.

65. Ferru E, Pantaleo A, Carta F, et al. Thalassemic erythrocytes release microparticles loaded with hemichromes by redox activation of p72Syk kinase. *Haematologica*. 2014;99(3):570–578.

66. Pantaleo A, Ferru E, Carta F, et al. Irreversible AE1 tyrosine phosphorylation leads to membrane vesiculation in G6PD deficient red cells. *PloS One*. 2011;6(1):e15847.

67. Minetti G, Piccinini G, Balduini C, Seppi C, Brovelli A. Tyrosine phosphorylation of band 3 protein in Ca2+/A23187-treated human erythrocytes. *Biochem. J.* 1996;320 (Pt 2):445–450.

68. Antonelou MH, Kriebardis AG, Stamoulis KE, et al. Red blood cell aging markers during storage in citrate-phosphate-dextrose-saline-adenine-glucose-mannitol. *Transfusion*. 2010;50(2):376–389.

69. Delobel J, Prudent M, Rubin O, et al. Subcellular fractionation of stored red blood cells reveals a compartment-based protein carbonylation evolution. *J. Proteomics*. 2012;76 Spec No.:181–193.

70. Delobel J, Prudent M, Tissot J-D, Lion N. Proteomics of the red blood cell carbonylome during blood banking of erythrocyte concentrates. *Proteomics Clin. Appl.* 2016;10(3):257–266.

71. Cox J, Matic I, Hilger M, et al. A practical guide to the MaxQuant computational platform for SILAC-based quantitative proteomics. *Nat. Protoc.* 2009;4(5):698–705.

72. Matz A, Halamoda-Kenzaoui B, Hamelin R, et al. Identification of new Presenilin-1 phosphosites: implication for γ-secretase activity and Aβ production. *J. Neurochem.* 2015;133(3):409–421.

73. Cox J, Mann M. MaxQuant enables high peptide identification rates, individualized p.p.b.-range mass accuracies and proteome-wide protein quantification. *Nat. Biotechnol.* 2008;26(12):1367–1372.

74. Cox J, Neuhauser N, Michalski A, et al. Andromeda: a peptide search engine integrated into the MaxQuant environment. *J. Proteome Res.* 2011;10(4):1794–1805.

75. Olsen JV, Blagoev B, Gnad F, et al. Global, in vivo, and site-specific phosphorylation dynamics in signaling networks. *Cell*. 2006;127(3):635–648.

76. Hubner NC, Mann M. Extracting gene function from protein-protein interactions using Quantitative BAC InteraCtomics (QUBIC). *Methods.* 2011;53(4):453–459.

77. R Core Team (2018). R: A language and environment for statistical computing. R Foundation for Statistical Computing, Vienna, Austria. Available at: https://www.R-project.org/.

78. Salzer U, Zhu R, Luten M, et al. Vesicles generated during storage of red cells are rich in the lipid raft marker stomatin. *Transfusion*. 2008;48(3):451–462.

79. Burger P, Korsten H, De Korte D, et al. An improved red blood cell additive solution maintains 2,3-diphosphoglycerate and adenosine triphosphate levels by an enhancing effect on phosphofructokinase activity during cold storage. *Transfusion*. 2010;50(11):2386–2392.

80. Huyer G, Liu S, Kelly J, et al. Mechanism of inhibition of protein-tyrosine phosphatases by vanadate and pervanadate. *J. Biol. Chem.* 1997;272(2):843–851.

81. Gordon JA. Use of vanadate as protein-phosphotyrosine phosphatase inhibitor. *Methods Enzymol.* 1991;201:477–482.

82. Leal JK, Adjobo-Hermans MJ, Bosman GJ. Red Blood Cell Homeostasis: Mechanisms and Effects of Microvesicle Generation in Health and Disease. *Front. Physiol.* 2018;9:703.

83. Reid TJ, Babcock JG, Derse-Anthony CP, et al. The viability of autologous human red cells stored in additive solution 5 and exposed to 25 degrees C for 24 hours. *Transfusion*. 1999;39(9):991–997.

84. Paglia G, D'Alessandro A, Rolfsson Ó, et al. Biomarkers defining the metabolic age of red blood cells during cold storage. *Blood*. 2016;29:128(13):e43-50.

85. Nemkov T, Sun K, Reisz JA, et al. Hypoxia modulates the purine salvage pathway and decreases red blood cell and supernatant levels of hypoxanthine during refrigerated storage. *Haematologica*. 2018;103(2):361–372.

86. Rinalducci S, D'Amici GM, Blasi B, et al. Peroxiredoxin-2 as a candidate biomarker to test oxidative stress levels of stored red blood cells under blood bank conditions. *Transfusion*. 2011;51(7):1439–1449.

87. D'Alessandro A, Dzieciatkowska M, Hill RC, Hansen KC. Supernatant protein biomarkers of red blood cell storage hemolysis as determined through an absolute quantification proteomics technology. *Transfusion*. 2016;56(6):1329–1339.

88. Roussel C, Dussiot M, Marin M, et al. Spherocytic shift of red blood cells during storage provides a quantitative whole cell-based marker of the storage lesion. *Transfusion*. 2017;57(4):1007–1018.

89. Jordan A, Chen D, Yi Q-L, et al. Assessing the influence of component processing and donor characteristics on quality of red cell concentrates using quality control data. *Vox Sang.* 2016;111(1):8–15.

90. Tzounakas VL, Georgatzakou HT, Kriebardis AG, et al. Donor variation effect on red blood cell storage lesion: a multivariable, yet consistent, story. *Transfusion*. 2016;56(6):1274–1286.

91. Tzounakas VL, Kriebardis AG, Papassideri IS, Antonelou MH. Donor-variation effect on red blood cell storage lesion: A close relationship emerges. *Proteomics Clin. Appl.* 2016;10(8):791–804.

92. Chassé M, McIntyre L, English SW, et al. Effect of Blood Donor Characteristics on Transfusion Outcomes: A Systematic Review and Meta-Analysis. *Transfus. Med. Rev.* 2016;30(2):69–80.

93. Chassé M, Tinmouth A, English SW, et al. Association of Blood Donor Age and Sex With Recipient Survival After Red Blood Cell Transfusion. *JAMA Intern. Med.* 2016;176(9):1307–1314.

94.   Kanias T, Lanteri MC, Page GP, et al. Ethnicity, sex, and age are determinants of red blood cell storage and stress hemolysis: results of the REDS-III RBC-Omics study. *Blood Adv.* 2017;1(15):1132–1141.

95.   D'Alessandro A, Culp-Hill R, Reisz JA, et al. Heterogeneity of blood processing and storage additives in different centers impacts stored red blood cell metabolism as much as storage time: lessons from REDS-III-Omics. *Transfusion*. 2019;59(1):89-100.

96.   Meer PF van der, Korte D de. The Effect of Holding Times of Whole Blood and Its Components During Processing on In Vitro and In Vivo Quality. *Transfus. Med. Rev.* 2015;29(1):24–34.

97.   Radwanski K, Garraud O, Cognasse F, et al. The effects of red blood cell preparation method on in vitro markers of red blood cell aging and inflammatory response. *Transfusion*. 2013;53(12):3128–3138.

98.   Tzounakas VL, Georgatzakou HT, Kriebardis AG, et al. Uric acid variation among regular blood donors is indicative of red blood cell susceptibility to storage lesion markers: A new hypothesis tested. *Transfusion*. 2015;55(11):2659–2671.

99.   Tzounakas VL, Kriebardis AG, Papassideri IS, Antonelou MH. Donor-variation effect on red blood cell storage lesion: A close relationship emerges. *Proteomics Clin. Appl.* 2016;10(8):791-804.

100.   Heaton A, Keegan T, Holme S. In vivo regeneration of red cell 2,3-diphosphoglycerate following transfusion of DPG-depleted AS-1, AS-3 and CPDA-1 red cells. *Br. J. Haematol.* 1989;71(1):131–136.

CHAPTER 2

EVOLUTION OF THE ANTIOXIDANT POWER IN THE RED CELL CONCENTRATES DURING STORAGE

INTRODUCTION

One major role of the Red Blood Cells (RBCs) is the transport of oxygen (O_2) and carbon dioxide (CO_2) between the lungs and tissues. To fulfill optimally this vital function, these cells have become highly specialized, *i.e.* their cytosolic content is composed at 92 % of Hemoglobin (Hb, dry mass), and they are capable of extensive deformation to cross the network of small capillaries for gas perfusion[1]. Because of their close interaction with O_2 and the high levels of iron (Fe) they contain, RBCs are exposed to metal-catalyzed oxidation[2], moreover, a high proportion of endogenous Reactive Oxygen Species (ROS) originate from oxyhemoglobin (OxyHb) autooxidation that generates Methemoglobin (MetHb) and superoxide anion ($O_2^{\cdot-}$).

To counteract the oxidative burden they are exposed to, RBCs thus possess powerful enzymatic and non-enzymatic antioxidant defenses (Figure 1), such as the catalase, Superoxide Dismutase (SOD), Peroxiredoxin (Prx), Glutathione Peroxidase (GPx), Thioredoxin (Trx), Thioredoxin Reductase (TrxR) and Glutathione Reductase (GR) enzymes; and the reduced Glutathione (GSH), methionine, vitamin C (or Ascorbic Acid [AA]) and vitamin E (tocopherols and tocotrienols), and Uric Acid (UA) molecules.
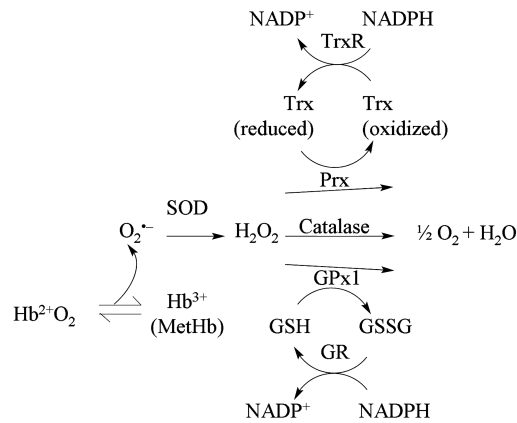
*Figure 1 – **Enzymatic antioxidant systems in red blood cells**. The different mechanisms are described in detail in the text below. Image taken from Low et al.[3]*

$O_2^{\cdot-}$ radical is eliminated or dismutated into hydrogen peroxide (H_2O_2) by the SOD (Reaction 1).

$$2O_2^{\cdot-} + 2H^+ \xrightarrow{SOD} O_2 + H_2O_2 \qquad \textit{Reaction 1}$$

H_2O_2 molecules are also produced during the divalent O_2 reduction by flavo- and metallo- oxidases. For example, two H_2O_2 molecules are produced during the successive degradation of the hypoxanthine into xanthine and of the xanthine into UA by the xanthine oxidase (XO, Reactions 2 and 3). Note that the presence of the XO enzyme has yet never been reported in RBCs.

$$Hypoxanthine + H_2O + O_2 \overset{XO}{\leftrightarrow} Xanthine + H_2O_2 \qquad \textit{Reaction 2}$$

$$Xanthine + H_2O + O_2 \overset{XO}{\leftrightarrow} Uric\ acid + H_2O_2 \qquad \textit{Reaction 3}$$
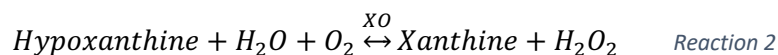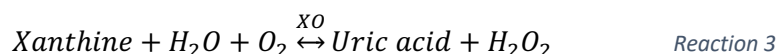
H_2O_2 crosses easily the cell membranes and can participate to the production of ferryl Hb as well as the highly reactive oxygen intermediates hydroxyl radical ($OH^\bullet$) in presence of transition metal ions such as Fe or copper (Cu) *via* the Haber-Weiss reaction. Ferric iron (Fe^{3+}) is first reduced into ferrous iron Fe^{2+} (Reaction 4). The second reaction corresponds to the Fenton reaction (Reaction 5).

$$O_2^{\cdot-} + Fe^{3+} \rightarrow Fe^{2+} + O_2 \qquad \textit{Reaction 4}$$

$$Fe^{2+} + H_2O_2 \rightarrow Fe^{3+} + OH^{\cdot} + OH^- \qquad \textit{Reaction 5}$$
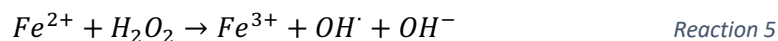
$OH^\bullet$ has a very short half-life and a high reduction potential. $OH^\bullet$ and ferryl Hb are highly reactive and can initiate the peroxidation of lipids and attack the proteins within the cytosol, the cytoskeleton and the membrane[4–8].

In cells, H_2O_2 is detoxified by the catalase, the GPx and Prx enzymes[2,9]. Catalase (ferriheme enzyme) converts two molecules of H_2O_2 to water and O_2 with an extremely high turnover rate (Reaction 6).

$$2H_2O_2 \xrightarrow{Catalase} 2H_2O + O_2 \qquad \textit{Reaction 6}$$

GPx (selenocysteine-containing enzymes) can convert H_2O_2 to water (Reaction 7), as well as lipid peroxides (ROOH) to their corresponding alcohols (ROH, Reaction 8) at the expense of GSH which is transformed into its oxidized form, *i.e.* GSSG.

$$2GSH + H_2O_2 \xrightarrow{GPx} GSSG + 2H_2O \qquad \textit{Reaction 7}$$

$$2GSH + ROOH \xrightarrow{GPx} GSSG + ROH + H_2O \qquad \textit{Reaction 8}$$
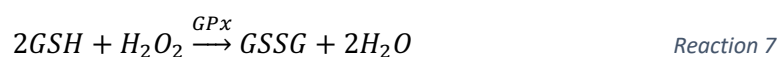
GSH (also named γ-glutamylcysteinylglycine) is a tripeptide comprise of glutamate, Cysteine (Cys) and glycine. It is a major antioxidant in RBCs. Recycling of GSSG into GSH by the GR requires the Nicotinamide Adenine Dinucleotide Phosphate (NADPH). A redox cofactor produced by the Pentose Phosphate Pathway (PPP).

Finally, H_2O_2 can be decomposed by the thiol-based Prxs (Reaction 9). Six isoforms of Prx are known in mammals, Prx 2 being the major form in RBCs. Moreover, it was estimated that Prx 2 is the third most abundant in RBCs after Hb and carbonic anhydrase[3,10,11]. During H_2O_2 detoxification, two highly conserved Cys residues in the Prx 2 catalytic site are involved. Cys51 is first oxidized into sulfenic acid and then reacts with Cys172 to form a disulfide bond[3].

$$Prx_{reduced} + H_2O_2 \rightarrow Prx_{oxidized} + H_2O \qquad \textit{Reaction 9}$$

Prx enzymes are recycled by the Trx and NADPH-dependent TrxR enzymes.

In the context of blood storage, oxidative stress was shown to be closely associated with storage lesions[4,6,12]. The antioxidant defense system thus plays an important preventive role. Likewise, an impaired antioxidant defense induces a cascade of events related to protein function impairment, proteasome inhibition, oxidized protein accumulation at the RBC membrane and their elimination through microvesiculation[5,13,14]. The Microvesicles (MVs) released during storage[15,16] could contribute to deleterious transfusion effects linked to hemostasis[17,18]. The quality of RBCs following storage also depends on the donor's characteristics[19–21], including antioxidant content, as a higher level of UA (a major antioxidant in plasma) contributes to the storability of RBCs[22].

Whereas the consequences of oxidative stress are well-documented (for more details, refer to the Introduction), the global antioxidant content has been poorly quantified during RBC storage. Different approaches exist to study and quantify the global Antioxidant Power (AOP) in biological fluids, including spectrophotometric, fluorescence and electrochemical methodologies. Some of the available assays are listed in Table 1.

*Table 1 – **Assays for the monitoring of the total antioxidant capacity in biological samples**[23].*

System		Assay
Colorimetric or Fluorometric	**Hydrogen Transfer (HAT)**	Oxygen Radical Absorbance Capacity (ORAC) Total Radical-Trapping Antioxidant Parameter (TRAP) Inhibited oxygen uptake (IOU)
	Electron Transfer (ET)	Trolox Equivalent Antioxidant Capacity (TEAC) Ferric ion Reducing Antioxidant Parameter (FRAP) Cupric ion Reducing Antioxidant Capacity (CUPRAC) Total phenolics by Folin-Ciocalteu (FC) DPPH-based (2,2-Di[4-tert-octylphenyl]-1-picrylhydrazyl) ABTS-based (2,2'-Azino-bis[3-ethylbenzothiazoline-6-sulfonic acid])
Electrochemical[23,24]		Cyclic Voltammetry (CV) or Linear Sweep Voltammetry (LSV) Differential pulse voltammetry Square wave voltammetry Reducing Antioxidant Capacity evaluated by Electrolysis (RACE) Rapid Electrochemical Screening of Antioxidant Capacity (RESAC) Pseudo-titration of water-soluble antioxidants

Each method has its advantages and drawbacks. These include whether the assay is time-consuming, easy to use, sufficiently sensitive, specific or global, direct or indirect. In general, the methods based on Hydrogen or Electron Transfer (HAT or ET) require several reagents and equipment. These methods are generally more complicated and time-consuming compared to the electrochemical systems which have multiple advantages for the quantification of AOP in a complex sample. First, they are rapid and do not require sample pre-treatment, such as dilution[23,25]. Moreover, they enable screening of complex matrices such as the blood samples.

The aim of the following study was to follow the global antioxidant content of RCCs and of extracellular samples. This study was done in collaboration with Philippe Tacchini from the Edel-for-Life company and a team from the "Laboratoire d'Electrochimie Physique et Analytique" (Ecole Polytechnique Fédérale de Lausanne [EPFL], Switzerland). The results presented in this Chapter are based on a paper published in *Vox Sanguinis*[26].

STUDY DESIGN

Six Red Cell Concentrates (RCCs) were prepared in Saline-Adenine-Glucose-Mannitol (SAGM) additive solution and followed for 43 days. The global antioxidant content of RCCs and extracellular samples were measured electrochemically using the Edel technology and compared with results obtained from a colorimetric assay. UA, suspected to be a major contributor to the extracellular AOP was quantified using High-Pressure Liquid Chromatography (HPLC) coupled to UV detection. Hematological data and percentage of hemolysis were also recorded, as before (see Material and Methods section of Chapter 1, Part 1). Finally, a kinetic model was developed to extract quantitative kinetic data on the AOP behavior.

MATERIAL AND METHODS

The six RCCs used in this study came from three women and three men (donors' characteristics are listed in Table 2).

*Table 2 – **Donor's characteristics**. Sex, age and blood group (ABO and Rhesus D) of the donor.*

Sample	Sex	Age /year	Blood group
RCC 1	Female	66	O+
RCC 2	Female	26	A+
RCC 3	Female	47	O+
RCC 4	Male	43	A+
RCC 5	Male	27	A+
RCC 6	Male	60	A+

RCC: Red Cell Concentrate.

Samples (3 mL per bag) were collected daily from day 1 to 10 and then weekly until day 43. Global AOP and hematological data were measured on RCCs. Supernatants were separated from RBCs by centrifugation (2000 g, 10 min at 4°C) and used for extracellular AOP and hemolysis measurements. Remaining supernatant was saved at –80°C until quantification of the extracellular UA.

Antioxidant power measurement in red cell concentrates with the Edel technology

The Edel technology (Edel-for-Life, Switzerland) is an electrochemical system where Screen-Printed Electrodes (SPE) are used as sensors for AOP quantification in liquid samples. This amperometric test measures the current generated by the oxidation at different potential off hydro-soluble redox active

species. The signal recorded (Linear Sweep Voltammogram [LSV]) being proportional to their concentration. In addition, pseudo-titration is used to discriminate the biologically relevant antioxidants.

For the AOP measurement with the Edel technology, three elements are required, *i.e.* an electrochemical sensor, a workstation, and a computer (Figure 2).
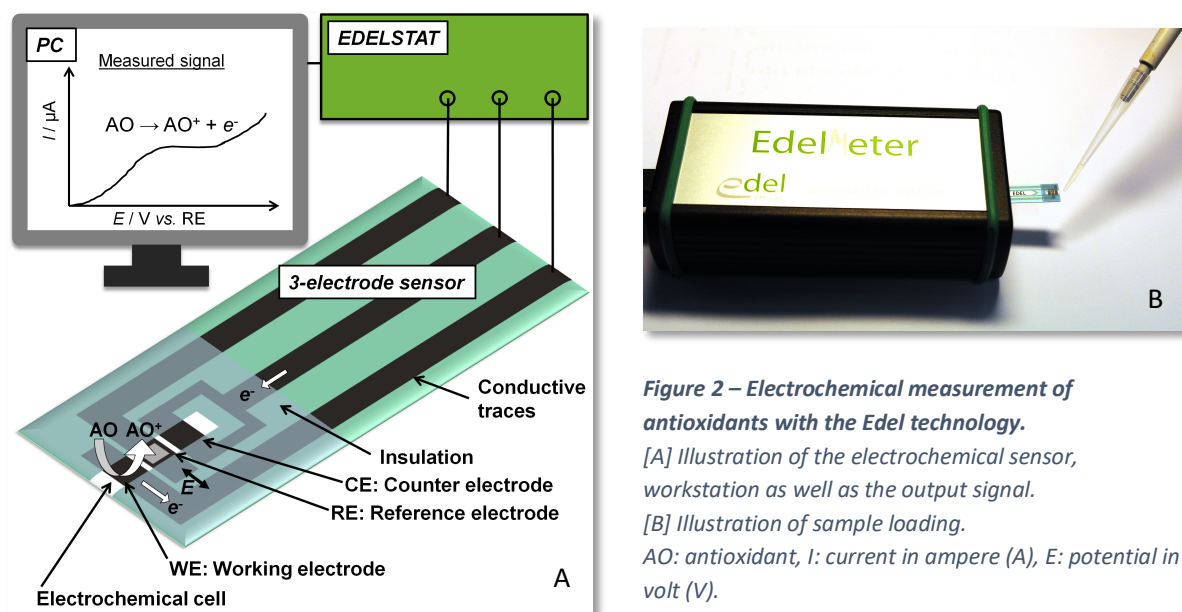
Figure 2 – Electrochemical measurement of antioxidants with the Edel technology.
[A] Illustration of the electrochemical sensor, workstation as well as the output signal.
[B] Illustration of sample loading.
AO: antioxidant, I: current in ampere (A), E: potential in volt (V).

The sensor part is a screen-printed, disposable, electrode strip (3-electrode sensor part), composed of carbon paste Working (WE) and Counter (CE) Electrodes, and a Ag/AgCl quasi-Reference (RE) Electrode (Figure 2A). A dielectric insulation layer is used to define the electrochemical cell above the electrode patterns (1 mm^2 left for each electrode), and a cover lid with small openings on both sides of the sensor structure is added on top to create a capillary. The principle of screen-printing is to deposit layer by layer inks on a solid surface through a screen to create the electrode area and to cover this conductive track with an insulating coating. Such fabrication technique has the advantage of being reproducible, inexpensive, fast and suitable for automatization and large-scale production. It also allows great design flexibility and enables electrode miniaturization, which limits the production costs, as well as the sample volume and analysis time[23,27–29]. Additionally, electrochemical workstations (*i.e.* potentiostats) are nowadays available in small and compact portable formats with wireless communication. As a result, electrochemical measurements can rapidly be performed at any location, *e.g.* in the field, in hospitals, at bedside or at home.

The strip is inserted in the potentiostat (EdelMeter), then the electrochemical cell is filled with liquid by capillary forces in a fraction of seconds which limits exposure time of the sample to air and electrodes surfaces (Figure 2B). Three seconds after loading, an LSV is recorded. To do so, a linear potential ramp is applied from 0 V to 1.2 V with a scan rate of 100 mV·s^{-1}. Each electrochemically active

substance in the sample will transfer one or more electrons from the antioxidant molecules to the biased WE at a particular redox potential. The recorded current is proportional to the antioxidant concentration (the potentials are reported with respect to the RE).
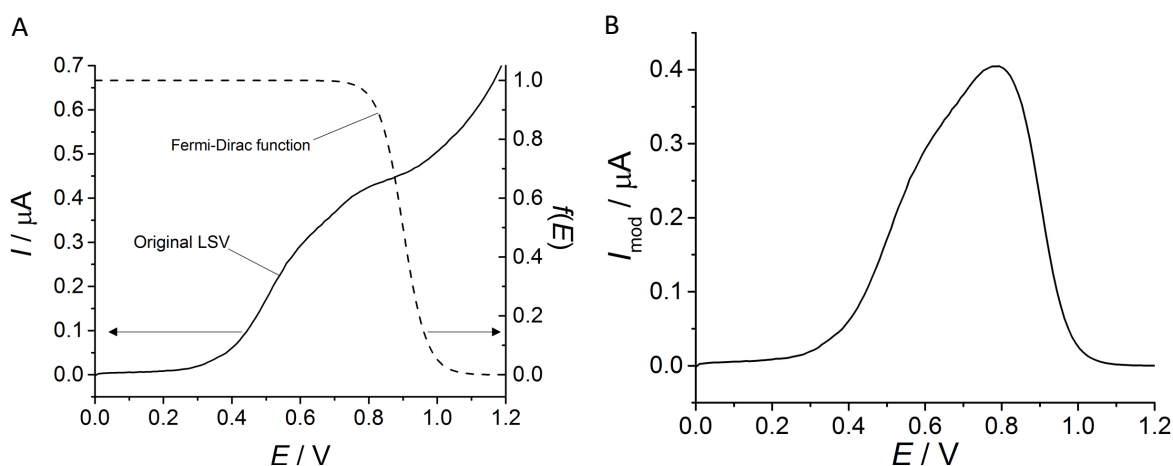
*Figure 3 – **Principle of electrochemical pseudo-titration voltammetry.** [A] Typical Linear Sweep Voltammogram (LSV) recorded with a scan rate of 100 mV·s⁻¹ (solid line) and Fermi-Dirac function with λ = 0.75 and E_threshold = 0.9 V (dashed line). [B] Result of pseudo-titration voltammetry by modulation of the LSV in [A]. I: Current in ampere (A), E: potential in volt (V).*

The LSVs are transformed from a current value in Ampere to an AOP in nW by using the electrochemical pseudo-titration voltammetry (Figure 3)[23,30]. This procedure is used to discriminate in a complex fluid the signals from biologically active antioxidants which are by nature easily converted at low redox potentials and are fast reactive species. In brief, a mathematical treatment of the recorded curves is applied to suppress the signals measured at high potentials (Figure 3A). To do so, the original LSVs are multiplied by a Fermi-Dirac function that contains curve points of unity at low potentials and become zero at higher potentials (Equation 1).

$$I_{mod} = I \cdot f(E) = I \cdot \frac{1}{1 + \exp\left(\dfrac{\lambda nF(E - E_{threshold})}{RT}\right)}$$

Equation 1

where n is the number of transferred electrons (herein n = 1), F is the Faraday constant, E the applied potential, R the universal gas constant and T the temperature. Two adjustable parameters, namely λ and $E_{threshold}$, are used as a factor modulating the slope and as a potential offset of the Fermi-Dirac function. The resulting I_{mod} vs. E curve is represented in Figure 3B. The AOP is then calculated by the integration of the I_{mod} over E and is expressed in nW (Equation 2).

$$AOP = \int I_{mod} \, dE$$

Equation 2
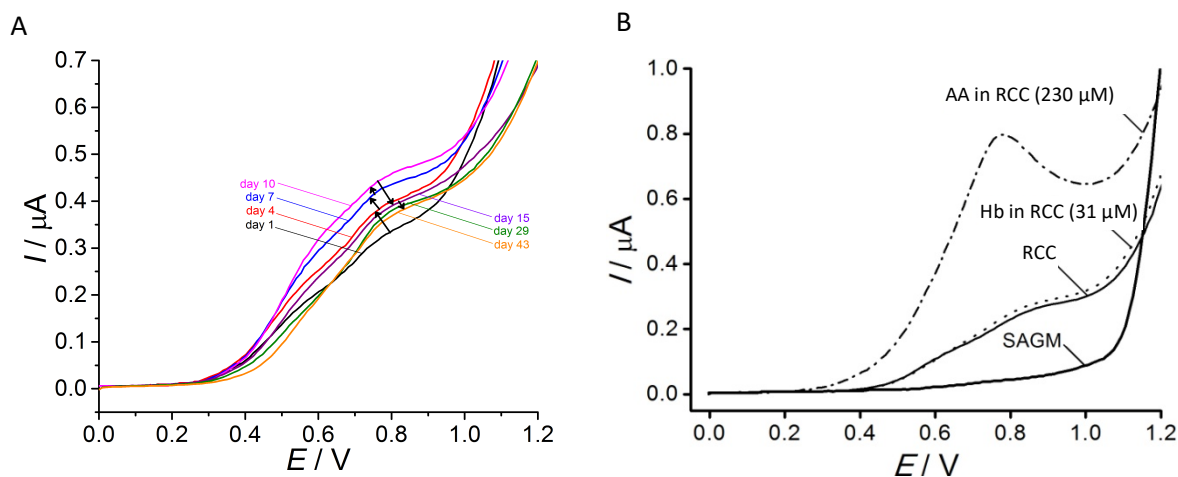
*Figure 4 – **Electrochemical pseudo-titration voltammetry for red cell concentrate (RCC) analysis.** [A] Evolution of the Linear Sweep Voltammogram (LSV) during storage for the extracellular content of a Red Cell Concentrate (RCC). [B] LSVs of additive solution Saline-Adenine-Glucose-Mannitol (SAGM), RCC, RCC enriched in Hemoglobin (Hb) and RCC enriched in Ascorbic Acid (AA). I: Current in Ampere, E: potential in Volt.*

Figure 4A shows the evolution of the LSV curves during storage. Figure 4B shows the original LSVs recorded in the additive SAGM solution, in one RCC sample, in the RCC sample enriched with 31 µM Hb, corresponding to approximately 0.4 % of hemolysis, and in the RCC sample enriched with additional 230 µM AA, a typical concentration for such sample. It demonstrates that this method is not affected by background colors or auto-fluorescence, as it is generally the case for other optical detection methods, which represents a tangible advantage for the study of RBCs that contain large amounts of Hb. The major drawback is that only the water-soluble antioxidants are quantified and that it is a bulk analysis that does not permit to establish individually the contribution of each antioxidant specie to the global signal.

Colorimetric antioxidant power measurement

The extracellular AOP was quantified using a colorimetric method based on the decolorization of the green 2,2'-Azino-bis-(3-ethylbenzothiazoline-6-sulfonic acid) radical cation (ABTS$^{\cdot+}$), which converts into colorless ABTS by reduction with antioxidants. The bleaching rate is proportional to the antioxidant concentration. Briefly, 80 µL of supernatant were mixed in a cuvette with 800 µL of acetate buffer (0.4 mM, pH 5.8) and 40 µL of ABTS$^{\cdot+}$ in acetate buffer (30 mM, pH 3.6), according to Erel's protocol[31], with slight modifications. The absorbance was measured (in duplicate) at 660 nm with a NanoDrop spectrophotometer. The assay was calibrated using AA as a standard.

Uric acid quantification

One hundred and fifty microliters of supernatant were transferred in Vivaspin 500 columns (Sartorius) and centrifuged at 15'000 *g*, 30 min at 4°C. Then, 30 µL of filtrate were dried (Genevac Ltd) for 45 min and stored at -28°C. Just before analysis, the dried samples were dissolved in 90 µL of ammonium

acetate (100 mM, pH 8) mixed with acetonitrile 45/55 (v/v), vortexed, sonicated for 10 min at room temperature and stored on ice for 20 min. After a final centrifugation at 20'800 g, 30 min at 4°C, 45 µL of supernatant were transferred into an injection vial.

One microliter of sample was injected in duplicate on a HPLC apparatus (Dionex UltiMate 3000 RSLCnano System, Thermo Scientific). The capillary column (ZIC-HILIC, 150 × 0.3mm, 5 µL, SeQuant Merck) was kept at 40°C. Chromatography conditions are summarized in Table 3.

*Table 3 – **High-PressureLliquid Chromatography (HPLC) gradient conditions.***

Time / min	% A	% B	Flow rate / µL/min
0	5	95	5
0.5	5	95	5
15	60	40	5
17	80	20	5
20	80	20	5
20.2	5	95	5
30	5	95	5

A: ammonium acetate 100 mM pH 8, B: acetonitrile.

UV signal was measured at 292 nm, specifically for UA detection. Peak integration was calculated using the HyStar post-processing software (Bruker Daltonics). The nature of the detected compound was confirmed by mass spectrometry (Bruker Daltonics, amazon ETD, negative ionization mode). For calibration, UA standard was dissolved in SAGM at concentrations ranging from 0 to 75.0 µM and prepared for injection in the same way as the supernatant samples (Figure 5).

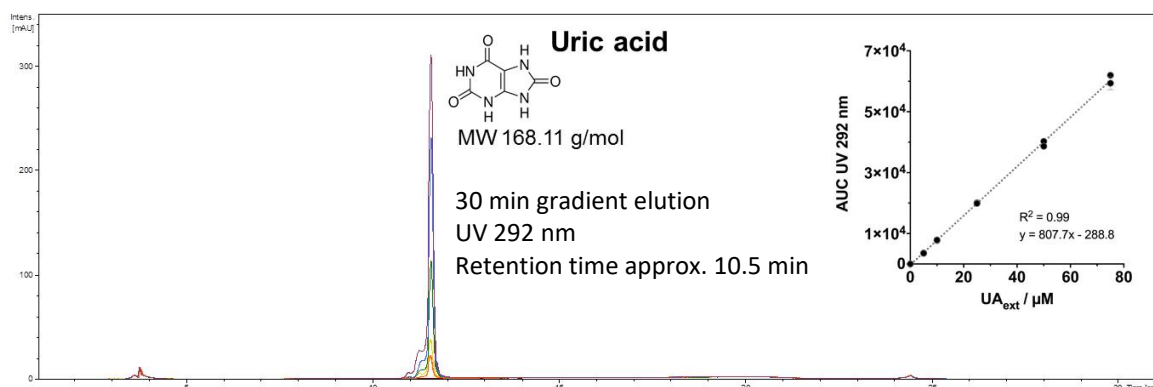*Figure 5 – **Uric Acid (UA) quantification by High-Pressure Liquid Chromatography (HPLC).** Chromatogram for UA standard at different concentration dissolved in Saline-Adenine-Glucose-Mannitol (SAGM, 30 min gradient) and calibration curves with linear regression (Area Under the Curve [AUC] calculated from the chromatogram, linear regression [dotted line] and regression coefficient [R^2]). Calibration was repeated twice.*

RESULTS AND DISCUSSION

Mean values for some of the observed parameters are summarized in Table 4.

*Table 4 – **Evolution of the Red Cell Concentrates (RCCs) during storage.***

	Day 1	Day 5 /4+ /6+/ 7+++	Day 29	Day 43
RBCs (1·1012/L)	6.65 ± 0.32	6.59 ± 0.30	6.53 ± 0.31	6.59 ± 0.34
MCV (fL)	85.2 ± 3.3	86.9 ± 3.7	91.6 ± 4.2	93.7 ± 4.0
SD-RDW (fL)	44.7 ± 2.4	46.8 ± 2.1	51.3 ± 4.1	51.6 ± 4.6
Hemolysis (%)	0.075 ± 0.013	0.077 ± 0.007	0.157 ± 0.041	0.221 ± 0.042
AOPEdel women (nW)	116.4 ± 19.6	147.8 ± 20.6	112.5 ± 10.0	107.4 ± 5.1
AOPEdel men (nW)	142.8 ± 18.0	193.9 ± 25.1	147.5 ± 15.9	138.9 ± 15.1
AOPcolor. women (µM AA equ.)	85.5 ± 19.5	128.7 ± 19.0 +	125.7 ± 13.7	130.7 ± 18.2
AOPcolor. men (µM AA equ.)	109.7 ± 23.4	184.8 ± 13.6 ++	159.1 ± 22.8	167.9 ± 23.3
UA women (µM)	53.4 ± 19.2	100.6 ± 22.6	53.7 ± 9.5	64.9 ± 10.1
UA men (µM)	70.1 ± 19.2	147.1 ± 13.8 +++	77.3 ± 14.9	77.1 ± 14.3

Main Red Blood Cell (RBC) aging parameters followed at day 1, 5 or 4 (+) or 6 (++) or 7 (+++), 29 and 43 of storage.
Mean values for the six RCCs ± standard deviation.
MCV: Mean Corpuscular Volume, SD-RDW: Standard Deviation of Distribution Width, AOP$_{Edel}$: Antioxidant Power measured with Edel electrochemical technology, AOP$_{color.}$: antioxidant power measured the colorimetric method, UA: Uric Acid.

The six RCCs exhibited standard hematological values over the storage period, *i.e.* a slight increase in RBC size and population anisocytosis (Figure 6A). Hemolysis reached 0.18, 0.19, 0.20, 0.29, 0.25 and 0.21 % for RCC 1 to 6, respectively, at the end of the storage period, remaining below the accepted 0.8 % (Figure 6B).
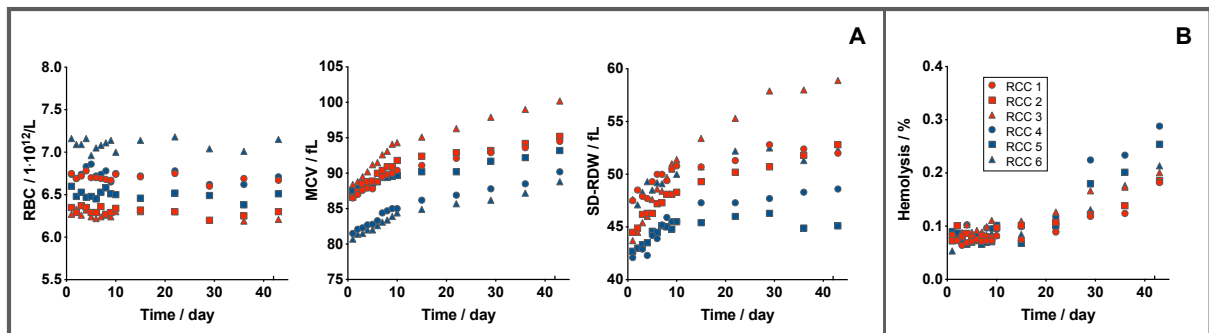
*Figure 6 – **Evolution of Red Blood Cell (RBC) hematological parameters and hemolysis in the six Red Cell Concentrates (RCCs) during storage**. [A] RBC count, Mean Corpuscular Volume (MCV) and Standard Deviation of Distribution Width (SD-RDW). [B] Percentage of hemolysis. Individual values for the six RCCs ± standard deviation. Red: women, blue: men.*

AOPs of all six samples exhibited a steep increase during the first week of storage followed by a decrease, until reaching a plateau (Figure 7A). The extracellular AOP is correlated with the AOP of the total RCC (R^2 = 0.75, Figure 7B) because of the hydrophilic antioxidants present in the extracellular medium. AOP levels in the six RCCs are related to the sex of the donor. Indeed, the AOP was generally lower in women and remained lower all along the storage compared to men (area under the curve for the extracellular AOP was 5063 ± 349 day·nW for women and 6547 ± 668 day·nW for men, p-value = 0.027).
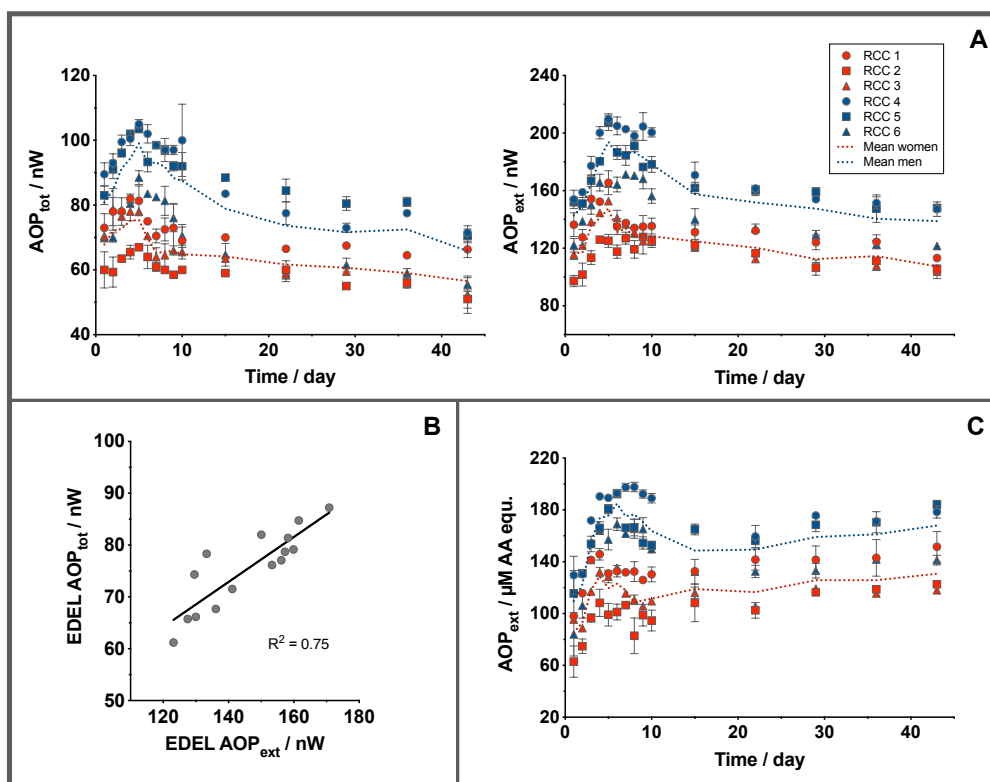
*Figure 7 – **Evolution of Antioxidant Power (AOP) in the six Red Cell Concentrates (RCCs) during storage**. [A] AOP in the whole RCC (AOP$_{tot}$) and extracellular AOP (in the supernatant, AOP$_{ext}$) measured with the electrochemical Edel technology. [B] Linear correlation (with regression coefficient [R^2]) between global AOP (AOP$_{tot}$) and AOP in supernatant (AOP$_{ext}$). [C] Extracellular AOP (AOP$_{ext}$) measured with the colorimetric assay. Individual (symbols) and mean values (dotted lines) for the six RCCs ± standard deviation. Red: women, blue: men.*

The trends for AOPs measured with the electrochemical method and colorimetric assay were similar for both early-storage trends and sex-related differences (Figure 7C). However, a slight increase was observed at the end of storage instead of a plateau, which is not related to extracellular Hb. One hypothesis to explain this effect could be the presence of lipophilic antioxidants stemming from aged RBCs at the end of the storage detected spectrophotometrically and not with the EdelMeter.

To quantitatively describe the observed trends, a kinetic model has been developed by the team from the EPFL. The kinetic model of consecutive reactions was selected. It consists of two consecutive, irreversible first order reactions converting a reagent *AO$_{pre}$* into an intermediate, *i.e.* the *AO* (which stands for antioxidant), and then the *AO* into a product *AO$_{ox}$*, that corresponds chemically to the oxidation of the antioxidant. In the human metabolism, antioxidants are permanently generated and/or released from various sources before becoming effective, herein simplified as *AO$_{pre}$*. The antioxidants are constantly consumed, for instance to reduce reactive oxygen species. Hence, the *AO* can be considered as an intermediate, generated with a heterogeneous reaction rate constant k_1 and degraded with a heterogeneous rate constant k_2 (Reaction 10).

$$AO_{pre} \xrightarrow{k_1} AO \xrightarrow{k_2} AO_{ox}$$

Reaction 10

CHAPTER 2
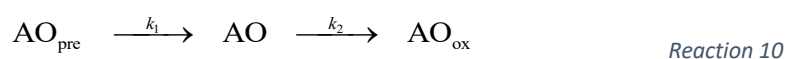
Where *AO* stands for antioxidant, *AO_pre* stands for precursors and *AO_ox* for the oxidized *AO*. k_1 and k_2 are kinetic constants that represent the production and the consumption of *AO*, respectively. The change of the concentrations of *AO_pre*, *AO* and *AO_ox* can be described as follows (Equations 3-7):

$$\frac{d[AO_{pre}]}{dt} = -k_1[AO_{pre}] \qquad \text{Equation 3}$$

$$[AO_{pre}] = [AO_{pre}]_0 e^{-k_1 t} + AO_{pre,const} \qquad \text{Equation 4}$$

$$\frac{d[AO]}{dt} = k_1[AO_{pre}] - k_2[AO] \qquad \text{Equation 5}$$

$$\frac{d[AO]}{dt} + k_2[AO] = k_1[AO_{pre}]_0 e^{-k_1 t} + k_1 AO_{pre,const} \qquad \text{Equation 6}$$

$$\frac{d[AO_{ox}]}{dt} = k_2[AO] \qquad \text{Equation 7}$$

The above differential equations are solved by the method of integral factors, which results the following equation describing the AOP development in the extracellular samples for the investigated period (Equation 8):

$$[AO] = [AO]_0 e^{-k_2 t} + \frac{k_1}{k_2 - k_1}[AO_{pre}]_0 \left(e^{-k_1 t} - e^{-k_2 t}\right) + \frac{k_1}{k_2} AO_{pre,const} \qquad \text{Equation 8}$$

This equation can be transferred to the AOP. The AOP as a function of time is thus expressed considering 1st-order reactions as follows (Equation 9):

$$AOP(t) = AOP_0 e^{-k_2 t} + \frac{k_1}{k_2 - k_1} AOP_{pre,0}\left(e^{-k_1 t} - e^{-k_2 t}\right) + \frac{k_1}{k_2} AO_{pre,const} \qquad \text{Equation 9}$$

This equation was applied to fit the measured AOP of the extracellular samples in Figure 8.
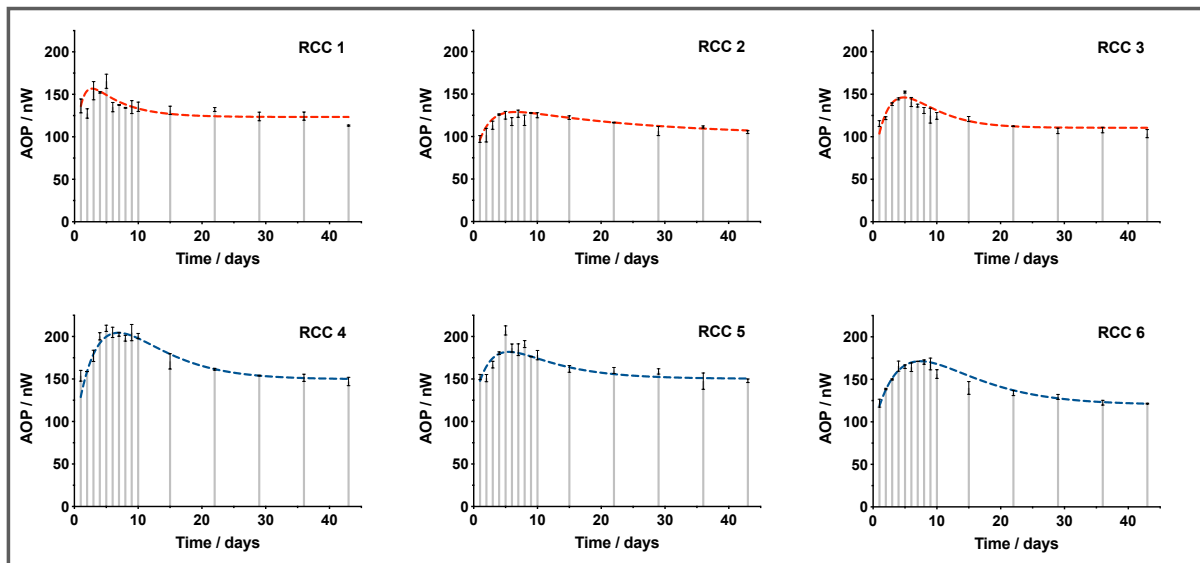
*Figure 8 – **Fitting of Antioxidant Power (AOP) curves.** Measured extracellular AOP (grey bars, mean values ± standard deviation) for the individual Red Cell Concentrates (RCCs) with curve-fits for the kinetic model (dashed lines). Red: women, blue: men.*

The values obtained from the fitting procedure are shown in Table 5.

*Table 5 – **Antioxidant Power (AOP) fitting parameters for each Red Cell Concentrate (RCC).** Fitting parameters for the AOP development using Equation 9 for the extracellular samples.*

	Women			Men		
	RCC 1	RCC 2	RCC 3	RCC 4	RCC 5	RCC 6
AOP_0 / nW	-49.15	-31.62	-47.34	-64.21	-29.94	-27.71
$AOP_{pre,0}$ / nW	96.73	66.09	136.95	203.42	84.98	164.58
$AOP_{pre,const}$ / nW	25.73	9.086	110.59	149.71	56.65	120.13
k_1 / days^{-1}	0.955	0.495	0.279	0.191	0.356	0.157
k_2 / days^{-1}	0.199	0.044	0.279	0.191	0.134	0.157

$k1$ and $k2$: reaction rate constants.

Kinetic constant k_2 was lower than k_1, which is supported by the slow decay observed during storage. The efflux phase represented by k_1 was on average higher in women, and the second phase (slower and represented by k_2) was independent from the donor's sex.

The AOP_0 is mathematically the AOP at day 0, but $AO_{pre,const}$ needs to be included to get the real AOP value at day 0, *i.e.* the date of donation and blood treatment (Equation 10).

$$AOP(day\ 0) = AOP_0 + \frac{k_1}{k_2} AOP_{pre,const}$$

Equation 10

The calculated AOP of the extracellular samples at day 0 was 74.2, 69.5, 63.2, 85.6, 120.3 and 92.4 nW for the RCC 1 to 6, respectively, values that are below the AOP after long storage periods.

The UA molecule makes a big contribution to the antioxidant defense of RCCs. As confirmed by the increase of UA concentration, similarly to the AOP, which occurred during the first week of storage (Figure 9A), reaching a maximum after five days for the women and seven days for the men (maximum UA of 100.6 ± 22.6 µM for women and 147.1 ± 13.8 µM for men, p-value = 0.038).
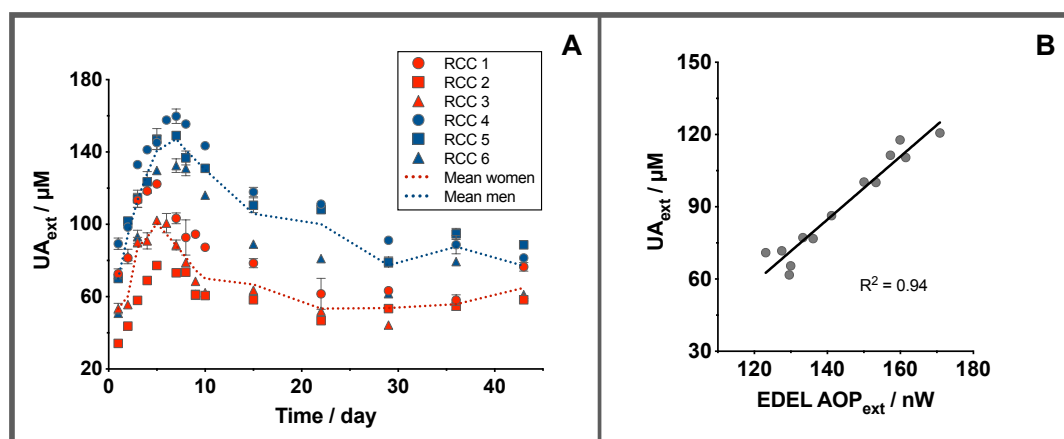
*Figure 9 – **Evolution of extracellular Uric Acid (UA) concentration in the six Red Cell Concentrates (RCCs) during storage.** [A] Extracellular UA concentration (UA_{ext}) measured by High-Pressure Liquid Chromatography (HPLC). [B] Linear correlation (with regression coefficient [R^2]) between the extracellular AOP (in the supernatant, AOP_{ext}) measured with the electrochemical Edel technology and the UA_{ext}. Individual (symbols) and mean values (dotted lines) for the six RCCs ± standard deviation. Red: women, blue: men.*

Men exhibited a higher UA concentration during the whole storage (area under the curve of 2687 ± 416 day·µM for women and 4231 ± 541 day·µM for men, p-value = 0.017). A plateau was reached after approximately three weeks in women and four weeks in men. Extracellular UA concentration and AOP are strongly positively correlated (R^2 = 0.94, Figure 9B).

CONCLUSIONS

The antioxidant capacity reflects the metabolic activity during the first two weeks of storage as previously reported[32,33]. The changes of AOP are visible earlier compared to other aging markers, *i.e.* hemolysis and microvesiculation, lactate accumulation, changes of morphology, etc., which only become significantly visible after several weeks of storage[14,33,34].

The increase in AOP during the first week could result from an initial boost in RBC metabolism, as shown by increasing intracellular Adenosine Triphosphate (ATP) and GSH concentrations during the first 10 days of storage[32]. Extracellular UA concentration evolved similarly. Equilibration between intracellular and extracellular media could also explain the observed trend, as suggested by the steep increase of extracellular UA and the decrease of intracellular UA observed by our group and by Bordbar *et al*[32]. Indeed, because of blood processing and SAGM addition to the RBCs, the residual plasma is diluted. In theory, the calculated dilution factor of plasma in the RCCs is 11. This number is however subject to large variations (*e.g.* because of different blood processing methods), as pointed out by Jordan and Acker[36]. Extracellular UA concentration, normally comprised between 120 and 450 µM in human plasma, is subsequently diluted by the same factor.

To have a quick glance at the AOP evolution throughout the *ex-vivo* journey of the RBCs for transfusion, a preliminary experiment was conducted where the AOP was measured from whole blood collection to RCC preparation and during storage (see ANNEX-7). The results obtained showed significant effect of blood processing on the RCC AOP and suggest that the RBCs are impacted by their new environment from the very beginning of the storage period.

The dynamic of UA concentration is governed by the active or passive transport of UA through the membrane. Active UA transport is probably ATP-dependent[37] and it was also shown that membrane permeability to UA increases with storage duration[38]. An equilibrium was reached after one week of storage (maxima of extracellular UA concentration at day five for women and day seven for men). In a second phase, AOP decreased because the glycolysis slowdown impairs intracellular antioxidant production (*e.g.* reduction of intracellular glutathione after 2 weeks). Subsequent accumulation of oxidative species and/or re-entry of UA to protect the intracellular space against oxidative stress could explain in part the decrease of extracellular UA concentration[22]. Moreover, as the purine pathway is not active since the Adenosine Monophosphate (AMP) is transformed in inosine monophosphate, consumed UA is not replaced[32,35]. The time at which the plateau is reached correlates

with the reactivation of the purine metabolism (inhibition of the nucleotide salvage pathway). The feeding of the glycolysis through the PPP and the production of ribose-5 phosphate releases hypoxanthine and xanthine. They partially participate to the synthesis of UA *in situ*. This could explain why the extracellular UA concentration and AOP did not decrease to zero. It must be noticed that the basal AOP level is reached earlier in women than in men. This loss of antioxidant capacity at the end of the storage corroborates the defect in metabolism activity[32], and the appearance of oxidative stress markers[11] and oxidized molecules[4–6].

In conclusion, the results obtained with the electrochemical and colorimetric AOP measurements suggest that the antioxidant capacity of the investigated RCCs is donor-dependent and impacted by changes in the RBC environment because of the blood processing. Moreover, the AOP was closely correlated to the UA concentration that accounts for 60-70 % of the extracellular AOP in RCCs[39]. UA level was proposed as a biomarker of RBCs storability[22]. The kinetics of the AOP and the extracellular concentration of UA during storage are in accordance with the three metabolic phases previously identified[32]. Notably, the kinetic constants might demonstrate a donor's specific release of AOP (k_1) and a consumption of UA (k_2), depending upon the storage conditions. The kinetic model could be integrated into general kinetic analyses related to the RBC metabolism[40,41] and therefore be used as predictive measurement for the evolution of lesions.

It must be emphasized that in the context of blood transfusion, the Edel technology has already been validated as a quality control test to assess the completeness of the pathogen (virus, bacteria and parasites) or cell inactivation procedures[42]. Indeed, Abonnenc *et al.*[25] demonstrated that the successful treatment with INTERCEPT™ of platelets and plasma decreased significantly the AOP, because this method (as well as the MIRASOL®) including photochemical inactivation technique and that relies on the application of a photosensitizer (amotosalem-HCl) and UVA illumination, is known to produce ROS.

REFERENCES

1.   Nemkov T, Reisz JA, Xia Y, Zimring JC, D'Alessandro A. Red blood cells as an organ? How deep omics characterization of the most abundant cell in the human body highlights other systemic metabolic functions beyond oxygen transport. *Expert Rev. Proteomics*. 2018;15(11):855–864.

2.   Cimen MY. Free radical metabolism in human erythrocytes. *Clin. Chim. Acta.* 2008;390(1–2):1–11.

3.   Low FM, Hampton MB, Winterbourn CC. Peroxiredoxin 2 and peroxide metabolism in the erythrocyte. *Antioxid. Redox Signal.* 2008;10(9):1621–1630.

4.   Kriebardis AG, Antonelou MH, Stamoulis KE, et al. Progressive oxidation of cytoskeletal proteins and accumulation of denatured hemoglobin in stored red cells. *J. Cell. Mol. Med.* 2007;11(1):148–155.

5.   Delobel J, Prudent M, Rubin O, et al. Subcellular fractionation of stored red blood cells reveals a compartment-based protein carbonylation evolution. *J. Proteomics*. 2012;76:181–193.

6.   Delobel J, Prudent M, Tissot J-D, Lion N. Proteomics of the red blood cell carbonylome during blood banking of erythrocyte concentrates. *Proteomics Clin. Appl.* 2016;10(3):257–266.

7.   Delobel J, Prudent M, Crettaz D, et al. Cysteine redox proteomics of the hemoglobin-depleted cytosolic fraction of stored red blood cells. *Proteomics Clin. Appl.* 2016;10(8):883–893.

8.   Wither M, Dzieciatkowska M, Nemkov T, et al. Hemoglobin oxidation at functional amino acid residues during routine storage of red blood cells. *Transfusion*. 2016;56(2):421–426.

9.   Yoshida T, Shevkoplyas SS. Anaerobic storage of red blood cells. *Blood Transfus.* 2010;8(4):220-236.

10.   Matte A, Bertoldi M, Mohandas N, et al. Membrane association of peroxiredoxin-2 in red cells is mediated by the N-terminal cytoplasmic domain of band 3. *Free Radic. Biol. Med.* 2013;55:27–35.

11.   Rinalducci S, D'Amici GM, Blasi B, et al. Peroxiredoxin-2 as a candidate biomarker to test oxidative stress levels of stored red blood cells under blood bank conditions. *Transfusion*. 2011;51(7):1439–1449.

12.   Kriebardis AG, Antonelou MH, Stamoulis KE, et al. Membrane protein carbonylation in non-leukodepleted CPDA-preserved red blood cells. *Blood Cells. Mol. Dis.* 2006;36(2):279–282.

13.   Prudent M, Rappaz B, Hamelin R, et al. Loss of Protein Tyr-phosphorylation During in vitro Storage of Human Erythrocytes: Impact on RBC Morphology. *Transfusion*. 2014;54:49A-50A.

14.   Prudent M, Tissot J-D, Lion N. The 3-phase evolution of stored red blood cells and the clinical trials: an obvious relationship. *Blood Transfus.* 2017;15(2):188–188.

15.   Rubin O, Crettaz D, Canellini G, Tissot J-D, Lion N. Microparticles in stored red blood cells: an approach using flow cytometry and proteomic tools. *Vox Sang.* 2008;95(4):288–297.

16.   Rumsby MG, Trotter J, Allan D, Michell RH. Recovery of membrane micro-vesicles from human erythrocytes stored for transfusion: a mechanism for the erythrocyte discocyte-to-spherocyte shape transformation. *Biochem. Soc. Trans.* 1977;5(1):126–128.

17.   Kriebardis A, Antonelou M, Stamoulis K, Papassideri I. Cell-derived microparticles in stored blood products: innocent-bystanders or effective mediators of post-transfusion reactions? *Blood Transfus.* 2012;10(Suppl 2):s25–s38.

18.   Rubin O, Delobel J, Prudent M, et al. Red blood cell-derived microparticles isolated from blood units initiate and propagate thrombin generation. *Transfusion*. 2013;53(8):1744–1754.

19.   Dern RJ, Gwinn RP, Wiorkowski JJ. Studies on the preservation of human blood. I. Variability

in erythrocyte storage characteristics among healthy donors. *J. Lab. Clin. Med.* 1966;67(6):955–965.

20. Tzounakas VL, Kriebardis AG, Papassideri IS, Antonelou MH. Donor-variation effect on red blood cell storage lesion: A close relationship emerges. *Proteomics Clin. Appl.* 2016;10(8):791–804.

21. Jordan A, Chen D, Yi Q-L, et al. Assessing the influence of component processing and donor characteristics on quality of red cell concentrates using quality control data. *Vox Sang.* 2016;111(1):8–15.

22. Tzounakas VL, Georgatzakou HT, Kriebardis AG, et al. Uric acid variation among regular blood donors is indicative of red blood cell susceptibility to storage lesion markers: A new hypothesis tested. *Transfusion*. 2015;55(11):2659–2671.

23. Lesch A, Cortés-Salazar F, Prudent M, et al. Large scale inkjet-printing of carbon nanotubes electrodes for antioxidant assays in blood bags. *J. Electroanal. Chem.* 2014;717–718:61–68.

24. Pisoschi AM, Cimpeanu C, Predoi G. Electrochemical Methods for Total Antioxidant Capacity and its Main Contributors Determination: A review. *Open Chem.* 2015;13(1): DOI: 10.1515/chem-2015-0099.

25. Abonnenc M, Crettaz D, Tacchini P, et al. Antioxidant power as a quality control marker for completeness of amotosalen and ultraviolet A photochemical treatments in platelet concentrates and plasma units. *Transfusion*. 2016;56(7):1819–1827.

26. Bardyn M, Maye S, Lesch A, et al. The antioxidant capacity of erythrocyte concentrates is increased during the first week of storage and correlated with the uric acid level. *Vox Sang.* 2017;112(7):638–647.

27. Renedo OD, Alonso-Lomillo MA, Martínez MJA. Recent developments in the field of screen-printed electrodes and their related applications. *Talanta*. 2007;73(2):202–219.

28. Kurita R, Yabumoto N, Niwa O. Miniaturized one-chip electrochemical sensing device integrated with a dialysis membrane and double thin-layer flow channels for measuring blood samples. *Biosens. Bioelectron.* 2006;21(8):1649–1653.

29. Couto R a. S, Lima JLFC, Quinaz MB. Recent developments, characteristics and potential applications of screen-printed electrodes in pharmaceutical and biological analysis. *Talanta*. 2016;146:801–814.

30. Tacchini P, Lesch A, Neequaye A, et al. Electrochemical Pseudo-Titration of Water-Soluble Antioxidants. *Electroanalysis*. 2013;25(4):922–930.

31. Erel O. A novel automated direct measurement method for total antioxidant capacity using a new generation, more stable ABTS radical cation. *Clin. Biochem.* 2004;37(4):277–285.

32. Bordbar A, Johansson PI, Paglia G, et al. Identified metabolic signature for assessing red blood cell unit quality is associated with endothelial damage markers and clinical outcomes. *Transfusion*. 2016;56(4):852-862.

33. D'Alessandro A, Kriebardis AG, Rinalducci S, et al. An update on red blood cell storage lesions, as gleaned through biochemistry and omics technologies. *Transfusion*. 2015;55(1):205–219.

34. Bardyn M, Rappaz B, Jaferzadeh K, et al. Red blood cells ageing markers: a multi-parametric analysis. *Blood Transfus.* 2017;15(3):239–248.

35. Hess JR, Lippert LE, Derse-Anthony CP, et al. The effects of phosphate, pH, and AS volume on RBCs stored in saline-adenine-glucose-mannitol solutions. *Transfusion*. 2000;40(8):1000–1006.

36. Jordan A, Acker JP. Determining the Volume of Additive Solution and Residual Plasma in

Whole Blood Filtered and Buffy Coat Processed Red Cell Concentrates. *Transfus. Med. Hemotherapy*. 2016;43(2):133–136.

37. Lucas-Heron B, Fontenaille C. Urate transport in human red blood cells. Activation by ATP. *Biochim. Biophys. Acta.* 1979;553(2):284–294.

38. Buzdygon KJ, Zydney AL. Effect of storage time on red blood cell membrane permeability to creatinine and uric acid. *ASAIO Trans.* 1989;35(3):693–696.

39. Tzounakas VL, Kriebardis AG, Georgatzakou HT, et al. Data on how several physiological parameters of stored red blood cells are similar in glucose 6-phosphate dehydrogenase deficient and sufficient donors. *Data Brief*. 2016;8:618–627.

40. Bordbar A, Jamshidi N, Palsson BO. iAB-RBC-283: A proteomically derived knowledge-base of erythrocyte metabolism that can be used to simulate its physiological and patho-physiological states. *BMC Syst. Biol.* 2011;5:110.

41. Nishino T, Yachie-Kinoshita A, Hirayama A, et al. Dynamic Simulation and Metabolome Analysis of Long-Term Erythrocyte Storage in Adenine–Guanosine Solution. *PLoS ONE*. 2013;8(8):e71060.

42. Abonnenc M, Tacchini P, Crettaz D, et al. Quality control assay to monitor the completeness of pathogen or targeted cell inactivation treatments in biological, foodstuff, drinks and cosmetics products. 2017; WO 2017/103661 Al.

CHAPTER 3

MODIFICATION OF THE ADDITIVE SOLUTION FORMULATIONS TO REDUCE RED BLOOD CELL STORAGE LESIONS

INTRODUCTION

From decades of research and as shown in the previous chapters, it is well known that the Red Blood Cells (RBCs) accumulate a broad range of physicochemical changes during their storage at 4°C, rendering these cells qualitatively different than the fresh ones[1,2]. Some of these lesions are reversible. Notably, the levels of Adenosine Triphosphate (ATP) and 2,3-Diphosphoglycerate (2,3-DPG) that were shown to be rapidly replenished after transfusion[3]. Later during storage (around week 4), irreversible lesions such as proteins post-translational modifications (*i.e.* carbonylation, glycation, and methylation[4]), fragmentation and aggregation start to appear. Lipids are also subject to peroxidation. Ultimately, Microvesicles (MVs) are released resulting in irreversible membrane surface reduction leading to spheroechino- and sphero-cystosis and to the reduction of the RBC deformability. RBCs stored for long periods also have tendency to lose the CD47 "do not eat me" signal. As a consequence, extensively damaged cells become targets for rapid removal from the circulation of the transfusion recipient. Luten *et al.* determined that the mean 24-hour Post-Transfusion Recovery (PTR) of RBCs stored in Saline-Adenine-Glucose-Mannitol (SAGM) for a short period of time (0-10 days) was of 86.4 ± 17.8 % and dropped to 73.5 ± 13.7 % after 25 to 35 days of storage[5]. To meet the official guidelines, it is accepted that up to 25 % of the RBCs are rapidly removed after a transfusion (or that at least 75 % of the RBCs should survive 24-hour post-transfusion). This opens the question of transfusion efficiency in function of storage duration.

Beyond mitigation of the beneficial impact of the transfusion, the storage-related changes in RBCs can even trigger deleterious side effects, affecting the patient clinical outcomes[6–9]. Hence, the MVs that progressively accumulate in the supernatant of the Red Cell Concentrates (RCCs) are known to have hemostatic, pro-thrombotic and pro-inflammatory effects[10–13]. Indeed, the exposure of negatively charged phospholipids make the MVs prone to initiate and propagate the generation of thrombin in plasma[13]. Bioactive lipids are also implicated in Transfusion-Related Acute Lung Injury (TRALI), and were shown to have immunomodulatory effects.

Moreover, prolonged storage of RCCs (*i.e.* six weeks) results in enhanced extravascular hemolysis and increased levels of Non-Transferrin Bound Iron (NTBI) in circulation, as demonstrated by Hod *et al.*[14]. Similarly, Rapido *et al.* observed, in a study were sixty healthy volunteers were randomly transfused with one autologous leukoreduced RCC after one to six weeks of storage, a decline of transfusion efficiency proportional to the storage duration (*i.e.* decreased 20-hour RBC recovery, elevation in Hematocrit [HCT] and serum ferritin)[15]. Moreover, the older units (six weeks) were associated with a significant increase in extravascular hemolysis (transferrin saturation and increased serum NTBI) after six weeks of storage. The consecutive accumulation of cell-free Hemoglobin (Hb) in organs such as the spleen, the kidney and/or the liver might alleviate adverse

reactions such as increased inflammation or predisposition to infections[16–21]. Long-term storage of RBC products also has vascular effects. Indeed, aged RBCs reduce the bioavailability of Nitric Oxide (NO) by impairing its *de novo* synthesis, as well as *via* its scavenging by free hemes and MVs for example[22,23]. NO is a powerful vasodilator, whose depletion could limit oxygen (O_2) perfusion to tissues and more particularly to end organs.

Some studies (randomized trials, retrospective researches and meta-analyses) suggested that patients transfused with short- or long-term stored RBCs have similar clinical outcomes[24–30], whereas others demonstrated the adverse effects of transfusing long-term stored RBCs[31–36]. Recently, Goel *et al.* showed in a retrospective study that transfusion of RCCs of more than 35 days was associated with increased morbidity, and even higher mortality for the most critically ill patients[36]. In 2018, Jones *et al.* analyzed data acquired during the PROPPR (Pragmatic, Randomized Optimal Platelet and Plasma Ratios) trial and concluded that massive transfusion (≥10) of packed RBC stored for 22 days or more increased the likelihood of 24-hour mortality[33].

Up to now, no consensus has been found in the transfusion community concerning the potential danger of transfusing "old" blood. The discrepancy between the different studies is imputable to the fact that in addition to storage duration, many other parameters can be associated with the transfusion outcomes. First, there is the fact that each transfused patient is unique, *i.e.* diagnostic and co-morbidities, number of blood products received, age, sex, etc. In addition, the donor characteristics surely affect the transfusion outcome[37–40]. For example, a retrospective study demonstrated that blood donated by women who were pregnant once increased the rate of mortality in male patients but not in other women, suggesting that more factors than only blood groups define the fine donor-recipient compatibility match[38]. Moreover, heterogenous results can be caused by the blood processing and type of additive solutions used for the preparation of the transfused blood products[41]. Finally, inconsistencies could be attributed to the categorization of the RCC age. Indeed, in clinical studies (mostly observational or retrospective), long-term stored RCCs have a mean age of 26 ± eight days whereas it was shown *in vitro* that irreversible lesions accumulate around four to five weeks of storage[42].

In conclusion, even if we assume that no adverse effects are associated with transfusion of long-term stored RBCs, despite the alterations they accumulate, we should wonder about the efficiency of such labile blood products. To answer this central question, more studies assessing the storage duration with the RBC post-transfusion recovery and survival are needed[43]. Overall, the above observations open the question of the transfusion practices related to the age of RBCs, but reduction of the RCC shelf life is probably not the best solution to this issue as it would induce shortage of blood product inventory[44]. Therefore, different strategies were proposed in the past decades[45], such as the development of acellular Hb-Based Oxygen Carriers (HBOCs)[46], or the *ex vivo* generation of RBCs from

stem cells[47–50], as well as the cryopreservation[51,52], anaerobic storage[53–57] or rejuvenation of the donated RBCs[58–60]. A lot of research was also devoted to the improvement of stored RBC quality *via* the modification of the additive solution formulations[61–63].

The studies presented in this Chapter will focus on this last approach. First, the aim will be to counteract the effects of blood processing. The strategy will consist in adding protective molecules naturally found in the human plasma at physiological levels. The choice of the added compound was based on the observations made during the study presented in Chapter 2[64]. Then, in Part 2, different molecules having potential antioxidant action will be added in the blood bags. The selection of the compound added was this time based on the literature.

PART 1: RESTORATION OF PHYSIOLOGICAL AMOUNTS OF ENDOGENOUS ANTIOXIDANTS

The normal Uric Acid (UA) levels measured in the serum is 120-420 µM, close to its limit of solubility[65]. Such high concentration is the result of a series of mutations that conducted to the silencing of the uricase gene (uricase enzyme degrades UA into allantoin). Moreover, UA is efficiently reabsorbed at the level of the kidneys.

UA is an endogenous antioxidant molecule capable of neutralizing a large range of ROS and more particularly the singlet O_2 and free radicals by accepting a single electron[66,67]. It is an end product of the purine metabolism. UA was estimated to contribute at 60 % to the Ferric Reducing Ability of Plasma (FRAP)[68]. Ames *et al.* even proposed that such powerful antioxidant system constitutes an evolutionary advantage by reducing the cellular oxidative stress and thus the occurrence of cancers, explaining the exceptional lifetime of the human beings[66].

As shown in Chapter 2, because of the preparation of the labile blood product, the plasma that normally surrounds the RBCs is almost completely replaced by additive solution. The exogenous antioxidant defenses are subsequently reduced, which in turn impacts the intracellular Antioxidant Power (AOP). Consequently, stored RBC are more sensitive to oxidative stress and accumulate oxidative lesions during storage.

In the framework of RBC storage, plasma UA level was shown to be a potential storability biomarker. Indeed, Tzounakas *et al.* observed that RBCs from donors with a high serum UA concentration (447.6 ± 29.8 µM) aged better in leukoreduced RCC collected in citrate-phosphate-dextrose (CPD) anticoagulant and stored in SAGM solution. Indeed, the RBCs from "high-UA" donors had reduced indicators of oxidative stress, of intracellular Ca^{2+} accumulation and of spheroechinocytosis, in comparison to those from donors with low levels of UA (281.5 ± 14.9 µM)[69]. In a more recent study, the same team confirmed the association between donor serum UA concentration and the fragility of RBCs stored in non-leukoreduced Citrate-Phosphate-Dextrose-Adenine-1 (CPDA-1) RCCs[70].

In the light of these observations and knowing that only residual amount of plasma remains in the RCCs[71], the aim of the two following studies was to supplement the RCCs with physiological amounts of UA and then with UA plus Ascorbic Acid (AA). Which could avoid a potential metabolic shift, prevent the depletion of intracellular antioxidants, as well as provide an extracellular protective environment.

PART 1.1: Supplementation of red cell concentrates with uric acid

Study design

To evaluate the effect of UA addition, four CPD-SAGM RCCs supplemented with physiological levels of UA were stored at 4°C and followed during 70 days (Figure 1).
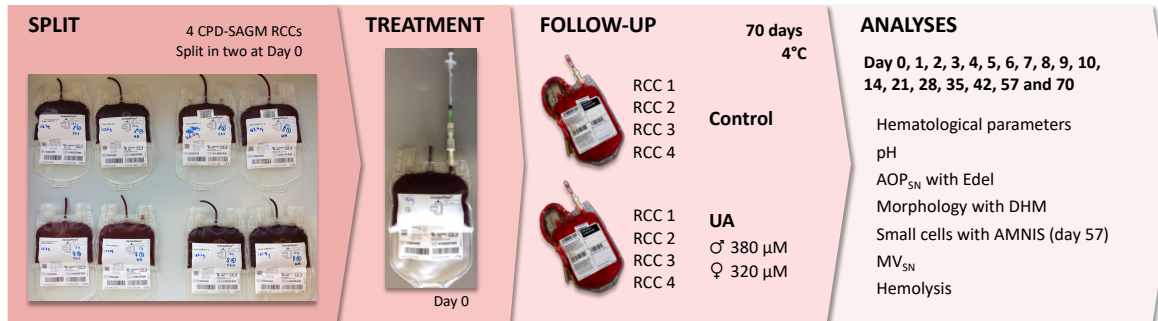
*Figure 1 – **Experimental workflow: preparation of the Red Cell Concentrates (RCCs), supplementation with Uric Acid (UA) and follow-up.** Split of the four RCCs in two subunits, treatment with 380 μM of UA for the RCCs donated by men and 320 μM in those given by women. The RCCs were followed during 70 days of storage at 4°C. The hematological parameters, pH, antioxidant power in the supernatant (AOP_{SN}), morphology, number of small cells, release of Microvesicles in the supernatant (MV_{SN}) and hemolysis were analyzed.*

After reception, each RCC was split in two subunits in sealed conventional storage bags and treated with control or UA stock solutions. According to the paper of Fathallah-Shaykh and Cramer[72], the UA concentration in serum of adults is 305.4 ± 74.4 μM for the men and 252.8 ± 65.4 μM for the women. Here, the RCCs were supplemented with the maximal UA extracellular concentration, *i.e.* 380 μM and 320 μM respectively. Then, a panel of analyses was done to evaluate the evolution of the storage lesions.

Material and methods

Preparation and treatment of the red cell concentrates

Four RCCs stored in CPD-SAGM at 4°C were used for this study (see donor's characteristics in Table 1).

*Table 1 – **Donor's characteristics**. Sex, age and blood group (ABO and Rhesus D) of the donor.*

Sample	Sex	Age / year	Blood group
RCC 1	Male	31	A +
RCC 2	Male	38	AB +
RCC 3	Female	62	O +
RCC 4	Female	26	A +

RCC: red cell concentrate.

The whole blood units were donated by two men and two women and stored overnight at Room Temperature (RT). Early the next morning, the products were processed using routine procedures and

sent to our laboratory as quickly as possible to limit as much as possible the delay between the plasma reduction and UA supplementation (Day 0).

The stock solutions (26x concentrated) were prepared by dissolving UA powder in SAGM in presence of NH_3 that helps to the UA dissolution. The same amount of NH_3 was added in the control. The solutions were then filtrated at 0.22 µM to limit bacterial contamination. As we assumed that the RBCs in the split RCCs are surrounded by 50 mL of SAGM additive solution (this quantity is probably slightly overestimated), 2 mL of 26x stock solution (*i.e.* 9.87 mM UA for men and 8.27 mM UA for women, in presence of 29.5 µM or 0.056 % NH_3) were injected in the blood bags in a laminar flow hood.

Follow-up during storage

Approximatively 2.5 mL of RCC were taken daily during the first 10 days of storage and then weekly until expiration at day 42, an additional time point was added at day 70. The percentage of small cells was also evaluated at day 57 by imaging flow cytometry. Hematological values were analyzed with a Sysmex automate and the pH of the RCC was measured (Orion SA 520 pH-meter and Orion Micro 8228 PerpHecT ROSS electrode). The samples were then centrifuged at 2000 *g* during 10 min at 4°C and the supernatant was collected for AOP quantification (EdelMeter potentiostat electrochemical analyzer), MV count (flow cytometry), and determination of percentage of hemolysis (Harboe direct spectrophotometric method with the Allen correction). In parallel, RBCs were washed twice in 0.9 % NaCl (centrifugation as before) and finally resuspended in two volumes of HEPA for morphology analysis by Digital Holographic Microscopy (DHM). More details about the analytical methods used can be found in Part 1 of Chapter 1.

Small cell analysis

The analysis of the small cells was done by Michael Dussiot and Pascal Amireault (Institut Imagine, Laboratory of Cellular and Molecular Mechanisms of Hematological Disorders and Therapeutic Implications, Laboratoire d'Excellence GR-Ex, Université Sorbonne Paris Cité, Université Paris Descartes, Inserm, CNRS, Paris, France). The projected surface area of the RBCs was characterized using imaging flow cytometry (ImageStream X Mark II, AMNIS part of EMD Millipore). The exact procedure is described in the paper from Roussel *et al.* published in *Transfusion* in 2017[73]. Shortly, the RBCs were diluted at 1 % HCT in a modified Krebs-albumin solution and imaged at 60x magnification with the AMNIS flow cytometer. The projected surface area of focused, front view RBCs was measured post-acquisition *via* the IDEAS software. The distribution of the projected surface area was then plotted on frequency histograms and the small cells were segregated from the "normal" ones using the nadir (local minima) of the bimodal distribution.

Results and discussion

The evolution observed at the level of the hematological parameters and the pH were similar between control or UA conditions for each RCC and evolved as usual (Figure 2A and 2B). The RBCs gained on average 6.6 fL over 70 days for the control as well as the UA samples and the anisocytosis increased gradually, reflecting morphological changes.

*Figure 2 – **Red Blood Cell (RBC) aging markers in Red Cell Concentrates (RCCs) supplemented with Uric Acid (UA). Part 1.** [A] Hematological data: RBC count, Mean Corpuscular Volume (MCV) and Standard Deviation of Distribution Width (SD-RDW) measured with Sysmex analyzer. [B] pH in the RCCs. [C] Antioxidant Power (AOP) in supernatant quantified by pseudotitration voltammetry with EdelMeter. Mean value ± standard deviation.*

The pH was about 7.1-7.2 at day 0 and dropped to 6.6-6.5 at day 42 and around 6.5-6.4 at day 70 for all RCCs. Such acidification can be imputed to rise of extracellular lactate levels and reflects the accumulation in the supernatant of cellular metabolic waste products.

The extracellular AOP was higher in the UA *versus* control RCCs all along the follow-up period (Figure 2C). This result was expected as UA is a redox active substance that contributes to the electrochemical signal. In treated samples, the AOP dropped rapidly during the first 6 days of storage and then diminished more progressively. In control units, the AOP was on average 15 % higher in men than women and exhibited the same pattern (an increase followed by a decrease), as observed before. The morphology of the RBCs treated with UA was slightly better (however not significantly, Figure 3). In the 4 RCCs, the percentage of discocytes was higher and for RCC 1, 2 and 4, the percentage of echinocytes and spherocytes was lower after 42 days of storage, the differences were less marked after 70 days.
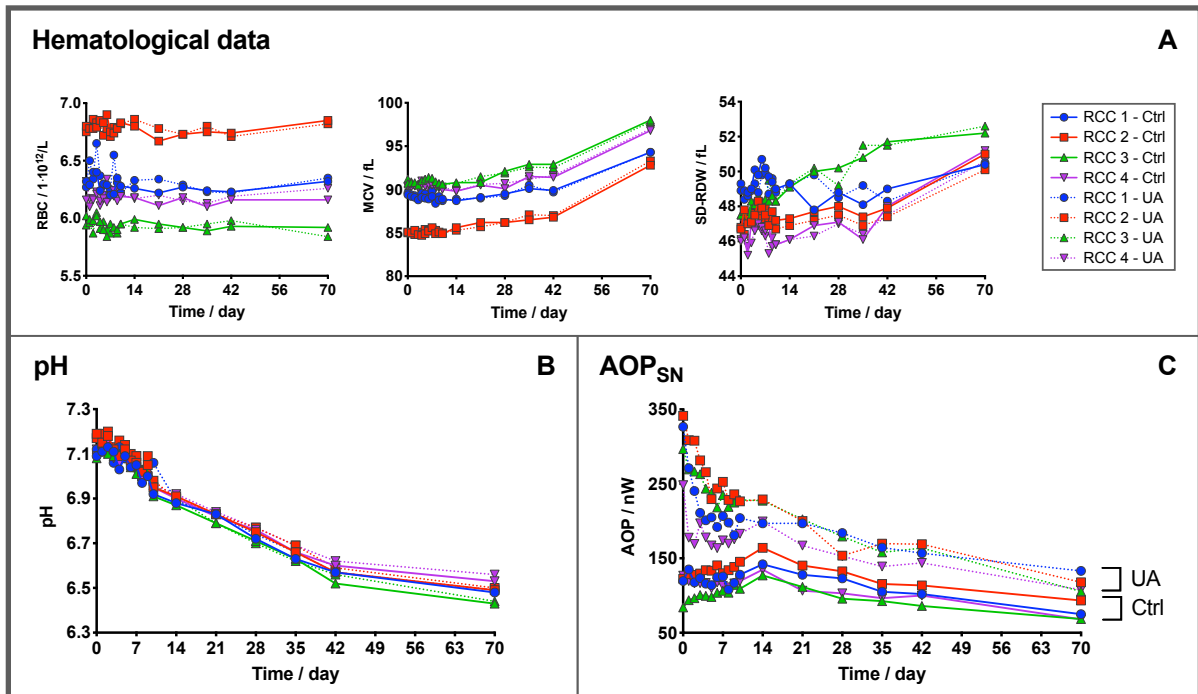
*Figure 3 – **Red Blood Cell (RBC) aging markers in Red Cell Concentrates (RCCs) supplemented with Uric Acid (UA). Part 2.** Morphology analysis with Digital Holographic Microscope (DHM): [A] single-cell morphology analysis with CellProfiler and CellProfiler Analyst (CPA), and [B] population analysis with Standard Deviation of Optical Path Difference parameter (SD-OPD). [C] Percentage of small cells at day 57 determined with the AMNIS imaging flow cytometer. Mean value ± standard deviation.*

At the level of the entire cell population, the Standard Deviation of Optical Path Difference (SD-OPD) was lower in UA *versus* Ctrl RCCs (Figure 3B). This parameter, as shown before, is positively correlated to the percentage of spherocytes (refer to ANNEX-3). To note that stomatocytic RBCs, certainly contribute positively to the SD-OPD signal because of their round and dense shape. It explains why the SD-OPD signal was higher in RCC 4 that counts a high basal level of stomatocytes. Then, these cells seemed to be progressively transformed in discocytes in the course of the storage, when looking at the individual cell morphology analysis (Figure 3A).

The percentage of small cells in the sample was not significantly different between the control and treated samples at day 57 (Figure 3C). The distribution of the projected surface area on the normalized frequency plot (not shown) exhibited the expected bimodal profile which reflects the appearance of a subpopulation of small cells during storage. The smaller RBCs were shown to be essentially echinocytes, spheroechinocytes and spherocytes[73].
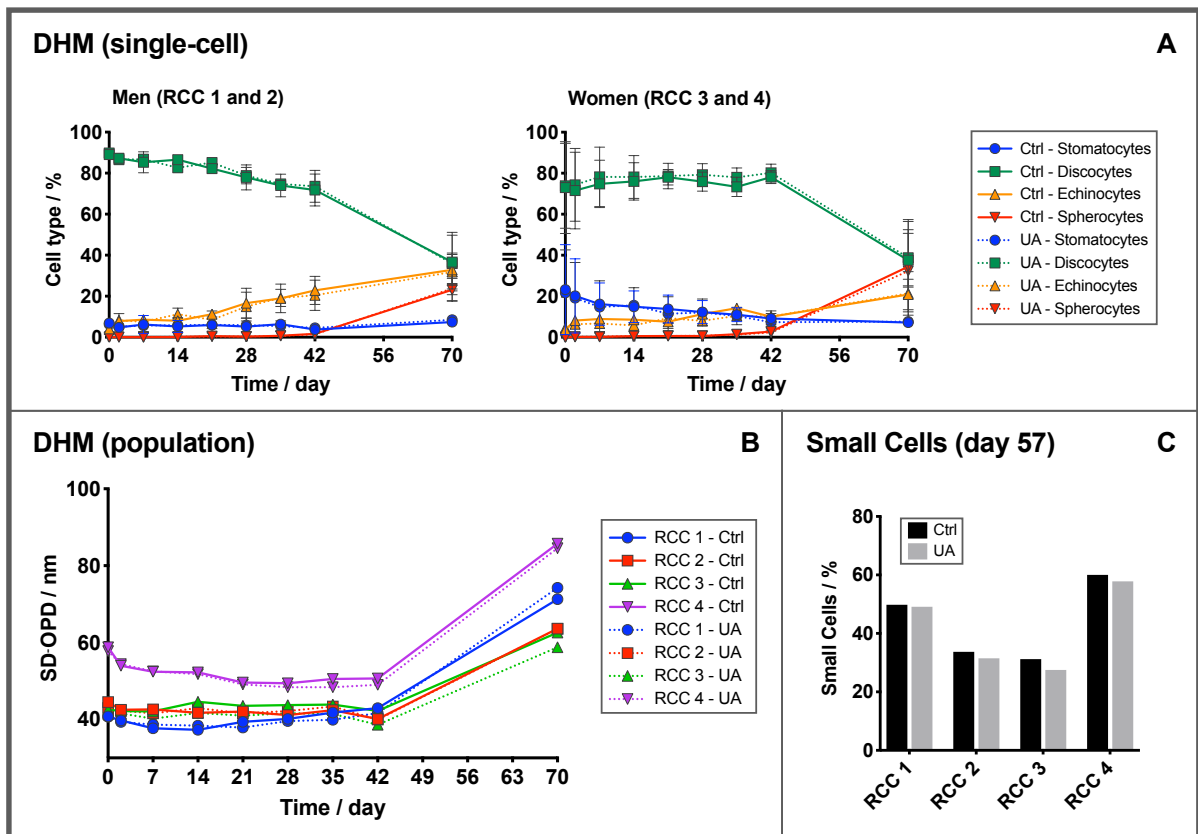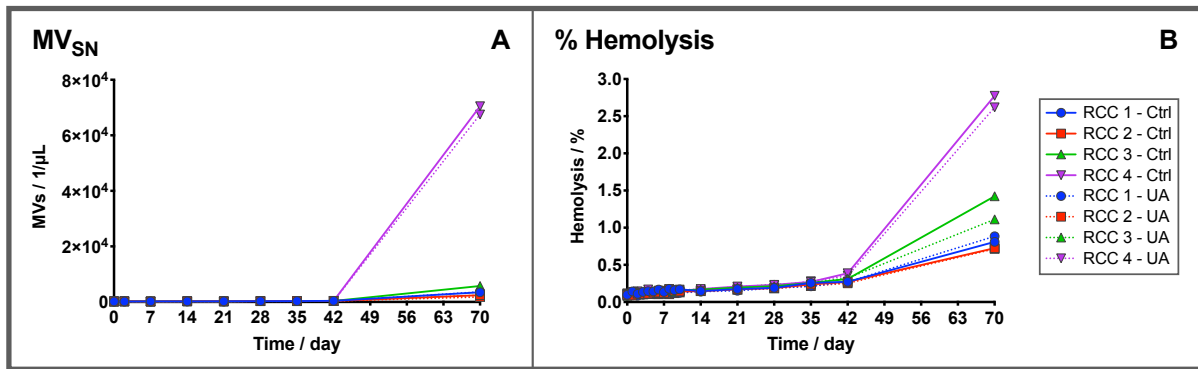
*Figure 4 – **Red Blood Cell (RBC) aging markers in Red Cell Concentrates (RCCs) supplemented with Uric Acid (UA). Part 3.** [A] Microvesicles (MVs) in the RCC supernatant counted by flow cytometry. [B] Percentage of hemolysis in the blood bag determined with the Harboe spectrophotometric method. Mean value ± standard deviation.*

Finally, the release of MVs and hemolysis were slightly lower (not significantly) in the RBCs treated with UA (Figure 4A and 4B). These two parameters are closely correlated as they both reflect irreversible lesions. RCC 4 was the least "storable" unit.

Conclusions

In conclusion, the addition of UA in the blood bag did not significantly improve or worsen RBC aging markers during storage. One reason might be that the antioxidant activity of UA is limited to hydrophilic environments[74] and that it can become a conditional prooxidant for lipids and membranes within the cells[75].

PART 1.2: Supplementation of the red cell concentrates with uric acid and ascorbic acid

The human plasma contains AA at a concentration comprised between 30 and 110 μM. It was shown in plasma, AA had to be present to prevent the prooxidant properties of UA[76]. In the light of such information and knowing that AA concentration is also drastically reduced by plasma dilution in the RCCs, it was decided to treat the RBCs with both AA and UA to reach extracellular levels close to the physiology.

Study design

The RCCs were prepared as follows (Figure 5).
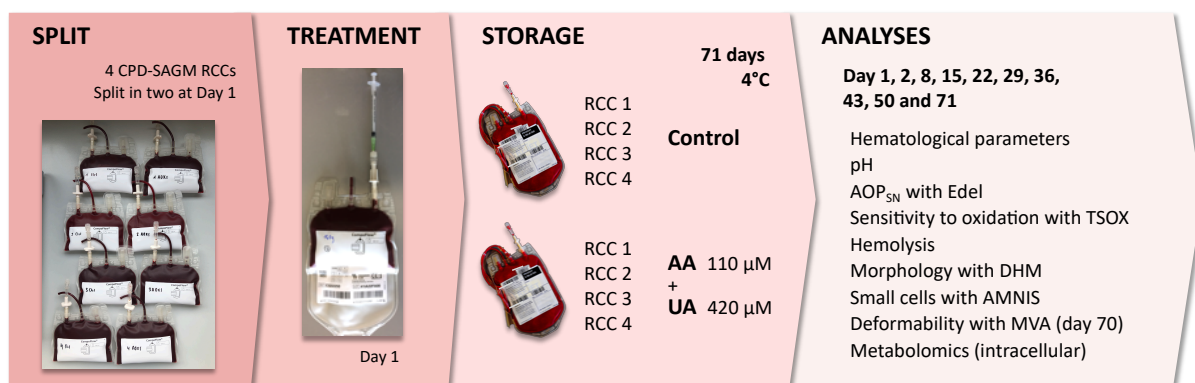
*Figure 5 – **Experimental workflow: preparation of the Red Cell Concentrates (RCCs), supplementation with Ascorbic Acid (AA) plus Uric Acid (UA) and follow-up.** Split of the four RCCs in two subunits, treatment with 110 µM AA and 420 µM UA. The RCCs were followed during 71 days of storage at 4°C. The hematological parameters, pH, Antioxidant Power in the supernatant (AOP$_{SN}$), sensitivity to oxidation, hemolysis, morphology, number of small cells, deformability and intracellular metabolite levels were analyzed.*

Standard aging markers, *i.e.* hematological parameters, pH, AOP, hemolysis and morphology were analyzed during the storage at 4°C of CPD-SAGM RCCs supplemented with 110 µM of AA and 420 µM of UA antioxidants. Again, in order to capture deep storage lesions, the follow-up period was extended to 10 weeks (71 days) instead of 6 (official expiration date). In addition to the parameters mentioned above, novel tests were added, such as the "Test of Sensitivity to Oxidation" (TSOX) developed to characterize the sensitivity of RBCs to oxidative stress and thus indirectly their antioxidant defenses. For this follow-up, the percentage of small cells in the sample was also determined at each time-point. In addition, a microfluidic device was used to evaluate the RBC rheological properties after 70 days of storage[53,77]. Finally, metabolomic analysis was conducted to evaluate the impact of the treatment on the RBC metabolism.

Material and methods

Four RCCs donated exclusively by male donors (Table 2) were selected for this experiment.

*Table 2 – **Donor's characteristics**. Sex, age and blood group (ABO and Rhesus D) of the donor.*

Sample	Sex	Age / year	Blood group
RCC 1	Male	52	A +
RCC 2	Male	54	A +
RCC 3	Male	27	B +
RCC 4	Male	61	A +

RCC: Red Cell Concentrate.

The whole blood was processed at day 0 and the antioxidants were added at day 1. Ideally, the separation and treatment should have been performed the same day to avoid early release of UA that probably results from the resuspension of the RBCs in a non-physiological environment (not 100 % plasma). Unfortunately, it was not possible because of logistic reasons.

After being split in two subunits in sealed conventional bags, the RCCs were supplemented with 2 mL of AA-UA stock solution (26x). The stock solution (2.95 mM AA and 10.83 mM UA) was prepared in 0.9 % NaCl and was supplemented with 36.9 µM NH_3 to help the dissolution of UA. The same amount of NH_3 was added in the control. As we assumed an extracellular volume of 50 mL SAGM, the final concentrations of AA and UA were thus theoretically of 110 µM AA and 420 µM UA respectively, which corresponds to the maximum of the UA concentration in plasma.

Follow-up during storage

The RCCs were sampled at day 1, 2, 8, 15, 22, 29, 36, 43, 50 and 71 of storage. The bags stored at 4°C were gently mixed, and 4.2 mL were collected with a syringe through a sampling site. A 1-mL sample was immediately put aside and shipped at 4°C to Paris (France) for the analysis of small cell (AMNIS imaging flow cytometry). Another 1 mL was used for the test of RBC sensitivity to oxidation. At day 70, 1 mL was also withdrawn to test a microfluidic device developed to assess RBC deformability (MVA system).

Sysmex analysis and pH measurement were performed on the whole RCC. The remaining 2 mL were centrifuged at 2000 g for 10 min at 4°C. The supernatant was kept for the quantification of the extracellular AOP (Edel) as well as for determination of the percentage of hemolysis (Harboe spectrophotometric method). The RBCs were further washed twice in 0.9 % NaCl. Aliquots of dry RBC pellet (HCT 0.821 ± 0.03) were snap-frozen in liquid Nitrogen (N_2) for metabolomics analysis. Some RBCs were also resuspended in two volumes of HEPA for morphology analysis by DHM.

Test red blood cell sensitivity to oxidation: "TSOX"

The TSOX is described more globally and with more details in Chapter 4. For this particular application, the RBCs were first washed by adding 14 mL of 0.9 % NaCl to the 1 mL RCC sample and centrifuging it during 10 min at 2000 g and 4°C. Then, the pelleted RBCs were resuspended at 10 % HCT in 0.9 % NaCl (1.8 mL final) and treated with 9 µL of 10 mM 2',7'-Dichlorofluorescin diacetate (DCFH-DA, Sigma-Aldrich) in 100 % DMSO (50 µM DCFH-DA and 0.5 % DMSO final). This dye is incorporated in the cells where it is de-esterified by the cytosolic esterases[78]. The DCFH molecule becomes fluorescent (Ex/Em 485/520 nm) upon oxidation by Reactive Oxygen Species (ROS). The RBCs were incubated 30 min at 37°C under agitation to enable the reporter probe incorporation within the cells. After this, the samples were centrifuged (as before) and the supernatant containing the excess of DCFH-DA was discarded. Finally, the RBCs were resuspended at 1 % HCT in 0.9 % NaCl, treated with 0, 0.001, 0.0025, 0.005 and 0.01 % hydrogen peroxide (H_2O_2) to generate oxidative stress. After 10 min at RT, the emitted fluorescence was quantified by flow cytometry (laser excitation at 488 nm and emission detection at FL1 533/30 nm, BD FACSVia and BD FACSVia Research Software, BD Biosciences). For the

analysis, the fluorescence emitted at different oxidant concentrations was reported and the Area Under the Curve (AUC, with a baseline corresponding to the value of fluorescence at 0 % H_2O_2) was calculated using PRISM software.

Red blood cell deformability analysis (MVA)

The experimental protocol was based on the papers of Burns *et al.*[53,77]. Shortly, the RCC samples were resuspended at HCT of 40 ± 0.5 % in 1x Phosphate Buffered Saline (PBS) and stored on ice (for maximum 1 h). Right before the analysis, 25 µL of the control and AA-UA samples were loaded, respectively, in the left and right inlets of a microfluidic device placed under an inverted brightfield microscope (IT415PH – 630-2729, VWR) equipped with a 20x objective (Plan-achromatic IOS LWD 20XPh, N.A. 0.40, W.D. 7.66 mm) and a CMOS camera (Flea3 1.3 MP Mono USB3 Vision [VITA 1300], Point Grey Research). To drive the RBCs throughout the microchannels network of the chip, the outlet was connected to a 20-cm water column to establish a differential pressure. The RBC deformability was evaluated by looking at the average flow rate Q (nL/s) below the microchannel network. Each sample was analyzed in duplicate.

Metabolomics

A panel of intracellular metabolites was quantified in treated and control RBCs, stored for 2, 8, 15, 29 and 43 days, that were put aside during the follow-up and frozen until analysis.

 The extraction of the intracellular RBC metabolites consisted in three successive extraction steps. For the first one, three volumes (450 µL) of cold methanol (-28°C) were added on the frozen pellets of washed packed RBCs (150 µL). The tubes were carefully vortexed during at least 1 min because the precipitated proteins have tendency to form dense aggregates difficult to homogenize. The samples were kept 5 min on ice before being sonicated in an ice bath during 10 min. The vortex and sonication steps were repeated twice. The tubes were then centrifuged during 15 min at 4°C and 21'000 *g*. The supernatant was transferred into another tube and kept on ice, and the bottom part which formed a solid aggregate was further processed. For the second extraction step, 1.5 volume (225 µL) of 50 % cold methanol (-28°C) was added on the aggregate, the sample was vortexed and sonicated once, and centrifuged, as before. The supernatant was added to the one obtained from the first round of extraction. Finally, for the third and last step, 1.5 volume (225 µL) of cold dH_2O (4°C) was added on the aggregate and the sample was processed as step 2. The combined supernatants for the three successive extraction steps were stored at -80°C prior to analysis. In total, the initial sample was diluted seven times.

The targeted metabolomics of the intracellular metabolites (amino acids, nucleotides, sugar phosphates and organic acids) was conducted at the Canada Research Chair in Applied Metabolic Engineering (Ecole Polytechnique de Montréal, Montréal, Québec) by Jingkui Chen and Professor Mario Jolicoeur. The frozen extracted samples were shipped by plane in dry ice. Before the analysis, the extracts were filtered through 0.2 µm filters. The quantification was done according to the method described in the paper from Ghorbaniaghdam *et al.*[79]. Shortly, the metabolites were separated by Ultra Performance Liquid Chromatography (UPLC) and analyzed by Mass Spectrometry (MS/MS). To achieve accurate and sensitive quantification, the Multiple Reaction Monitoring (MRM) approach was applied. The resulting AUC (elution time *versus* MRM signal) was calculated and compared to calibrations curves obtained with commercial standards for each series of analysis.

Results and discussion

The hematological parameters evolved similarly for both subunits (Ctrl and AA-UA, Figure 6A). For the four RCCs, the number of RBCs remained stable during the whole storage, the Mean Corpuscular Volume (MCV) increased linearly and the anisocytosis became more pronounced with cell aging.

The mean pH for the four RCCs before the split was of 7.39 ± 0.05 and increased to 7.47 ± 0.04 for the control and to 7.50 ± 0.06 for the AA-UA units after the split and treatment. The pH became gradually more acidic during storage as a results of lactate accumulation in the supernatant (Figure 6B). The pH reached 6.78 ± 0.06 *versus* 6.77 ± 0.06, and 6.46 ± 0.04 *versus* 6.42 ± 0.06 for the control *versus* AA-UA at day 43, and 71, respectively.

As expected, the AOP was much higher in the units treated with the antioxidants (*i.e.* 106.9 ± 19.5 nW in Ctrl *versus* 328.4 ± 17.3 nW in AA-UA at day 2, Figure 6C). Indeed, both UA and AA are hydrosolubles antioxidants that positively contribute to the redox potential of the sample. The AOP followed the expected trend in the control RCCs, *i.e.* an increase during the first week of storage followed by a decrease and a plateau. The reduction of the AOP signal in the treated units could results from: 1) the degradation, 2) the extracellular oxidation or 3) the uptake and consumption of the added antioxidants by the RBCs. Interestingly, the drop of AOP was more rapid in the first part of the storage. The slope of the linear regression curve was -7.87 nW/day (R^2 = 0.99) between days 2 and 22, and -1.07 nW/day (R^2 = 0.91) between days 22 and 71. Until the end of the follow-up, the AOP remained significantly higher in the treated units. The mean AOP in the four control *versus* AA-UA was 85.2 ± 20.1 *versus* 158.9 ± 17.4 nW at day 43 and 83.0 ± 8.2 *versus* 128.0 ± 13.0 nW at day 71, respectively.

*Figure 6 – **Red Blood Cell (RBCs) aging markers in Red Cell Concentrates (RCCs) supplemented with Ascorbic Acid (AA) and Uric Acid (UA). Part 1.** [A] Hematological data: RBC count, Mean Corpuscular Volume (MCV) and Standard Deviation of Distribution Width (SD-RDW) measured with Sysmex analyzer. [B] Evolution of the pH in the RCCs. [C] Antioxidant Power (AOP) in supernatant quantified by pseudotitration voltammetry with EdelMeter. [D] Test of RBC sensitivity to oxidation ("TSOX") under hydrogen peroxide (H_2O_2) treatment, reported with the 2',7'-Dichlorofluorescin diacetate (DCFH-DA) fluorescent dye. The higher the Area Under the Curve (AUC), the most intracellular Reactive Oxygen Species (ROS) generated. [E] Percentage of hemolysis in the blood bag determined using the Harboe spectrophotometric method. Mean value ± standard deviation.*

Surprisingly and despite the addition of exogenous antioxidants, the sensitivity to oxidative stress was not statistically different between control and AA-UA RBCs (Figure 6D). In both cases, the amount of intracellular ROS generated under H_2O_2 treatment increased significantly with storage time. The RBC antioxidant defenses were stronger during the first 15 days and the sensitivity to oxidative stress clearly increased at the beginning of the third week of storage (day 22). These results are in accordance with the observation made by D'Alessandro *et al.* who reported an accumulation of ROS during the first 3 weeks of storage in SAGM[80]. After this, the control and AA-UA RBCs became 2.5 and 2.3 (at day 43) and 3.7 and 3.4 (at day 71) times more sensitive to oxidation in comparison to day 2.

It seems that the addition of AA and UA antioxidants did globally not improve nor worsen RBC storage lesions. This observation was confirmed when looking at the percentage of hemolysis (Figure 6E). In the four RCCs, the cell lysis increased linearly up to day 36 and then followed an exponential trend. At day 43, the mean hemolysis was 0.345 ± 0.089 % for the control and 0.360 ± 0.065 % for the AA-UA units, below the accepted 0.8 %. At day 71, it reached 1.198 ± 0.819 % and 1.270 ± 0.903 % in the control and AA-UA RCCs.

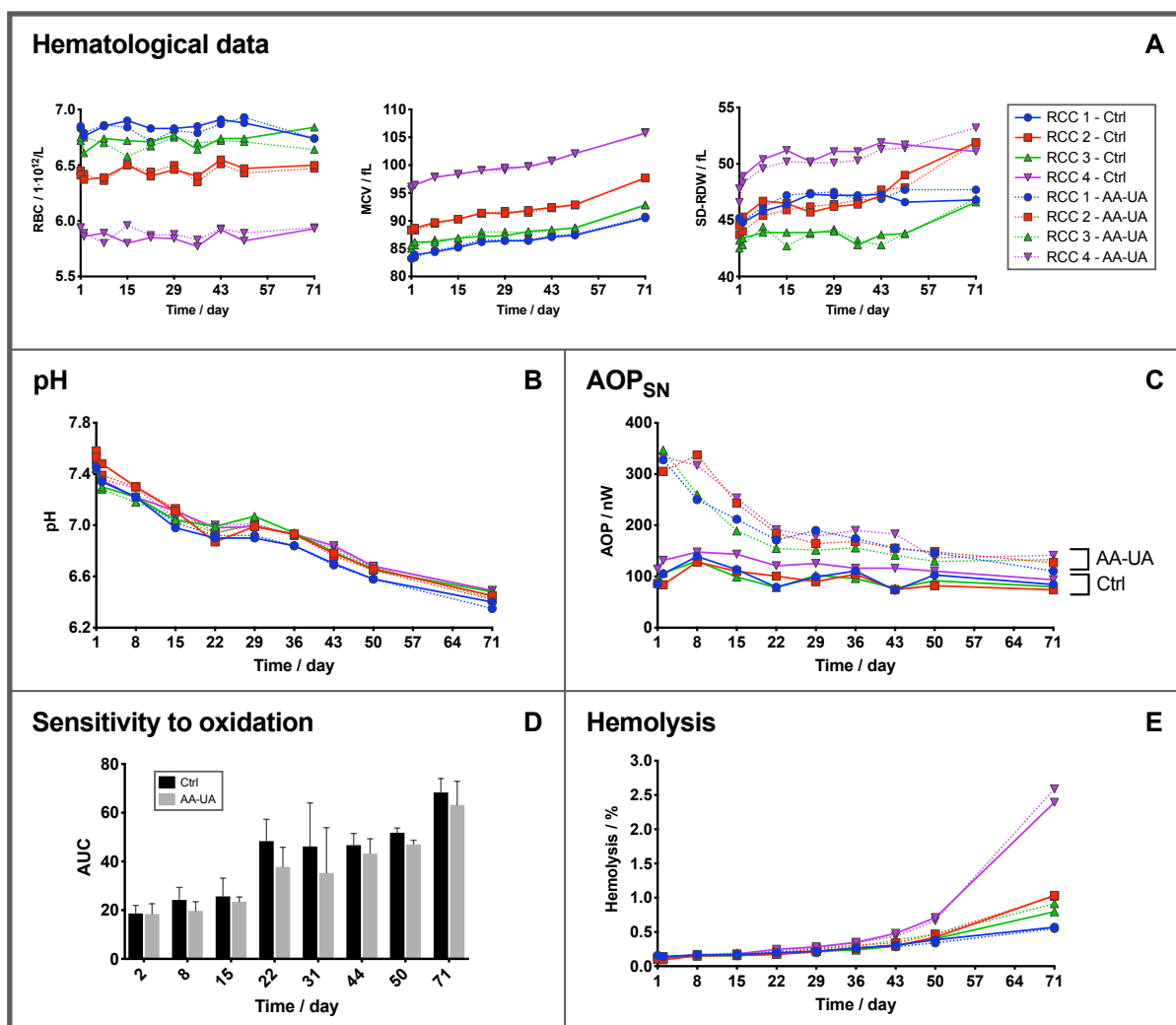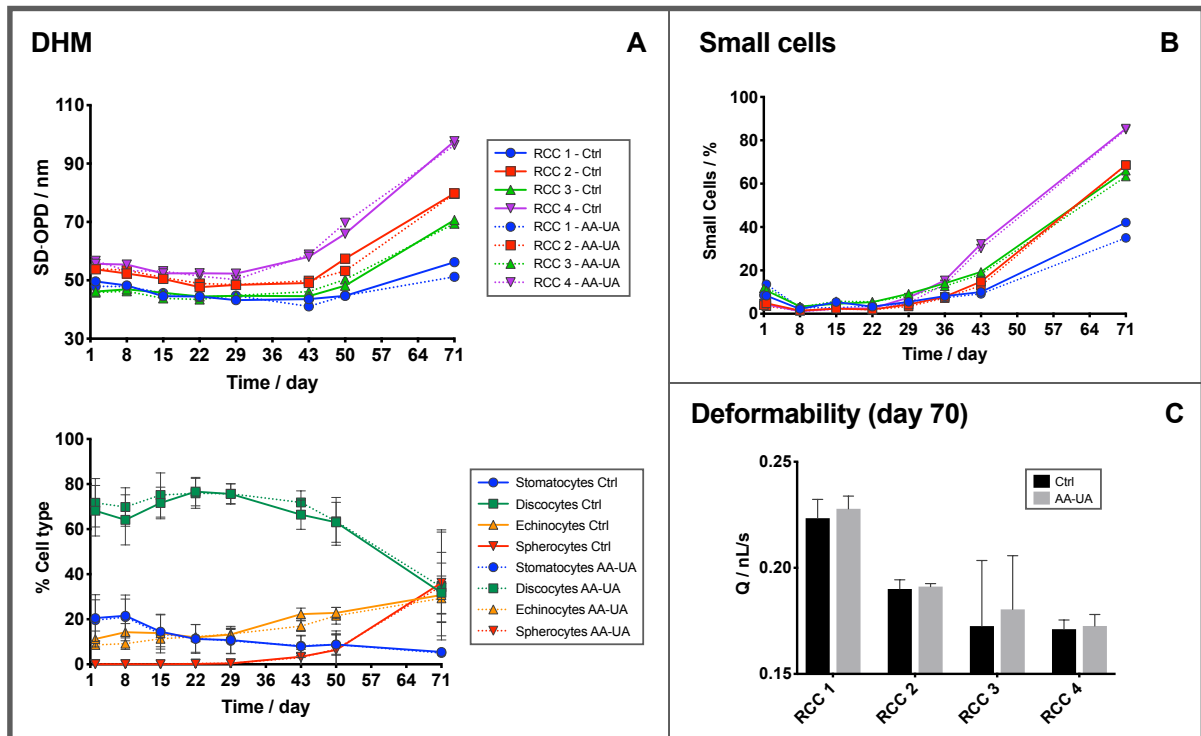*Figure 7 – **Red Blood Cell (RBCs) aging markers in Red Cell Concentrates (RCCs) supplemented with Ascorbic Acid (AA) and Uric Acid (UA). Part 2.** Morphology analysis with Digital Holographic Microscope (DHM): [A, top] population analysis with Standard Deviation of Optical Path Difference parameter (SD-OPD), and [A, bottom] single-cell morphology analysis with CellProfiler and CellProfiler Analyst (CPA). [B] Percentage of small cells determined with the AMNIS imaging flow cytometer. [C] Deformability at day 70 assessed with the MVA system. Mean value ± standard deviation.*

Similarly to other aging markers, the rheological properties of the RBCs were not radically improved by the antioxidant treatment. In all RCCs, the integrity of the cell shape was maintained during at least four weeks with a low SD-OPD (Figure 7A, top), a low percentage of spherocytes (Figure 7A, bottom) and few small cells (Figure 7B). At day 43, the treated samples had a slightly better morphology compared to control, *i.e.* 71.8 ± 5.2 % *versus* 66.4 ± 6.5 % of discocytes, 17.0 ± 2.4 % *versus* 22.3 ± 2.7 % of echinocytes and 3.0 ± 3.6 % *versus* 3.4 ± 4.2 % of spherocytes.

This tendency was confirmed when looking at the mean percentage of small cells that reached 17.6 ± 9.1 % in the AA-UA *versus* 19.1 ± 9.5 % in the control RCCs. Finally, the perfusion rate through the artificial microvascular network[53,77], that reflects the rheological properties of the RBCs was measured. The deformability of the cells was similar in both conditions at day 70 (Figure 7C).

Metabolism under uric acid and ascorbic acid supplementation

Although no macroscopic effects of UA and AA supplementation were observed, the results of the metabolomics analysis indicated that the RBC metabolism was in fact impacted. Indeed, the level of a certain number of intracellular metabolites (refer to ANNEX-8), *i.e.* Adenosine Monophosphate (AMP), Nicotinamide Adenine Dinucleotide (NAD), glucose 6-phosphate, malate, methionine, serine, glutamine, glycine, ribulose 5-phosphate & xylose 5-phosphate, ribose 5-phosphate, phenylalanine and threonine was significantly modified under treatment (at least for one time point). ATP and pyruvate concentrations were also different whereas not statistically. Finally, the intracellular UA was depleted within eight days of storage in control RBCs (as reported in Chapter 2), but was, as expected, maintained in the treated cells.

The evolution of the level of the different metabolites, as well as the fact that divergent behaviors were observed from the very beginning of the storage suggested that the treatment helped the RBCs to better support the perturbation triggered by the RCC preparation and storage.

Indeed, the evolution of the metabolism in the control RBCs seems to indicate that because UA is a metabolic end-product, its rapid depletion would pull the reactions toward the oxidative Pentose Phosphate Pathway (PPP) and then in the direction of the purine pathway as a compensatory mechanism (Figure 8, red path). Such behavior could explain why lower levels of ribose 5-phosphate and higher levels of AMP and glutamine were observed in the control samples.
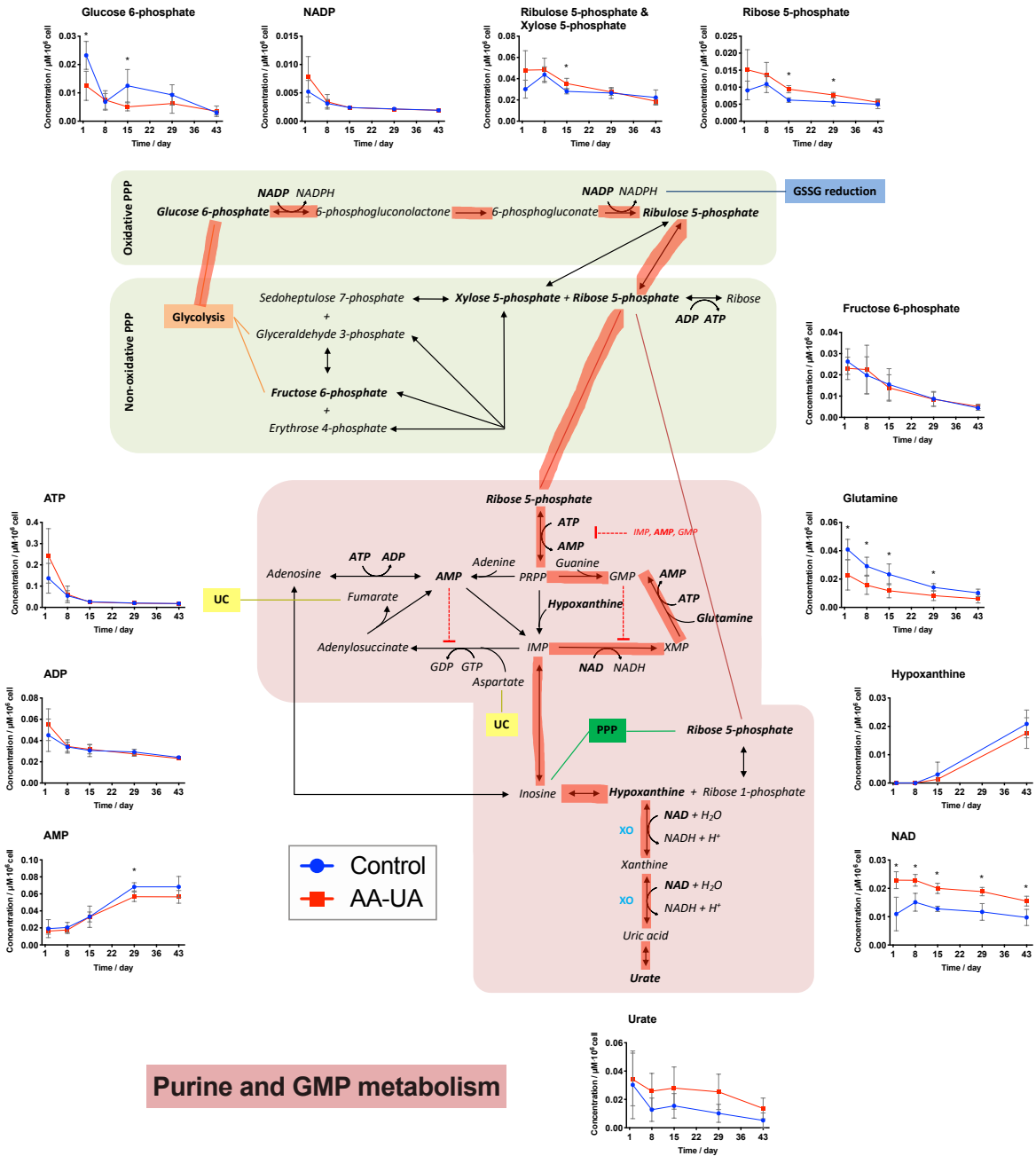
*Figure 8 – **Effect of Ascorbic Acid (AA) and Uric Acid (UA) supplementation on Red Blood Cell (RBC) metabolism. Part 1.** Oxidative and non-oxidative Pentose Phosphate Pathway (PPP), and purine and GMP metabolism in control vs AA-UA samples. Time-course metabolomics analysis of several intracellular RBC metabolites. In the control RBCs, the metabolism is pulled in the direction (red path) of non-oxidative PPP and toward the purine and GMP metabolism, probably as a result of the depletion of intracellular UA pool.*

The difference of NAD concentration could also come from this metabolic rerouting, if we assume that the RBCs contain the Xanthine Oxidase (XO) enzyme (which has not yet been reported). Indeed, the XO catalyzes the following reactions (Reactions 1 and 2).

$$Hypoxanthine + NAD^+ + H_2O + O_2 \rightleftarrows Xanthine + NADH + H_2O_2 \qquad \text{Reaction 1}$$

$$Xanthine + NAD^+ + H_2O + O_2 \rightleftarrows Urate + NADH + H_2O_2 \qquad \text{Reaction 2}$$
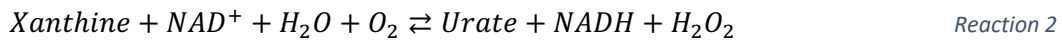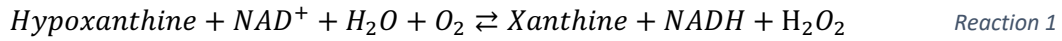
Because each of these reactions releases ROS (*i.e.* H_2O_2), urate depletion could itself further participate to the build-up of oxidative stress that was reported during the RCC storage.

*Figure 9 – **Effect of Ascorbic Acid (AA) and Uric Acid (UA) supplementation on Red Blood Cell (RBC) metabolism. Part 2.** S-Adenosylmethionine cycle (SAM), and reduced Glutathione (GSH) synthesis and oxidized Glutathione (GSSG) reduction pathways in control vs AA-UA samples. Time-course metabolomics analysis of several intracellular RBC metabolites. In the treated RBCs, GSH synthesis is favored (green path).*

The data also indicate that the treatment favored the *de novo* synthesis of reduced glutathione (GSH, Figure 9, green path). It is suggested by the lower levels of methionine, serine, as well as GSH precursors glutamine and glycine in the AA-UA samples. As such, methionine could be consumed by the S-Adenosylmethionine (SAM) cycle to produce the homocysteine metabolite. The latter then reacts with the serine to produce cysteine. The reduced concentration of glutamine and glycine tends to corroborate this hypothesis, as well as the increased consumption of pyruvate by the urea cycle and remnant of the Tricarboxylic Acid cycle (TCA or Krebs cycle) to produce more glutamate, a glutathione precursor. Unfortunately, the GSH concentration was not measured.

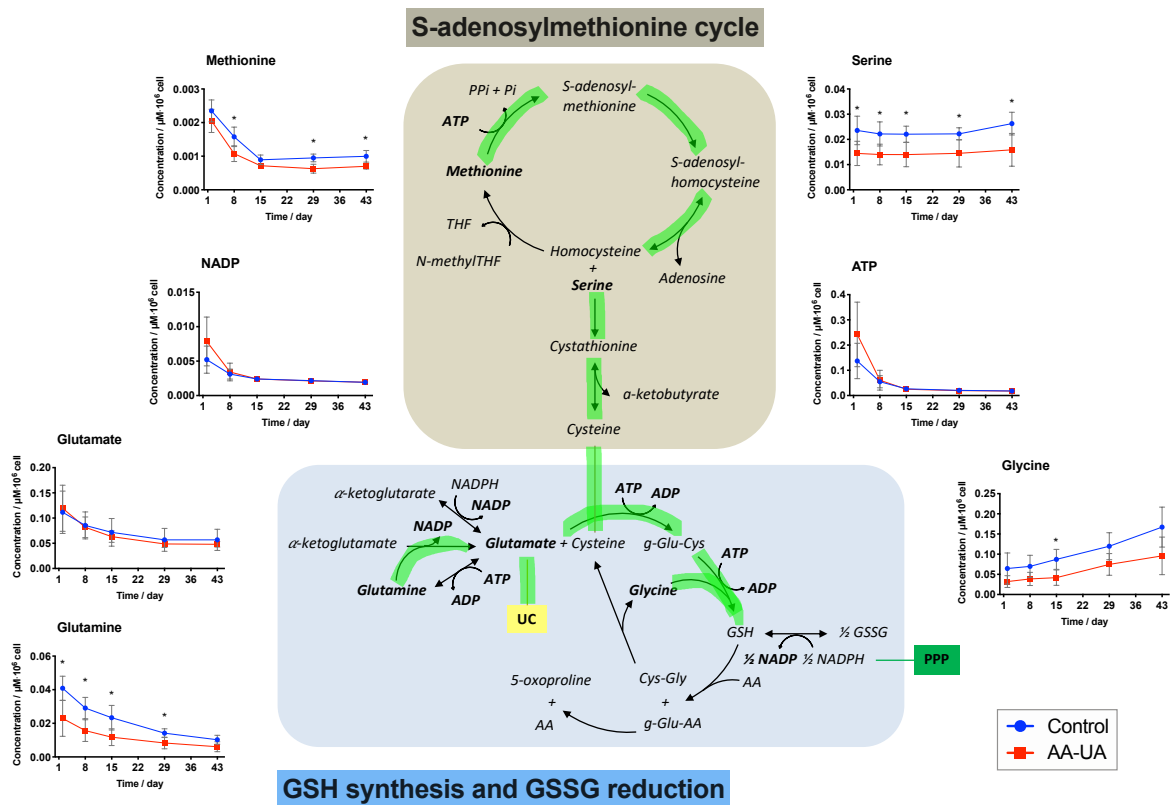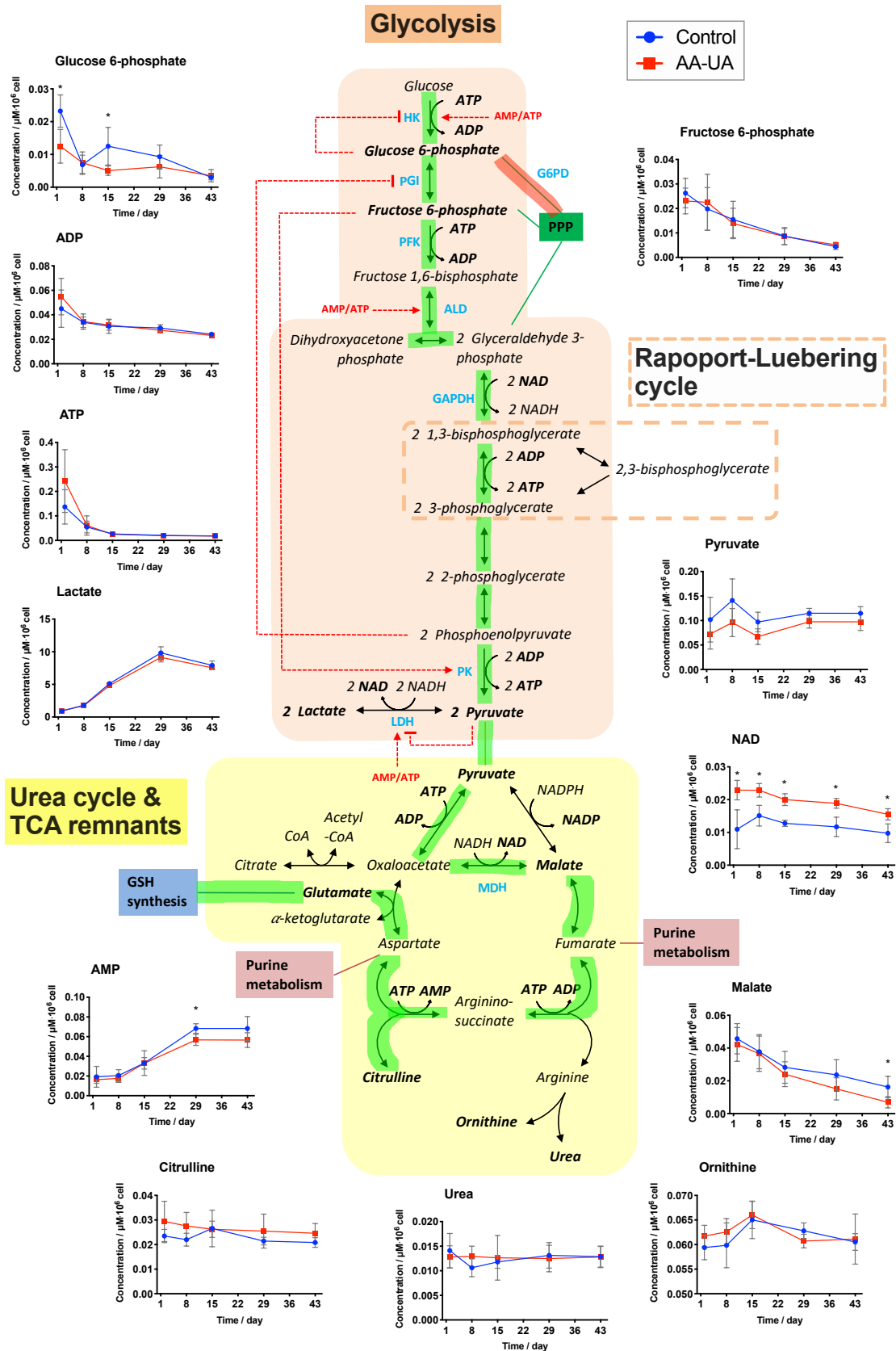*Figure 10 – **Effect of Ascorbic Acid (AA) and Uric Acid (UA) supplementation on Red Blood Cell (RBC) metabolism. Part 3.** Urea cycle and remnants of the tricarboxylic acid cycle (TCA or Krebs cycle) in control vs AA-UA samples. Time-course metabolomics analysis of several intracellular RBC metabolites. In the treated RBCs the glycolysis is favored (green path).*

A more active GSH synthesis in treated RBCs could be explained by the fact that these cells maintain a higher energy level. Indeed, preventing the switch toward the non-oxidative PPP and purine metabolism, would leave the glycolytic intermediates available for ATP (and 2,3-DPG) generation by the glycolysis (Figure 10, green path). Moreover, the reduction of the oxidative stress by the antioxidant supplementation could also limit the metabolism rerouting triggered by the RBC salvage mechanisms, *e.g.* the shift toward the non-oxidative PPP that produces reduced Nicotinamide Adenine Dinucleotide Phosphate (NADPH). Such phenomena was shown to occur in the second metabolic phase as consequence of the oxidation of the redox sensitive amino acids in the active site pocket of the Glyceraldehyde 3-Phosphate Dehydrogenase (GAPDH) enzyme[81]. Finally, higher levels of 2,3-DPG could also limit rerouting toward the PPP as it would help the cells to maintain a lower oxygenation state.

Conclusions

In a general way, the AA-UA treatment seemed to have positively impacted the RBC metabolism, *i.e.* it helped to maintain a more active glycolysis and therefore sustained key cellular functions such as the GSH synthesis. A combination of two mechanisms probably explains these effects, the first one being that the addition of UA at physiological levels prevents or at least limits the export of intracellular UA and the consequent metabolic dysregulation, and the second that addition of antioxidants prevented, at least partially, the metabolic rerouting triggered by the accumulation of oxidative stress. AA-UA addition also reduced slightly the sensitivity of the RBCs to oxidation, as shown by the TSOX assays. Unfortunately, not enough to prevent efficiently the changes of morphology, deformability and ultimately the hemolysis of the RBCs.

Independently of the effect of the treatment and as generally observed, all RCCs did not behave exactly the same way. It highlights the donor-dependent capacity for storage ("storability"). In this study, the RBCs contained in RCC 1 aged the best, *i.e.* limited anisocytosis, lower number of MVs released, best morphology and deformability and lower hemolysis. Those in RCC 4 exhibited an increased susceptibility to storage lesions. It confirms that the loss of membrane by microvesiculation reduces the surface to area ratio rendering the cells less deformable. These RBCs are probably rapidly cleared from the transfusion recipient circulation. Indeed, RBCs with more than 18 % average area loss (*i.e.* 27 % of area-to-volume ratio) were shown to be sequestered by human spleen in an *ex vivo* setting[82].

PART 2: SUPPLEMENTATION OF THE RED CELL CONCENTRATES WITH PROTECTIVE MOLECULES

Aim of the study

In the following study, the impact of the supplementation of the RCCs with several compounds having potential direct or indirect antioxidant actions during storage will be evaluated. Indeed, a higher load of antioxidant defenses could help the RBCs to deal with oxidative stress during storage. The molecules that will be added in the blood bags have all been reported to have antioxidant activities (

Table 3) and have been tested as potential therapeutic agents in Sickle Cell Disease (SCD), a pathology associated with an increased production of pro-oxidants species[83].

*Table 3 – **Properties and antioxidant activities of the tested compounds.***

Compound	Properties and antioxidant activities
Ascorbic acid (AA, vitamin C)	Reducing agent against ROS, recycling of other antioxidants (*e.g.* vitamin E).[84]
N-Acetylcysteine (NAC)	Increased intracellular thiols (GSH precursor), direct antioxidant action.[85]
Glutamine	Preservation of intracellular NAD(P)H levels, glutathione precursor.[86]
Hydroxyurea (HU)	Antiradical activity and amine oxidase inhibition. Conversion of HU to NO that stimulates HbF synthesis.[87,88]
α-lipoic acid	Lipo- and hydrosoluble, and antioxidant properties in both its reduced (dihydrolipoic acid) and oxidized (lipoic acid) forms. Reacts with the ROS, interacts with vitamin C, E and GSH, and metal-chelator.[89–91]
Acetyl-L-carnitine	Decrease lipid peroxidation, ROS scavenger and metal-chelator.[92]
α-tocopherol (vitamin E)	Vitamin E isoform with the highest bioavailability. Lipophilic antioxidant. Peroxyl radical scavenger, decrease lipid peroxidation. Synergistic interaction with ascorbic acid.[93,94]

ROS: Reactive Oxygen Species, GSH: reduced Glutathione, NADH: reduced Nicotinamide Adenine Dinucleotide (Phosphate), NO: Nitric Oxide, HbF: Fetal Hemoglobin.

The antioxidant action of the selected compounds is either direct or indirect. Indeed, some of these molecules are precursors for antioxidants or promote their recycling, and thus promote indirectly the cellular defenses, whether others are direct scavengers or reducing agents for oxidative species. The protective effect of the same molecules in the framework of RBC storage, in *in vitro* experiments or even in *in vivo* trials is described in Table 4.

*Table 4 – **State of the art for the protective effect of the tested compounds.** Improvements observed under treatment with the different compounds. Experimental conditions are specified in brackets.*

Compound	Protective effect in Red Blood Cells
Ascorbic acid (AA, vitamin C)	Higher antioxidant status, reduced osmotic fragility and increased membrane integrity (RCC in SAGM, 3 mM AA)[95]. Reduced membrane fragility and hemolysis (RCC in AS-5, 5.86 and 8.78 mM AA)[96]. Maintenance of 2,3-DPG levels (RCC in CPD-adenine, 0.5 mM AA)[97].

N-acetyl cysteine (NAC)	Decreased MV formation and improved 24-hour posttransfusion recovery (stored murine RBCs, 3.6-10.8 mM AA)[98].
	Maintenance of GSH levels and scavenger capacity against H_2O_2 and amelioration of cell lysis (RCC in SAGM, 5 and 20-25 mM NAC)[99].
	Replenishment of the intracellular reductive reservoir (RBC exposed to oxidant agents *in vitro*, 5 mM NAC)[100].
	Increase GSH blood levels, and decreased PS exposure, plasma levels of advanced glycation end-products (AGEs) and cell free-Hb (SCD patients, 2.4 mg NAC during 6 weeks)[101].
Both	Decreased energy metabolic fluxes (glycolysis and PPP), promotion of glutathione homeostasis, and less hemolysis, MDA and oxidation by-products (RCC, SAGM, 0.23 mM AA plus 0.5 mM NAC)[102].
Glutamine	Antisickling property (RBCs in vitro, 3.8 mM glutamine)[103].
	Maintain ATP, lipid content and phospholipid asymmetry, and decreased vesiculation and hemolysis (RCC in Adsol, 10 mM glutamine plus 20 mM phosphate)[104].
Hydroxyurea (HU)	Significant increase in antioxidant enzymes at RBC membrane and increase in tyrosine-phosphorylation of catalase (RBC *in vitro*, 50 µM HU)[105].
	Higher values of GSH and Trolox Equivalent Antioxidant Capacity (TEAC), and lower lipid peroxidation (Sickle Cell Anemia [SCA] patients)[106,107].
α-lipoic acid	Reduction of MDA, increase of 2.3-DPG and elevation of glycolytic activity (RCC in SAGM, 100 µM)[108].
	Protection against the oxidative damages induced by gamma irradiation (Gy), maintenance of rheological, mechanical properties and permeability of the erythrocytes (RBC exposed to 25 Gy in vitro, 123 µM α-lipoic acid)[109].
Acetyl-L-carnitine	Retards osmotic cell swelling linked to calcium and potassium imbalance (RCC in SAGM, 5 mM L-carnitine)[110].
	Scavenging of ROS, first line of defense during storage (rat RBCs, whole blood in CPDA-1, 10/30/60 mM L-carnitine)[111].
	Decreased plasma MDA and increase of antioxidant enzymes (catalase, SOD and GPx) activity in RBCs (Coronary Artery Disease [CAD] patients, 1000 mg/d L-carnitine during 12 weeks)[112].
Both	α-lipoic acid reverses oxidative stress arising from iron overload, action further enhanced in combination with L-carnitine (iron-overloaded human fibroblasts, 5/25/125 µM α-lipoic acid plus L-carnitine)[113].
α-tocopherol (vitamin E)	Inhibition of oxidative damages induced by glucose (hemolysis, restoration of catalase, SOD and GSH levels), decreased levels of Thiobarbituric Acid Reactive Substances (TBARS) (RBCs incubated with 5/10/20 mM glucose, 18 µg/mL vit. E)[114].
	Reduced levels of TBARS, improved morphology, prevention of hemolysis (rat RBCs treated with acetone *in vitro*, 200 mg/kg α-tocopherol per day *i.m.*)[115].
	Decreased percentage of irreversibly sickled RBCs (SCD patients, 450 IU α-tocopherol per day for 6 to 35 weeks)[116].
	Decrease of ROS production (RCC in SAGM, vitamin E nanoemulsion)[117].

RCC: Red Cell Concentrate, SAGM: Saline-Adenine-Glucose-Mannitol, AS: Additive solution, 2,3-DPG: 2,3-Diphosphoglycerate, CPD: Citrate-Phosphate-Dextrose, MV: Microvesicle, RBC: Red Blood Cell, GSH: reduced Glutathione, H_2O_2: hydrogen peroxide, Hb: Hemoglobin, PS: Phosphatidylserine, SCD: Sickle Cell Disease, MDA: Malondialdehyde, ATP: Adenosine Triphosphate, CPDA: Citrate-Phospate-Dextrose-Adenine, SOD: Superoxide Dismutase, GPx: Glutathione Peroxidase.

In the following study, RBCs were treated with the above compounds and the evolution of several aging markers were followed for 71 days.

Material and methods

Addition of protective molecules in the red blood cell concentrates

The modified additive solutions were kindly prepared in the Pharmaceutical Development department of B. Braun (Crissier, Switzerland) under aseptic conditions (composition and preparation are described in ANNEX-9). The compounds of interest were dissolved in SAGM and nitrogen was bubbled in the bottles to protect the molecules from oxidation. The stock solutions were 28.5 times concentrated and were frozen until use.
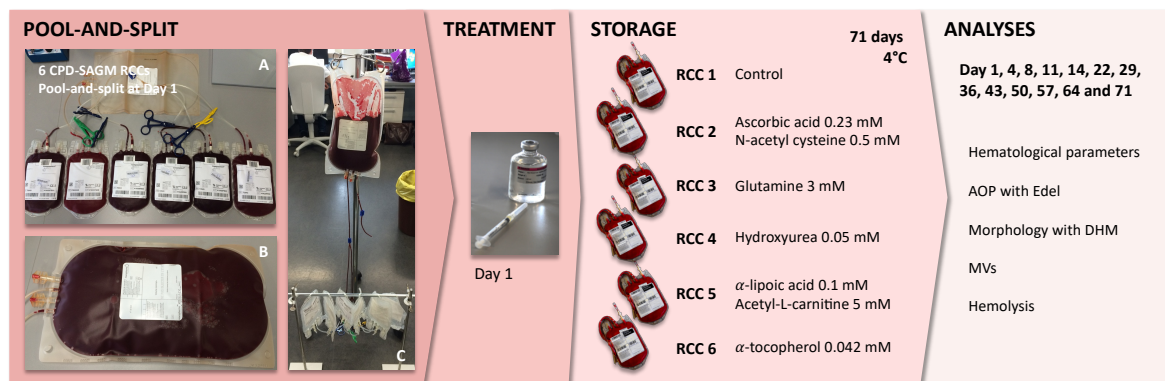
*Figure 11 – **Experimental workflow: pool-and-split of the Red Cell Concentrates (RCCs), supplementation with protective molecules and follow-up.** [A] Connection of six RCCs to one big transfer bag, [B] pool and [C] split in six units, treatment with the protective molecules, and follow-up during 71 days of storage at 4°C. The hematological parameters, global Antioxidant Power (AOP), morphology, microvesicle count (MVs) and hemolysis were analyzed.*

Six RCCs coming from six men, all B Rhesus-D positive and aged of 37, 39, 39, 40, 49 and 67 years at the time of the donation were pooled in a large transfer bag (3.5 L, Macopharma) and split in six pouches. The pooled RCCs having a volume of 275 ± 75 mL were treated with 10 mL of antioxidant solution or SAGM for the control (Figure 11).

Follow-up during storage

The RCCs stored at 4°C were analyzed at day 1, 4, 8, 11, 14, 22, 29, 36, 43, 50, 57, 64 and 71 of storage. Each time, the blood bags were gently mixed to homogenize their content and 3 mL of RCCs were withdrawn. Sysmex, AOP and MV count analyses were done on the whole RCC. Then, the samples were centrifuged at 2000 *g* and 4°C for 10 min. The supernatants were used for measurement of the hemolysis percentage. After that, the RBCs were washed twice in 0.9 % NaCl (centrifugation as before). Finally, the RBC pellets were resuspended in two volumes of HEPA and used for morphology analysis with DHM. For more details about the methods, please refer to the "material and methods" section of Chapter 1, Part 1.

Results and discussion

Among the five conditions tested, RCC 5 and RCC 6 exhibited significant differences with the control. In RCC 5, supplementation of α-lipoic acid and acetyl-L-carnitine reduced the release of MVs and delayed RBC lysis (Figure 12E and F), but did not seem to prevent spherocytosis (Figure 12C and D). In

RCC 6, addition of α-tocopherol was deleterious rather than protective. Indeed, this molecule induced a rapid drop of the discocyte population that transformed into stomatocytes and spherocytes, along with microvesiculation and hemolysis (Figure 12C-F). This "unexpected role" has already been described in a study that demonstrated α-tocopherol-mediated peroxidation in the RBCs treated with low concentrations of 2,2'-Azobis(2-amidinopropane) dihydrochloride (AAPH) oxidant[118]. Interestingly, the only noticeable effect of AA (RCC 2) was an increase of the global AOP level. Reason for this could be that in RBCs, the vitamin C is mainly taken up in its oxidized form (Dehydroascorbic Acid [DHA]) *via* GLUT1 (solute carrier family 2, facilitated glucose transporter member 1). To enter the cell *via* this transporter, abundantly expressed in the erythrocyte membrane, DHA enters in competition with glucose. Once in the cytoplasm, DHA can exert a pro-oxidant effect because its reduction requires expansion of endogenous GSH[119]. Addition of AA could thus only protect the RBCs from surrounding oxidative attacks rather than provide efficient intracellular defenses.
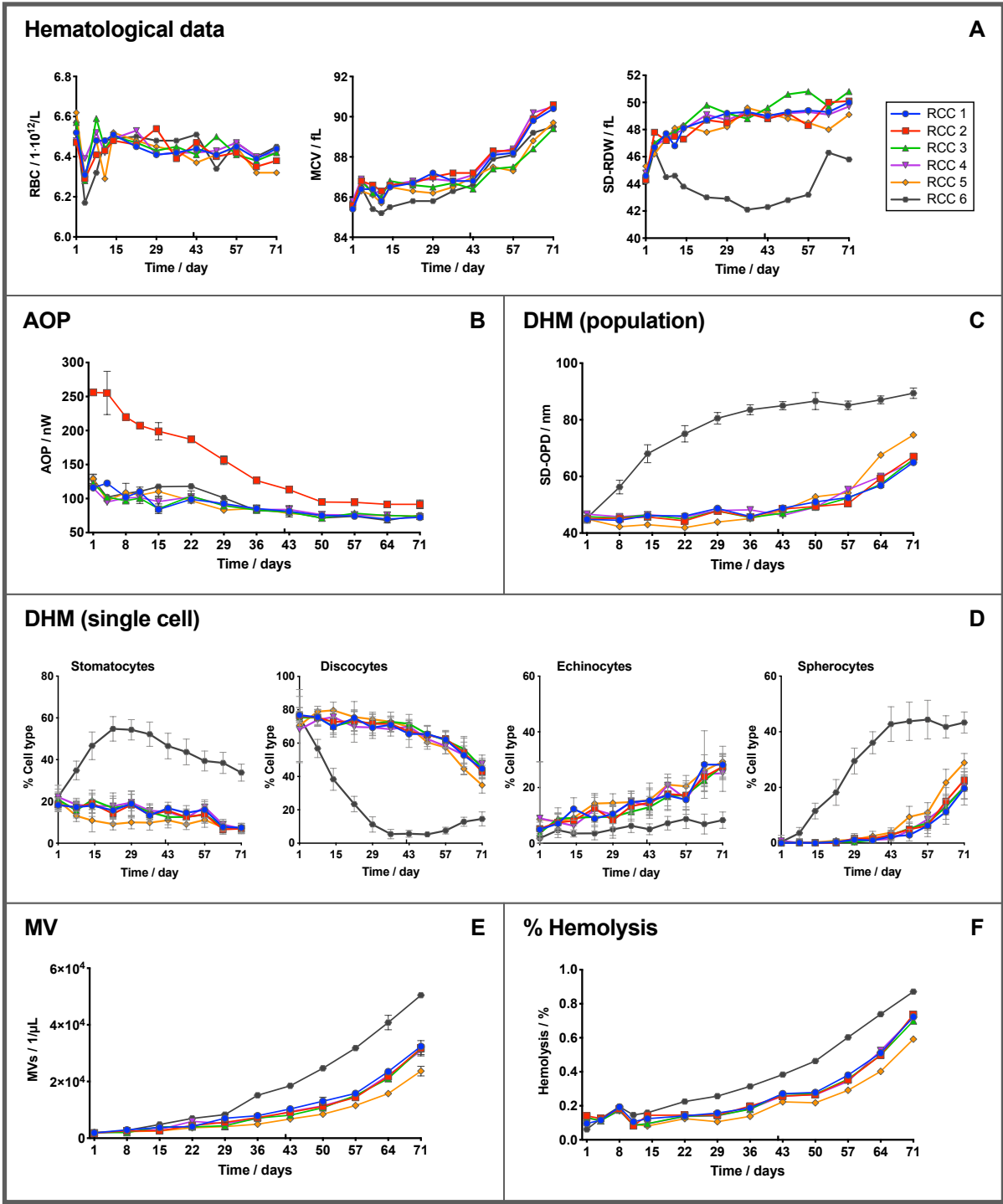
*Figure 12 – **Red Blood Cell (RBC) aging markers in Red Cell Concentrates (RCCs) supplemented with the different compounds.** [A] Hematological data: RBC count, Mean Corpuscular Volume (MCV) and Standard Deviation of Distribution Width (SD-RDW) measured. [B] Antioxidant Power (AOP) quantified by pseudotitration voltammetry with EdelMeter. Morphology analysis using Digital Holographic Microscopy (DHM): [C] population analysis with Standard Deviation of Optical Path Difference parameter (SD-OPD), and [D] single-cell morphology analysis with CellProfiler and CellProfiler Analyst (CPA). [E] Microvesicles (MVs) in the supernatant counted by flow cytometry. [F] Percentage of hemolysis in the blood bag determined with the Harboe spectrophotometric method. Mean value ± standard deviation.*

Conclusions

Globally, the results of this preliminary study were surprising (see Figure 12). Indeed, all the RCCs including the control, with the exception of the one supplemented with α-tocopherol, aged better compared to previous studies when looking at parameters such as the MCV, anisocytosis (reflected by the standard deviation of the RBC distribution width [SD-RDW] parameter), number of MVs, percentage of hemolysis or morphology (population and single-cell). Therefore, it was even more difficult to assess with confidence the beneficial impact of the different treatments. We suspect the pool-and-split to be the reason of these unexpected results. One hypothesis is that one (or more) donor is a "super-storer", *i.e.* who possesses some characteristics that helps to the storability of the RBCs (for example a higher plasmatic UA concentration[69]). This advantage could be "shared" during the pool-and-split. It would also explain why the increase of AOP during the first week of storage (mostly due to the equilibration of UA concentration between the intra- and extra-cellular space) was not observed. To avoid such bias, each solution formulation such be test on several individual RCCs (at least 3).

In summary, the pool-and-split enabled to reduce the unit-to-unit variability and could therefore be useful when multiple conditions need to be compared. However, we observed in this study that some individual donor's characteristics can impact the aging of the entire RBC population and thus potentially distort the results of the experiments.

GENERAL CONCLUSIONS

Oxidative stress results from the imbalance between the production of oxidants and the antioxidative system. Three measures can be taken to reduce such burden, *i.e.* reduce the O_2 levels, sustain the cellular antioxidant protective system, or directly provide antioxidant molecules. To be beneficial, a protective molecule should fulfill different criteria such as being specific, the product of its reaction with the oxidant should not be armful, and its half-life should be long enough to let the molecule produce its effect[120]. In addition, when thinking about ways to sustain indirectly the cellular antioxidant system, one should keep in mind that favorizing one metabolic pathway could destabilize the entire cellular machinery and result in the exhaustion of key metabolites or in the accumulation of unwanted waste products.

Even in the case of a major breakthrough, the feasibility, the risk *versus* benefit and finally the cost *versus* benefit (maybe less for us researchers) need to be evaluated before modifying routine procedures that are generally well established. For us, the feasibility of adding a protective molecule in the blood bags will mainly depend on its stability. Indeed, a molecule sensitive to light, and/or to O_2, and/or to temperature, and/or degrading over time will determine the manufacturing process, the packaging and the storage of the blood collection set. Cold storage, for example, requires complex storage infrastructure and could thus limit its use (*e.g.* in countries with limited access to electricity). In the health field, every action should result in more good than harm for the patient. Careful evaluation of the possible side effects of the added molecules, first at the level of the RBCs in the blood bags and then once transfused in the patient is necessary. One example is the HU addition tested in the last part of this chapter. Indeed, despite its potential protective properties, it is a molecule not naturally found in living organisms that is used for the treatment of sickle cell disease and for chemotherapy in hemato-oncology. Similarly, external supply of UA could be deleterious for patients with gout. The final criteria to be evaluated is the cost of antioxidant supplementation. Weighting the utility of a medical intervention is generally calculated in terms of QALY (Quality-Adjusted Life Year), that provides an economical value of one year in good health[121].

Unfortunately, none of the strategies developed in this chapter resulted in a major improvement of the stored RBC quality, although all the tested compounds were shown to have antioxidant and/or protective properties in other contexts (disease, *in vitro* experiments, etc.). For some of these compounds, we could wonder if the absence of conclusive results is not simply due to the experimental conditions, *e.g.* the concentrations tested, or if the aging markers targeted by our panels of tests are the most pertinent. In the future, we should surely test different concentrations for each molecule and probably update the choice of the tested compounds. It is the reason why efforts were put for the development of the TSOX assay, that will be presented in the Chapter 4.

REFERENCES

1. D'Alessandro A, Kriebardis AG, Rinalducci S, et al. An update on red blood cell storage lesions, as gleaned through biochemistry and omics technologies. *Transfusion*. 2015;55(1):205–219.

2. Yoshida T, Prudent M, D'Alessandro A. Red blood cell storage lesion: causes and potential clinical consequences. *Blood Transfus.* 2019;17(1):27–52.

3. Valeri CR, Hirsch NM. Restoration in vivo of erythrocyte adenosine triphosphate, 2,3-diphosphoglycerate, potassium ion, and sodium ion concentrations following the transfusion of acid-citrate-dextrose-stored human red blood cells. *J. Lab. Clin. Med.* 1969;73(5):722–733.

4. Reisz JA, Nemkov T, Dzieciatkowska M, et al. Methylation of protein aspartates and deamidated asparagines as a function of blood bank storage and oxidative stress in human red blood cells. *Transfusion*. 2018;58(12):2978–2991.

5. Luten M, Roerdinkholder-Stoelwinder B, Schaap NP, et al. Survival of red blood cells after transfusion: a comparison between red cells concentrates of different storage periods. *Transfusion*. 2008;48(7):1478–1485.

6. Grimshaw K, Sahler J, Spinelli SL, Phipps RP, Blumberg N. New frontiers in transfusion biology: Identification and significance of mediators of morbidity and mortality in stored red cell concentrates. *Transfusion*. 2011;51(4):874–880.

7. García-Roa M, Del Carmen Vicente-Ayuso M, Bobes AM, et al. Red blood cell storage time and transfusion: current practice, concerns and future perspectives. *Blood Transfus.* 2017;15(3):222–231.

8. Bosman GJ, Werre JM, Willekens FL, Novotný VM. Erythrocyte ageing in vivo and in vitro: structural aspects and implications for transfusion. *Transfus. Med.* 2008;18(6):335–347.

9. Francis RO, Spitalnik SL. Red blood cell components: Meeting the quantitative and qualitative transfusion needs. *Presse Med*. 2016;45(7–8):e281–e288.

10. Gao Y, Lv L, Liu S, Ma G, Su Y. Elevated levels of thrombin-generating microparticles in stored red blood cells. *Vox Sang.* 2013;105(1):11–17.

11. Jy W, Johansen ME, Bidot C, et al. Red cell-derived microparticles (RMP) as haemostatic agent. *Thromb. Haemost.* 2013;110(4):751–760.

12. Rubin O, Canellini G, Delobel J, Lion N, Tissot J-D. Red Blood Cell Microparticles: Clinical Relevance. *Transfus. Med. Hemotherapy*. 2012;39(5):342–347.

13. Rubin O, Delobel J, Prudent M, et al. Red blood cell-derived microparticles isolated from blood units initiate and propagate thrombin generation: RMPs Generate Thrombin. *Transfusion*. 2013;53(8):1744–1754.

14. Hod EA, Brittenham GM, Billote GB, et al. Transfusion of human volunteers with older, stored red blood cells produces extravascular hemolysis and circulating non–transferrin-bound iron. *Blood*. 2011;118(25):6675–6682.

15. Rapido F, Brittenham GM, Bandyopadhyay S, et al. Prolonged red cell storage before transfusion increases extravascular hemolysis. *J. Clin. Invest.* 2016;127(1):375–382.

16. Schaer DJ, Buehler PW, Alayash AI, Belcher JD, Vercellotti GM. Hemolysis and free hemoglobin revisited: exploring hemoglobin and hemin scavengers as a novel class of therapeutic proteins. *Blood*. 2013;121(8):1276–1284.

17. Hod EA. Red blood cell transfusion-induced inflammation: myth or reality. *ISBT Sci. Ser.* 2015;10(Suppl 1):188–191.

18. Hod EA, Spitalnik SL. Stored red blood cell transfusions: Iron, inflammation, immunity, and

infection. *Transfus. Clin. Biol.* 2012;19(3):84–89.

19. Hod EA, Zhang N, Sokol SA, et al. Transfusion of red blood cells after prolonged storage produces harmful effects that are mediated by iron and inflammation. *Blood*. 2010;115(21):4284–4292.

20. Spitalnik SL. Stored red blood cell transfusions: iron, inflammation, immunity, and infection. *Transfusion*. 2014;54(10):2365–2371.

21. Baek JH, D'Agnillo F, Vallelian F, et al. Hemoglobin-driven pathophysiology is an in vivo consequence of the red blood cell storage lesion that can be attenuated in guinea pigs by haptoglobin therapy. *J. Clin. Invest.* 2012;122(4):1444–1458.

22. Roback JD. Vascular Effects of the Red Blood Cell Storage Lesion. *Hematology Am Soc Hematol Educ Program.* 2011;2011(1):475–479.

23. Donadee C, Raat NJH, Kanias T, et al. Nitric oxide scavenging by red blood cell microparticles and cell-free hemoglobin as a mechanism for the red cell storage lesion. *Circulation*. 2011;124(4):465–476.

24. Steiner ME, Ness PM, Assmann SF, et al. Effects of Red-Cell Storage Duration on Patients Undergoing Cardiac Surgery. *N. Engl. J. Med.* 2015;372(15):1419–1429.

25. Steiner ME, Assmann SF, Levy JH, et al. Addressing the question of the effect of RBC storage on clinical outcomes: The Red Cell Storage Duration Study (RECESS) (Section 7). *Transfus. Apher. Sci.* 2010;43(1):107–116.

26. Lacroix J, Hébert PC, Fergusson DA, et al. Age of Transfused Blood in Critically Ill Adults. *N. Engl. J. Med.* 2015;372(15):1410–1418.

27. Alexander PE, Barty R, Fei Y, et al. Transfusion of fresher vs older red blood cells in hospitalized patients: a systematic review and meta-analysis. *Blood*. 2016;127(4):400–410.

28. Heddle NM, Cook RJ, Arnold DM, et al. Effect of Short-Term vs. Long-Term Blood Storage on Mortality after Transfusion. *N. Engl. J. Med.* 2016;375(20):1937–1945.

29. McQuilten ZK, French CJ, Nichol A, Higgins A, Cooper DJ. Effect of age of red cells for transfusion on patient outcomes: a systematic review and meta-analysis. *Transfus. Med. Rev.* 2018;32(2):77–88.

30. Cook RJ, Heddle NM, Lee K-A, et al. Red blood cell storage and in-hospital mortality: a secondary analysis of the INFORM randomised controlled trial. *Lancet Haematol.* 2017;4(11):e544–e552.

31. Koch CG, Li L, Sessler DI, et al. Duration of red-cell storage and complications after cardiac surgery. *N. Engl. J. Med.* 2008;358(12):1229–1239.

32. Middelburg RA, van de Watering LMG, Briët E, van der Bom JG. Storage Time of Red Blood Cells and Mortality of Transfusion Recipients. *Transfus. Med. Rev.* 2013;27(1):36–43.

33. Jones AR, Patel RP, Marques MB, et al. Older Blood Is Associated With Increased Mortality and Adverse Events in Massively Transfused Trauma Patients: Secondary Analysis of the PROPPR Trial. *Ann. Emerg. Med.* 2019;73(6):650-661.

34. Wang D, Sun J, Solomon SB, Klein HG, Natanson C. Transfusion of older stored blood and risk of death: a meta-analysis. *Transfusion*. 2012;52(6):1184–1195.

35. Ng MSY, David M, Middelburg RA, et al. Transfusion of packed red blood cells at the end of shelf life is associated with increased risk of mortality – a pooled patient data analysis of 16 observational trials. *Haematologica*. 2018;103(9):1542–1548.

36. Goel R, Johnson DJ, Scott AV, et al. Red blood cells stored 35 days or more are associated with adverse outcomes in high-risk patients. *Transfusion*. 2016;56(7):1690–1698.

37.   Chassé M, McIntyre L, English SW, et al. Effect of Blood Donor Characteristics on Transfusion Outcomes: A Systematic Review and Meta-Analysis. *Transfus. Med. Rev.* 2016;30(2):69–80.

38.   Chassé M, Tinmouth A, English SW, et al. Association of Blood Donor Age and Sex With Recipient Survival After Red Blood Cell Transfusion. *JAMA Intern. Med.* 2016;176(9):1307–1314.

39.   Caram-Deelder C, Kreuger AL, Evers D, et al. Association of Blood Transfusion From Female Donors With and Without a History of Pregnancy With Mortality Among Male and Female Transfusion Recipients. *JAMA*. 2017;318(15):1471.

40.   Van Den Hurk K, Peffer K, Habets K, et al. Blood donors' physical characteristics are associated with pre- and postdonation symptoms - Donor InSight. *Blood Transfus.* 2017;15(5):405-412.

41.   D'Alessandro A, Culp-Hill R, Reisz JA, et al. Heterogeneity of blood processing and storage additives in different centers impacts stored red blood cell metabolism as much as storage time: lessons from REDS-III-Omics. *Transfusion*. 2019;59(1):89-100.

42.   Prudent M, Tissot J-D, Lion N. In vitro assays and clinical trials in red blood cell aging: Lost in translation. *Transfus. Apher. Sci.* 2015;52(3):270–276.

43.   Roussel C, Buffet PA, Amireault P. Measuring Post-transfusion Recovery and Survival of Red Blood Cells: Strengths and Weaknesses of Chromium-51 Labeling and Alternative Methods. *Front. Med.* 2018;5:130. DOI: 10.3389/fmed.2018.00130.

44.   Jackson BP, Triulzi DJ, Yazer MH. Reducing red blood cell shelf life would frequently compromise inventory. *Transfusion*. 2016;56(1):271–272.

45.   Zolla L, D'Alessandro A, Rinalducci S, et al. Classic and alternative red blood cell storage strategies: seven years of "-omics" investigations. *Blood Transfus.* 2015;13(1):21–31.

46.   Kluger R. Red cell substitutes from hemoglobin--do we start all over again? *Curr. Opin. Chem. Biol.* 2010;14(4):538–543.

47.   Douay L. Why industrial production of red blood cells from stem cells is essential for tomorrow's blood transfusion. *Regen. Med.* 2018;13(6):627–632.

48.   Giarratana M-C, Rouard H, Dumont A, et al. Proof of principle for transfusion of in vitro-generated red blood cells. *Blood*. 2011;118(19):5071–5079.

49.   Giarratana M-C, Kobari L, Lapillonne H, et al. Ex vivo generation of fully mature human red blood cells from hematopoietic stem cells. *Nat. Biotechnol.* 2005;23(1):69–74.

50.   Rousseau GF, Giarratana M-C, Douay L. Large-scale production of red blood cells from stem cells: What are the technical challenges ahead? *Biotechnol. J.* 2014;9(1):28–38.

51.   Henkelman S, Noorman F, Badloe J f., Lagerberg JWM. Utilization and quality of cryopreserved red blood cells in transfusion medicine. *Vox Sang.* 2015;108(2):103–112.

52.   Valeri CR, Pivacek LE, Cassidy GP, Ragno G. Posttransfusion survival (24-hour) and hemolysis of previously frozen, deglycerolized RBCs after storage at 4°C for up to 14 days in sodium chloride alone or sodium chloride supplemented with additive solutions. *Transfusion*. 2000;40(11):1337–1340.

53.   Burns JM, Yoshida T, Dumont LJ, et al. Deterioration of red blood cell mechanical properties is reduced in anaerobic storage. *Blood Transfus.* 2016;14(1):80.

54.   Yoshida T, Shevkoplyas SS. Anaerobic storage of red blood cells. *Blood Transfus.* 2010;8(4):220-236.

55.   Dumont LJ, Yoshida T, AuBuchon JP. Anaerobic Storage of Red Blood Cells in a Novel Additive Solution Improves In vivo Recovery. *Transfusion*. 2009;49(3):458–464.

56.   Yoshida T, Blair A, D'alessandro A, et al. Enhancing uniformity and overall quality of red cell

concentrate with anaerobic storage. *Blood Transfus*. 2017;15(2):172–181.

57. Yoshida T, AuBuchon JP, Tryzelaar L, Foster KY, Bitensky MW. Extended storage of red blood cells under anaerobic conditions. *Vox Sang.* 2007;92(1):22–31.

58. Gehrke S, Srinivasan AJ, Culp-Hill R, et al. Metabolomics evaluation of early-storage red blood cell rejuvenation at 4°C and 37°C. *Transfusion*. 2018;58(8):1980–1991.

59. Meyer EK, Dumont DF, Baker S, Dumont LJ. Rejuvenation capacity of red blood cells in additive solutions over long-term storage. *Transfusion*. 2011;51(7):1574–1579.

60. Barshtein G, Arbell D, Livshits L, Gural A. Is It Possible to Reverse the Storage-Induced Lesion of Red Blood Cells? *Front. Physiol.* 2018;9:914.

61. Hess JR. An update on solutions for red cell storage. *Vox Sang.* 2006;91(1):13–19.

62. Lagerberg JW, Korsten H, Van Der Meer PF, De Korte D. Prevention of red cell storage lesion: a comparison of five different additive solutions. *Blood Transfus.* 2017;1–7.

63. Sparrow RL. Time to revisit red blood cell additive solutions and storage conditions: a role for "omics" analyses. *Blood Transfus.* 2012;10(Suppl 2):s7-11.

64. Bardyn M, Maye S, Lesch A, et al. The antioxidant capacity of erythrocyte concentrates is increased during the first week of storage and correlated with the uric acid level. *Vox Sang.* 2017;112(7):638–647.

65. Furger P. Guidelines SURF-med© : scientific - units - recommendations - formulas. Neuhausen: Editions D&F; 2010.

66. Ames BN, Cathcart R, Schwiers E, Hochstein P. Uric acid provides an antioxidant defense in humans against oxidant- and radical-caused aging and cancer: a hypothesis. *Proc. Natl. Acad. Sci. U. S. A.* 1981;78(11):6858–6862.

67. Becker BF. Towards the physiological function of uric acid. *Free Radic. Biol. Med.* 1993;14(6):615–631.

68. Benzie IF, Strain JJ. The ferric reducing ability of plasma (FRAP) as a measure of "antioxidant power": the FRAP assay. *Anal. Biochem.* 1996;239(1):70–76.

69. Tzounakas VL, Georgatzakou HT, Kriebardis AG, et al. Uric acid variation among regular blood donors is indicative of red blood cell susceptibility to storage lesion markers: A new hypothesis tested. *Transfusion*. 2015;55(11):2659–2671.

70. Tzounakas VL, Karadimas DG, Anastasiadi AT, et al. Donor-specific individuality of red blood cell performance during storage is partly a function of serum uric acid levels. *Transfusion*. 2018;58(1):34–40.

71. Jordan A, Acker JP. Determining the Volume of Additive Solution and Residual Plasma in Whole Blood Filtered and Buffy Coat Processed Red Cell Concentrates. *Transfus. Med. Hemotherapy*. 2016;43(2):133–136.

72. Fathallah-Shaykh SA, Cramer MT. Uric acid and the kidney. *Pediatr. Nephrol.* 2014;29(6):999–1008.

73. Roussel C, Dussiot M, Marin M, et al. Spherocytic shift of red blood cells during storage provides a quantitative whole cell-based marker of the storage lesion. *Transfusion*. 2017;57(4):1007–1018.

74. Sautin YY, Johnson RJ. Uric acid: the oxidant-antioxidant paradox. *Nucleosides Nucleotides Nucleic Acids*. 2008;27(6):608–619.

75. Abuja PM. Ascorbate prevents prooxidant effects of urate in oxidation of human low density lipoprotein. *FEBS Lett.* 1999;446(2):305–308.

76. Turner R, Brennan SO, Ashby LV, et al. Conjugation of urate-derived electrophiles to proteins

during normal metabolism and inflammation. *J. Biol. Chem.* 2018;293(51):19886–19898.

77. Burns JM, Yang X, Forouzan O, Sosa JM, Shevkoplyas SS. Artificial microvascular network: a new tool for measuring rheologic properties of stored red blood cells. *Transfusion*. 2012;52(5):1010–1023.

78. Gomes A, Fernandes E, Lima JLFC. Fluorescence probes used for detection of reactive oxygen species. *J. Biochem. Biophys. Methods*. 2005;65(2–3):45–80.

79. Ghorbaniaghdam A, Chen J, Henry O, Jolicoeur M. Analyzing clonal variation of monoclonal antibody-producing CHO cell lines using an in silico metabolomic platform. *PloS One*. 2014;9(3):e90832.

80. D'Alessandro A, D'Amici GM, Vaglio S, Zolla L. Time-course investigation of SAGM-stored leukocyte-filtered red bood cell concentrates: from metabolism to proteomics. *Haematologica*. 2012;97(1):107–115.

81. Reisz JA, Wither MJ, Dzieciatkowska M, et al. Oxidative modifications of glyceraldehyde 3-phosphate dehydrogenase regulate metabolic reprogramming of stored red blood cells. *Blood*. 2016;128(12):e32–e42.

82. Safeukui I, Buffet PA, Deplaine G, et al. Quantitative assessment of sensing and sequestration of spherocytic erythrocytes by the human spleen. *Blood*. 2012;120(2):424–430.

83. Silva DGH, Belini Junior E, de Almeida EA, Bonini-Domingos CR. Oxidative stress in sickle cell disease: An overview of erythrocyte redox metabolism and current antioxidant therapeutic strategies. *Free Radic. Biol. Med.* 2013;65:1101–1109.

84. Cimen MYB. Free radical metabolism in human erythrocytes. *Clin. Chim. Acta Int. J. Clin. Chem.* 2008;390(1–2):1–11.

85. Aruoma OI, Halliwell B, Hoey BM, Butler J. The antioxidant action of N-acetylcysteine: its reaction with hydrogen peroxide, hydroxyl radical, superoxide, and hypochlorous acid. *Free Radic. Biol. Med.* 1989;6(6):593–597.

86. Morris CR, Suh JH, Hagar W, et al. Erythrocyte glutamine depletion, altered redox environment, and pulmonary hypertension in sickle cell disease. *Blood*. 2008;111(1):402–410.

87. Huang J, Kim-Shapiro DB, King SB. Catalase-Mediated Nitric Oxide Formation from Hydroxyurea. *J. Med. Chem.* 2004;47(14):3495–3501.

88. Liu YH, Wu WC, Lu YL, Las YJ, Hou WC. Antioxidant and Amine Oxidase Inhibitory Activities of Hydroxyurea. *Biosci. Biotechnol. Biochem.* 2010;74(6):1256–1260.

89. Packer L, Witt EH, Tritschler HJ. Alpha-lipoic acid as a biological antioxidant. *Free Radic. Biol. Med.* 1995;19(2):227–250.

90. Navari-Izzo F, Quartacci MF, Sgherri C. Lipoic acid: a unique antioxidant in the detoxification of activated oxygen species. *Plant Physiol. Biochem.* 2002;40(6–8):463–470.

91. Biewenga GP, Haenen GR, Bast A. The pharmacology of the antioxidant lipoic acid. *Gen. Pharmacol. Vasc. Syst.* 1997;29(3):315–331.

92. Gülçin İ. Antioxidant and antiradical activities of L-carnitine. *Life Sci.* 2006;78(8):803–811.

93. Niki E. Role of vitamin E as a lipid-soluble peroxyl radical scavenger: in vitro and in vivo evidence. *Free Radic. Biol. Med.* 2014;66:3–12.

94. Packer L, Weber SU, Rimbach G. Molecular Aspects of α-Tocotrienol Antioxidant Action and Cell Signalling. *J. Nutr.* 2001;131(2):369S-373S.

95. Sanford K, Fisher BJ, Fowler E, Fowler AA, Natarajan R. Attenuation of Red Blood Cell Storage Lesions with Vitamin C. *Antioxidants*. 2017;6(3):55.

96. Raval JS, Fontes J, Banerjee U, et al. Ascorbic acid improves membrane fragility and decreases

haemolysis during red blood cell storage. *Transfus. Med.* 2013;23(2):87–93.

97.   Wood LA, Beutler E. The effect of ascorbate on the maintenance of 2,3-diphosphoglycerate (2,3-DPG) in stored red cells. *Br. J. Haematol.* 1973;25(5):611–618.

98.   Stowell SR, Smith NH, Zimring JC, et al. Addition of ascorbic acid solution to stored murine red blood cells increases posttransfusion recovery and decreases microparticles and alloimmunization. *Transfusion*. 2013;53(10):2248–2257.

99.   Amen F, Machin A, Touriño C, et al. N-acetylcysteine improves the quality of red blood cells stored for transfusion. *Arch. Biochem. Biophys.* 2017;621(Supplement C):31–37.

100.   Mazor D, Golan E, Philip V, et al. Red blood cell permeability to thiol compounds following oxidative stress. *Eur. J. Haematol.* 1996;57(3):241–246.

101.   Nur E, Brandjes DP, Teerlink T, et al. N-acetylcysteine reduces oxidative stress in sickle cell patients. *Ann. Hematol.* 2012;91(7):1097–1105.

102.   Pallotta V, Gevi F, D'Alessandro A, Zolla L. Storing red blood cells with vitamin C and N-acetylcysteine prevents oxidative stress-related lesions: a metabolomics overview. *Blood Transfus.* 2014;12(3):376–387.

103.   Rumen NM. Inhibition of sickling in erythrocytes by amino acids. *Blood*. 1975;45(1):45–48.

104.   Dumaswala UJ, Wilson MJ, José T, Daleke DL. Glutamine- and phosphate-containing hypotonic storage media better maintain erythrocyte membrane physical properties. *Blood*. 1996;88(2):697–704.

105.   Ghatpande SS, Choudhary PK, Quinn CT, Goodman SR. Pharmaco-Proteomic Study of Hydroxyurea-Induced Modifications in the Sickle Red Blood Cell Membrane Proteome. *Exp. Biol. Med.* 2008;233(12):1510–1517.

106.   Silva DGH, Belini Junior E, Torres L de S, et al. Relationship between oxidative stress, glutathione S-transferase polymorphisms and hydroxyurea treatment in sickle cell anemia. *Blood Cells. Mol. Dis.* 2011;47(1):23–28.

107.   Torres L de S, da Silva DGH, Belini Junior E, et al. The influence of hydroxyurea on oxidative stress in sickle cell anemia. *Rev. Bras. Hematol. Hemoter.* 2012;34(6):421–425.

108.   Geise W, Conrad F, Henrich HA. Protection of Stored Erythrocytes against Oxidative Stress and Insufficient Physiological Function by Enantiomers of α-Lipoic Acid. *Transfus. Med. Hemotherapy*. 1999;26(1):26–32.

109.   Desouky OS, Selim NS, Elbakrawy EM, Rezk RA. Impact evaluation of α-lipoic acid in gamma-irradiated erythrocytes. *Radiat. Phys. Chem.* 2011;80(3):446–452.

110.   Arduini A, Minetti G, Ciana A, et al. Cellular properties of human erythrocytes preserved in saline-adenine-glucose-mannitol in the presence of L-carnitine. *Am. J. Hematol.* 2007;82(1):31–40.

111.   Soumya R, Carl H, Vani R. L-carnitine as a Potential Additive in Blood Storage Solutions: A Study on Erythrocytes. *Indian J. Hematol. Blood Transfus.* 2016;32(3):328–334.

112.   Lee BJ, Lin JS, Lin YC, Lin PT. Effects of L-carnitine supplementation on oxidative stress and antioxidant enzymes activities in patients with coronary artery disease: a randomized, placebo-controlled trial. *Nutr. J.* 2014;13:79.

113.   Lal A, Atamna W, Killilea DW, Suh JH, Ames BN. Lipoic acid and acetyl-carnitine reverse iron-induced oxidative stress in human fibroblasts. *Redox Rep.* 2008;13(1):2–10.

114.   Marar T. Amelioration of glucose induced hemolysis of human erythrocytes by vitamin E. *Chem. Biol. Interact.* 2011;193(2):149–153.

115.   Armutcu F, Coskun Ö, Gürel A, et al. Vitamin E protects against acetone-induced oxidative

stress in rat red blood cells. *Cell Biol. Toxicol.* 2005;21(1):53–60.

116. Natta CL, Machlin LJ, Brin M. A decrease in irreversibly sickled erythrocytes in sicle cell anemia patients given vitamin E. *Am. J. Clin. Nutr.* 1980;33(5):968–971.

117. Silva CAL, Azevedo Filho CA, Pereira G, et al. Vitamin E nanoemulsion activity on stored red blood cells. *Transfus. Med.* 2017;27(3):213–217.

118. Liu ZQ. The "unexpected role" of vitamin E in free radical-induced hemolysis of human erythrocytes. *Cell Biochem. Biophys.* 2006;44(2):233–239.

119. Zhang ZZ, Lee EE, Sudderth J, et al. Glutathione Depletion, Pentose Phosphate Pathway Activation, and Hemolysis in Erythrocytes Protecting Cancer Cells from Vitamin C-induced Oxidative Stress. *J. Biol. Chem.* 2016;291(44):22861–22867.

120. Systems Biology of Free Radicals and Antioxidants. Berlin, Heidelberg: Springer Berlin Heidelberg; 2014.

121. Nelson AL, Cohen JT, Greenberg D, Kent DM. Much cheaper, almost as good: decrementally cost-effective medical innovation. *Ann. Intern. Med.* 2009;151(9):662–667.

CHAPTER 3

CHAPTER 4

DEVELOPMENT OF THE TSOX ASSAY, *I.E.* TEST OF SENSITIVITY TO OXIDATION

INTRODUCTION

An antioxidant is by definition a molecule, protein or enzyme that counteracts oxidation. In living organisms like humans, such protection can: 1) be provided by enzymes (*e.g.* the catalase, Glutathione Peroxidase [GPx] and Reductase [GR], Superoxide Dismutase [SOD]), 2) by chain breaking antioxidants that directly scavenge free radicals by receiving or donating an electron (*e.g.* the liposoluble tocopherols, ubiquinol, carotenoids and flavonoids, or the hydrosoluble Ascorbic Acid [AA], Uric Acid [UA] and thiols), and finally 3) by metal binding proteins (*i.e.* transferrin, ferritin and lactoferrin) that scavenge Fe^{2+} and Cu^+ transitions metals and thus prevent the formation of the highly reactive hydroxyl radical ($OH^\bullet$) *via* the Fenton reaction[1].

In Chapter 3, the protective effect of different molecules was assessed in the context of Red Blood Cell (RBC) storage. First, Red Cell Concentrates (RCCs) were supplemented with UA with the aim to restore its normal plasmatic concentration and therefore prevent the loss of Antioxidant Power (AOP) and metabolic dysregulation subsequent to blood products preparation (see Chapter 2). As a corrective action, RCCs were supplemented with plasma levels of UA, *i.e.* 380 µM and 320 µM UA in RCCs donated by men and women, respectively (Chapter 3, Part 1.1). Because no benefices were noticed, a second experiment was conducted where AA was supplemented in addition of UA in order to reduce its pro-oxidant effect. To do so, 420 µM UA and 110 µM AA were added in four RCCs donated by men (Chapter 3, Part 1.2). Despite the variations in metabolism, such treatment neither positively impacted the RBCs. Finally, the blood bags were treated with five different combinations of protective molecules. Each compound was tested at a given concentration (230 µM AA and 500 µM N-Acetylcysteine [NAC]; 3 mM glutamine; 50 µM Hydroxyurea [HU]; 100 µM α-lipoic acid and 5 mM acetyl-L-carnitine; and 42 µM α-tocopherol), selected on the basis of the literature (Chapter 3, Part 2). Against all odds, none of the conditions tested resulted in improvement of the standard aging parameters, even for the compounds known as potent antioxidants (such as AA). Such results triggered the following reflection: 1) "are these compounds indeed protective against oxidative stress accumulation?", 2) "are they efficient in RBCs in such context?" and 3) "were the tested concentrations high enough?".

Despite the limited impacts of molecules added, chemical supplementation is an option that deserves to be taken into account and investigated because this approach is probably the most straightforward and cheapest manner to improve the RCC quality. Indeed, adjustment of the additive solution composition does not require to modify the design of the blood collection kits, the way of processing the blood or the storage conditions of the labile blood products. The production lines and supply chain in the transfusion centers should thus not be affected by such strategy.

Therefore, to provide a tool to answer such questions, a test of sensitivity against oxidative stress, named TSOX has been developed. It is intended to help to determine if a compound provides protection to RBCs against oxidative stress and at which concentration. Such assay is more functional than a simple "test-tube" chemical-based assay, like the well-known Oxygen Radical Absorbance Capacity (ORAC) assay that only observes the direct quenching capacity of an antioxidant toward an oxidant. Indeed, a cell-based test also takes into account the uptake and metabolism of the compounds of interest and could thus provide better predictions for the situation in complex systems and potentially also enable detection of indirect antioxidants. Moreover, the aim was also to propose a test compatible with High-Throughput Screening (HTS), that would allow, similarly to the method used for drug discovery, to monitor the activity of a high number (thousands) of molecules at once for discovery of hit molecules. Then the same assay could be used for a secondary screen to generate the dose response curves for the hits.

A representative HTS assay needs to be robust, reliable and should fulfill the following criteria: 1) the technical manipulations should be limited to few steps consisting in simple operations such as addition, 2) the volume should not exceed a hundred of μL to avoid waste of reagent and ensure that a microtiter plate can be used as a container, 3) to simplify the process, the handling should be robotized which necessitates a particular instrumentation, *i.e.* a robotic arm, a pipettor and dispenser for liquid handling, a plate centrifuge, washer and shaker, *etc.*, 4) the variables should be restricted to the compound and compound concentration, 5) the measurement time should be limited to minutes or hours and 6) finally, the assay must include a precise detection method, the readout provided by a reader (microplate reader or automated microscope) and the analysis automatically reported using statistical criteria.

ASSAY DESIGN

The TSOX was thus designed keeping in mind the questions raised previously, as well as criteria to have an HTS-compatible assay (Figure 1).
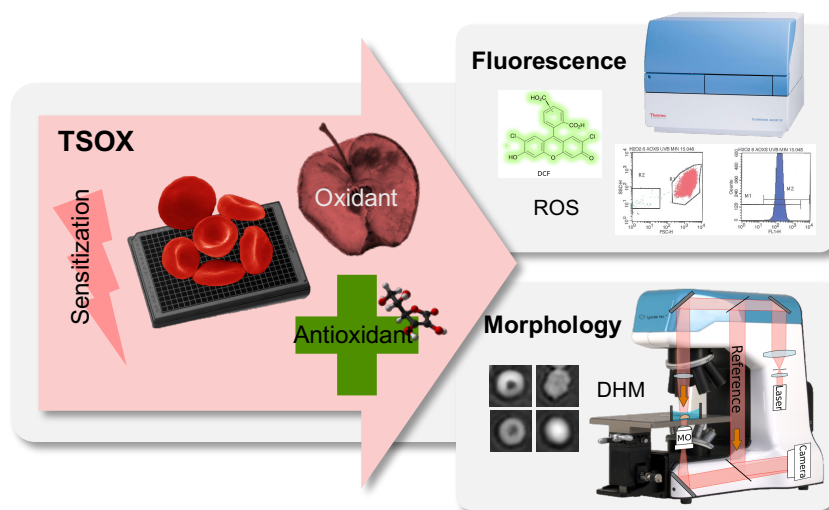

*Figure 1 – **Principle of the "TSOX",** i.e. **"test of sensitivity to oxidation" assay.** Red Blood Cells (RBCs) seeded in a microplate are treated with an oxidant and/or an antioxidant. Two possible readouts giving complementary information were proposed. The first one is based on the detection of the fluorescence emitted by the 2'-7'-Dichlorofluorescin Diacetate (DCFH-DA) reporter probe, activated when intracellular Reactive Oxygen Species (ROS) are generated[2]. The second consists in the analysis by Digital Holographic Microscopy (DHM) of the morphological changes triggered by a particular treatment.*

The workflow of the TSOX assay consisted to dispense the RBCs in 96-well microplate. 384- or 1536-well microplates could also be used depending on the number of conditions to test. Then different treatments can be applied successively or simultaneously, and be executed in specific orders according to the question asked.

First sensitization of the RBCs could be done by applying an exogenous stress. This step is optional and was only used to amplify pre-existing oxidative stress in order to exacerbate differences that would otherwise not be visible. RCC storage could also be considered as a kind of sensitization. Then, the protection will be provided by addition of molecules having direct antioxidant properties (Reactive Oxygen Species [ROS] scavenger) or indirect effect (*e.g.* by sustaining the RBC metabolism and therefore promoting the recycling or the *de novo* synthesis of endogenous antioxidants). It can work intracellularly, extracellularly or both. Finally, the phase of oxidation will consist in challenging oxidatively the platted RBCs by the addition of oxidant molecules (or with a UV treatment, oxygen-enriched atmosphere, etc.)

In this Chapter, three oxidants were tested. The use of diverse oxidants with different properties is advised as it will maximize the power of the TSOX assay to detect antioxidants with various mechanisms of action. The first one was the hydrogen peroxide (H_2O_2), that is also an endogenous ROS. This water-soluble molecule can easily cross the cell membranes and participates

via the Fenton Haber-Weiss reaction to the formation of the highly reactive OH$^\bullet$ radical, responsible for lipid peroxidation, damages to the DNA and protein oxidation. H_2O_2 can thus be considered as a transmitter, to propagate oxidative stress and induce oxidative damages in various locations. 2,2'-Azobis(2-methylpropionamidine) dihydrochloride (AAPH) was also evaluated as a source of oxidative stress. Indeed, this hydrophilic azo compound has a higher oxidant capacity than H_2O_2[3], and is capable to trigger nucleophilic reactions and free radical oxidations[4]. Shortly, the generation of free radical occurs when the azo compound in solution undergoes thermal decomposition or hydrolysis at a constant rate (first order reaction) and forms a nitrogen (N_2) and two carbon radicals (R$^\bullet$) that can either combine and form stable products or react with oxygen (O_2) to generate peroxyl radicals (ROO$^\bullet$) (see Table 1 for chemical structure)[4]. Such radical can trigger chain oxidation of lipids and proteins and ultimately lead to oxidative hemolysis[5]. The last oxidant to be tested was the diamide. It is a thiol-oxidizing agent that targets sulfhydryl groups in glutathione and amino acids such as the cysteine, (selenocysteine) and methionine.

Two readouts were selected for this assay (Figure 1). The first one was based on the detection of the fluorescence emitted by the 2'-7'-Dichlorofluorescin Diacetate (DCFH-DA)[2] reporter probe, activated when intracellular ROS are generated. The use of the redox-sensitive DCFH-DA molecule for oxidative stress quantification in a cell model is not new and was already described by Wang and Joseph in 1999[6]. The first Cellular Antioxidant Assay (CAA) using DCFH-DA as reporter probe was developed by Wolfe and Liu in 2007 on HepG2 cells to test the antioxidant activity of phytochemical food extracts and dietary supplements[7]. Then, different research teams have adapted it on diverse cell lines to test various substances. RBCs were also used as cell models, such as in the CAP-e assay proposed by Honzel *et al.* in 2008[8]. A flow cytometer was first used for the quantification of the fluorescence in the early TSOX development phase; however, this method is barely compatible with HTS and was therefore replaced by a microplate fluorometer. Flow cytometry could be used to after the initial screening phase to decipher the mechanism of action of the hit molecules. The second readout based on image analysis by DHM was proposed as it delivers complementary information. DHM was introduced in Chapter 1 and has previously been validated for HTS applications (automation available)[9,10]. Moreover, a fluorescent camera can also be mounted on the DHM.

MATERIAL AND METHODS

Oxidative stress induction

The different compounds tested to generate oxidative stress are listed in Table 1.

Table 1 – Compounds tested for oxidative stress generation.

Compound and MW	Mechanism of ROS generation	Structure	References
H_2O_2 34.01 g/mol	Water-soluble oxidizing agent, inorganic peroxide		Sigma-Aldrich, H1009. PubChem CID 784
Diamide 172.19 g/mol	Thiol-oxidizing agent, oxidizes sulfhydryl groups to disulfide form		Sigma-Aldrich, D3648. PubChem CID 5353800
AAPH 271.19 g/mol	Water-.soluble azo compound, peroxyl radicals (ROO•) generation, temperature-dependent degradation at constant rate[4]		Sigma-Aldrich. 440914. PubChem CID 76344

ROS: Reactive Oxygen Species, H_2O_2: hydrogen peroxide, AAPH: 2,2'-Azobis(2-methylpropionamidine) dihydrochloride.

Oxidative stress generation using UVB (280-350 nm) was also tested (data no shown). To do so, RBC samples in tubes were put inside a dark cabinet and were illuminated with UVB lamps (Philips UVB broadband TL 20W/12, Elevite) for a given duration, at room temperature (RT) under agitation. Details of experimental conditions will be provided directly within the "Results and discussion" section.

Readouts for the TSOX assay

Analysis of reactive oxygen species generation using DCFH-DA fluorescent reporter probe

The DCFH-DA probe was used for the monitoring of the general oxidative stress as it detects non-specifically different ROS within live-cells[11–16]. The DCFH-DA molecule is non-ionic and non-polar, which enables its passage through the plasma membrane[11]. After entering the cells, the DA moieties are hydrolyzed (deacetylation) by the cellular esterases. The resulting DCFH molecule is more polar and is therefore retained within the cell. In presence of ROS, the reporter probe becomes fluorescent (green highlighted molecule in Figure 2).
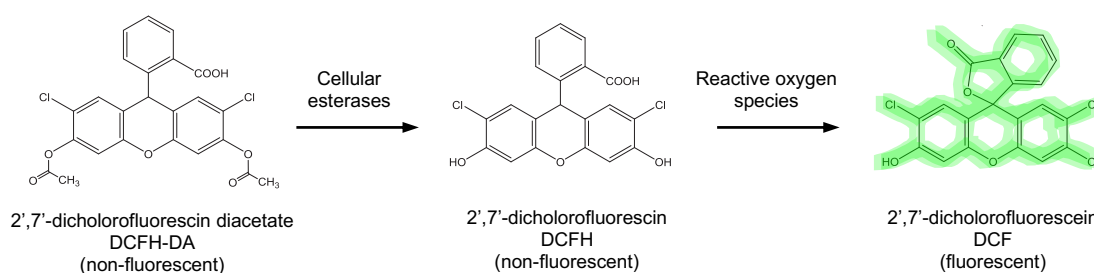

*Figure 2 – **Activation of 2'-7'-Dichlorofluorescin Diacetate (DCFH-DA),** i.e. **reactive oxygen species fluorescent reporter.** Modified from Kellet et al., Food Chemistry, 2018[11].*

The DCF is excited at a wavelength of 504 nm and emits at 529 nm (in ethanol) and is thus compatible with the common Fluorescein (FITC) filter set. For the analyses, DCFH-DA (D6883 purchased from Sigma-Aldrich) was prepared at 10 mM in 100 % DMSO and aliquots were stored at -28°C.

Treatment of the red blood cells with DCFH-DA reporter probe

RBCs sampled in RCCs (using a sterile syringe through a sample site) were washed 1-2x with 0.9 % NaCl (10 min of centrifugation at 2000 g and 4°C). Then, the RBCs were resuspended at 10 % Hematocrit (HCT) in 0.9 % NaCl, treated with 50 µM DCFH-DA (0.5 % DMSO) and incubated during 30 min at 37°C under agitation to enable incorporation of the dye within the cells. Finally, the tubes were centrifuged (as before) and the supernatant containing the excess of DCFH-DA was discarded.

Quantification of fluorescence emission using a microplate fluorometer

For fluorescence analysis, the RBCs treated with the DCFH-DA probe were further diluted at 1 % HCT in 0.9 % NaCl and dispensed in a 96-well imaging plate (ref. 353219, Black/Clear, Falcon). Then, 10 µL of oxidant and/or antioxidant stock solutions (20x) were added. The final volume in each well was 200 µL. The plate was incubated at 37°C during the timelapse analysis.

The microplate fluorometer that was used is a Fluoroskan Ascent (and Ascent Software, Thermo Fisher Scientific), equipped with a fluorometric filter pair (Ex/Em 492/527 nm). This device can be programmed to perform automatically a list of steps, and possesses orbital shaking, dispenser and incubator functions. The main advantage of such device in comparison to the flow cytometry is the possibility to analyze simultaneously and with kinetic measurements a high number of conditions. However, it only provides a picture of the bulk fluorescence (cells and surrounding) within the wells.

Analysis of morphological changes using digital holographic microscopy

The impact of oxidative stress on RBC morphology was assessed using a Digital Holographic Microscope (DHM) equipped with a motorized microscope stage, an incubator system, and 20x/0.40 NA objective. More details about this technology are provided in Chapter 1.

The RBCs were taken in RCCs using a sterile syringe through a sample site and were washed (1-2x) with 0.9 % NaCl (10 min of centrifugation at 2000 g and 4°C). Before the analysis, the pellet was resuspended in HEPA (composition described in ANNEX-1). Then, 80'000 RBCs were seeded per well in a 96-well black imaging plate coated with poly-L-ornithine (procedure in ANNEX-2). To sediment the cells more rapidly, the plate was gently centrifuged (2 min, 140 g, RT). Then, 10 µL of oxidant and/or antioxidant stock solutions (10x) were added per well. The final volume in each well was of 100 µL. For imaging, the plate was put under the microscope in the incubation chamber set at 37°C and 5 % CO_2, and four images were taken per well at 20x magnification. The evolution of the treated RBCs was followed during timelapse analysis.

As described before, the output of DHM analyses are 1) the phase images and 2) a quantitative value, *i.e.* optical path difference (OPD) for each pixel of the phase image. For the TSOX, the average of the OPD distribution (OPD avg), as well as the confluency parameter were retained. The confluency refers here to the percentage of the phase image occupied by RBCs, the evolution of such parameter will thus be impacted by cell swelling or shrinkage and is strongly reduced in case of hemolysis. In general, confluency was normalized (divided by the confluency measured at right after the oxidant addition), as this parameter depends on the cell seeding.

RESULTS AND DISCUSSION

TSOX development: generation of oxidative stress

The first step in the TSOX development consisted in testing the effect of various sources of oxidative stress on RBCs and to determine if the changes induced were quantifiable with the proposed readouts, *i.e.* measurements of DCFH-DA fluorescence emission using the Fluoroskan fluorometer and evaluation of morphological changes by DHM.

Fluorescence as readout to monitor reactive oxygen species generation under H_2O_2, diamide and AAPH treatment

The effect of H_2O_2, diamide and AAPH oxidants at three concentrations was evaluated as shown in Figure 3. Two control experiments were also conducted to determine: 1) if fluorescence was emitted when DCFH (after -DA group cleavage) was submitted to oxidative stress outside the cell ("Lysed RBCs" control) and 2) if the DCFH-DA probe could be activated by the oxidants even in absence of cells ("No RBCs" control).
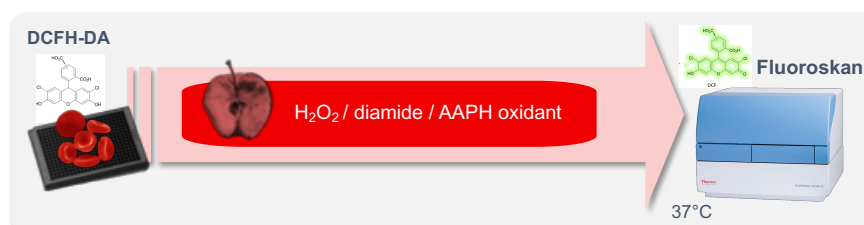

*Figure 3 – **Analysis workflow for the monitoring of the oxidative stress triggered by oxidant treatment using fluorescence readout.** Red blood cells treated with the 2',7'-Dichlorofluorescin Diacetate (DCFH-DA) probe are plated in a multiwell imaging plate and treated with hydrogen peroxide (H_2O_2), diamide, or 2'-Azobis(2-amidinopropane) dihydrochloride (AAPH). A fluorometer is used to quantify the fluorescence emitted which increases when intracellular reactive oxygen species are generated.*

RBCs taken from an RCC were treated with DCFH-DA and resuspended at 1 % HCT either in 0.9 % NaCl, or in dH_2O for cell lysis. The lysed RBCs were vortexed during 2 min at RT, centrifuged during 5 min at 3200 g and 4°C to pellet the cell membranes, and the supernatant was collected ("Lysed RBCs"

control). For the "No RBCs" control, DCFH-DA was diluted at 50 µM in 0.9 % NaCl and kept 30 min under agitation at 37°C to mimic the standard protocol. Finally, 190 µL of the RBCs, "Lysed RBCs" and "No RBCs" samples were dispensed in different wells and treated with 10 µL of 10x H_2O_2, diamide and AAPH stock solutions (two wells per condition). The concentrations tested were 0, 0.001, 0.005 or 0.01 % H_2O_2, with 0, 250, 500 or 1000 µM diamide, as well as 0, 100, 500 or 1000 µM AAPH. After that, fluorescence was recorded overnight with the Fluoroskan fluorometer (plate incubated at 37°C).
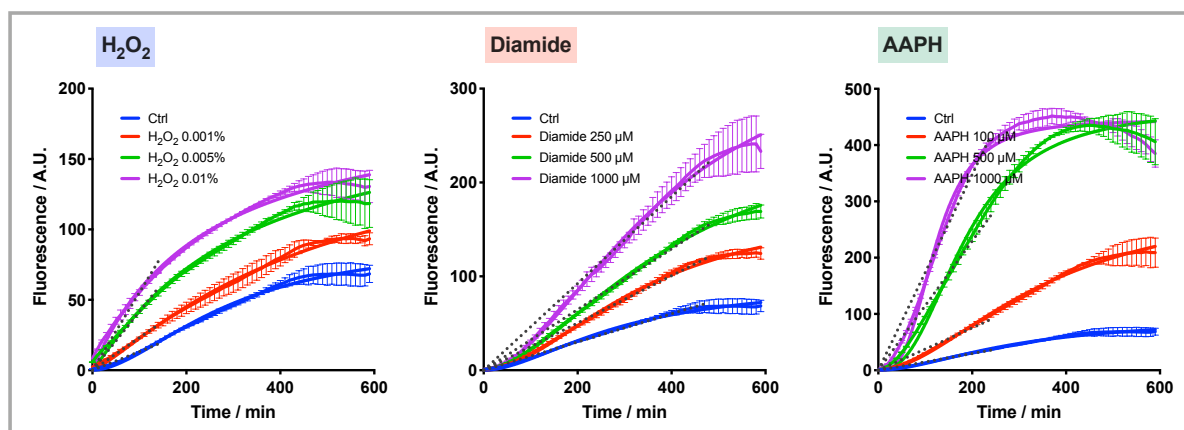

*Figure 4 – **Fluorescence emission triggered in red blood cells by different concentrations of hydrogen peroxide (H_2O_2), diamide, or 2'-Azobis(2-amidinopropane) dihydrochloride (AAPH).** Timelapse analysis of fluorescence emission by the 2',7'-Dichlorofluorescin Diacetate (DCFH-DA) reporter probe (i.e. intracellular reactive oxygen species generation) triggered by 0, 0.001, 0.005 or 0.01 % H_2O_2, by 0, 250, 500 or 1000 µM diamide, or by 0, 100, 500 or 1000 µM AAPH treatment. Mean value for two wells $\pm$ standard deviation.*

As expected, the fluorescence emission was positively correlated to the oxidant concentration (Figure 4). The reaction onset was fast for H_2O_2 and slower for diamide and AAPH (see initial slopes). The signal also increased in the control, suggesting that endogenous and/or exogenous ROS were spontaneously generated.

The fluorescence curves are full of information about the kinetics of the reactions and could help to decipher the mechanisms of action of the different molecules tested. However, this kind of data presentation can become dense and difficult to analyze when the number of conditions increases. It is the reason why, with a view of applying the TSOX to HTS, different quantitative analysis parameters were proposed. Two quantitative parameters were selected for the statistical analysis of fluorescence (Figure 5). First, the slopes (A.U. per minute) were extracted. To do so, linear regression was calculated using PRISM software (GraphPad Prism version 8 for Mac) on the basis of the least squares approach. It should be noted that the lines were forced to go through x = 0 and y = 0. The fitting was restricted to the linear part of the curve, *i.e.* limited to the first 140 min of the timelapse for H_2O_2, 480 min for diamide and 240 min for AAPH. The second parameter proposed was the Area Under the Curve (AUC). It was again calculated with PRISM software that computes it by the trapezoidal method. The baseline fluorescence was assumed to be equal to 0 A.U.
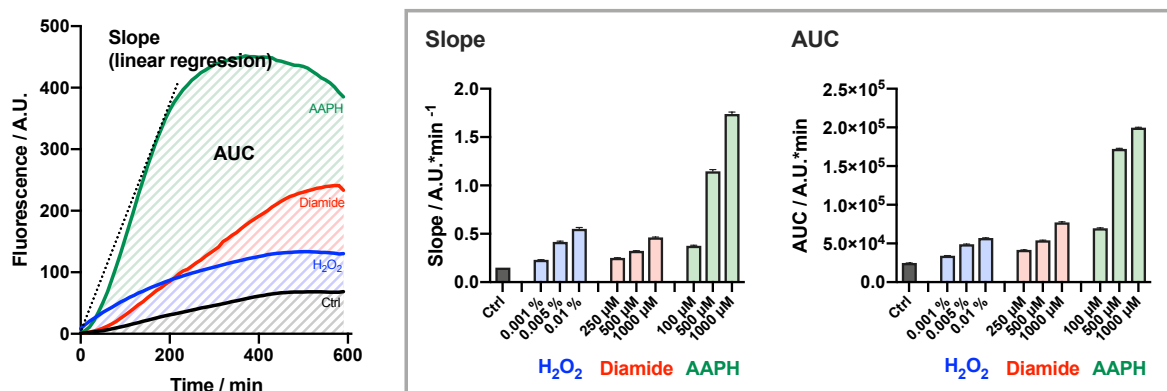
*Figure 5 – **Quantitative analysis of fluorescence emission triggered in red blood cells by different concentrations of hydrogen peroxide (H₂O₂), diamide, or 2'-Azobis(2-amidinopropane) dihydrochloride (AAPH).** [Left] Illustration of the selected analysis parameters for fluorescence curves. [In box] slope and Area Under the Curve (AUC) calculated from the fluorescence curves presented in Figure 4. Mean value for two wells ±standard deviation.*

Both parameters selected enabled to discriminate control from RBCs treated either with H_2O_2, diamide or AAPH. In the TSOX, increased values of initial slope and AUC are expected in presence of oxidants, which was the case here. Moreover, the values were positively correlated to the oxidant concentration, *i.e.* the slope steepness indicating more particularly at which rate ROS are generated and the AUC informing about the global quantity of ROS produced. The reason that a maximum is reached could be that all DCFH within the cell has been converted to DCF. However, in such case the value of the plateau should be identical when RBCs are treated with similar amounts of fluorescent probe. Another reason could be that all oxidant molecules were quenched or degraded, *e.g.* by the cellular endogenous antioxidant defenses. Finally, cell lysis that certainly occurs during the incubation in 0.9 % NaCl at 37°C under oxidative stress also impacts the global fluorescence. Indeed, lower levels of fluorescence were emitted in the "Lysed RBCs" controls (Figure 6, top). Finally, the signal remained almost null in the "No RBCs" samples, confirming that the -DA group must be cleaved to enable fluorescence emission (Figure 6, bottom).
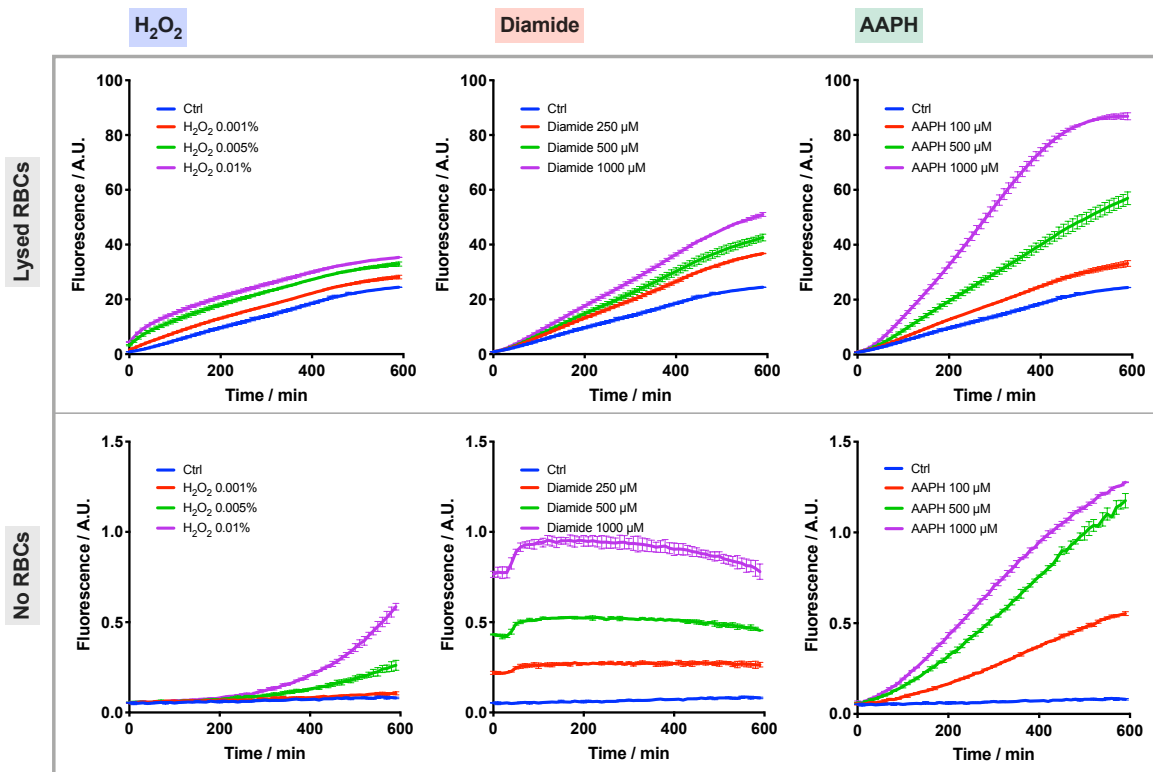
*Figure 6 – **Fluorescence emission triggered in "Lysed RBCs" and "No RBCs" controls by different concentrations of hydrogen peroxide (H_2O_2), diamide, or 2'-Azobis(2-amidinopropane) dihydrochloride (AAPH).** Timelapse analysis of fluorescence emission by the 2',7'-Dichlorofluorescin Diacetate (DCFH-DA) reporter probe (i.e. intracellular reactive oxygen species generation) triggered by 0, 0.001, 0.005 or 0.01 % H_2O_2, by 0, 250, 500 or 1000 μM diamide, or by 0, 100, 500 or 1000 μM AAPH treatment in "Lysed RBCs" [top] and "No RBCs" [bottom] control samples. Mean value for two wells ± standard deviation. RBC: red blood cell.*

Morphology readout: analysis of morphological changes under H_2O_2, diamide and AAPH treatment

After evaluating the DCFH-DA ROS reporter probe to study the effect of H_2O_2, diamide or AAPH treatment, the same approach was applied to determine if the oxidation induced lesions to the RBCs that would be observable and quantifiable by DHM, *i.e.* significant variation of OPD, the quantitative DHM output (Figure 7).
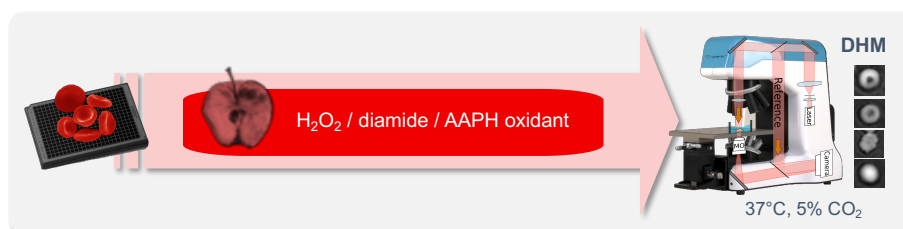

*Figure 7 – **Analysis workflow for the monitoring of the oxidative stress triggered by oxidant treatment using Digital Holographic Microscopy (DHM) readout.** Red blood cells are plated in a multiwell imaging plate and treated with hydrogen peroxide (H_2O_2), diamide or 2,2'-Azobis(2-amidinopropane) dihydrochloride (AAPH). The DHM is used to quantify the changes of morphology.*

To do so, RBCs taken from a RCC were prepared as usual for DHM imaging (3 wells/condition). They were treated with 0, 0.001, 0.005, 0.01 or 0.1 % H_2O_2, with 0, 0.5, 1, 2.5, 5, 7.5 or 10 mM diamide, as well as 0, 1, 2.5, 5, 7.5 or 10 mM AAPH and incubated (with frequent imaging) during approximatively 10h at 37°C and 5 % CO_2.
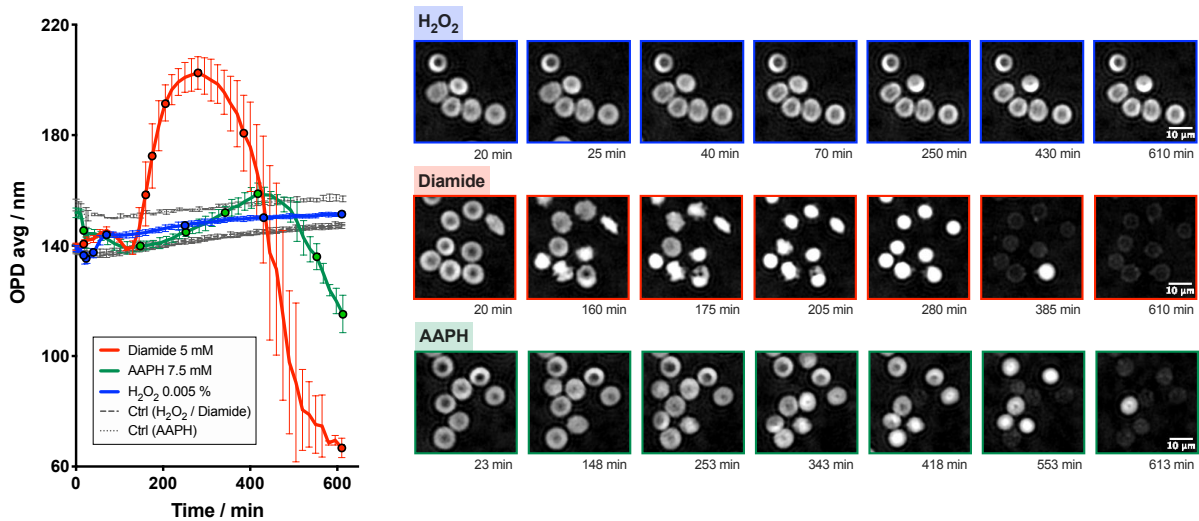

*Figure 8 – **Morphological changes triggered in red blood cells (RBCs) by hydrogen peroxide (H_2O_2), diamide, or 2'-Azobis(2-amidinopropane) dihydrochloride (AAPH), analyzed by Digital Holographic Microscopy (DHM).** [Left] Timelapse analysis of the Average of the Optical Path Difference distribution (OPD avg) parameter. [Right] Illustrative phase images acquired by DHM of treated RBCs at given time points. Mean value for three wells ± standard deviation.*

Each oxidant induced a unique change of RBC morphology (Figure 8). H_2O_2 did not modified the apparent RBC biconcave shape but leaded to a loss of the projected area. The response of RBCs to diamide treatment exhibited a delayed onset during which the discocytic morphology was maintained for a short period of time. Then, the sudden increase of OPD reflected a complete membrane destabilization leading to formation of echinocytes exhibiting large spicules, accompanied with loss of large portions of membrane. The maximum of the curve corresponding to the formation of spherocytes (*e.g.* see image at 280 min in Figure 8). The spherocytic RBCs have a strong OPD signal, because they are thicker and more dense (higher Mean Corpuscular Hemoglobin Concentration [MCHC]). Finally, the OPD signal dropped because of cell lysis, leaving only crenated ghosts (end-point image in Figure 8). AAPH also ultimately leaded to RBC hemolysis, but in a more progressive and controlled way than the diamide.
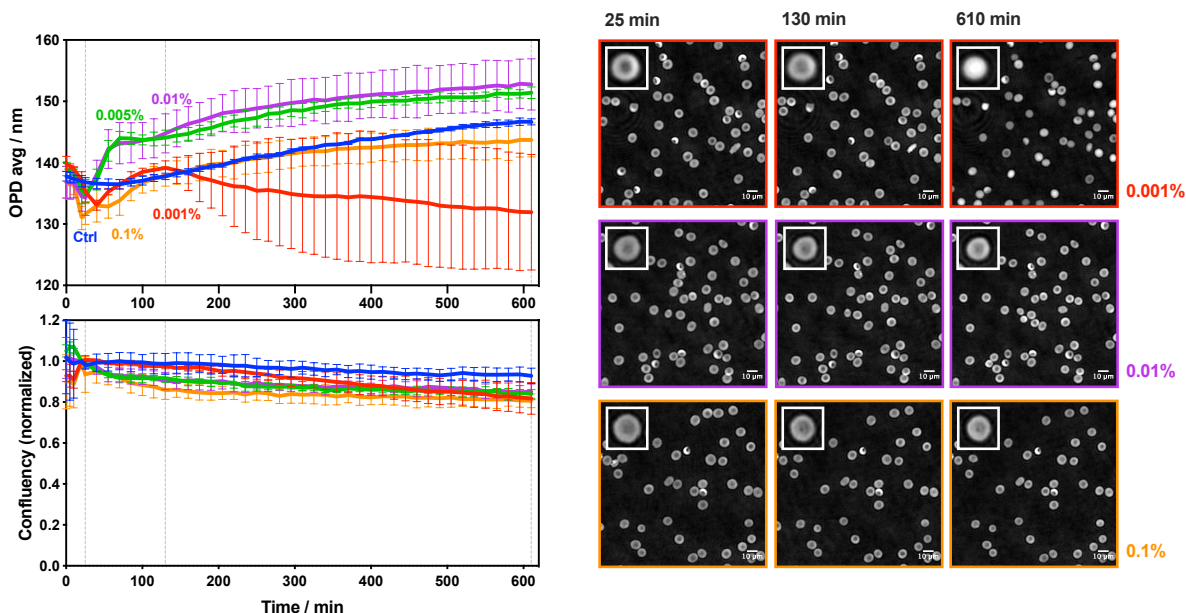
*Figure 9 – **Morphological changes triggered in Red Blood Cells (RBCs) by different concentration of hydrogen peroxide (H₂O₂).** Timelapse analysis by Digital Holographic Microscopy (DHM) of morphological changes under 0, 0.001, 0.005, 0.01 or 0.1 % H₂O₂ treatment. [Left] Evolution of Average of the Optical Path Difference distribution (OPD avg) and confluency. Mean value for three wells ±standard deviation. [Right] Illustrative phase images acquired by DHM of RBCs treated with 0.001, 0.01 or 0.1 % H₂O₂ at three time points, with zoom on a random RBC.*

As described before, the H_2O_2 treatment induced the formation of smaller RBCs that generally kept their discocytic shape. As for fluorescence, the changes occurred rapidly after treatment. Interestingly, the response pattern differed according to the concentrations tested (Figure 9). Indeed, at 0.005 % and 0.01 % H_2O_2, the OPD signal increased mostly within the first 30 min following the exposition to the oxidative stress and reached a plateau, whereas it decreased at the same time with 0.001 and 0.1 % H_2O_2. Interestingly, the lower concentration tested (*i.e.* 0.001 % H_2O_2), impacted the most the OPD avg and the highest (*i.e.* 0.1 % H_2O_2) the least.

*Figure 10 – **Quantitative analysis of the morphological changes triggered in red blood cells by different concentrations of hydrogen peroxide (H₂O₂)**. [Left box] Area Under the Curve (AUC) and end-point calculated from the Average of the Optical Path Difference distribution (OPD avg) curves presented in Figure 9. [Right box] AUC and end-point calculated from the confluency curves presented in Figure 9. Mean value for three wells ±standard deviation.*

The problem of using H_2O_2 for the TSOX assay was the effect of this oxidant on the RBCs that was poorly reflected by the DHM variables like the OPD avg and confluency (Figure 10). Therefore, none of the potential quantitative analysis parameters, such as AUC or end-point were significantly different between untreated and treated RBCs. Unfortunately, higher concentrations of H_2O_2 could not be used because formation of bubbles occurred and strongly biased the OPD signal.
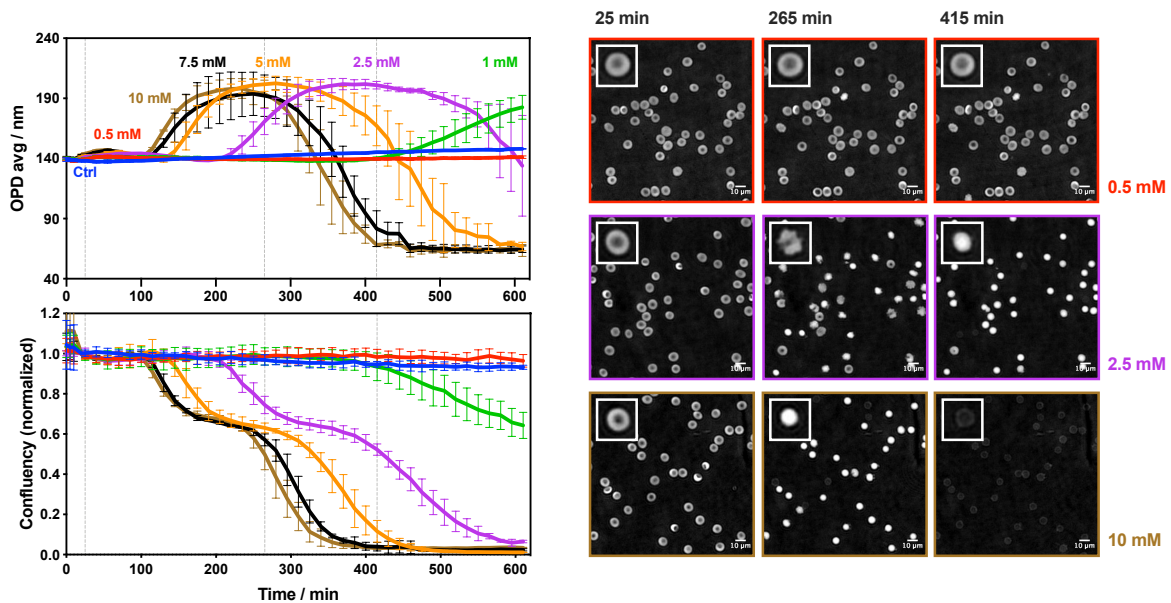
Figure 11 – **Morphological changes triggered in Red Blood Cells (RBCs) by different concentrations of diamide.** *Timelapse analysis by Digital Holographic Microscopy (DHM) of morphological changes under 0, 0.5, 1, 2.5, 5, 7.5 or 10 mM diamide treatment. [Left] Evolution of Average of the Optical Path Difference distribution (OPD avg) and confluency. Mean value for three wells ± standard deviation. [Right] Illustrative phase images acquired by DHM of RBCs treated with 0.5, 2.5 or 10 mM diamide at three time points, with zoom on a random RBC.*

The response of the RBCs to the diamide treatment was proportional to the concentration tested (Figure 11). Higher diamide concentrations shortened the lag time. All RBCs in the sample responded in a synchronized manner to the treatment. The amplitude of the change was comparable for all conditions with similar maximum (spherocytes formation) and minimum (complete cell lysis) OPD avg values. However, after reaction onset, the duration of the process, *i.e.* membrane destabilization, spherocyte formation and hemolysis, was inversely proportional to the diamide concentration because RBCs treated with lower oxidant concentrations resisted longer. The overall process was also reflected by the confluency parameter that decreased first because of spherocytosis (reduction of the projected area) and then because of the hemolysis.

Several quantitative parameters that could serve as output data for the TSOX assay were extracted from the OPD avg and confluency curves, *i.e.* the lag time, time to Max, cross-control time, time to Min and AUC (Figure 12).

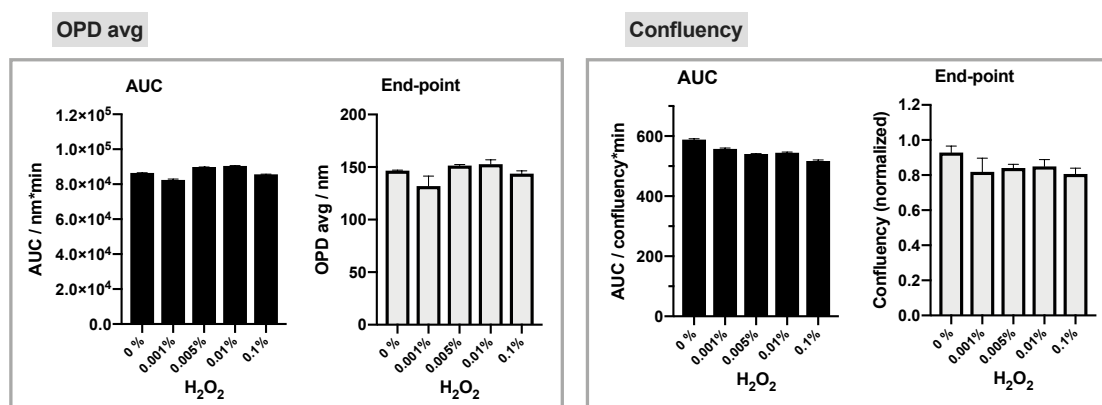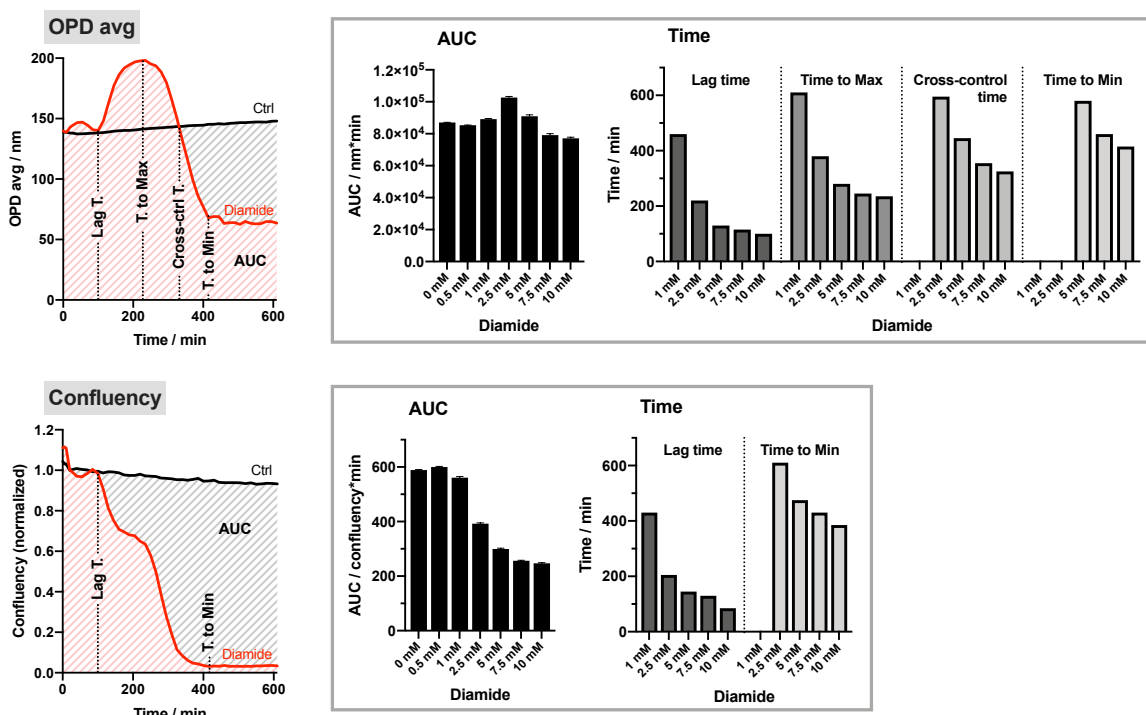*Figure 12 – **Quantitative analysis of the morphological changes triggered in red blood cells by different concentrations of diamide. [Left]** Illustrations of the selected analysis parameters for Average of the Optical Path Difference distribution (OPD avg) and confluency curves. **[Top box]** Area Under the Curve (AUC) and Time-related, i.e. Lag time (Lag T.), Time to Max (T. to Max), Cross-control time (Cross-ctrl T.) and Time to Min (T. to Min) calculated from the Average of the OPD avg curves presented in Figure 11. **[Bottom box]** AUC and Time-related, i.e. Lag time (Lag T.) and Time to Min (T. to Min) calculated from the confluency curves presented in Figure 11. Mean value for three wells ± standard deviation.*

The time-related values were not reported when the curves are flat such as for the control and the oxidant concentrations that are too low to induce quantifiable morphologic alterations within the timeframe of the experiment. It does not mean that nothing happened. Indeed, response to 0.5 mM diamide was comparable to control with DHM readout, whereas fluorescence was detected. Each parameter varied proportionally to the oxidant concentration, at the exception of the AUC of OPD avg that did not decrease when oxidant concentration increased.

Finally, various concentrations of AAPH were tested (Figure 13). Interestingly, not all the RBCs in the sample responded at the same time to the treatment, explaining why the maximal OPD avg value was lower in comparison to the diamide treatment. Again, the changes observed were proportional to the AAPH concentration.
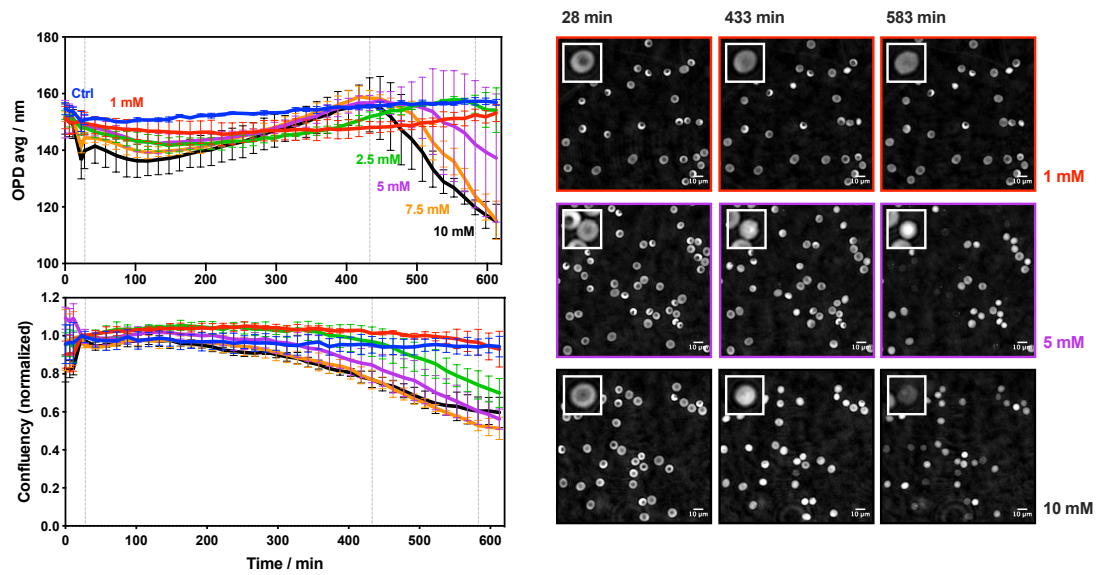
*Figure 13 – **Morphological changes triggered in Red Blood Cells (RBCs) by different concentrations of 2'-Azobis(2-amidinopropane) dihydrochloride (AAPH).** Timelapse analysis by Digital Holographic Microscopy (DHM) of morphological changes under 0, 1, 2.5, 5, 7.5 or 10 mM AAPH treatment. [Left] Evolution of Average of the Optical Path Difference distribution (OPD avg, top) and confluency (bottom). Mean value for three wells ± standard deviation. [Right] Illustrative phase images acquired by DHM of RBCs treated with 1, 5 or 10 mM AAPH at three time points, with zoom on a random RBC.*

The AUC, Time to Max and End-point parameters could be used for the quantitative analysis of oxidative stress induced by AAPH (Figure 14). The main differences were observed with the End-point parameter allowing the comparison to any concentrations.
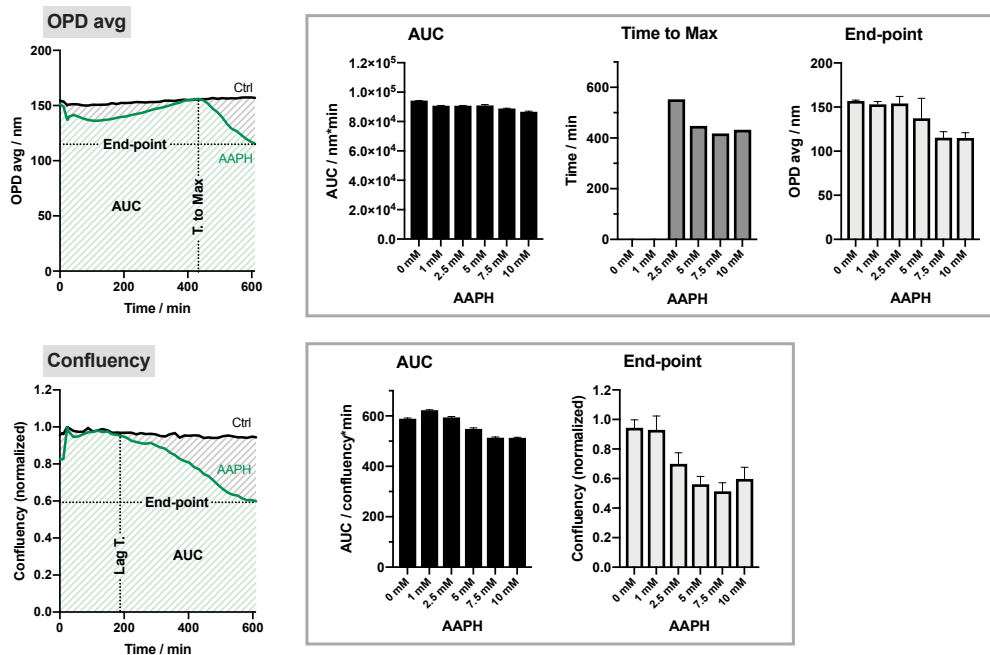
*Figure 14 – **Quantitative analysis of the morphological changes triggered in red blood cells by different concentrations of 2'-Azobis(2-amidinopropane) dihydrochloride (AAPH).** [Left] Illustrations of the selected analysis parameters for Average of the Optical Path Difference distribution (OPD avg) and confluency curves. [Top box] Area Under the Curve (AUC), Lag time (Lag T.), and End-point calculated from the OPD avg curves presented in Figure 13. [Bottom box] AUC and End-point calculated from the confluency curves presented in Figure 13. Mean value for three wells ± standard deviation.*

TSOX development: identification of antioxidant molecules

The second step in the TSOX assay development was to demonstrate its ability to effectively detect antioxidant molecules. To do so, various compounds with proven antioxidant properties were used as positive controls. Again, both the fluorescence and morphology readouts were tested.

Fluorescence readout: proof-of-concept with a "miniscreen" of known antioxidants

To validate the TSOX assay using fluorescence as readout, a "miniscreen" was conducted to test the well-known AA, UA, Trolox (water-soluble analog of vitamin E) and resveratrol (natural polyphenol) antioxidants. The pipeline of the experiment is pictured out in Figure 15.

*Figure 15 – **Analysis workflow for the identification of antioxidant molecules using fluorescence readout.** Red blood cells treated with the 2',7'-Dichlorofluorescin Diacetate (DCFH-DA) probe are plated in a multiwell imaging plate and treated with the molecules of interest during 60 min. Then hydrogen peroxide (H_2O_2), diamide or 2,2'-Azobis(2-amidinopropane) dihydrochloride (AAPH) 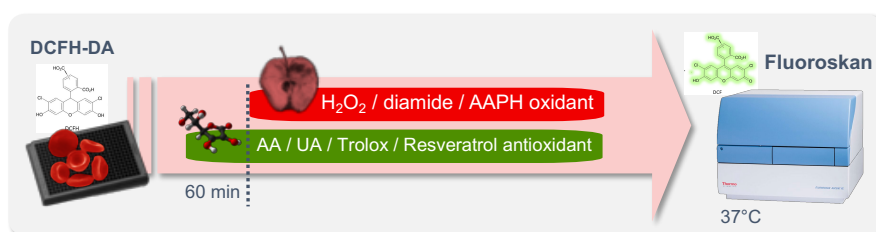are added. A fluorometer is used to quantify the fluorescence emitted which increases when intracellular reactive oxygen species are generated.*

RBCs were taken from an RCC, treated with DCFH-DA probe and 180 µL of 1 % HCT RBC sample were loaded per well in a 96-well plate. Then the molecules to analyze were added at three different concentrations, *i.e.* 0, 10, 100 or 1000 µM (2 wells/condition). The antioxidant stock solutions (20x) were prepared at 20 mM and diluted at 2 and 0.2 mM in 0.9 % NaCl. AA was dissolved in 0.9 % NaCl, UA in 0.9 % NaCl plus 0.07 % NH_3 (37 µM), Trolox and Resveratrol were solubilized in 100 % DMSO. Consequently 1.85 µM NH_3 was used as control for UA, and 5% DMSO for Trolox and Resveratrol. The RBCs were treated with 10 µL of antioxidants and incubated at 37°C during 60 min before addition of the oxidant. After that, 10 µL of 20x oxidant stock solution prepared in 0.9 % NaCl were added. In addition to the control, two concentrations were tested for each oxidant, *i.e.* 250 and 1000 µM AAPH and diamide, and 0.0001 and 0.001 % H_2O_2. Fluorescence was recorded overnight (590 min from oxidant addition) in the Fluoroskan fluorometer, the plate was kept at 37°C. The experiment was repeated for three consecutive days using the same RCC stored for three, four and five days of storage. The first day, the oxidative stress was induced with AAPH, the second with diamide and the third with H_2O_2. The difference in storage was negligible since the metabolism variations are equivalent in this phase of the storage (see Chapter 1).

The results for the three experiments, which aimed to analyze the effects of four antioxidants at three concentrations against three oxidants at two concentrations are presented in Figure 16.
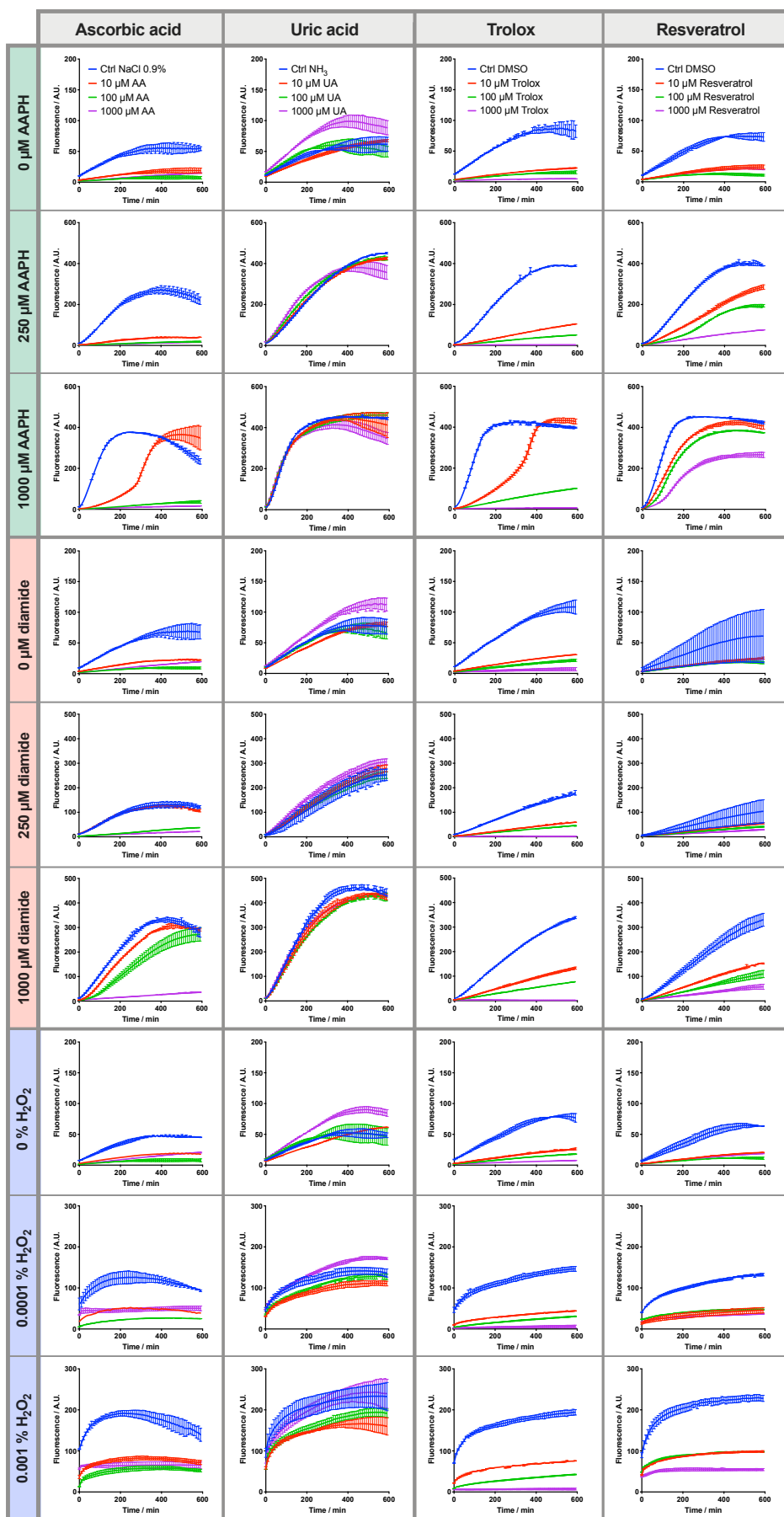
Figure 16 – "Miniscreen" with the TSOX assay coupled to fluorescence readout to assess the protective effects of known antioxidants against 2,2'-Azobis(2-amidinopropane) dihydrochloride (AAPH), diamide or hydrogen peroxide (H₂O₂) oxidant. Timelapse analysis of fluorescence emission by the 2',7'-Dichlorofluorescin Diacetate (DCFH-DA) reporter probe (i.e. intracellular reactive oxygen species generation). The protective effect of 0, 10, 100 or 1000 µM Ascorbic Acid (AA), Uric Acid (UA), Trolox or resveratrol antioxidants against oxidative stress generated by 0, 250 or 1000 µM AAPH, by 0, 250 or 1000 µM diamide, or by 0, 0.0001 or 0.001 % H₂O₂ was assessed. Mean value for two wells ± standard deviation.

For analysis, the AUC was calculated, as before using PRISM software, baseline fluorescence was assumed to be null (Figure 17).
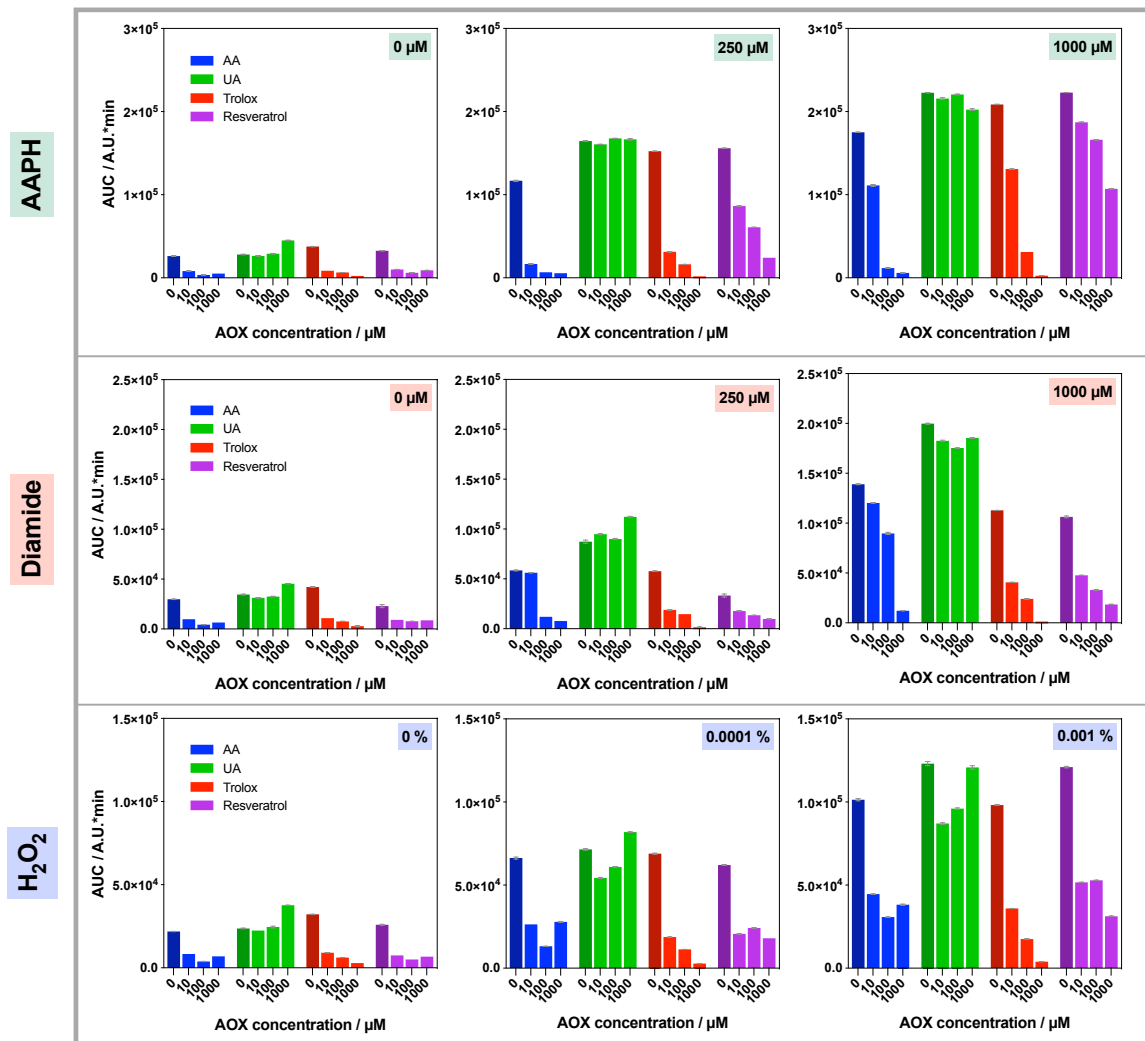
*Figure 17 – **Analysis of the results obtained during the "Miniscreen with the TSOX assay"**. The Area Under the Curve (AUC) was calculated from the fluorescence curves presented in Figure 16. Mean value for two wells $\pm$ standard deviation.*

The "no oxidant" controls (0 μM AAPH, 0 μM diamide and 0 % H_2O_2 controls) are presented in the first column of graphics. They can serve as a reference to compare the different experiments. As seen before, fluorescence raised even without exogenous oxidant addition, because of the incubation conditions that elicited spontaneous ROS generation. In such case, the protective effect of AA, Trolox and resveratrol was already quantifiable, excepted for UA that even further exacerbated the oxidative stress.

As expected, the global fluorescence was correlated to the amount of oxidant added in the "no antioxidant" controls (0 μM AA, 0 μM UA, 0 μM Trolox and 0 μM resveratrol, corresponding to the bar with shaded color). It seems that the solvent used for the dissolution of the antioxidants impacted the sensitivity of the RBCs to the oxidants. Indeed, the 5 % DMSO in the Trolox and resveratrol controls

and even more the 1.85 µM NH_3 UA control samples increased the amount of ROS generated when compared to the 0 µM AA control, only composed of 0.9 % NaCl.

Within the experiment timeframe, addition of 10 µM, 100 µM and 1000 µM AA fully protected the RBCs from 250 µM AAPH. It is not certain that the signal would not have increased if the experiment had been prolonged. For the 1000 µM AAPH treatment, 10 µM AA was not sufficient, but delayed the onset of the reaction. AA was less potent against diamide for the same concentrations tested but was protective against 0.0001 and 0.001 % H_2O_2. UA was not effective against AAPH, diamide or H_2O_2 and even worsened the situation, which confirms that it can function as a pro-oxidant. It could explain why the addition of this molecule in the RCCs did not improved the aging markers of the RBCs in the first part of Chapter 3. It is important to mention that the apparent protective effect of 1000 µM Trolox treatment (lower AUC) was in fact related to RBC hemolysis. This phenomenon was visible by eye on the plate (brown color). Finally, resveratrol also limited the production of ROS. The kinetic analysis shows that this compound lowered the maximum of fluorescence (plateau value) and also modified the initial slopes of the curves (rate of ROS generation), either suggesting that resveratrol is a direct antioxidant, but could also indicate that this molecule induces cell lysis.

Morphology readout: proof-of-concept with ascorbic acid and uric acid antioxidants

Proof-of-concept experiments were also conducted to demonstrate that the TSOX could be coupled to the DHM readout to detect antioxidants (Figure 18). Hence, the protective effect of AA combined with UA against diamide and AAPH oxidants was assessed. These two molecules have already been tested in pair in Chapter 3, Part 1.2.
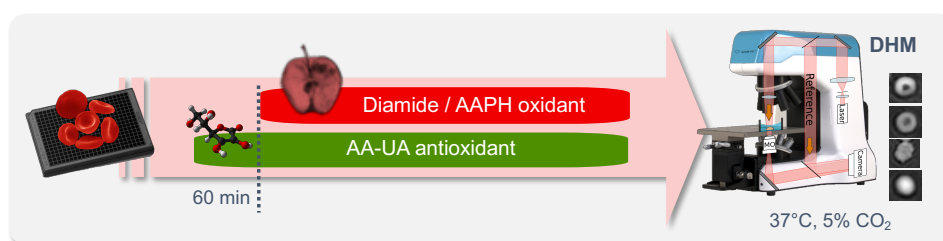
*Figure 18 – **Analysis workflow for the identification of antioxidant molecules using Digital Holographic Microscopy (DHM) readout.** Red Blood Cells (RBCs) are plated in a multiwell imaging plate and treated with the molecules of interest during 60 min (e.g. Ascorbic Acid plus Uric Acid [AA-UA]). Then diamide or 2,2'-Azobis(2-amidinopropane) dihydrochloride (AAPH) are added. The DHM is used to quantify the changes of RBC morphology.*

For the first experiment, RBCs were treated with 113.7 µM AA plus 416.3 µM UA (plasma levels) and oxidized with 0, 1, 2 or 5 mM diamide (three wells per condition). To do so, RBCs were taken from an RCC (stored 2 days under standard conditions), washed 2x in 0.9 % NaCl and diluted in HEPA at a final concentration of $8.89 \cdot 10^8$ RBC/L. The cells were treated in tube with the antioxidants or control SAGM. The AA-UA stock solution (26x) was prepared by solubilizing first AA in SAGM (at 3.0 mM) and then UA

(at 10.8 mM) in the AA-SAGM solution, 1/500 volume of 28 % NH₃ was added to favor UA dissolution. Immediately after supplementation of the antioxidants, 90 µL of sample were dispensed per well (80'000 RBCs/well) in a 96-well poly-L-ornithine coated imaging plate. The plate was placed in the DHM incubation chamber during 60 min and images were taken each 15 min. Finally, the RBCs were treated with 10 µL of diamide stock solution (10x) or control 0.9 % NaCl, *i.e.* 0, 1, 2 or 5 mM diamide final and again incubated at 37°C for timelapse analysis during 479 min (images acquisition each 15 min).

*Figure 19 – **Assessment of protection provided by the Ascorbic Acid plus Uric Acid (AA-UA) antioxidant pair against diamide oxidant using TSOX assay with digital holographic microscopy readout.** Timelapse analysis of morphological changes triggered by 0, 1, 2 or 5 mM diamide treatment and 113.7 µM AA plus 416.3 µM UA. [Top] Evolution of Average of the Optical Path Difference distribution (OPD avg) and confluency. [Bottom] Area Under the Curve (AUC) calculated from the OPD avg or confluency curves. Mean value for three wells ± standard deviation.*

The addition of the antioxidants did not changed the lag-time (onset of the reaction), at least with 5 mM diamide, but improved the resistance of the RBCs to the oxidant (retarded spherocytosis and hemolysis, Figure 19). The AUC calculated for both the OPD avg and confluency were significantly different between RBCs treated or not with antioxidants for the three concentrations of diamide. It must be emphasized that for the OPD avg, other analysis parameters such as the "Time to Max" or "Cross-control time" could have been more instructive, and that the "end-point" value would also have been interesting for analysis of the confluency.

*Figure 20 – **Antioxidant treatment (i.e. Ascorbic Acid plus Uric Acid [AA-UA]) reduces the morphological changes triggered by diamide.** Illustrative phase images acquired by digital holographic microscopy of red blood cells treated with 0, 1, 2 or 5 mM diamide and then without [top] or with 113.7 µM AA plus 416.3 µM UA [bottom] after 404 min of incubation. The images were taken during the timelapse analysis presented in Figure 19.*

When looking at the phase images (*e.g.* after 404 min of analysis), differences of morphology were visible between RBCs treated or not with the antioxidants (Figure 20). At this time, all control RBCs were already transformed into spherocytes while discocytes and echinocytes were still visible in the AA-UA sample under treatment with 2 mM diamide. With 5 mM diamide, all the RBCs already became spherocytes and began to lyse. Hemolysis occurred earlier and faster in the control *versus* AA-UA sample.

In a second experiment, the protective effect of the same pair of molecules, was evaluated when the oxidative stress was triggered by 10 mM AAPH. To do so, RBCs (RCC stored for three days) were prepared as before and treated in tube with different concentration of antioxidants, *i.e.* 0, 1, 2.5, 5, 7.5, 10, 25, 50, 75, 100 or 200 % AA-UA, the 100 % concentration corresponding to a treatment with 113.8 µM AA plus 415.1 µM UA (plasmatic levels). The RBCs were pre-incubated with the antioxidants during 60 min in the incubation chamber set at 37°C, 5 % CO_2 and high humidity, before treatment with 10 mM AAPH. In total, the RBCs were analyzed during 990 min.
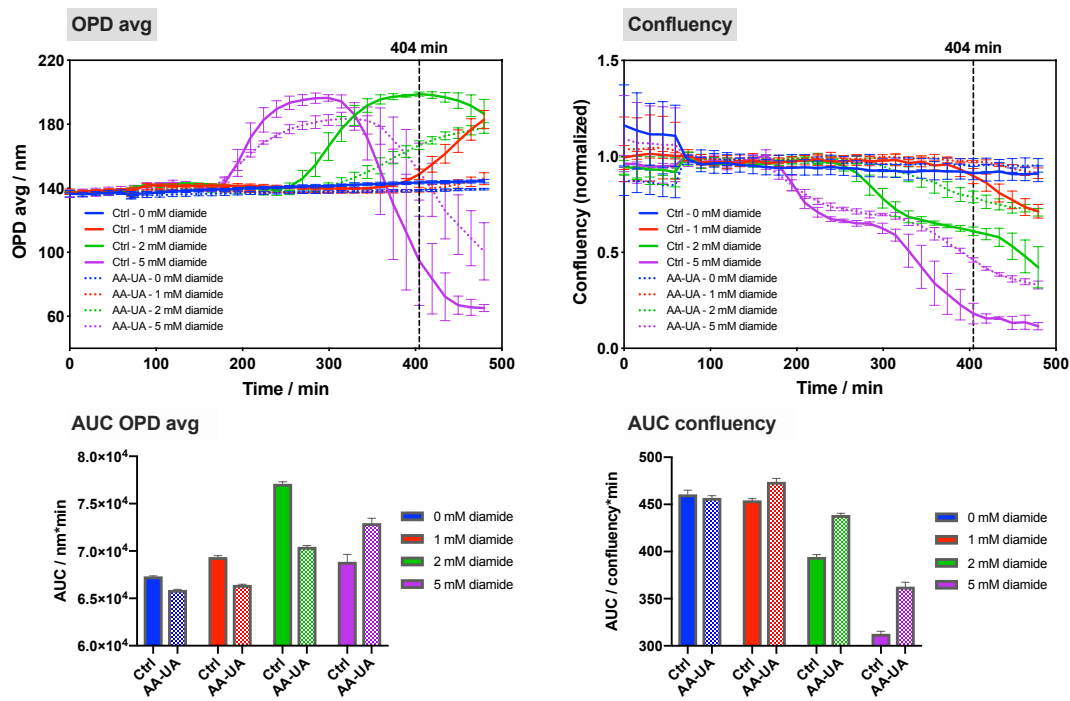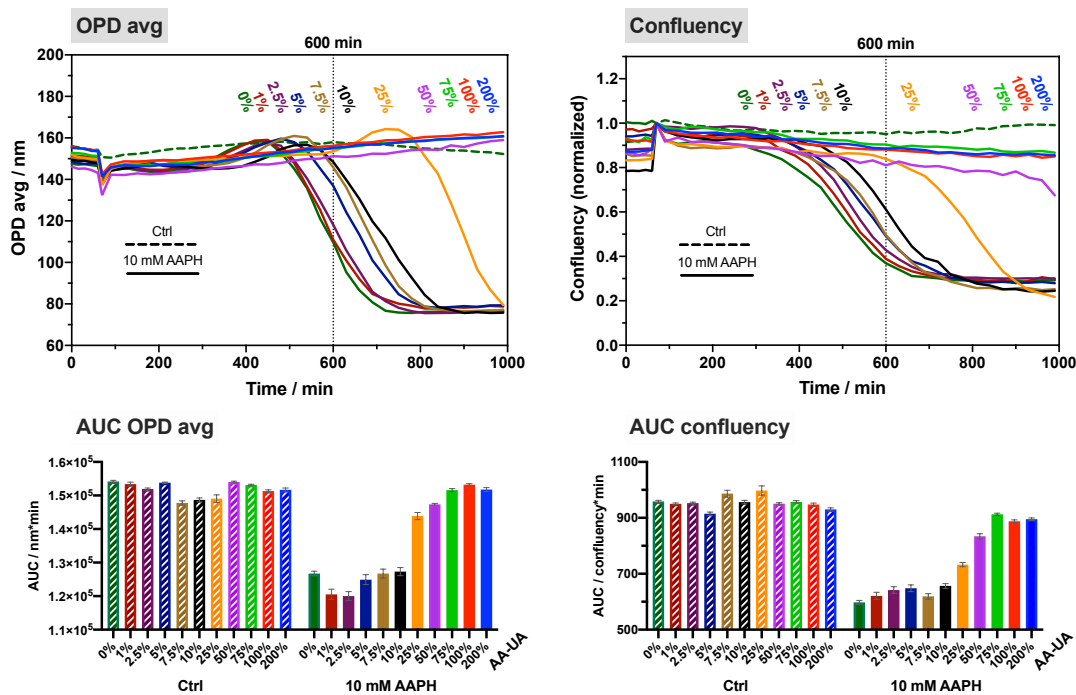
*Figure 21 – **Assessment of protection provided by the Ascorbic Acid plus Uric Acid (AA-UA) antioxidant pair against 2,2'-Azobis(2-amidinopropane) dihydrochloride (AAPH) oxidant using TSOX assay coupled to digital holographic microscopy readout.** Timelapse analysis of morphological changes triggered by 0 or 10 mM 2,2'-Azobis(2-amidinopropane) dihydrochloride (AAPH) treatment and 0, 1, 2.5, 5, 7.5 10, 75, 50, 100 or 200 % of AA-UA antioxidant pair (100 % corresponding to 113.8 µM AA plus 415.1 µM UA). [Top] Evolution of Average of the Optical Path Difference distribution (OPD avg) and confluency. [Bottom] Area Under the Curve (AUC) calculated from the OPD avg or confluency curves. Mean value for three wells ± standard deviation.*

Without antioxidants (*i.e.* 0 %), the morphology was rapidly affected by AAPH oxidation (Figure 21), whereas with antioxidants the drop of OPD avg and confluency was shifted to the right proportionally to the percentage added. Such effect was reflected by the AUC analysis parameter (baseline at 0 nm).

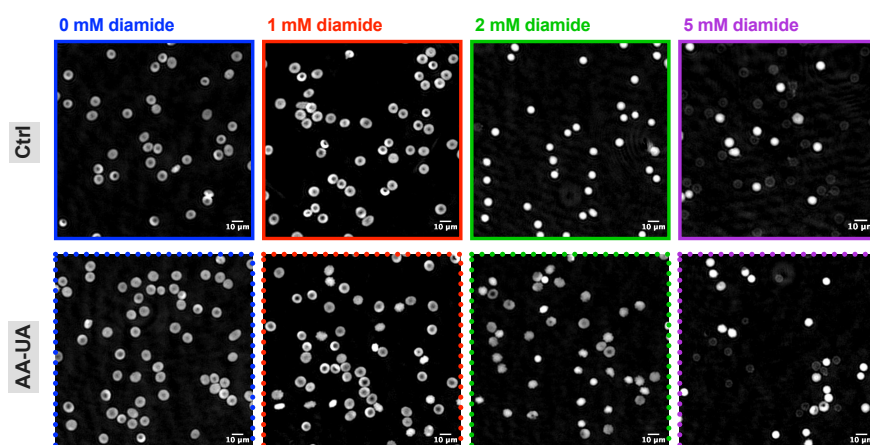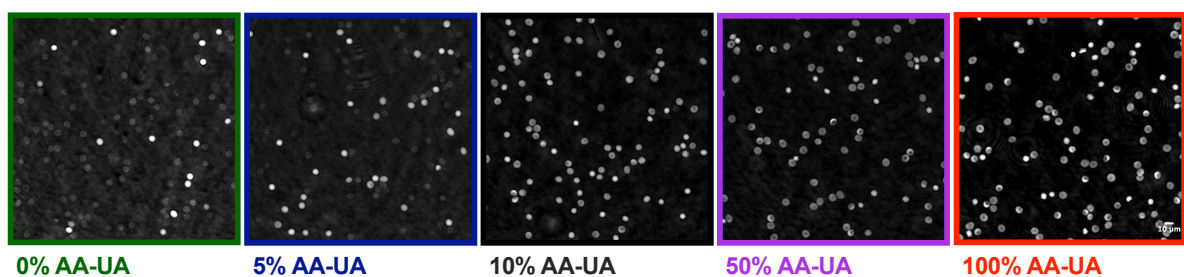*Figure 22 – **Antioxidant treatment (i.e. Ascorbic Acid plus Uric Acid [AA-UA]) reduces the morphological changes triggered by 2,2'-Azobis(2-amidinopropane) dihydrochloride (AAPH).** Illustrative phase images aquired by digital holographic microscopy of red blood cells treated with 10 mM AAPH and 0, 5, 10, 50 or 100 % of AA-UA antioxidant pair (100 % corresponding to 113.8 µM AA plus 415.1 µM UA) after 600 min of incubation. The images were taken during the timelapse analysis presented in Figure 21.*

The observation of the phase images confirmed that antioxidant treatment slowed down the effect of AAPH on RBC morphology (Figure 22). A 10 %-supplementation already partly preserved the RBCs and a 100 %-supplementation clearly preserved the cell morphology.

Various applications for the TSOX assay

More than only being a tool for HTS, the TSOX can be useful for a large panel of applications such as the monitoring of the oxidative lesions in the framework of RCC storage (see Chapter 3 Part 1.2). In the context of drug discovery, the TSOX could also be used in the primary screen to provide detailed information about a hit, such as its dose-response activity.

As an example, the suitability of the TSOX for determination of an EC_{50} was tested for AA antioxidant against 10 mM AAPH oxidant (arbitrarily fixed) using changes of morphology as readout. Samples were taken from 3 RCCs at day three of storage. The RBCs were prepared as usual for DHM analysis and were treated in tube with 0, 0.25, 0.5, 1, 2, 3, 5 or 7 mg/dL AA (which corresponds to 0, 14.2, 28.4, 56.8, 113.6, 170.5, 284.1 or 397.7 µM AA). Immediately after antioxidant addition, the cells were plated and incubated 60 min before addition of 10 mM AAPH or control 0.9 % NaCl. The evolution of morphology was followed during approximatively 19 hours (at 37°C and 5 % CO_2).
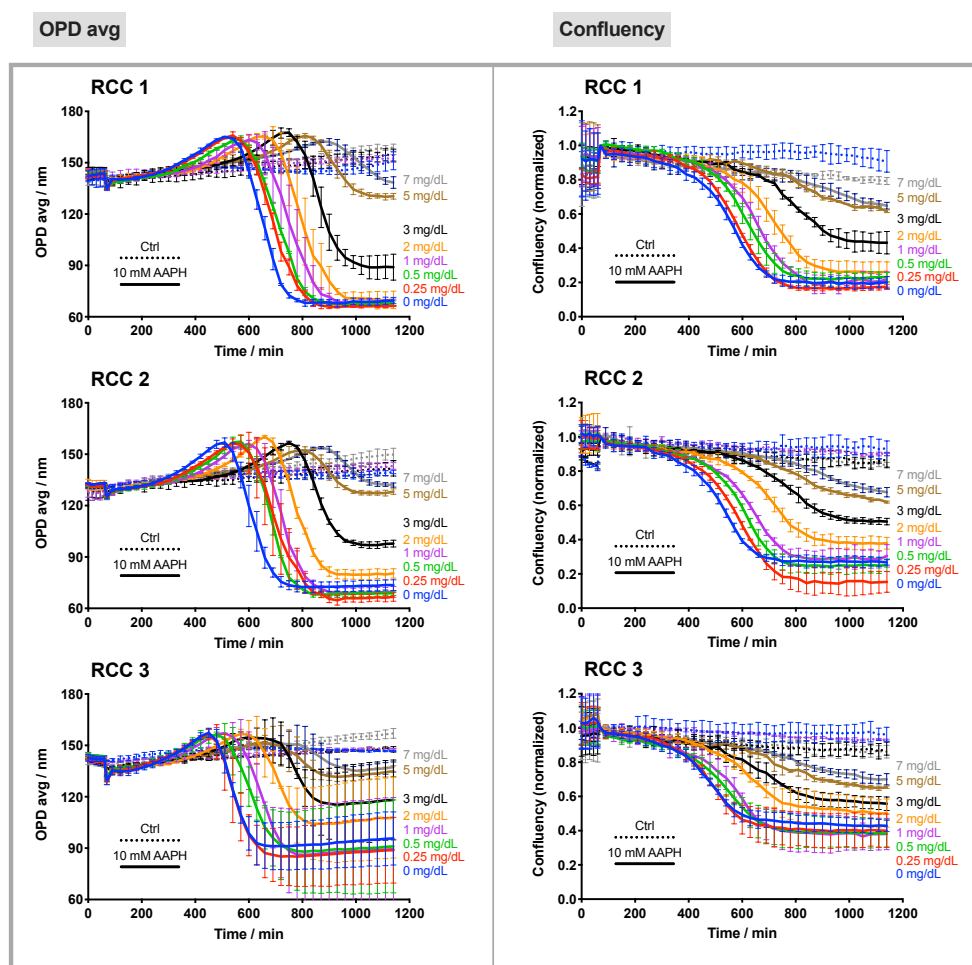
*Figure 23 – **Determination of dose-response activity of Ascorbic Acid (AA) antioxidant against 2,2'-Azobis(2-amidinopropane) dihydrochloride (AAPH) oxidant using TSOX assay coupled to digital holographic microscopy readout.** Timelapse analysis of morphological changes triggered by 0 or 10 mM AAPH and 0, 0.25, 0.5, 1, 2, 3, 5 or 7 mg/dL AA (which corresponds to 0, 14.2, 28.4, 56.8, 113.6, 170.5, 284.1 or 397.7 µM) in three Red Cell Concentrates (RCCs). Evolution of Average of the Optical Path Difference distribution (OPD avg, left) and confluency (right). Mean value for three wells $\pm$ standard deviation.*

Without AA (0 mg/dL AA), the RBCs began to lyse after 510 min for RCC 1 and 2 and after 450 min for RCC 3, all RBCs disappeared after 720 min for RCC 1 and 2 and 630 min for RCC 3 (Figure 23). As before, addition of an antioxidant modified the effect of AAPH. For the smallest concentrations, *i.e.* 0.25, 0.5, and 1 mg/dL, AA only delayed the reaction which could indicate that the antioxidant was exhausted before total elimination of the oxidant. Then, higher concentrations progressively prevented hemolysis (increase of end-point OPD avg and confluency values), suggesting that the protection level became sufficient to protect the RBCs upon complete degradation of all AAPH molecules.

Prism software was used to compute the AUC analysis parameter, and then to fit the dose-response curve in order to report the EC_{50} value, *i.e.* the antioxidant concentration that provides half-maximal protection (response halfway between the baseline and maximum values). The PRISM equation that was selected for fitting is defined as the "[Agonist] vs. response – Variable slope (four parameters) equation".
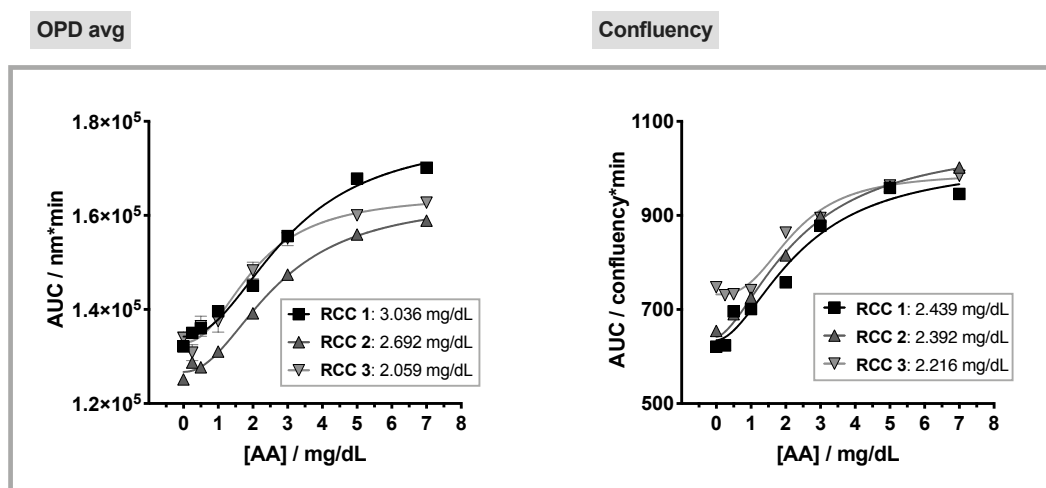
*Figure 24 – EC_{50} **values for Ascorbic Acid (AA) against 10 mM 2,2'-Azobis(2-amidinopropane) dihydrochloride (AAPH).** Fitted Area Under the Curve (AUC) values calculated from the Average of the Optical Path Difference distribution (OPD avg) or confluency curves presented in Figure 23. Mean value for three wells $\pm$ standard deviation. [In frame] Best-fit EC_{50} values for AA antioxidant against 10 mM AAPH oxidant for the three Red Cell Concentrates (RCCs).*

The AUC computed for both OPD avg and confluency parameters was plotted in Figure 24. The selected model fitted well the data with R^2 of 0.991, 0.995 and 0.989 for RCC 1, 2 and 3 AUC of OPD avg, and of 0.965, 0.991, 0.984 for the AUC of confluency of RCC 1, 2 and 3, respectively. Moreover, the fittings as well as the best-fit EC_{50} values were comparable for the three RCCs.

CONCLUSIONS AND PERSPECTIVES

The aim of this chapter was to show the process followed for the development of the test of sensitivity to oxidation, coined TSOX, that aim to become a tool to monitor and quantify the impact of oxidation on RBCs based on ROS quantification and morphology changes.

The three oxidants tested, namely H_2O_2, diamide and AAPH could be proposed for the TSOX assay using DCFH-DA fluorescent signal as an output, whereas for the DHM, only diamide and AAPH produced quantifiable changes of RBC morphology. The preliminary results suggested that H_2O_2 would not enable robust, reproductive and sensitive identification of hit molecules, necessary for an HTS-compatible assay. Higher concentrations of oxidant had to be used for the experiments with DHM compared to fluorescence. It is certainly because the label-free DHM imaging technique provides quantitative data about the phenotypic changes yielded by a compound and thus an indication of the consequences of a particular treatment, whereas DCFH-DA fluorescence enables straightforward quantification of the ROS generated.

The kinetic rates were close for both analysis technics and were in accordance with the mechanism of action of each oxidant. Hence, H_2O_2 that is by itself a physiologic ROS and a highly reactive species almost immediately produced its effect, leading to a sudden increase of fluorescence and OPD signals. For its part, a lag time was observed with diamide. It is probably because this thiol oxidant does not directly generate ROS but perturbs the cell redox balance by depleting glutathione. Diamide was also shown to induce structural changes of spectrin, a major constituent of the RBC cytoskeleton, and reduced its ability to bind protein 4.1[17], which could explain the major structural alterations observed. Finally, the AAPH known to degrade into peroxyl radicals at a constant rate, generated a linear increase of fluorescence and a progressive effect on RBC morphology.

Then, proof was given that potent antioxidants will indeed be detected by the TSOX and therefore that this assay is suitable for screening campaigns as well as robust enough the determination of dose-response curves as shown by the obtained data. Fluorescence analysis turned out to be a sensitive and convenient readout to have a quick glance at the antioxidant properties of molecules. Its major limitation was that it only provided a bulk picture of what happens at the level of the RBC population within the entire well. Moreover, it is a relatively "blind" method of analysis and is thus prone to be biased. For example, in an HTS including only fluorescence as readout, Trolox that triggers RBC lysis would have certainly be taken for a hit (false positive), as it reduces the fluorescence. With DHM, such side effect would have been more easily detected. It is the reason why, DHM is certainly a valuable throughput method. However, it has the disadvantage, similarly to other image-based methods to generate large amounts of data, and that the assessment of single-cell phenotype can necessitate a lot of time and resources (human and computer).

A multitude of assay designs and parameters for a broad range of applications

The design of the TSOX assay can be easily modulated to answer a particular question. Indeed, the different steps can be arranged and combined in multiple ways. Possible assay designs are presented in Figure 25.
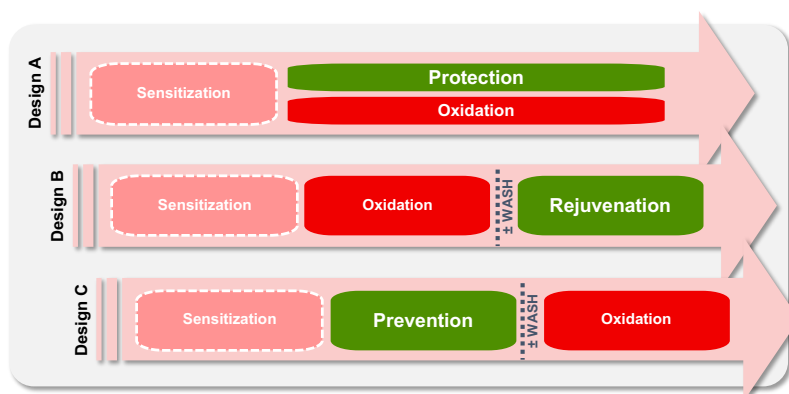
*Figure 25 – **Non-exhaustive presentation of the possible designs for the "TSOX" assay.***

The Design A can be used to test the protective role of the molecules. It is the most straightforward design for HTS as it simply consists in treating the cells and apply simultaneously the oxidative stress without washing the cells in between. The Design B can provide information about the rejuvenation properties of a compound. To do so, the RBCs are first exposed to the oxidants and then put in contact with the molecules to see if one of them could potentially rescue some reversible oxidative damages. A washing step can be added. However, such experimental design is hardly applicable for the HTS with RBCs as it is almost impossible to wash non adherent cells in multi-well plates. It will thus require performing the first treatment in tubes. Finally, the Design C can serve as determining the preventive role of the molecules. For that the RBCs are incubated with the compounds to test before the oxidation step. Again, a washing step can be included in between, with the same constraints. The molecules that give a positive result in such situation will be those that are incorporated within the cells and exhibit a direct antioxidant effect intracellularly or those that provide an indirect protection *via* the activation of the endogenous antioxidant system.

In addition to the various possible designs, each individual parameter of the TSOX assay can be modified and adjusted to best meet the needs. For example, rather than using a single oxidant, combination of multiple oxidants with distinct properties could be interesting to best mimic complex environments. Other types of oxidants with distinct mode of action could also be included such as the liposoluble cumene hydroperoxide (CumOOH) that targets preferentially the inner part of the membrane lipid bilayer and causes lipid peroxidation. Similarly, the 2,2'-azobis(2,4-dimethylvaleronitrile) (AMVN) is a lipophilic azo compound that generates at constant rate radical formation within the lipid environment. Even the readout can be optimized. Indeed, multiple detection

reagents are available to detect a large variety of ROS. For example, preliminary tests were conducted using the BODIPY[18] probe to sense lipid peroxidation induced by CumOOH (data not shown).

TSOX for high-throughput screening

After designing and optimization, the next step in the assay development workflow will be to validate statistically the assay by calculating for example the Z'-factor. This parameter is widely used in assay development to determine if the difference observed between positive and negative controls is large enough to guarantee the reliability, robustness and significance of an assay. This dimensionless value was proposed by Zhang *et al.* in 1999[19] is defined as (Equation 1):

$$Z' = 1 - \frac{(3\,SD_+ + 3\,SD_-)}{|Ave_+ - Ave_-|}$$ Equation 1

where SD_+ and SD_- and Ave_+ and Ave_- represent the standard deviations and averages for the positive and negative controls, respectively. The categorization of the assay is the following: if Z' is almost 1 the assay is ideal with a huge dynamic range and no standard deviation. When Z' is comprised between 0.5 and 1 the assay is good, and it is poor/marginal between 0 and 0.5. If the Z'=0, the assay only provides a yes or no answer. Below 0, the screening is not applicable, because the signals from the positive and negative controls are possibly overlapped.

Finally, the assay will have to be automatized, maybe miniaturized and again validate in final conditions. After that, a pilot screen can be launched. In the near future, it is planned to the TSOX to screen the library of natural products (NPs) extracts available at the biomolecular screening facility (BSF) of the Ecole Polytechique Fédérale de Lausanne (EPFL, Lausanne, Switzerland). This library provided by Analyticon - InterBioscreen contains 2'654 organic molecules purified from plants and bacteria.

In conclusion, the data presented in this Chapter showed that the TSOX is a promising tool to determine the antioxidant properties of various compounds and answer a broad range of questions using one or both readout methods, *i.e.* fluorescence and morphology analyses provide complementary information. Currently, final developments and validation for the TSOX assay are ongoing. It is also planned to use artificial intelligence (AI) in a close future for the automated on-line analysis of the phenotypic changes triggered by a treatment.

The roles of such assay are multiple. They can provide information for the development of additive solutions and other storage strategies in blood banking in order to improve RBC storage and transfusion medicine. Moreover, links between metabolic pathways and cell morphology can be investigated. The use of different TSOX designs and strategies will be useful to decipher the modes of action of toxic or protective molecules. In a close future, the use of the AI for the RBC morphology classification.

REFERENCES

1. Young IS, Woodside JV. Antioxidants in health and disease. *J. Clin. Pathol.* 2001;54(3):176–186.

2. Rota C, Chignell CF, Mason RP. Evidence for free radical formation during the oxidation of 2'-7'-dichlorofluorescin to the fluorescent dye 2'-7'-dichlorofluorescein by horseradish peroxidase: Possible implications for oxidative stress measurements. *Free Radic. Biol. Med.* 1999;27(7–8):873–881.

3. Shiva Shankar Reddy CS, Subramanyam MVV, Vani R, Asha Devi S. In vitro models of oxidative stress in rat erythrocytes: Effect of antioxidant supplements. *Toxicol. In Vitro*. 2007;21(8):1355–1364.

4. Werber J, Wang YJ, Milligan M, Li X, Ji JA. Analysis of 2,2'-azobis (2-amidinopropane) dihydrochloride degradation and hydrolysis in aqueous solutions. *J. Pharm. Sci.* 2011;100(8):3307–3315.

5. Niki E. Free radical initiators as source of water- or lipid-soluble peroxyl radicals. *Methods Enzymol.* 1990;186:100–108.

6. Wang H, Joseph JA. Quantifying cellular oxidative stress by dichlorofluorescein assay using microplate reader. *Free Radic. Biol. Med.* 1999;27(5–6):612–616.

7. Wolfe KL, Liu RH. Cellular Antioxidant Activity (CAA) Assay for Assessing Antioxidants, Foods, and Dietary Supplements. *J. Agric. Food Chem.* 2007;55(22):8896–8907.

8. Honzel D, Carter SG, Redman KA, et al. Comparison of chemical and cell-based antioxidant methods for evaluation of foods and natural products: generating multifaceted data by parallel testing using erythrocytes and polymorphonuclear cells. *J. Agric. Food Chem.* 2008;56(18):8319–8325.

9. Kühn J, Shaffer E, Mena J, et al. Label-Free Cytotoxicity Screening Assay by Digital Holographic Microscopy. *Assay Drug Dev. Technol.* 2013;11(2):101–107.

10. Rappaz B, Breton B, Shaffer E, Turcatti G. Digital Holographic Microscopy: A Quantitative Label-Free Microscopy Technique for Phenotypic Screening. *Comb. Chem. High Throughput Screen.* 2014;17(1):80–88.

11. Kellett ME, Greenspan P, Pegg RB. Modification of the cellular antioxidant activity (CAA) assay to study phenolic antioxidants in a Caco-2 cell line. *Food Chem.* 2018;244:359–363.

12. Eruslanov E, Kusmartsev S. Identification of ROS Using Oxidized DCFDA and Flow-Cytometry. *Methods Mol Biol.* 2010;57–72.

13. Bresolí-Obach R, Busto-Moner L, Muller C, Reina M, Nonell S. NanoDCFH-DA: A Silica-based Nanostructured Fluorogenic Probe for the Detection of Reactive Oxygen Species. *Photochem. Photobiol.* 2018;94(6):1143–1150.

14. Kim E, Winkler TE, Kitchen C, et al. Redox Probing for Chemical Information of Oxidative Stress. *Anal. Chem.* 2017;89(3):1583–1592.

15. Fan LM, Li J-M. Evaluation of methods of detecting cell reactive oxygen species production for drug screening and cell cycle studies. *J. Pharmacol. Toxicol. Methods*. 2014;70(1):40–47.

16. Gomes A, Fernandes E, Lima JLFC. Fluorescence probes used for detection of reactive oxygen species. *J. Biochem. Biophys. Methods*. 2005;65(2–3):45–80.

17. Becker PS, Cohen CM, Lux SE. The effect of mild diamide oxidation on the structure and function of human erythrocyte spectrin. *J. Biol. Chem.* 1986;261(10):4620–4628.

18. Makrigiorgos GM. Detection of lipid peroxidation on erythrocytes using the excimer-forming

property of a lipophilic BODIPY fluorescent dye. *J. Biochem. Biophys. Methods*. 1997;35(1):23–35.

19. Zhang JH, Chung TD, Oldenburg KR. A Simple Statistical Parameter for Use in Evaluation and Validation of High Throughput Screening Assays. *J. Biomol. Screen.* 1999;4(2):67–73.

CHAPTER 4

CONCLUSIONS &

PERSPECTIVES

CONTEXT

In Switzerland, blood and blood-derived products are regarded as drugs, and are thus under the control of Swissmedic, *i.e.* the Swiss agency for therapeutic products. Like any treatment, blood transfusion implies risks which must be minimized as much as possible using methods that are economically justified (*e.g.* in terms of Quality-Adjusted Life Year [QALY]).

Today, the risk *versus* benefit ratio of blood transfusion is still positive, and lives are saved everyday thanks to the latter. Recently, however, the scientific community raised the question of negative effects associated with the transfusion of long-term stored Red Cell Concentrates (RCCs)[1]. So far, no consensus has been reached on whether RCCs stored for a long period of time can be dangerous to transfused patients, and recent clinical trials are reassuring regarding standard practices[2,3]. It is clear, however, that the properties of Red Blood Cells (RBCs) within RCCs are changing over time[4–6]. In particular, their efficiency for oxygen perfusion and their circulation lifetime after transfusion are affected.

Changes that occur *ex vivo* are reversible, such as the metabolic reprogramming which likely begins right after (or even during) blood collection, and provides a starting point for the avalanche of lesions appearing afterward[7]. Lesions to the metabolism include the early loss of 2,3-Diphosphoglycerate (2,3-DPG), the accumulation of lactate, a drop in pH and an ion unbalance (K^+, Ca^{2+}, Fe^{3+}, etc.). Next, oxidative lesions which are often irreversible accumulate due to an increase in oxygen saturation within RCC units[8,9], and to reductions in antioxidant defenses (after removal of the plasma, which contains antioxidant molecules, and the loss of reduced Nicotinamide Adenine Dinucleotide Phosphate [NADPH], reduced Nicotinamide Adenine Dinucleotide [NADH], reduced Glutathione [GSH], and Uric Acid [UA] metabolites). Oxidative lesions appear at the level of proteins[10,11] (*e.g.* sulfenic acid and carbonylation[12,13]), triggering their degradation, dimerization (*e.g.* band 3), and delocalization to the membrane (*e.g.* Peroxiredoxin 2 [Prx 2][14] or denatured hemoglobin [Hb])[15]. Lipids are also progressively oxidized. Finally, the cell phenotype and functions are affected: aged RBCs present senescence markers such as phosphatidylserine, which release microvesicles (MVs)[16,17] and change their shape (from stomatocytes/discocytes to echinocytes, and finally spherocytes)[18,19]. Such markers lead to a reduction in RBC deformability[20], and finally to hemolysis. Once transfused, irreversible lesions affecting RBCs make them more likely to be removed from circulation in transfused recipients, while reversible lesions delay the efficiency of transfused RBCs.

The above changes can be attributed in part to the donor itself, in part to blood collection and processing, which are likely causes of cellular stress (mechanical constraints, temperature variations, anticoagulant addition, etc.), and mostly to storage conditions themselves, which are not

physiological: lower temperature, surrounding plastic bag, static conditions, closed environment allowing only gas exchanges, and the adapted, though still non-physiological, additive solution.

In this context, the aim of this thesis was to optimize the quality of RBCs for transfusion by modifying the additive solution.

SUMMARY OF RESULTS

Chapter 1: "Changes in the red blood cells during storage"

The purpose of the experiments presented in the first chapter was to qualify and quantify storage lesions (metabolic, oxidative and morphological). To this aim, five RCCs stored at 4°C in Citrate-Phosphate-Dextrose and Saline-Adenine-Glucose-Mannitol (CDP-SAGM) were followed for 71 days. Weekly analyses demonstrated the accumulation of various types of lesions at different chemical and cellular levels. Overall, the RBCs stored within RCCs showed a linear increase in Mean Corpuscular Volume (MCV) and anisocytosis (SD-RDW). Early during storage, the main changes that were observed concerned the Antioxidant Power (AOP) and the intracellular concentration of reduced Glutathione (GSH), which increased in the 10 days, only to decrease afterwards. After four weeks, significant irreversible lesions were observed, while lactate levels were seen to saturate to a maximum. From week 5, discocytes were progressively replaced by transient echinocytes, and ultimately spherocytes. In addition, the steady increase in the percentage of hemolysis and the number of generated MVs became exponential. After six weeks of storage (expiration date), the ratio of GSH to oxidized Glutathione (GSSG) was down by 25.3 %, reflecting the increase in levels of oxidative stress. Finally, at week 8 of storage, glucose consumption stopped, and at the end of the follow-up, the only remaining discocytes had lost 10 % of their dynamic membrane fluctuations. Interestingly, the severity of changes differed among donors, in line with previous studies[21,22].

In the second part of Chapter 1, the focus was on the impact of the membrane protein phosphorylations on RBC morphology. Specifically, the targets and effects of Tyrosine-phosphorylations (pY) were investigated using an inhibitor of Protein Tyrosine Phosphatases (PTP), *i.e.* sodium Orthovanadate (OV). The Western Blot (WB) analysis of the pY showed that the capacity for phosphorylation was gradually lost during storage, due to the depletion of Adenosine Triphosphate (ATP). The rejuvenation replenishing the cellular ATP was shown to restore pY levels. Then, phosphoproteomic analysis revealed the presence of 7'764 phosphosites (609 phosphoproteins), of which 40 pY sites belonging to 21 different proteins were upregulated upon OV treatment. The first 20 upregulated pY sites belong mostly to proteins involved in cell structure, *i.e.* band 3, α- and β- spectrin, α- and β- adducin, protein 4.1, ankyrin-1, dematin, tensin-1, and flotillin-2. Finally, Digital Holographic Microscopy (DHM) experiments showed that OV treatments induced

the formation of spherocytes via transient echinocytes. In the near future, the plan is to use specific Kinase Inhibitors (KIs) to further decipher the reactions controlling phosphorylation.

Chapter 2: "Evolution of the antioxidant power in red cell concentrates during storage"

In Chapter 2, six RCCs were prepared in CPD-SAGM additive solution, and followed for 43 days. The AOP was quantified electrochemically using disposable electrode strips, and compared with results obtained from a colorimetric assay. With both methods, the AOP reached a maximum after one week of storage prior to decaying and reaching a plateau. Variations in AOP were correlated to the extracellular UA levels. This major antioxidant found in plasma (120 to 450 µM) seems to be progressively exported from RBCs due to the their changing environment (due to the dilution of the residual plasma, among others). The AOP behavior could therefore reflect the changes in metabolism activity triggered by the preparation and storage of the blood product. Particularly noteworthy is the link between AOP and UA levels and the sex of donors: the AOP was generally lower (approximatively 30 %) in RCCs donated by women than by men.

Chapter 3: "Modification of the additive solution formulations to reduce red blood cell storage lesions"

The experiments presented in Chapter 3 explored possible modifications of the additive solution formulation *per se*, to improve RBC storage.

The first strategy consisted in restoring physiological levels of UA in RCCs to reduce its export from the cells, as the loss of intracellular UA can: 1) trigger a metabolic shift, and 2) reduce the intracellular antioxidant pool. Four CPD-SAGM RCCs were split into two subunits, supplemented at day 1 either with UA (380 and 320 µM for donations from men and women, respectively), or with SAGM only for the control, and followed for 42 days (with an additional time point at day 70). The first results showed only small differences between treated and untreated units, possibly because of the conditional pro-oxidant effect of urate. The concentration of supplements was perhaps also too low to be efficient.

Next, Ascorbic Acid (AA, 110 µM) was supplemented in addition to UA (420 µM) to prevent its pro-oxidant side effect. Again, no significant improvement was observed across the majority of storage markers (pH, hemolysis, morphology, or deformability). Nevertheless, the RBC metabolism was particularly modified by such storage conditions: quantitative metabolomic analysis of targeted intracellular metabolites demonstrated that the treatment had a positive impact on RBCs, leading in particular to a better maintenance of glycolysis and GSH syntheses.

Finally, preliminary tests of addition of protective molecules against oxidative stress (ascorbic acid, N-Acetylcysteine [NAC], glutamine, Hydroxyurea [HU], α-lipoic acid, acetyl-L-carnitine, and α-tocopherol) were not conclusive.

The fact that none of the above treatments led to positive results at the cellular level (mainly hemolysis and morphology) raised the following questions: first, are the standard markers for aging sensitive enough and/or are they the most appropriate? Could the standard analytical methods somehow distort the results? For example, the preparation of RBC samples for imaging includes a washing step, the resuspension in HEPA buffer (composition described in ANNEX-1), and the plating of the RBCs in a multiwell plate coated with poly-L-ornithine (ANNEX-2). Each of these steps could introduce variability in the results. In addition, one could wonder if tested molecules are inefficient or not efficient enough? This not only calls into question the selection of compounds, but also the amount that was supplemented. Metabolomic analysis showed significant differences in this regard, potentially emphasizing the importance of dosage. Finally, one should think about the experimental approach. For example, what is the impact of a pool-and-split method? What is the effect of the temperature on the mechanism of action of a particular compound in terms of activity and uptake?

Together, the above questions highlight the need to develop tools to predict more easily and rapidly (faster than with a whole follow-up) if a given compound meets important requirements to efficiently protect RBCs.

Chapter 4: "Development of the TSOX assay, *i.e.* Test of Sensitivity to Oxidation"

The goal of the project presented in the last chapter was to develop a test compatible with High-Throughput Screening (HTS), making it possible to evaluate simply and quickly the antioxidant properties of a wide variety of compounds. The assay that was developed was named TSOX for "Test of Sensitivity to Oxidation". It consists in treating RBCs with different compounds that have potentially protective effects (direct, indirect, or both), and to expose them to oxidative stress. Two readout methods were proposed: first, a fluorescent one, where a 2,7-Dichlorofluorescin Diacetate (DCFH-DA) fluorescent probe (a reporter of intracellular Reactive Oxygen Species (ROS) generation) was used, and second, DHM, allowing us to measure the effects of specific treatments on the RBC morphology.

The initial phase of development consisted in treating RBCs with various concentrations of different oxidants (hydrogen peroxide [H_2O_2], diamide and 2,2'-Azobis(2-methylpropionamidine) dihydrochloride [AAPH]), to generate various kinds of stress. Each oxidant triggered a specific behavior that was shown to be dose-dependent. Then, the TSOX was challenged with known antioxidants such as AA, vitamin E, resveratrol and UA. Few adjustments are required before adding the screening assay to the library of Natural Products (NPs) extracts available at the Biomolecular

Screening Facility (BSF) of the Ecole Polytechique Fédérale de Lausanne (EPFL, Lausanne, Switzerland). This library provided by Analyticon – InterBioscreen contains 2'654 organic molecules purified from plants and bacteria. Finally, lead molecules could be supplemented in RCC bags.

CONCLUSIONS & PERSPECTIVES

The RBCs accumulate lesions during storage, which can impact their *in vivo* recovery and, hence, reduce the efficiency of transfusions. As these lesions appear through a succession of events, it seems suitable to reconsider storage conditions at an early stage. In this thesis, modifications of the additive solution formulation were proposed, providing a cost-effective strategy.

The primary goal was not to increase the storage duration. Indeed, a study regarding this aspect conducted at the Centre Hospitalier Universitaire Vaudois (CHUV, Lausanne, Switzerland, 31'352 RCCs between 2011 and 2012, Figure 1A) showed that the majority of RCCs are used around the second week of storage, following the first-in-first-out principle (Figure 1B). When looking more carefully at the repartition of blood groups, however, it appears that more common blood groups (O Rhesus + and A Rhesus +) are transfused earlier during storage, while less frequent ones (AB, B and Rhesus -) are mostly transfused with old RCCs (Figure 1C). For example, at the CHUV, 56.6 % of the AB Rhesus + RCCs are transfused after 35 days of storage.
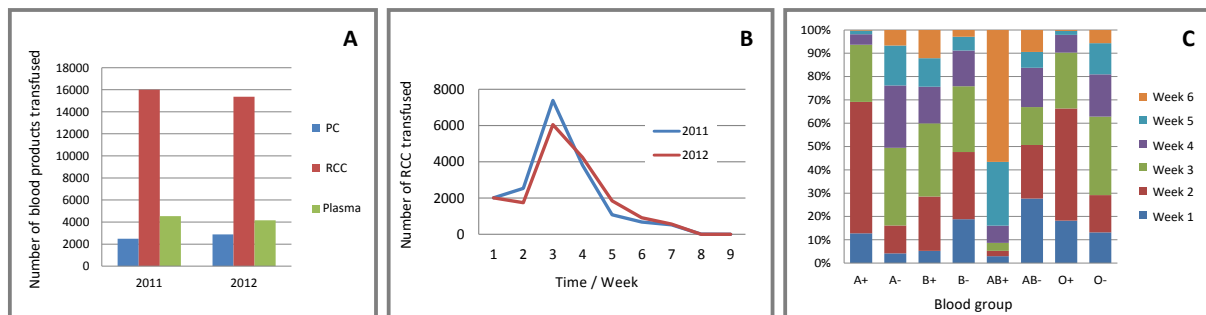
*Figure 1 – **Blood transfusion at the Centre Hospitalier Universitaire Vaudois** (CHUV, Lausanne, Switzerland). [A] Number of labile blood products, i.e. Platelets Concentrates (PCs), Red Cell Concentrates (RCCs) and plasma units transfused in 2011 and 2012 at the CHUV (more than 15'000 products each year). [B] Storage duration of transfused RCCs. [C] Percentage of transfused RCCs, for different donor's blood groups and storage times. Adapted from the Medicine Master thesis of Marine Gossin, 2016.*

Improving the quality of storage is thus a more important goal, to provide a better product to more patients, and limit as much as possible adverse effects of storage lesions.

Understand to improve

The approach followed throughout this thesis was to observe and understand in more detail what happens to RBCs stored within RCCs, and to propose suitable corrective strategies. Accordingly, the supplementation of UA was based on the observation that the depletion of extracellular UA levels

after plasma removal triggers a metabolic remodeling, potentially reducing intracellular antioxidant defenses. The observation that none of the added antioxidant molecules protect RBCs efficiently led us to propose the TSOX assay as a practical means to determine whether a molecule is indeed protective. This test was intended to provide a rational tool for making decisions regarding possible modifications of the additive solution formulation, instead of conducting trials which often consume a lot of time and resources. Its versatility offers a wide range of possibilities to understand the mechanisms of action of a specific molecule. For example, one could imagine to test the effects of different compounds at various concentrations, temperatures, and oxygen levels. It would even be possible to use the TSOX assay to mimic a transfusion, *e.g.* by incubating the RBCs in plasma at 37°C in a controlled atmosphere.

The data presented in this thesis provides novel information about the *ex vivo* aging of RBCs, and a better understanding thereof. New functions and behaviors were observed, such as the reported phosphorylation events and AOP evolution. Furthermore, metabolomic approaches have highlighted the influence of metabolite uptakes, opening up new avenues for investigation of metabolite fluxes and regulations within the purine salvage pathways and the PPP. More broadly, the results presented in this thesis contribute to our general knowledge of RBCs.

Predicting the aging of red blood cells and the post-transfusion recovery: still looking for a gold standard

Today, the perfect marker to predict post-transfusion recovery of transfused RBCs is still missing, even though metabolites such as hypoxanthine have been shown to be correlated with post-transfusion recovery (mainly in mouse models[23]). It is currently impossible to say with a sufficient level of confidence whether RBCs in blood bags will fulfil their task of oxygenation efficiently after transfusion, and, hence, there is currently no way of knowing whether such blood products are useful. Tomorrow's research and innovation will surely help fill this gap.

Existing examples are omic approaches, *i.e.* lipidomics, proteomics and metabolomics, which are used broadly around the world today. One of our collaborators, Professor Jolicoeur from Polytechnique Montréal (Canada), is developing an *in silico* model of the RBC metabolism to predict the evolution thereof as a function of the initial conditions and, hence, to predict the effects of a particular treatment. Such tools are of particular interest to boost research on RBCs, and, more generally, on blood cells and blood products.

Rheological properties may be the best way to predict the efficiency of RBCs after transfusion. Microfluidics devices (such as the MVA devices developed by Hemanext) enabling to measure the cell deformability are particularly promising. Such approaches could both serve as a

research tool and a quality control assay, whereas applications to bedside use will require improvements in terms of ease of use and suitability to the needs of patients.

Last but not least, donor characteristics themselves influence the storage[24–27]: their level of antioxidant, saturation of oxygen, and hormones are a few parameters involved in RBC aging. A better characterization of these parameters and a deeper understanding of the link between storage and donors are also important to properly process and store collected blood.

LAST WORDS

In conclusion, the future of transfusion is full of challenges, but also of promises. There is still room for improvements, emphasizing the essential role of research and innovation.

This PhD thesis was conducted at Transfusion Interrégionale CRS SA (TIR), who provides labile blood products for the regions of Bern, Vaud and Valais in Switzerland. The company slogan is "Be together for the donors and the patients". In this context, the mission of the R&D laboratory of Epalinges is to study the *ex vivo* journey of blood components (mainly plasma, platelets and RBCs) from donors to patients, to deliver the best products to the latter. It is this leitmotiv which motivated me to choose this research project, and guides my work every day.
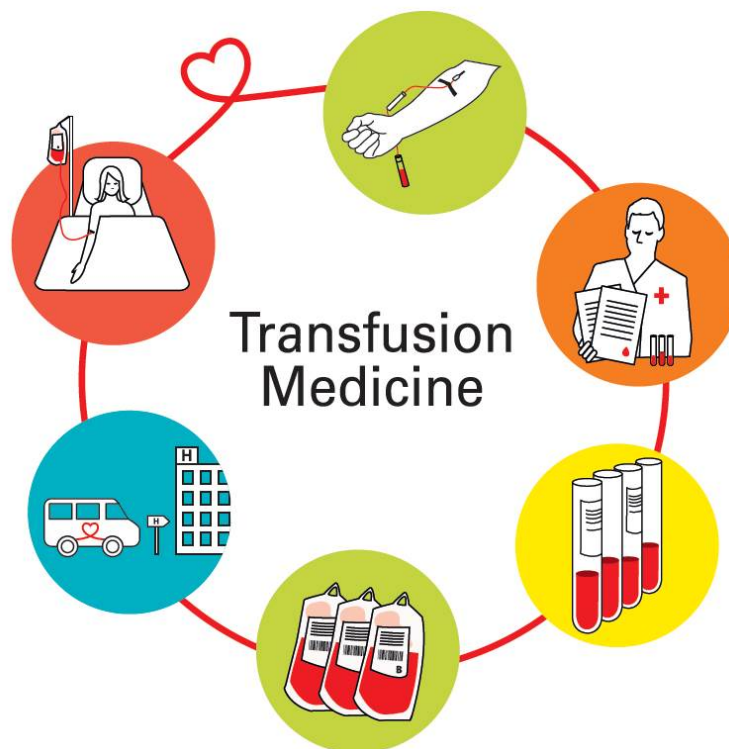
REFERENCES

1.   Tissot J-D, Bardyn M, Sonego G, Abonnenc M, Prudent M. The storage lesions: From past to future. *Transfus. Clin. Biol.* 2017;24(3):277-284.

2.   Prudent M, Tissot J-D, Lion N. In vitro assays and clinical trials in red blood cell aging: Lost in translation. *Transfus. Apher. Sci.* 2015;52(3):270–276.

3.   Prudent M, Tissot J-D, Lion N. The 3-phase evolution of stored red blood cells and the clinical trials: an obvious relationship. *Blood Transfus.* 2017;15(2):188–188.

4.   D'Alessandro A, Kriebardis AG, Rinalducci S, et al. An update on red blood cell storage lesions, as gleaned through biochemistry and omics technologies. *Transfusion.* 2015;55(1):205–219.

5.   Bardyn M, Rappaz B, Jaferzadeh K, et al. Red blood cells ageing markers: a multi-parametric analysis. *Blood Transfus.* 2017;15(3):239–248.

6.   Yoshida T, Prudent M, D'Alessandro A. Red blood cell storage lesion: causes and potential clinical consequences. *Blood Transfus*. 2019;17(1):27–52.

7.   Bordbar A, Johansson PI, Paglia G, et al. Identified metabolic signature for assessing red blood cell unit quality is associated with endothelial damage markers and clinical outcomes. *Transfusion*. 2016;56(4)852-62.

8.   Bardyn M, Tissot J-D and Prudent M. Oxidative stress and antioxidant defenses during blood processing and storage of erythrocyte concentrates. *Transfus. Clin. Biol.* 2018;25(1):96–100.

9.   Yoshida T, Blair A, D'alessandro A, et al. Enhancing uniformity and overall quality of red cell concentrate with anaerobic storage. *Blood Transfus.* 2017;15(2):172–181.

10. Kriebardis AG, Antonelou MH, Stamoulis KE, et al. Progressive oxidation of cytoskeletal proteins and accumulation of denatured hemoglobin in stored red cells. *J. Cell. Mol. Med.* 2007;11(1):148–155.

11. Kriebardis AG, Antonelou MH, Stamoulis KE, et al. Membrane protein carbonylation in non-leukodepleted CPDA-preserved red blood cells. *Blood Cells. Mol. Dis.* 2006;36(2):279–282.

12. Delobel J, Prudent M, Tissot J-D, Lion N. Proteomics of the red blood cell carbonylome during blood banking of erythrocyte concentrates. *Proteomics Clin. Appl.* 2016;10(3):257–266.

13. Delobel J, Prudent M, Crettaz D, et al. Cysteine redox proteomics of the hemoglobin-depleted cytosolic fraction of stored red blood cells. *Proteomics Clin. Appl.* 2016;10(8):883–893.

14. Rinalducci S, D'Amici GM, Blasi B, et al. Peroxiredoxin-2 as a candidate biomarker to test oxidative stress levels of stored red blood cells under blood bank conditions. *Transfusion.* 2011;51(7):1439–1449.

15. Delobel J, Prudent M, Rubin O, et al. Subcellular fractionation of stored red blood cells reveals a compartment-based protein carbonylation evolution. *J. Proteomics.* 2012;76:181–193.

16. Rubin O, Crettaz D, Canellini G, Tissot J-D, Lion N. Microparticles in stored red blood cells: an approach using flow cytometry and proteomic tools. *Vox Sang.* 2008;95(4):288–297.

17. Kriebardis A, Antonelou M, Stamoulis K, Papassideri I. Cell-derived microparticles in stored blood products: innocent-bystanders or effective mediators of post-transfusion reactions? *Blood Transfus.* 2012;10(Suppl 2):s25–s38.

18. Blasi B, D'Alessandro A, Ramundo N, Zolla L. Red blood cell storage and cell morphology.

Transfus. Med. 2012;22(2):90–96.

19. Roussel C, Dussiot M, Marin M, et al. Spherocytic shift of red blood cells during storage provides a quantitative whole cell-based marker of the storage lesion. *Transfusion.* 2017;57(4):1007–1018.

20. Berezina TL, Zaets SB, Morgan C, et al. Influence of Storage on Red Blood Cell Rheological Properties*. J. Surg. Res.* 2002;102(1):6–12.

21. Tzounakas VL, Kriebardis AG, Papassideri IS, Antonelou MH. Donor-variation effect on red blood cell storage lesion: A close relationship emerges. *Proteomics Clin. Appl.* 2016;10(8):791–804.

22. Tzounakas VL, Georgatzakou HT, Kriebardis AG, et al. Donor variation effect on red blood cell storage lesion: a multivariable, yet consistent, story. *Transfusion.* 2016;56(6):1274–1286.

23. Nemkov T, Sun K, Reisz JA, et al. Hypoxia modulates the purine salvage pathway and decreases red blood cell and supernatant levels of hypoxanthine during refrigerated storage. *Haematologica.* 2018;103(2):361–372.

24. Reisz JA, Tzounakas VL, Nemkov T, et al. Metabolic Linkage and Correlations to Storage Capacity in Erythrocytes from Glucose 6-Phosphate Dehydrogenase-Deficient Donors. *Front. Med.* 2017;4:248.

25. Kanias T, Lanteri MC, Page GP, et al. Ethnicity, sex, and age are determinants of red blood cell storage and stress hemolysis: results of the REDS-III RBC-Omics study. *Blood Adv.* 2017;1(15):1132–1141.

26. Tzounakas VL, Kriebardis AG, Georgatzakou HT, et al. Glucose 6-phosphate dehydrogenase deficient subjects may be better "storers" than donors of red blood cells. *Free Radic. Biol. Med.* 2016;96:152–165.

27. Chassé M, McIntyre L, English SW, et al. Effect of Blood Donor Characteristics on Transfusion Outcomes: A Systematic Review and Meta-Analysis. *Transfus. Med. Rev.* 2016;30(2):69–80.

CONCLUSIONS & PERSPECTIVES

ANNEXES

ANNEX-1: COMPOSITION OF HEPA AND HEPA_{NOCALCIUM} BUFFER

Table 1 – Composition of HEPA and HEPA_{noCalcium} buffers.

Compound	[mM]	g / 1 L	g / 500 mL	MW / g / mol
NaCl	130	7.597	3.799	58.44
KCl	5.4	0.403	0.201	74.55
CaCl$_2$*2H$_2$O	1	0.147	0.074	147.02
MgCl$_2$*6H$_2$O	0.5	0.102	0.051	203.3
Glucose	10	1.800	0.900	180
Hepes	15	3.575	1.787	238.31
BSA	1 mg/mL	1	0.500	

In grey: compound not added in the HEPA_{noCalcium} buffer.

Adjust pH at 7.4 with HCl or NaOH. Filtrate at 0.22 μm and store at 4°C. Theoretical osmolarity is approximatively 298 mOsm. Chemicals came from MSD Merk Sharp & Dohme and Sigma-Aldrich.

ANNEX-2: COATING OF IMAGING PLATE WITH POLY-L-ORNITHINE

The poly-L-ornithine (Sigma-Aldrich, P3655) is prepared in deionized water (dH$_2$O) at 100 mg/L and filtrated. Then the wells of the 96-well multiplate are field with 100 μL of this solution using a MultiDrop dispenser (ThermoFisher Scientific) and incubated at 37°C during 3 to 4 hours. After that, the plate is washed (3x) with dH$_2$O using a washer (Biotek EL405). Finally the plate is tapped onto an absorbing paper to remove as much water as possible and is finally placed under a laminar flow hood until being completely dry. They can then be stored at 4°C during at least 2 weeks.
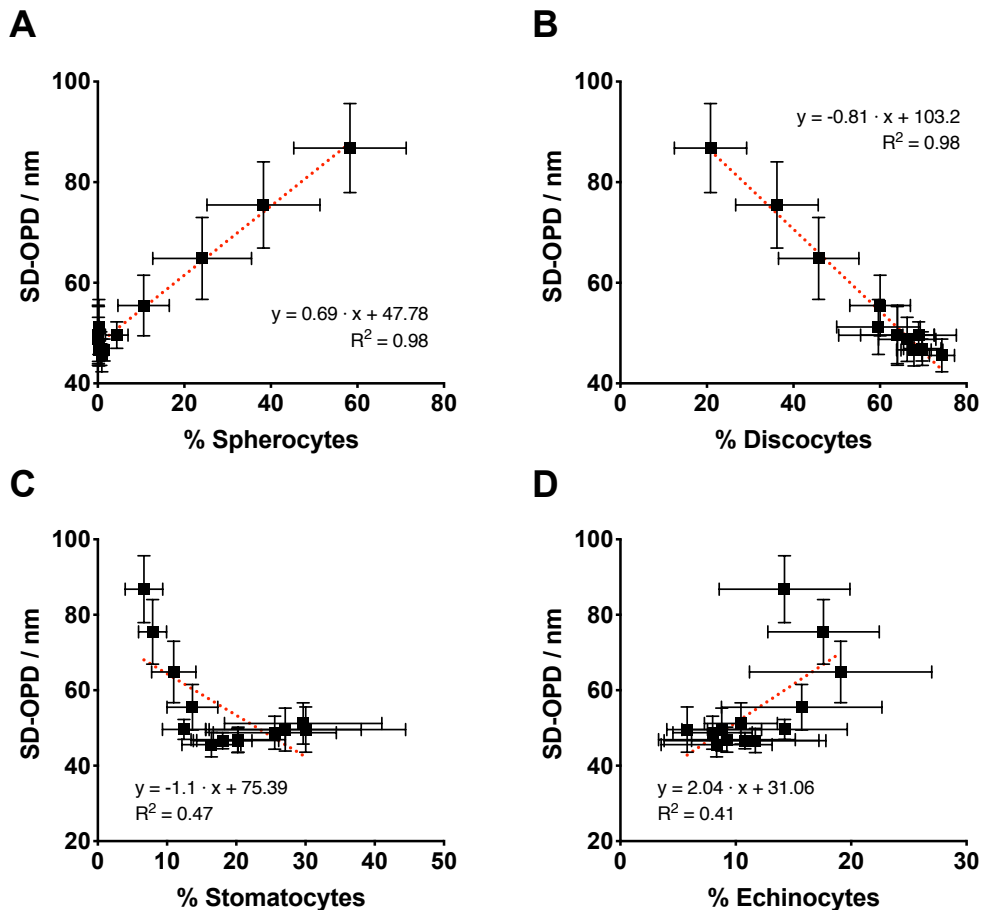
*Figure 1 – **Single-cell versus population analysis.** Correlation between the percentage of [A] spherocytes, [B] discocytes, [C] stomatocytes and [D] echinocytes (from CellProfiler) and the Standard Deviation of Optical Path Difference (SD-OPD) value. Mean values for five Red Cell Concentrates (RCCs) are presented ± Standard Deviation (SD). The equation of linear correlation curve (dotted line) and regression coefficient R^2 are specified.*

The analysis of correlation between Red Blood Cell (RBC) morphology (based on the results obtained with CellProfiler and CellProfiler Analyst) and the Digital Holographic Microscopy (DHM) quantitative value demonstrated that the Standard Deviation of Optical Path Difference (SD-OPD) was linearly correlated (from day 15 of storage) to the percentage of spherocytes (positively, $R^2 = 0.98$) and discocytes (negatively, $R^2 = 0.98$) in the sample, but not to the percentage of stomatocytes and echinocytes (Figure 1). The data come from the study presented in Chapter 1, Part 1. DHM images of RBCs were acquired weekly during 71 days at a 20x magnification.

ANNEX-4: DETAILS ON CELL MEMBRANE FLUCTUATIONS MEASUREMENTS

Fluctuations rate can be measured using Equation 1.

$$Var\big(\varphi_{cell} + \varphi_{background}\big) = Var(\varphi_{cell}) + Var\big(\varphi_{background}\big) + 2Cov\big(\varphi_{cell} + \varphi_{background}\big) \qquad \textit{Equation 1}$$

The temporal deviation of each pixel at position $(i,j)^{th}$ can be measured using Equation 2:

$$std(\varphi_{cell})_{(i,j)} = \sqrt{(std(\varphi_{cell} + \varphi_{background})_{(i,j)})^2 - (std(\varphi_{background}))^2} \qquad \textit{Equation 2}$$

Eventually, the Cell Membrane Fluctuations (CMFs) is measured with Equation 3:

$$\mathrm{CMF_{OPD}(nm)}_{(i,j)} = \mathrm{std}(\varphi_{cell})_{(i,j)} \qquad \textit{Equation 3}$$

In which $Var(\varphi_{cell})$ and $Var\big(\varphi_{background}\big)$ are the temporal variance in Optical Path Difference (OPD) corresponding to the CMFs and to the background fluctuations, respectively, and $Cov(\varphi_{cell}, \varphi_{background})$ is the covariance of the two variables. Assuming that the two variables are independent, $Cov\big(\varphi_{cell}, \varphi_{background}\big) = 0$. All the simulations were implemented in Matlab 2015.

ANNEX-5: PREPARATION OF SODIUM ORTHOVANADATE SOLUTION

Solution of 100 mM Sodium Orthovanadate (OV, Sigma-Aldrich, S6508) is prepared in dH_2O. The pH is set to 9.0 which makes the solution turn yellow. The solution is boiled until colorless and cooled at Room Temperature (RT). The pH was set again to 9.0 and the solution was boiled again. The cycle was repeated a few times. Such procedure accelerates the depolymerization of the decavanadate into monovanadate. Stock solution was aliquoted and stored at -28°C.

ANNEX-6: RESULTS OF THE PHOSPHOPROTEOMICS ANALYSIS.

On next two pages: list of the Tyrosine-phosphorylated (pY) after 1 hour of treatment with 2 mM OV.

Upregulated (part 1)

Protein names	Uniprot Identifier	Log P value	Difference	Position	Phospho..STY..Probabilities	PEP
Band 3	P02730	26.64	8.17	359	YQSSPAKPDSSFY(1)K	7.48E-277
Band 3	P02730	19.42	11.35	904	DEY(1)DEVAMPV	1.05E-82
Alpha-spectrin	P02549	18.82	7.86	610	LADDEDY(1)KDIQNLKSR	0
Beta-adducin	P35612	18.54	7.47	31	FSEDDPEY(1)MR	2.47E-59
Protein 4.1	P11171;Q4VB86	18.47	8.64	660;418	LDGENIY(1)IRHS(1)NLMLEDLDK	5.31E-268
Protein 4.1 *	P11171;Q4VB86	16.99	5.68	660;418	LDGENIY(1)IRHS(1)NLMLEDLDK	5.31E-268
Beta-spectrin	P11277	13.48	7.28	16	T(0.333)S(0.333)AT(0.333)EFENVGNQPPY(0.888)S(0.111)R	0
Ankyrin-1	H0YBS0;P16157	12.86	5.15	708;1386	Y(0.914)S(0.086)ILSESTPGSLSGTEQAEMK	5.20E-172
Lck-interacting transmembrane adapter 1	A0A087WUJ1	12.24	5.23	227	GQGAILALAGDLAY(1)QTLPLR	6.20E-83
Alpha-spectrin	P02549	12.03	3.94	81	VNILTDKS(0.006)Y(0.994)EDPTNIQGK	2.18E-138
Lck-interacting transmembrane adapter 1	A0A087WUJ1	11.73	3.45	192	TEVTPAAQVDVLY(0.842)S(0.158)R	2.39E-86
Dematin	Q08495	11.60	6.13	293	SSSLPAY(1)GR	0.0025765
Beta-spectrin *	P11277	11.54	4.60	2137	LSSSWESLQPEPS(0.021)HPY(0.979)	1.26E-07
Alpha-adducin	P35611	11.37	5.20	550	EY(1)QPHVIVSTTGPNPFTTLTDRELEEYRR	1.32E-166
Dematin	Q08495	10.72	4.96	141	TSLPHFHHPETSRPDS(0.001)NIY(0.999)K	2.68E-38
Ankyrin-1	P16157	10.39	4.23	3	PY(1)S(1)VGFR	1.50E-07
Ankyrin-1	P16157	10.19	5.99	1867	QIDLSSADAAQEHEEVTVEGPLEDPSELEVDIDY(1)FMK	6.49E-138
Tensin-1	H0Y4U1	8.97	3.47	434	HVAY(1)GGYSTPEDR	1.01E-11
Beta-adducin	P35612	7.93	3.55	489	IENPNQFVPLY(0.996)T(0.004)DPQEVLEMR	1.94E-51
Flotillin-2	Q14254	7.55	2.98	163	DVYDKVDY(1)LSSLGK	6.83E-75
Tensin-1	H0Y4U1	7.39	3.04	365	HPAGVY(1)QVSGLHNK	9.71E-07
Alpha-spectrin	P02549	7.17	2.43	2280	EFS(0.001)T(0.003)IY(0.996)KHFDENLTGR	3.81E-29
Aquaporin-1	P29972	6.76	1.55	253	VWTSGQVEEY(1)DLDADDINSR	1.62E-94
Plasma membrane calcium-transporting ATPase 1	P20020	6.51	2.73	1129	SSLY(1)EGLEKPESR	3.79E-74
Junctional adhesion molecule A	Q9Y624	6.48	2.67	280	VIY(0.997)S(0.003)QPSAR	0.00020914

Upregulated (part 2)

Protein names	Uniprot Accession number	Log P value	Difference	Position	Phospho...STY...Probabilities	PEP
Alpha-adducin	P35611	6.00	2.93	24	Y(1)FDRVDENNPEYLR	7.48E-10
Alpha-adducin	P35611	5.63	2.85	35	YFDRVDENNPEY(1)LR	8.95E-22
Myelin protein zero-like protein 1	O95297	5.59	2.20	263	SESVVY(1)ADIR	0.00119487
Lck-interacting transmembrane adapter 1	A0A087WUJ1	5.45	1.90	246	ALDVDSGPLENVY(0.997)ES(0.003)IR	6.57E-43
Myelin protein zero-like protein 1	O95297	5.08	3.11	241	SLPSGSHQGPVIY(1)AQLDHSGGHHSDK	5.48E-68
Beta-spectrin	P11277	4.82	4.44	1302	LLTSQDVS(0.032)Y(0.968)DEAR	4.81E-28
Dematin	Q08495	4.38	3.47	70	AILDIERPDLMIYEPHFT(0.01)Y(0.865)S(0.125)LLEHVELPR	5.85E-283
Phosphatidylinositol 3,4,5-trisphosphate 5-phosphatase 1	Q92835	3.97	2.46	1022	NAGDTLPQEDLPLT(0.001)KPEMFENPLY(0.969)GS(0.723)LS(0.232)S(0.075)FPKPAPR	6.36E-91
Beta-spectrin	P11277	3.79	2.62	2137	LSSSWESLQPEPS(0.021)HPY(0.979)	1.26E-07
Tyrosine-protein kinase; Tyrosine-protein kinase Fyn	J3QRU1;P06241	3.55	1.86	431;420	LIEDNEY(0.993)T(0.007)AR	7.78E-14
Tyrosine-protein kinase Lyn	P07948	3.12	1.86	397	VIEDNEY(0.889)T(0.111)AR	0.00066243
Platelet endothelial aggregation receptor 1	Q5VV43	2.86	1.92	925	GLISEEELGASVASLSSENPY(0.962)AT(0.038)IR	9.51E-22
Plasma membrane calcium-transporting ATPase 4	P23634	2.63	1.97	1158	AFHSLHESIQKPY(1)NQK	3.95E-08
Ephrin type-B receptor 4	Q96L35	2.25	1.40	574	EAEY(0.994)GS(0.006)DKHGQYLIGHGTK	9.53E-13
Phosphatidylinositol 3,4,5-trisphosphate 5-phosphatase 1	Q92835	2.04	3.04	865	EKLY(1)DFVK	3.02E-11

Downregulated

Protein names	Uniprot Accession number	Log P value	Difference	Position	Phospho...STY...Probabilities	PEP
Proteasome subunit beta type-3 **	A0A087WXQ8	4.34	-3.50	85	QIKPY(1)T(1)LMS(0.972)MVANLLY(0.029)EKR	0.00687676
MARVEL domain-containing protein 2 *	A1BQX2	3.87	-2.72	159	DPY(0.974)GS(0.026)LDRHT(0.977)QT(0.022)VR	0.00077313
Receptor-interacting serine/threonine-protein kinase 1	Q13546	2.65	-1.52	94	YSLVMEY(1)MEK	0.016447
DNA excision repair protein ERCC-6-like 2	Q5T890	2.29	-2.68	653	VLRLSLGTVEEIMY(1)LR	0.00987153
Band 3 *	P02730	1.57	-3.24	359	YQSSPAKPDSSFY(1)K	7.48E-277

*mult_2; **mult_3; PEP (Peptide posterior error probability)

ANNEX-7: IMPACT OF BLOOD PROCESSING: A QUICK GLANCE ON ANTIOXIDANT POWER FROM WHOLE BLOOD COLLECTION TO RED BLOOD CELL CONCENTRATE STORAGE

Aim of the study

The aim of the present experiment was to first to evaluate the impact of the blood product processing on the Antioxidant Power (AOP) within the bag by following its evolution from donation, throughout the different steps of the Red Cell Concentrate (RCC) preparation and as well as during its storage at 4°C upon expiry.

Material and methods

Whole blood was donated by a healthy young man (28 years old) with informed consent at the transfusion center of Epalinges, Switzerland. This donor has a lifetime deferral because he had received a transfusion in the past. Consequently, his blood could only be used for research purposes.
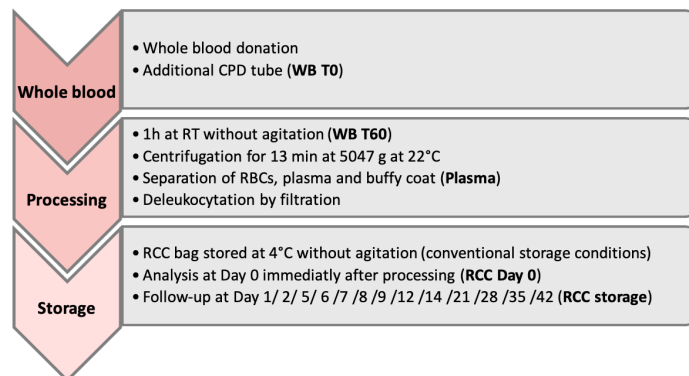
Immediately after donation, the hematological parameters and AOP were analyzed (**WB T0** sample). Then, the same sample was centrifuged 10 min at 2000 g and 4°C and the supernatant collected. The proteins concentration was determined using the A$_{280}$ Absorbance protein method of the NanoDrop spectrophotometer that uses the Beer's Law (with 1 Abs = 1 mg/mL), the blank was done in 0.9 % NaCl. The AOP was also measured in the supernatant. The whole blood bag was left 1h at RT without agitation. A sample was taken and analyzed as before (**WB T60** sample). Then, the WB bag was centrifuged during 13 min at 5047 g and 22°C to separate the RBCs from the plasma and buffy coat. The different blood components were transferred aseptically in distinct storage bags. A sample was taken from the plasma bag (**Plasma** sample) for the same analyses. After being mixed with Saline-Adenine-Glucose-Mannitol (SAGM) additive solution, the final processing step for the RBCs consisted in filtration to remove the residual leukocytes.

The RCC was stored under standard conditions (4°C without agitation). It was analyzed immediately (**RCC Day 0** sample), and at Day 1, 2, 5, 6, 7, 8, 9, 12, 14, 21, 28, 35, 42 (**RCC storage** samples). To do so, RCC samples were withdrawn with a syringe through a sampling site. Hematological parameters and AOP were measured on the whole RCC. Then, the samples were centrifuged at 2000 g during 10 min at 4°C and the supernatant collected for the determination of the percentage of hemolysis, the protein concentration and the AOP.

Results and discussion

The hematological parameters were normal. During storage, the RBC count remained stable and the Mean Corpuscular Volume (MCV) and anisocytosis (reflected by the Standard Deviation of Red Blood Cell Distribution Width [SD-RDW]) increased, as usually observed (Figure 2, blue curves). At Day 42, the percentage of hemolysis was of 0.287 ± 0.002 %, well below the accepted 0.8 % (Figure 2, red curve).
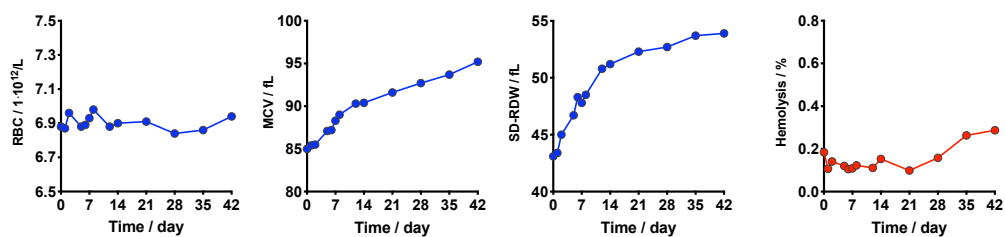

Figure 2 – Red Blood Cell (RBC) aging markers. Hematological data: RBC count, mean corpuscular volume (MCV) and Standard deviation of Standard Deviation of Red Blood Cell Distribution Width (SD-RDW) measured with Sysmex analyzer. Percentage of hemolysis in the blood bag determined using the Harboe spectrophotometric method.
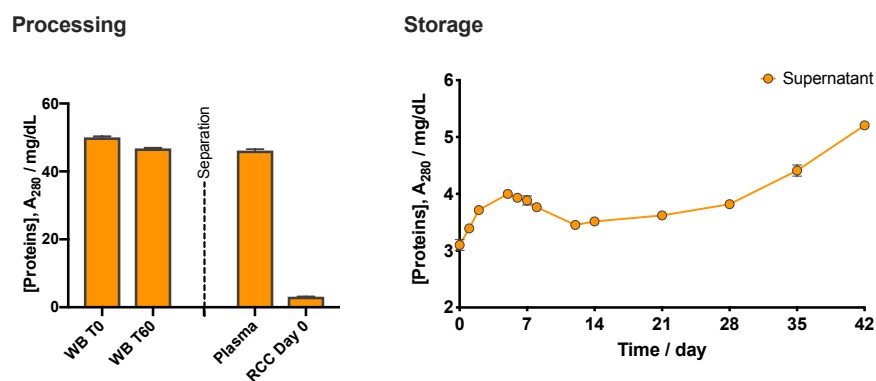
Figure 3 – Evolution of the protein concentration in the supernatant during blood processing and Red Cell Concentrate (RCC) storage. Determined with the NanoDrop spectrophotometer using A_{280} Absorbance. Mean value ± Standard Deviation (SD).

The concentration of proteins (Figure 3) in the whole blood supernatant (*i.e.* plasma) was of 50.05 ± 0.32 mg/mL at T0 and 46.79 ± 0.22 mg/mL after 60 min of rest. After processing, the quantity measured was similar, *i.e.* 46.15 ± 0.42 mg/mL, in the sample taken from the plasma bag. As expected, the

amount of proteins was strongly reduced in the RCC supernatant because of plasma removal and addition of SAGM solution. At Day 0, the protein concentration dropped to 3.099 ± 0.095 mg/dL. At the beginning of storage period, the protein concentration followed a pattern similar to the AOP, because UA (a main contributor to the extracellular AOP) has a maximum of absorbance at 292 nm and thus interferes with the measure of the A_{280} Absorbance. Later, the increase in protein concentration was related to the hemolysis of the RBCs.
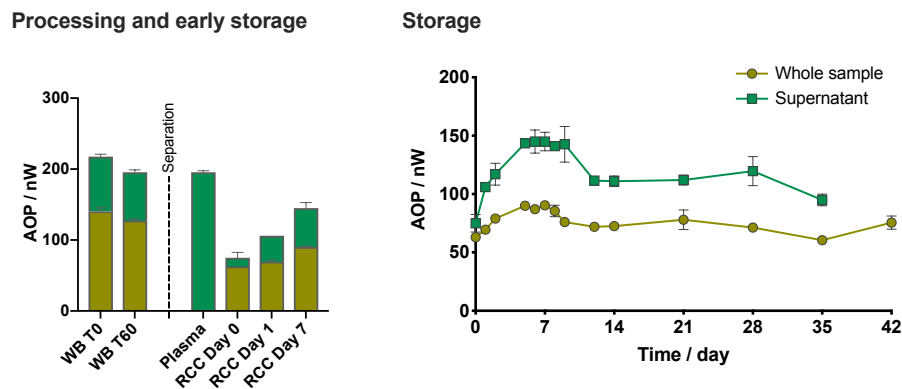

Figure 4 – Evolution of the Antioxidant Power (AOP) in the supernatant and whole sample during blood processing and Red Cell Concentrate (RCC) storage. Quantified by pseudotitration voltammetry with Edelmeter. Mean value ± Standard Deviation (SD).

Immediately after donation, the AOP was of 140.5 ± 4.95 nW in the WB and 217.5 ± 3.54 nW in its supernatant (*i.e.* plasma). After 60 min of rest, it dropped to 127.5 ± 2.12 nW and 195.5 ± 3.54 nW, which correspond to a loss of 9.3 and 10.1 %, respectively, suggesting that even before processing, the exposure to an *ex vivo* environment and the stress induced by the collection procedure increases the oxidative burden and/or depletes the WB antioxidant defenses. The extracellular AOP remained stable during WB centrifugation and separation. Removal of plasma and addition of SAGM solution drastically decreased the AOP in the RCC compared to the WB. Right after processing, the RCC AOP dropped to 63.0 ± 0.0 nW in the whole sample and 75.0 ± 7.52 nW in the supernatant. To be noted that the bare SAGM solution has a basal AOP of approximately 20 nW. During the first week of storage, and as reported in the Part 2 of Chapter 2, the RCC AOP raised sharply subsequently to the release of intracellular UA by the RBCs. A maximum was reached at 90.3 ± 1.15 nW for the whole RCC and 145.0 ± 7.94 after 7 days, probably because of the exhaustion of the intracellular UA pool.

Conclusion

The results obtained during this experiment illustrated the effects of blood processing on the RCC AOP and suggest that the RBCs are impacted by their new environment from the very beginning of the storage period.
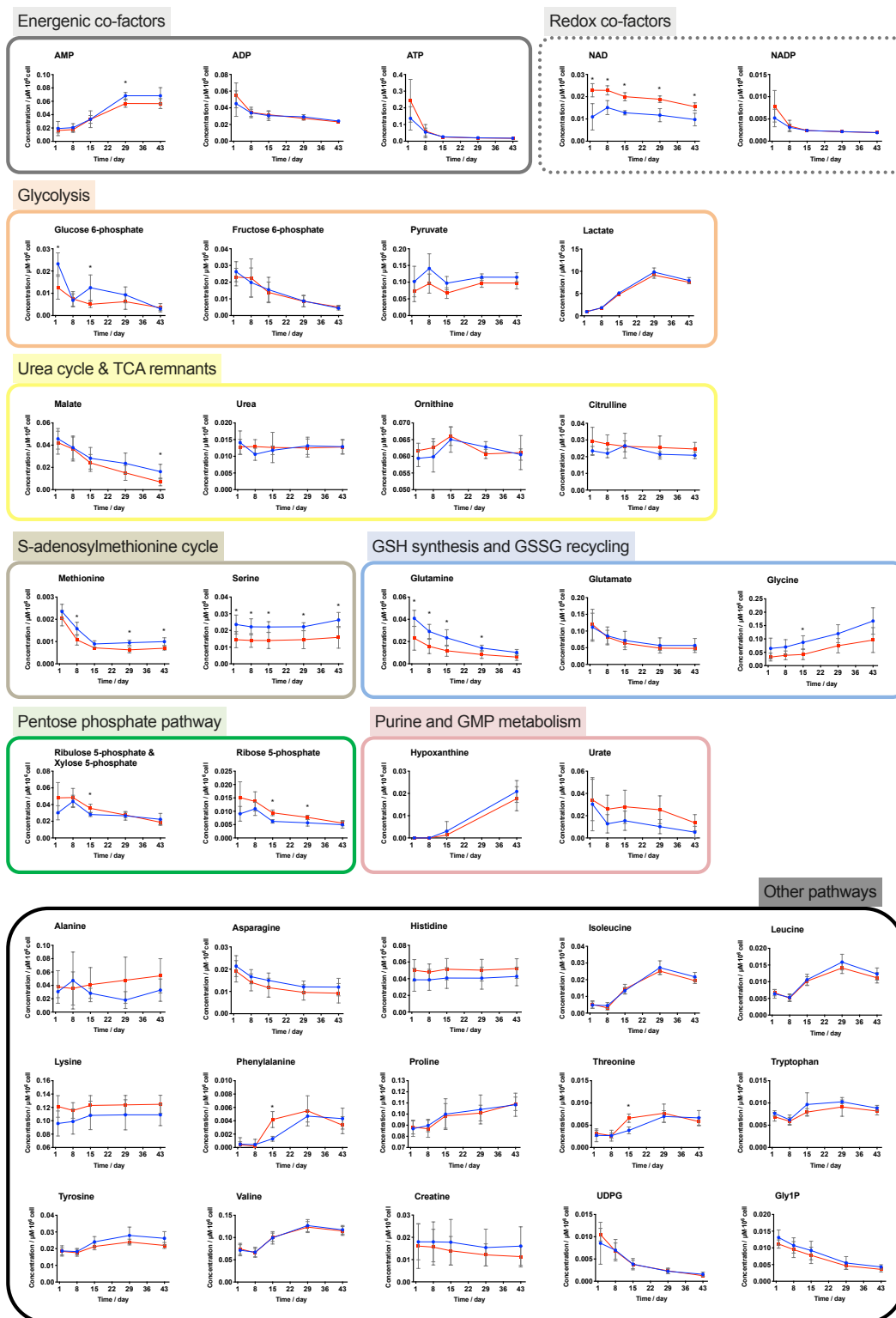
*Figure 5 – **Quantitative data of the time-course metabolomics analysis for control RBCs stored in standard conditions (SAGM only, blue lines) or for RBCs supplemented with ascorbic acid-uric acid antioxidant (red lines).** Only intracellular metabolites were measured. Each point corresponds to the mean value ±SD of metabolite concentration measured in 4 red cell concentrates.*

ANNEX-9: COMPOSITION OF THE ANTIOXIDANT STOCK SOLUTIONS

<table>
<tr>
<td rowspan="2">B|BRAUN</td>
<td>– Summary Note –</td>
<td>B. Braun Medical AG
Pharmaceutical Development Crissier</td>
</tr>
<tr>
<td>Manufacturing of Red Blood Cell Additive Solutions</td>
<td>Project: Ma Vie Ton Sang
Date.: 17-April-2015
Version: 01
Page: 1 of 5</td>
</tr>
</table>

1. Introduction

In general, blood collected by blood banks is combined with additive solutions to extend storage time and quality of red blood cells.

Lausanne Blood Bank ("Service Régional Vaudois de Transfusion Sanguine") has initiated a research program to investigate the effect of additive solutions on red blood cells.

In this context, B. Braun Crissier Pharmaceutical Development department will manufacture at labscale small quantities of these new additive solutions which will be used for preliminary *in vitro* evaluation at Lausanne Blood Bank.

This document lists the raw materials which will be used and summarizes the compositions of the additive solutions to be prepared.

2. References

- Study proposal, Service Régional Vaudois de Transfusion Sanguine, Lausanne "New routes and new additive solution formulations to improve the quality of stored red blood cells".

3. Definitions and Abbreviations

API	Active Pharmaceutical ingredient
BCR	B. Braun Crissier (Switzerland)
Blood Bank	Service Régional de Transfusion Sanguine
N/A	Not Applicable
n.r.	Not Relevant
QS	Sufficient Quantity
RBCAS	Red Blood Cells Additive Solution
SAGM	Saline Adenine Glucose Mannitol
tbd	To Be Defined
WFI	Water for Injections

4. Materials and methods

4.1 Raw materials

Raw materials used for red blood cells additive solution preparation are listed in the Table below.

	Compound or Component	Mw (g/mol)	Supplier	Art Nb
1	Ascorbic acid	176.12	DSM	0408050
2	N-Acetyl cysteine	163.19	BCR	DA30057
3	L-Glutamine	146.14	Sigma Aldrich	G5792
4	Hydroxyurea	76.05	Sigma Aldrich	H8627
5	α-lipoic acid	206.33	BCR	DT19075
6	O-Acetyl-L-carnitine hydrochloride	239.70	Sigma Aldrich	A6705
7	α-Tocopherol	430.71	BASF	50371444
8	NaCl	58.44	BCR	DS49957
9	Phospholipid based solubilizer	608.7	BCR	N/A
10	Adenine	135.13	Sigma Aldrich	A8626
11	D-Glucose monohydrate	198.17	BCR	1620071
12	D-Mannitol	182.17	BCR	DM38037
13	HCl 20%	n.r.	BCR	R720
14	NaOH 40%	n.r.	BCR	R710
15	WFI	n.r.	BCR	DA01072

Table 1 :   Components of red blood cells additive solutions

- Safety consideration

Red blood cells additive solutions components are biologically active compounds and adequate safety precautions should be observed for storage, handling and waste disposable. Detailed information are provided in their respective MSDS.

B|BRAUN

– Summary Note –

Manufacturing of Red Blood Cell Additive Solutions

B. Braun Medical AG
Pharmaceutical Development Crissier
Project: **Ma Vie Ton Sang**
Date.: **17-April-2015**
Version: **01**
Page: **3 of 5**

4.2   Samples Packaging

The following packaging materials will be used for the study.

Component	Description	Supplier*
50 ml clear glass bottle	Type I tubular glass 20 mm Crimp neck	Schott AG (Germany)
20 mm stopper	Omniflex Plus coated stoppers	Daetwyler AG (Switzerland)
20 mm flip off cap	Alu cap with red flip off cap	Daetwyler AG (Switzerland)

*: Alternative suppliers could be used assuming comparable quality

Table 2 :   Samples packaging description

Vials and stoppers will be rinsed with WFI and autoclaved before use.

4.3   Methods

Preparation of red blood cells additive solutions will be performed at labscale in BCR Pilot Laboratory and filtered through a 0.2 µm prior filling. Solution will be considered as low bioburden but not sterile *per se*.

Details of the manufacturing operations will be documented in BCR formulation and process operators logbooks.

5.   Analytical Program and Storage Conditions

5.1   Analytical Program

Analyses will be performed after manufacturing within BCR Pharmaceutical Development department and Lausanne Blood Bank according to the Table below.

Parameter	Method Reference	Preliminary Acceptance Limit	Testing Site
Visible particles	Ph. Eur. 2.9.20	Practically free from particles	BCR
Clarity and degree of opalescence of solution	Ph. Eur. 2.2.1	Clear (≤ 3 NTU)	BCR
Degree of coloration of solution	Ph. Eur. 2.2.2	Record data	BCR
pH	Ph. Eur. 2.2.3	7.0 – 7.5	BCR
API content	tbd	tbd	Lausanne Blood Bank

Table 3 :   Red blood cells additive solutions analytical program

5.2   Storage Conditions

Samples will be stored frozen at BCR and at Lausanne Blood Bank before use. Solution will be thawed shortly before use, checked for absence of precipitation and kept protected from light and oxygen. At the current stage of the study, it is not foreseen to perform a stability study on the red blood cells additive solutions.

6. Red blood cells additive solutions composition

Composition of SAGM and red blood cells additive solutions RBCAS-01 and RBCAS-02 are provided in the Table below.

Compound or Component		SAGM		RBCAS-01		RBCAS-02	
		(g/l)	*mM*	(g/l)	*mM*	(g/l)	*mM*
1	Ascorbic acid	-	-	1.154	*6.555*	-	-
2	N-Acetyl cysteine	-	-	2.326	*14.250*	-	-
3	L-Glutamine	-	-	-	-	12.495	*85.500*
4	NaCl	8.770	*150.068*	8.770	*150.068*	8.770	*150.068*
5	Adenine	0.169	*1.251*	0.169	*1.251*	0.169	*1.251*
6	D-Glucose monohydrate	9.000	*45.416*	9.000	*45.416*	9.000	*45.416*
7	D-Mannitol	5.250	*28.819*	5.250	*28.819*	5.250	*28.819*
8	HCl 20%	QS to pH 5.5 – 5.9		QS to pH 7.0 – 7.5		QS to pH 7.0 – 7.5	
9	NaOH 40%	QS to pH 5.5 – 5.9		QS to pH 7.0 – 7.5		QS to pH 7.0 – 7.5	
10	WFI	QS to 1L		QS to 1L		QS to 1L	

Table 4 : Composition of SAGM and Red Blood Cells Additive Solutions 01 and 02

ANNEXES

Chemin des Ecoliers 4
2013 Colombier, Switzerland
+41 79 427 68 69
manon.bardyn1@gmail.ch
31.01.1989, married, Swiss

Manon Bardyn

Life Sciences and Technologies

Personal skills and competences

- PhD in Life Sciences conducted in the research laboratory of a blood transfusion center
- Master diploma in Life Sciences and Technologies, specializing in Molecular Medicine
- Engineer with polytechnic education based on multidisciplinary competencies
- Professional experience in industrial and academic institutions
- Interest in innovation, health and life sciences

Relevant work experiences and internships

2014–2019   **PhD in Life Sciences, Transfusion Interrégionale CRS SA**, Epalinges, Switzerland
Faculty of Biology and Medicine, Université de Lausanne (UNIL), Lausanne, Switzerland
Research project focused on the red blood cells storage under blood banking conditions. Understand the lesions occurring in red blood cells during their storage, using standard and innovative analytical methods (Metabolomics, Proteomics, immunoblots, flow cytometry, digital holographic microscopy, microfluidics, etc.). The project was then dedicated on finding new routes and new additive solution formulations to improve the quality of the red cell concentrates. In parallel, time was dedicated to the supervision of interns, collaborative work on different side-projects, scientific writing and publishing, conferences attendance, and participation to courses and tutorials at UNIL (metabolomics, risk perception, linear multiple regression, fluorescence imaging, etc.).

2013
(2 months)   **Consulting experience in Tanzania**
Assessment of current health care waste management practices in the Dodoma region of Tanzania, in collaboration with the **Swiss Tropical and Public Health Institute** and **EssentialMed** (Switzerland). Carried out audits of 73 health facilities in the Dodoma region. After analysis of the collected data, a detailed report of the situation, including advice on future actions, was transmitted to the Tanzanian Ministry of Health.

2012–2013
(9 months)   **Master thesis**, **Biocartis SA**, Scientific Park of the EPFL, Switzerland
Development of an amplification strategy to improve sensitivity of nucleic acid detection assay on the multiplex detection platform of Biocartis. As a result of this development, sensitivity was improved by a factor of 100, reducing the need for target pre-amplification.

2011
(6 weeks)   **Internship at the Institute of Micro and Nano technics**, HEIG-VD, Switzerland
Characterization of the physical properties of a shape memory fiber. This fiber was intended for use in a medical application.

Higher education

2007–2013   **Master of Science (MSc) in Life Sciences and Technologies**
Specialization in Molecular Medicine,
Swiss Federal Institute of Technology in Lausanne (EPFL), Switzerland
Courses: animal experimentation, bioactive compound screening, biosafety, cancer biology, infection biology, stem cells, pharmaceutical biotechnology, immunology, biomimetic materials and tissue engineering, genetics, neurosciences, mathematics (analysis, probabilities and statistics, linear algebra, etc.), chemistry (general, organic, biologic), informatic, physics, fluid mechanics, introduction to law and ethics in Life Sciences, management of technology, etc.

2004–2007   **High school Diploma in Biology and Chemistry**
Lycée Denis-de-Rougemont, Neuchâtel, Switzerland

Languages

French   Native speaker
English   Fluent (B2)

Publications

Original articles

Manon Bardyn, Sunny Maye, Andreas Lesch, Julien Delobel, Jean-Daniel Tissot, Fernando Cortés-Salazar, Philippe Tacchini, Niels Lion, Hubert H. Girault, Michel Prudent
The antioxidant capacity of erythrocyte concentrates is increased during the first week of storage and correlated with the uric acid level.
Vox Sanguinis, 2017, 112(7):638-647

Manon Bardyn, Benjamin Rappaz, Keyvan Jaferzadeh, David Crettaz, Jean-Daniel Tissot, Inkyu Moon, Gerardo Turcatti, Niels Lion, Michel Prudent
Red blood cells ageing markers, a multi-parametric analysis.
Blood Transfusion, 2017, 15(3):239-248

Keyvan Jaferzadeh, Inkyu Moon, Manon Bardyn, Michel Prudent, Jean-Daniel Tissot, Benjamin Rappaz, Bahram Javidi, Gerardo Turcatti, Pierre Marquet
Quantification of stored red blood cell fluctuations by time-lapse holographic cell imaging.
Biomedical Optics Express, 2018, 9(10): 4714–4729

Mélanie Abonnenc, David Crettaz, Laure Marvin, Baptiste Grund, Giona Sonego, Manon Bardyn, Jean-Daniel Tissot, Michel Prudent, Bertrand Rochat, Niels Lion
Metabolomic profiling highlights oxidative damages in platelet concentrates treated for pathogen inactivation and shows protective role of urate.
Metabolomics, 2016, 12:188

Sangeeta Dey, Leila Laredj, Katarina Damjanovic, Manon Bardyn, Peter Beard
Growth of osteosarcoma cells in a three-dimensional bone-like matrix alters their susceptibility to adeno-associated virus.
Journal of General Virology, 2014, 95:1539-1543

Reviews

Manon Bardyn, Jean-Daniel Tissot, Michel Prudent
Oxidative stress and antioxidant defenses during blood processing and storage of erythrocyte concentrates.
Transfusion Clinique et Biologique, 2018, 25(1):96-100

Jean-Daniel Tissot, Manon Bardyn, Giona Sonego, Mélanie Abonnenc, Michel Prudent
The storage lesions: From past to future.
Transfusion Clinique et Biologique, 2017, 24(3):277-284

Posters

Michel Prudent, Manon Bardyn, Sunny Maye, Andreas Lesch, Julien Delobel, Jean-Daniel Tissot, Fernando Cortès-Salazar, Philippe Tacchini, Hubert H Girault and Niels Lion
The antioxidant defense system of erythrocyte concentrates is increased during the first week of storage.
AABB, Orlando, Florida, USA, October 2016

Manon Bardyn, Michel Prudent, Benjamin Rappaz, Sunny Maye, Andreas Lesch, David Crettaz, Jean-Daniel Tissot, Hubert H. Girault, Gerardo Turcatti, Philippe Tacchini and Niels Lion
How to measure oxidant/antioxidant status in erythrocytes?
Swisstransfusion, Annual Meeting, Bern, August 2016

Manon Müller, Benjamin Rappaz, David Crettaz, Jean-Daniel Tissot, Gerardo Turcatti, Niels Lion and Michel Prudent
Erythrocytes storage lesions, a multi-parametric analysis.
D.Day 2016, University of Lausanne, Lausanne, Switzerland, March 2016

Manon Müller, Michel Prudent, Benjamin Rappaz, Romain Hamelin, Florence Armand, Julien Delobel, Pierre Marquet, Jean-Daniel Tissot, Marc Moniatte, Gerardo Turcatti and Niels Lion
Loss of tyrosine phosphorylation during in vitro storage of erythrocytes and role of Lyn and Syk kinases in cell morphology.
Swiss Image-Based Screening Conference, Basel, September 2015